

MANAGING AGRICULTURAL SYSTEMS IN A VARIABLE, NON-STATIONARY CLIMATE:

PART II. NATURAL RESOURCE MANAGEMENT AND GRAZING SYSTEMS

Authors: Steven Crimp, Neil Flood, Greg McKeon and Mark Howden



**Land and Water Australia Project QNR31
Managing Climate Variability Program**

FINAL REPORT

August 2004



Queensland Government
Natural Resources and Mines



Department of Natural Resources, and Mines, Queensland

General Disclaimer

The Department of Natural Resources, and Mines, Queensland (NRM) have produced this final report for "Managing Climate Variability Program" administered by Land and Water Australia. NRM may not necessarily adopt and / or formulate any views and / or conclusions expressed in this report. Whilst all reasonable steps and due care has been taken to ensure that the information contained in this publication is accurate at the time of production, NRM expressly excludes all liability for errors or omissions whether made negligently or otherwise for loss, damage or other consequences, which may result from this publication.

Photos Courtesy of: Mr Robert Hassett Climate Impacts and Natural Resource Systems Group,
NRM

ABSTRACT

Australia's grazing lands are important to its Agricultural economy as they occupy over 50% of the continent and support approximately 120 million sheep and 25 million cattle. In Queensland, grazing of native pastures is the major land use (85% of State) and contributes approximately \$2.5 billion in gross agriculture value (i.e. approximately 40% of total agriculture).

Analyses of national climate variability have revealed that climatic events (e.g. drought, flood and extreme temperatures) are increasingly falling outside the long-term historical experience, as a consequence of anthropogenic climate change. As current agricultural practices have been strongly shaped by historical climate conditions, predicted changes in future climate, resulting from enhanced greenhouse gas concentrations, may result in loss of productivity and environmental degradation.

In order to ensure that natural resource and related on-farm management strategies take into account both changes in variability and non-stationarity, detailed climatic analysis quantifying historical trends and projected changes/impacts are required. These analyses need to be both scalable and transferable - principles that have been carried through the analyses undertaken for this project.

Trend analyses have been performed on rainfall and temperature data in Queensland's Burnett district, with the data used to simulate historical time sequences of deep drainage and run-off as well as on-farm management issues such as pasture productivity/condition and heat stress in cattle.

The results showed that annual rainfall for the Burnett study region (made up of an East, North, Central and South sub-region) has declined over the period 1890 to 2002. Of the four stations examined in the East sub-region half demonstrated statistically significant declining trends (i.e. $P < 0.05$), all the stations (4) in the North sub-region demonstrated statistically significant declining trends (i.e. $P < 0.05$) and the Central and South sub-regions demonstrated 2 and 1 statistically significant declining trends respectively. The analysis of both historical maximum and minimum temperatures revealed a consistent pattern of warming across the study region although only the warming trends in minimum temperature were statistically significant (i.e. $P < 0.05$).

The simulations of annual pasture production, revealed consistent declining trends across all stations and sub-regions except for the driest station in the Central sub-region (Auburn). While the simulation results returned a consistent declining trend in pasture production for all sub-regions analysed, there was no instance where the linear trends were statistically significant or explained more than 1% of the production variability. Similarly the simulation of deep drainage returned declining trends across all 16 stations examined in the Burnett study region, although these declines were almost non-existent in both the Central and South sub-regions for the analysis period 1890 to 2002. The simulated runoff data returned three instances where positive trends occurred. These instances occurred in the East, Central and South sub-regions in predominantly drier locations. Again, even though both positive and negative trends were simulated no statistically significant results were returned.

Projections of change in deep drainage, runoff, pasture production and heat stress were made through modification of the historical climate data. Projections of change in average temperature and rainfall were used to modify a range of other climate inputs such as daily measures of solar radiation, vapour pressure and evaporation. The climate change experiments were limited by

the coarse resolution of the climate projections, with individual climate model projections varying little for the entire study region. The greatest variation was as a result of inter-model differences with the climate models used producing a possible +6% to -6% change in rainfall by 2030 and +19% to -19% change in rainfall by 2070 (in response to 0.85 and 2.55°C of global warming).

Even though both positive and negative changes in rainfall were projected for the Burnett Study region and the CO₂ fertilisation effects were considered, the average simulated pasture production still demonstrated small declines (less than 1%) in productivity by 2030 (although productivity changes were highly variable between stations). By 2070 declines in pasture production of -4.5% were simulated.

Projected changes in deep drainage in response to enhanced greenhouse gas concentrations were greater than for pasture production with a relatively consistent pattern of decline across almost all of the 16 locations simulated. Stations in the South sub-region did show a number of instances where deep drainage increased in 2030, but declined by 2070.

Similarly runoff demonstrated a consistent pattern of decline across the East, North and Central sub-regions, with the South sub-region demonstrating both increases and decreases. The runoff values highlighted the water-limiting environment of both the South and Central sub-regions with runoff and deep drainage relatively small compared to the wetter North and East sub-regions.

The impact of climate change on heat stress was large with significant increases experienced across all sub-regions. The impacts were greatest in the Central and North sub-regions with over 100% increase in heat stress simulated by 2070.

PROJECT DETAILS

Project Title: Managing Agricultural Systems in a Variable, Non-Stationary Climate: Part II. Natural Resource Management and Grazing Systems

LWA Project No: QNR31

Research Organisation: Queensland Department of Natural Resources, Mines and Energy

Funding Organisations: Land and Water Australia (Climate Variability in Agriculture)

Principal Investigator: Mr Steven Crimp
Principal Climate Change Impacts Scientist
QCCA Building
Gate 4
80 Meiers Road
Indooroopilly
QLD 4068

Collaborators: Queensland Department of Primary Industries and Fisheries
CSIRO Sustainable Ecosystems

Project duration

The project officially started in June 2003 and has continued till June 2004.

Due date for Final Report

The Final Report was due for delivery on 1 June 2004.

Project objectives

The overall objective of this two-part project is the assessment of recent climate trends and the exploration of the resultant impacts on the cropping and grazing industries. In addition a consideration of the implications of current and projected climate changes for on-farm and government policy decisions will be addressed.

The research undertaken for Part II of the project (this report) is focussed on the Burnett study region. The sub-objectives under Part II (this report) include:

- quantifying historical trends in key climate factors such as temperature, rainfall (amount, duration and intensity)

- quantifying the consequences of these trends on natural resource management issues such as deep drainage and runoff as well as on-farm enterprise issues such as pasture production, and heat stress in cattle
- assessing the impact of a range of likely climate change projections on natural resource management issues as well as heat stress and pasture production using the most recent consensus climate change scenarios for the Burnett study region; and
- discussing possible management responses to these issues.

Final Report Milestones and achievement criteria

The Final Report includes a detailed analysis of climate trends in the Burnett study region as well as an assessment of the impact of these trends, on deep drainage, runoff, native pasture production and heat stress. In addition, projections of future heat stress, pasture productivity, runoff and deep drainage were prepared, analysed and included in the final report. The formal milestones as set out in the original contract include:

1. A detailed trend analysis of climatic indicators
2. Assessment of impacts of current climate trends on heat stress, pasture productivity and deep drainage
3. Assessment of impacts of project climate change on heat stress, pasture productivity and deep drainage
4. Assessment of potential adaptation options available to offset or mitigate impacts on heat stress, pasture productivity and deep drainage

Each of the milestones has been addressed in this report and will be considered completed on acceptance of the Final Report by Land & Water Australia (LWA).

Detailed trend analysis of climatic indicators

Detailed comparisons of raw and interpolated data were performed for all representative stations in the Burnett Study region. The raw and interpolated rainfall data showed strong agreement across all stations (except Moolboolaman, The Cedars, Auburn, Gayndah and Kumbia) exhibiting correlation co-efficient values above 0.92. In the case of the stations listed above the correlation co-efficient values ranged from 0.82 to 0.88. The strong correlation with raw rainfall data provided some confidence in the use of the interpolated data in the subsequent trend analyses and biophysical modelling. The raw and interpolated temperature data revealed weaker agreement with maximum temperature data consistently less well correlated than minimum temperature data.

An examination of the interpolated rainfall across all stations revealed consistent declining annual rainfall trends, with nine climate stations returning statistically significant declining trends and seven climate stations returning declining trends below the 95% confidence interval. This would suggest that the trends are strongly influenced by intra-seasonal climate variability (substantiated by summer and winter linear trend analyses).

An examination of the entire interpolated temperature data time series revealed consistent warming trends in both average maximum and minimum temperatures. While the minimum temperature trends were significant, the maximum temperature trends did not return statistically significant trends at the 95% confidence interval. These results correspond well with the official

Bureau of Meteorology trend analyses, which show minimum temperatures warming far more rapidly than maximum temperatures.

The analysis of extreme daily climate indices revealed consistent warming trends in the daily temperature data. Daily maximum temperature indices in the North, Central and South sub-regions returned the strongest daily warming trends in the winter months. The East sub-region did not reveal any statistically significant warming trends in average maximum temperatures but did exhibit statistically significant warming trends in extreme maximum temperature events.

In terms of rainfall changes, all sub-regions exhibited declining rainfall trends although these trends were not revealed in changes in average rainday amounts but through measures of extreme rainfall and wet spell persistence. Most of the stations in the East sub-region demonstrated statistically significant declines in extreme rainday amounts i.e. 60th, 80th, 90th and 95th percentile for the DJF period. In addition declines in maximum number of consecutive wet days, wet spell persistence and mean wet spell length all exhibited declines in the DJF and in some cases the MAM period.

The majority of stations in the North sub-region demonstrated statistically significant increasing trends in extreme percentile rainday amounts (i.e. 60th, 80th, 90th and 95th percentile) across all seasons with most significant increases found in the SON period. In addition stations in this sub-region also exhibited increasing trends in maximum consecutive dry days as well as declines in wet spell persistence across all periods.

The rainfall analysis for the Central sub-region return more equivocal trend results. For the most part stations demonstrated a mix of increases in lower percentile rainfall i.e. 20th to 50th as well as extremes i.e. 80th to 95th percentile rainday amounts. Consistent to all but one station was a decline in wet spell persistence and mean wet spell length for the summer rainfall period (i.e. DJF and SON). In this region three of the five stations analysed did return statistically significant declines in average daily rainfall for both JJA and annual periods.

The South sub-region, as with the Central sub-region returned few statistically significant rainfall trends. Consistent across all stations was the decline in mean wet spell length and wet spell persistence during the DJF period. Two of the five stations (i.e. Kingaroy and Kumbia) returned statistically significant increases in extreme daily rainfall amounts (i.e. 80th, 90th and 95th percentiles) for the SON period.

Assessment of impacts of current climate trends on heat stress, pasture productivity and deep drainage

On the whole the Burnett study region exhibited consistent declines in pasture, deep drainage, runoff and heat stress.

The simulation of historical annual pasture production, revealed consistent declining trends across all stations and sub-regions. While the simulation results returned a consistent declining trend in pasture production for the study region, there was no instance where the linear trends were statistically significant or explained more than 1% of the production variability.

Similarly the simulation of historical deep drainage returned no instances where drainage increased although both the Central and South sub-regions returned almost no linear trends for the period 1890 to 2002. These results, as with pasture production, were not statistically significant at the 95% confidence interval.

Again, while the simulation results returned, for the most part, declines in runoff for the study region, there were no instance where the linear trends were statistically significant or explained more than 1% of the runoff variability.

The simulation of historical heat stress (i.e. the occurrence of THI above 80) returned a predominantly negative trend across the Burnett Study region. The North and South sub-regions did demonstrate instance where positive trends were returned. However the linear trends for all sub-regions were below the 95% confidence limit. The anomalously high THI values at the beginning of the time series across all stations may well be an artificial feature of the interpolation process. This is an extremely difficult issue to resolve and has thus for the purposes of this project been included in the analyses.

While the linear trend analysis for the entire period did not indicate significant long-term changes, the 5, 10, and 30 year moving averages revealed the existence of important short and longer-term variability. Most notable were above average conditions in the late 1960s and 1970s consistent with above average rainfall and below average conditions since the early 1990s, consistent with anomalously low rainfall

Assessment of impacts of project climate change on heat stress, pasture productivity and deep drainage

The impacts of projected climate change on simulated of pasture production, deep drainage and runoff were modest, with most marked changes in drainage and runoff. The impacts of climate change on pasture productivity were marginal using global warming projections of 0.85°C by 2030 and 2.55°C by 2070. The simulations did reveal that although no large changes in pasture production occurred in most cases the changes indicated declining productivity.

The impact of climate change on heat stress was large with significant increases experienced across all sub-regions, with the Central and North sub-regions most pronounced.

Assessment of potential adaptation options available to offset or mitigate impacts on heat stress, pasture productivity and deep drainage

This research has demonstrated that the Burnett Study region is characterised by large spatial and temporal climate variability. The analysis of historical records for this region has demonstrated the importance of this variability in determining both industry reliability and economic returns within the agricultural sector.

History also reveals that the grazing industry is already intrinsically linked to natural climate variability and thus adapting to the range of climate change impacts identified in this project will represent an additional component of the property management process. One view is that by adopting methods to track year to year climate variability effectively, climate change over decades to centuries will automatically be accommodated. However increases in heat stress for the majority of the Burnett study region by 2070 may pose a series threat to industry sustainability.

Current pastoral management problems in this region include undesirable grass species, shrub invasion, soil erosion, animal nutrition, health and to a lesser degree salinisation and soil acidification. However many of these problems may become more of a challenge in the future and will require further technological advances to resolve. For this reason climate change adaptation options were discussed in light of current management issues.

Even though both positive and negative changes in rainfall were projected for the Burnett Study region, and the CO₂ fertilisation effect was considered, the average simulated pasture production

still demonstrated small declines (less than 1%) in productivity by 2030 (although productivity changes were highly variable between stations). By 2070 declines of almost 4.5% were simulated for pasture productivity.

Thus opportunities to improve pasture productivity will be limited with the maintenance of current productivity levels a greater challenge in the future. Some options available to maintain or enhance current forage production may include: (1) sowing new pastures which are better adapted to higher temperatures, water constraints and changes in soil fertility; and/or (2) providing additional nitrogen through use of sown legumes. However introducing new pasture species is likely to be considered a controversial strategy given the possible impacts on regional biodiversity.

The breeding cultivars having high non-structural carbohydrate levels may represent a viable adaptation option to maintaining herbage quality although any efforts to improve pasture would be limited by cost and scale of the individual grazing enterprise. The major risk to the grazing industry from climate change relates to the potential change in the distribution of pests, diseases and weeds. In some cases the change may be gradual, for example, with increasing temperature and go undetected until episodic events trigger widespread outbreaks

Under conditions of lower rainfall and warmer temperatures the resultant reduction in pasture productivity and drier conditions would limit the use of fire as a management tool. Current methods for controlling pests and disease in the grazing industry have proved useful in controlling pests and disease in response to natural climate variability and will continue to do so under project climate change. The increasing costs and resistance to chemical sprays may make this form of strategic adaptation more problematic in the future although technological advances may counter this trend.

The historical climate trends demonstrated by the Burnett Study region, revealed a reduction in rainfall, but increased incidence of extreme events (i.e. increase in the 80th to 95th percentile rainfall amounts). This, coupled with the slight reduction in pasture production by 2070 may result in greater susceptibility to soil erosion.

The climate change experiments showed a significant increase in the occurrence of heat stress by 2030 and most certainly by 2070. Adaptation to heat stress for the extensive grazing industry will be very difficult although the planting of shade trees and increased frequency of watering points may offset stress to some degree. For the intensive grazing industry such as feedlots and dairying, shading and spraying may represent viable adaptation options

TABLE OF CONTENTS

ABSTRACT	3
PROJECT DETAILS	5
Project duration.....	5
Due date for Final Report	5
Project objectives	5
Final Report Milestones and achievement criteria	6
Detailed trend analysis of climatic indicators	6
Assessment of impacts of current climate trends on heat stress, pasture productivity and deep drainage	7
Assessment of impacts of project climate change on heat stress, pasture productivity and deep drainage	8
Assessment of potential adaptation options available to offset or mitigate impacts on heat stress, pasture productivity and deep drainage	8
TABLE OF CONTENTS	10
BACKGROUND	20
1. Study region	20
2. Climate station selection and data integrity	21
3. Trend analysis methodology	23
4. Climate Indices	26
RAW CLIMATE DATA ANALYSES	27
1. Rainfall	27
2. Temperature	31
3. Summary of Raw Climate Data Trends	35

ANALYSIS OF INTERPOLATED CLIMATE DATA	37
1. Rainfall Correlation Analyses	38
2. Temperature Correlation Analysis	56
3. Summary of Interpolated and Raw Climate Data Comparisons	61
LINEAR TREND ANALYSIS OF EXTREME AND DAILY CLIMATE INDICES	62
1. Linear Trend Analysis of Climate Indices for the East Sub-Region	63
2. Linear Trend Analysis of Climate Indices for the North Sub-Region	66
3. Linear Trend Analysis of Climate Indices for the Central Sub-Region	69
4. Linear Trend Analysis of Climate Indices for the South Sub-Region	72
5. Summary of linear trend analyses of Interpolated Climate Data	75
LINEAR TREND ANALYSIS OF SIMULATED BIOPHYSICAL DATA FOR THE BURNETT STUDY REGION	77
1. Simulations of historical pasture production, deep drainage, runoff and cattle heat stress for the East sub-region	80
2. Simulations of historical pasture production, deep drainage, runoff and cattle heat stress for the North sub-region	87
3. Simulations of historical pasture production, deep drainage, runoff and cattle heat stress for the Central sub-region	91
4. Simulations of historical pasture production, deep drainage, runoff and cattle heat stress for the South sub-region	96
5. Summary of the results from simulations of historical pasture production, deep drainage, runoff and cattle heat stress for the Burnett study region	101
SIMULATED CHANGE IN PASTURE PRODUCTION, RUN-OFF, DRAINAGE AND HEAT STRESS IN RESPONSE TO GLOBAL WARMING	103
1. Climate Change Projections for the East sub-region	107
2. Climate Change Projections for the North sub-region	115
3. Climate Change Projections for the Central sub-region	123

4.	Climate Change Projections for the South sub-region	131
5.	Summary of the results from climate change simulations of pasture production, deep drainage, runoff and cattle heat stress for the Burnett study region.....	139
DISCUSSION AND CONCLUSIONS		141
Possible impacts on the Burnett's Grazing Industry.....		144
	Impacts on Pasture Productivity and Possible Adaptation Measures.....	145
	Impacts on Herbage Quality and possible amelioration options	145
	Impacts on Pests, Diseases and Weeds and Possible Adaptation Measures.....	146
	Impacts on Species Change in Native Pasture and Possible Adaptation Measures	146
	Impacts on Soil Erosion, Runoff and Deep Drainage and Possible Adaptation Measures	147
	Impacts on Animal Husbandry and Health and Possible Adaptation Options	147
REFERENCES.....		148
APPENDIX A		154

LIST OF FIGURES

Figure 1: A locality map of the Burnett study area.	20
Figure 2: A locality map of the Burnett study region showing long-term average annual rainfall (April to March) for the period 1889 to 2002 and selected climate stations for all four sub-regions.	21
Figure 3: A rainfall time series for a) "Bundaberg", b) "Gin Gin", c) "Moolboolaman" and d) "The Cedars" stations within the East sub-region. The linear trends were as follows a) Trend = $0.0292x + 1082.1$ $r^2 = 0.000005$, b) Trend = $-0.6028x + 2196.4$ $r^2 = 0.0035$, c) Trend = $-0.7881x + 2426.1$ $r^2 = 0.0023$ and d) Trend = $-1.7098x + 4228.3$ $r^2 = 0.021$. The smoothed red line represents the 10 year moving average of rainfall.	28
Figure 4: A rainfall time series for a) "Tecoma", b) "Kalpowar", c) "Malakof" and d) "Bancroft" stations within the North sub-region. The linear trends were as follows a) Trend = $-5.5504x + 11584.1$ $r^2 = 0.1989$, b) Trend = $-2.6541x + 6063.1$ $r^2 = 0.0487$, c) Trend = $-2.8897x + 6455.5$ $r^2 = 0.0638$ and d) Trend = $2.4682x + 4243.2$ $r^2 = 0.0308$. The smoothed red line represents the 10 year moving average of rainfall.	29
Figure 5: A rainfall time series for a) "Auburn", b) "Gayndah", c) "Eidsvold" and d) "Biggenden" stations within the Central sub-region. The linear trends were as follows a) Trend = $1.5635x + 2496.6$ $r^2 = 0.0108$, b) Trend = $-0.486x + 1710.9$ $r^2 = 0.0062$, c) Trend = $-0.8452x + 2373$ $r^2 = 0.0172$ and d) Trend = $0.0934x + 679.55$ $r^2 = 0.0001$. The smoothed red line represents the 10 year moving average of rainfall.	30
Figure 6: A rainfall time series for a) "Mounefontein", b) "Goomeri", c) "Kingaroy" and d) "Kumbia" stations within the South sub-region. The linear trends were as follows a) Trend = $-3.0358x + 6723.6$ $r^2 = 0.073$, b) Trend = $-0.4919x + 1755.7$ $r^2 = 0.0043$, c) Trend = $0.7694x + 723.71$ $r^2 = 0.0122$ and d) Trend = $1.3942x + 1980.4$ $r^2 = 0.0249$. The smoothed red line represents the 10 year moving average of rainfall.	31
Figure 7: A time series of average annual maximum temperature for a) the South sub-region (40112 - Kingaroy), b) the North sub-region (39057 - Kalpowar), c) the East sub-region (39015 - Bundaberg) and d) the Central sub-region (39039 - Gayndah). The linear trends were as follows a) Trend = $0.0098x + 5.1456$ $r^2 = 0.0256$, b) Trend = $-0.2677x + 550.95$ $r^2 = 0.6442$, c) Trend = $-0.0059x + 38.153$ $r^2 = 0.0847$ and d) Trend = $0.001x + 26.068$ $r^2 = 0.0011$	32
Figure 8: A time series of average annual minimum temperature for a) the South sub-region (40112 - Kingaroy), b) the North sub-region (39057 - Kalpowar), c) the East sub-region (39015 - Bundaberg) and d) the Central sub-region (39039 - Gayndah). The linear trends were as follows a) Trend = $0.0365x - 60.896$ $r^2 = 0.3086$, b) Trend = $-0.0181x + 46.139$ $r^2 = 0.013$, c) Trend = $0.0128x - 8.7306$ $r^2 = 0.2798$ and d) Trend = $0.0201x - 25.701$ $r^2 = 0.4194$	33
Figure 9: A time series of highest annual maximum temperature for a) the South sub-region (40112 - Kingaroy), b) the North sub-region (39057 - Kalpowar), c) the East sub-region (39015 - Bundaberg) and d) the Central sub-region (39039 - Gayndah). The linear trends were as follows a) Trend = $0.0196x - 1.7203$ $r^2 = 0.0234$, b) Trend = $-0.0304x + 96.758$ $r^2 = 0.0224$, c) Trend = $-0.0092x + 53.074$ $r^2 = 0.0275$ and d) Trend = $-0.0194x + 77.974$ $r^2 = 0.0881$	34
Figure 10: A time series of lowest annual minimum temperature for a) the South sub-region (40112 - Kingaroy), b) the North sub-region (39057 - Kalpowar), c) the East sub-region (39015 - Bundaberg) and d) the Central sub-region (39039 - Gayndah). The linear trends were as follows a) Trend = $0.0508x - 104.04$ $r^2 = 0.1653$, b) Trend = $0.1188x - 238.66$ $r^2 = 0.2155$, c) Trend = $-0.0055x + 12.58$ $r^2 = 0.0053$ and d) Trend = $0.0261x - 52.196$ $r^2 = 0.3085$	35
Figure 12: Raw annual rainfall (dark blue) and interpolated (light blue) annual rainfall time series data for the a) Tecoma b) Kalpowar c) Malakof and d) Bancroft rainfall stations. The straight line represents the linear regression for the interpolated annual rainfall series from 1889 to 2003.	53
Figure 13: Raw annual rainfall (dark blue) and interpolated (light blue) annual rainfall time series data for the a) 42059 (Auburn), b) 39039 (Gayndah), c) 39036 (Eidsvold) and d) 40021 (Biggenden) rainfall stations. The straight line represents the linear regression for the interpolated annual rainfall series from 1889 to 2003.	54
Figure 14: Raw annual rainfall (dark blue) and interpolated (light blue) annual rainfall time series data for the a) 40138 (Mounefontein), b) 40090 (Goomeri), c) 40112 (Kingaroy), and d) 40113 (Kumbia) rainfall stations. The straight line represents the linear regression for the interpolated annual rainfall series from 1889 to 2003.	55
Figure 15: A time series of average annual maximum temperature for a) the South sub-region (40112 - Kingaroy), b) the North sub-region (39057 - Kalpowar), c) the East sub-region (39015 - Bundaberg) and d) the Central sub-region (39039 - Gayndah). The red line represents the interpolated data and the black line represents the raw data.	60
Figure 16: A time series of average annual minimum temperature for a) the South sub-region (40112 - Kingaroy), b) the North sub-region (39057 - Kalpowar), c) the East sub-region (39015 - Bundaberg) and d) the Central sub-region (39039 - Gayndah). The blue line represents the interpolated data and the black line represents the raw data.	60
Figure 17: A locality map of the Burnett study area showing both the original climate station selection (highlighted in red) and the additional sites (highlighted in green) for all four sub-regions.	62

- Figure 18: A time series of annual pasture production for a) “Bundaberg”(39015), b) “Gin Gin” (39040), c) “Moolboolaman” (39218) and d) “The Cedars” (39234) stations within the East sub-region. The linear trends were calculated from the annual data as follows a) Trend = $-2.025x + 7108.64$ $r^2 = 0.0016$, b) Trend = $-3.540x + 10129.48$ $r^2 = 0.0041$, c) Trend = $-2.576x + 8303.08$ $r^2 = 0.0021$ and d) Trend = $-3.2688x + 9222.44$ $r^2 = 0.0049$. The smoothed green line represents the 5 year moving average of pasture production and the smoothed red line represents the 10 year moving average of pasture production.82
- Figure 19: A time series of annual ‘safe’ stocking rate for a) “Bundaberg”(39015), b) “Gin Gin” (39040), c) “Moolboolaman” (39218) and d) “The Cedars” (39234) stations within the East sub-region. The linear trends were calculated from the annual data as follows a) Trend = $-0.0002x + 0.53$ $r^2 = 0.0016$, b) Trend = $-0.0003x + 0.75$ $r^2 = 0.0041$, c) Trend = $-0.0002x + 0.62$ $r^2 = 0.0021$ and d) Trend = $-0.0002x + 0.68$ $r^2 = 0.0049$. The smoothed brown line represents the 5-year moving average of ‘Safe’ Stocking rate and the smoothed blue line represents the 30-year moving average of pasture production.83
- Figure 20: A time series of annual drainage for a) “Bundaberg”(39015), b) “Gin Gin” (39040), c) “Moolboolaman” (39218) and d) “The Cedars” (39234) stations within the East sub-region. The linear trends were calculated from the annual data as follows a) Trend = $-0.429x + 880.10$ $r^2 = 0.031$, b) Trend = $-0.479x + 1036.19$ $r^2 = 0.012$, c) Trend = $-1.158x + 2386.90$ $r^2 = 0.051$ and d) Trend = $-0.0266x + 544.71$ $r^2 = 0.021$. The smoothed blue line represents the 5-year moving average of drainage and the smoothed red line represents the 30-year moving average of drainage.84
- Figure 21: A time series of annual runoff for a) “Bundaberg”(39015), b) “Gin Gin” (39040), c) “Moolboolaman” (39218) and d) “The Cedars” (39234) stations within the East sub-region. The linear trends were calculated from the annual data as follows a) Trend = $-0.078x + 190.36$ $r^2 = 0.0071$, b) Trend = $-0.028x + 104.12$ $r^2 = 0.0003$, c) Trend = $-0.132x + 314.28$ $r^2 = 0.0089$ and d) Trend = $0.087x - 137.73$ $r^2 = 0.0081$. The smoothed turquoise line represents the 5-year moving average of runoff and the smoothed red line represents the 30-year moving average of runoff.85
- Figure 22: A time series of annual cattle heat stress for a) “Bundaberg”(39015), b) “Gin Gin” (39040), c) “Moolboolaman” (39218) and d) “The Cedars” (39234) stations within the East sub-region. The linear trends were calculated from the annual data as follows a) Trend = $-0.102x + 232.07$ $r^2 = 0.054$, b) Trend = $-0.039x + 120.33$ $r^2 = 0.0071$, c) Trend = $-0.054x + 154.18$ $r^2 = 0.0121$ and d) Trend = $-0.081x + 211.19$ $r^2 = 0.0257$. The smoothed orange line represents the 5-year moving average of THI days above 80 and the smoothed blue line represents the 30-year moving average of THI days above 80.86
- Figure 23: A time series of annual pasture production for a) “Tecoma”(39248), b) “Kalpowar” (39057), c) “Malakof” (39129) and d) “Bancroft” (39103) stations within the North sub-region. The linear trends were calculated from the annual data as follows a) Trend = $-0.288x + 3722.22$ $r^2 = 0.00004$, b) Trend = $-4.015x + 10932.89$ $r^2 = 0.0056$, c) Trend = $-2.124x + 7413.67$ $r^2 = 0.0015$ and d) Trend = $-5.114x + 13074.88$ $r^2 = 0.0094$. The green line represents the 5 year moving average of pasture production and the red line represents the 10 year moving average of pasture production.87
- Figure 24: A time series of ‘Safe’ Stocking Rate for a) “Tecoma”(39248), b) “Kalpowar” (39057), c) “Malakof” (39129) and d) “Bancroft” (39103) stations within the North sub-region. The linear trends were calculated from the annual data as follows a) Trend = $-0.288x + 3722.22$ $r^2 = 0.00004$, b) Trend = $-4.015x + 10932.89$ $r^2 = 0.0056$, c) Trend = $-2.124x + 7413.67$ $r^2 = 0.0015$ and d) Trend = $-5.114x + 13074.88$ $r^2 = 0.0094$. The smoothed brown line represents the 5 year moving average of ‘safe’ stocking rate and the smoothed blue line represents the 10 year moving average of ‘safe’ carrying capacity.88
- Figure 25: A time series of simulated drainage for a) “Tecoma”(39248), b) “Kalpowar” (39057), c) “Malakof” (39129) and d) “Bancroft” (39103) stations within the North sub-region. The linear trends were calculated from the annual data as follows a) Trend = $-0.508x + 1073.18$ $r^2 = 0.0168$, b) Trend = $-0.668x + 1368.48$ $r^2 = 0.0393$, c) Trend = $-1.124x + 2343.08$ $r^2 = 0.0360$ and d) Trend = $-0.551x + 1158.60$ $r^2 = 0.0216$. The smoothed blue line represents the 5 year moving average of drainage and the smoothed red line represents the 30 year moving average of drainage.89
- Figure 26: A time series of simulated runoff for a) “Tecoma”(39248), b) “Kalpowar” (39057), c) “Malakof” (39129) and d) “Bancroft” (39103) stations within the North sub-region. The linear trends were calculated from the annual data as follows a) Trend = $-0.138x + 326.81$ $r^2 = 0.0086$, b) Trend = $-0.091x + 218.60$ $r^2 = 0.0046$, c) Trend = $-0.152x + 356.62$ $r^2 = 0.0102$ and d) Trend = $-0.034x + 112.63$ $r^2 = 0.0007$. The smoothed turquoise line represents the 5 year moving average of runoff and the smoothed red line represents the 30 year moving average of runoff.90
- Figure 27: A time series of simulated annual cattle heat stress for a) “Tecoma”(39248), b) “Kalpowar” (39057), c) “Malakof” (39129) and d) “Bancroft” (39103) stations within the North sub-region. The linear trends were calculated from the annual data as follows a) Trend = $-0.091x + 261.52$ $r^2 = 0.0217$, b) Trend = $0.070x - 104.09$ $r^2 = 0.0296$, c) Trend = $0.049x - 60.78$ $r^2 = 0.0130$ and d) Trend = $0.012x - 24.25$ $r^2 = 0.0006$. The smoothed orange line represents the 5 year moving average of days with THI above 80 and the smoothed blue line represents the 30 year moving average of days with THI above 80.91
- Figure 28: A time series of annual pasture production for a) “Auburn”(42059), b) “Gayndah” (39039), c) “Eidsvold” (39036) and d) “Biggenden” (40021) stations within the Central sub-region. The linear trends were calculated from the annual data as follows a) Trend = $2.042x - 2505.84$ $r^2 = 0.0051$, b) Trend = $-1.578x + 6388.56$ $r^2 =$

0.001, c) Trend = $-0.489x + 4026.79$ $r^2 = 0.0001$ and d) Trend = $-4.029x + 11079.08$ $r^2 = 0.0063$. The smoothed green line represents the 5 year moving average of pasture production and the smoothed red line represents the 10 year moving average of pasture production. 92

Figure 29: A time series of annual 'safe' stocking rate for a) "Auburn"(42059), b) "Gayndah" (39039), c) "Eidsvold" (39036) and d) "Biggenden" (40021) stations within the Central sub-region. The linear trends were calculated from the annual data as follows a) Trend = $0.00015x - 0.19$ $r^2 = 0.0051$, b) Trend = $-0.0001x + 0.47$ $r^2 = 0.00087$, c) Trend = $-0.00004x + 0.30$ $r^2 = 0.0001$ and d) Trend = $-0.0003x + 0.82$ $r^2 = 0.0064$. The smoothed brown line represents the 5 year moving average of 'safe' stocking rate and the smoothed blue line represents the 10 year moving average of 'safe' stocking rate. 93

Figure 30: A time series of annual deep drainage for a) "Auburn"(42059), b) "Gayndah" (39039), c) "Eidsvold" (39036) and d) "Biggenden" (40021) stations within the Central sub-region. The linear trends were calculated from the annual data as follows a) Trend = $-0.017x + 62.18$ $r^2 = 0.0001$, b) Trend = $-1.041x + 2186.54$ $r^2 = 0.0355$, c) Trend = $-0.290x + 607.31$ $r^2 = 0.0169$ and d) Trend = $-0.379x + 785.29$ $r^2 = 0.0203$. The blue line represents the 5 year moving average of deep drainage and the red line represents the 10 year moving average of deep annual drainage. 94

Figure 31: A time series of annual deep drainage for a) "Auburn"(42059), b) "Gayndah" (39039), c) "Eidsvold" (39036) and d) "Biggenden" (40021) stations within the Central sub-region. The linear trends were calculated from the annual data as follows a) Trend = $0.00064x + 47.33$ $r^2 = 0.00004$, b) Trend = $-0.237x + 538.24$ $r^2 = 0.0196$, c) Trend = $-0.074x + 190.33$ $r^2 = 0.0032$ and d) Trend = $-0.153x + 338.65$ $r^2 = 0.0157$. The turquoise line represents the 5 year moving average of annual runoff and the red line represents the 10 year moving average of annual runoff. 95

Figure 32: A time series of annual cattle heat stress for a) "Auburn"(42059), b) "Gayndah" (39039), c) "Eidsvold" (39036) and d) "Biggenden" (40021) stations within the Central sub-region. The linear trends were calculated from the annual data as follows a) Trend = $-0.075x + 210.85$ $r^2 = 0.0181$, b) Trend = $-0.096x + 263.00$ $r^2 = 0.028$, c) Trend = $-0.059x + 185.83$ $r^2 = 0.0104$ and d) Trend = $-0.097x + 244.70$ $r^2 = 0.0343$. The orange line represents the 5 year moving average of total number of days where THI was above 80 and the blue line represents the 10 year moving average of total number of days where THI was above 80. 96

Figure 33: A time series of annual pasture production for a) "Mounefontein"(40138), b) "Goomeri" (40090), c) "Kingaroy" (40112) and d) "Kumbia" (40113) stations within the South sub-region. The linear trends were calculated from the annual data as follows a) Trend = $-3.818x + 10460.60$ $r^2 = 0.006$, b) Trend = $-3.342x + 9761.54$ $r^2 = 0.005$, c) Trend = $-4.685x + 12427.75$ $r^2 = 0.0084$ and d) Trend = $-3.715x + 10492.98$ $r^2 = 0.005$. The green line represents the 5 year moving average of pasture production and the red line represents the 10 year moving average of pasture production. 97

Figure 34: A time series of annual 'safe' stocking rate for a) "Mounefontein"(40138), b) "Goomeri" (40090), c) "Kingaroy" (40112) and d) "Kumbia" (40113) stations within the South sub-region. The linear trends were calculated from the annual data as follows a) Trend = $-0.0003x + 0.77$ $r^2 = 0.0062$, b) Trend = $-0.0002x + 0.72$ $r^2 = 0.0046$, c) Trend = $-0.0003x + 0.92$ $r^2 = 0.00839$ and d) Trend = $-0.0003x + 0.78$ $r^2 = 0.00496$. The brown line represents the 5 year moving average of annual 'safe' stocking rate and the blue line represents the 30 year moving average of annual 'safe' stocking rate. 98

Figure 35: A time series of annual deep drainage for a) "Mounefontein"(40138), b) "Goomeri" (40090), c) "Kingaroy" (40112) and d) "Kumbia" (40113) stations within the South sub-region. The linear trends were calculated from the annual data as follows a) Trend = $-0.082x + 190.76$ $r^2 = 0.0019$, b) Trend = $-0.205x + 446.89$ $r^2 = 0.0085$, c) Trend = $-0.0042x + 126.79$ $r^2 = 0.0004$ and d) Trend = $-0.142x + 311.92$ $r^2 = 0.0065$. The blue line represents the 5 year moving average of annual deep drainage and the red line represents the 30 year moving average of annual deep drainage. 99

Figure 36: A time series of annual runoff for a) "Mounefontein"(40138), b) "Goomeri" (40090), c) "Kingaroy" (40112) and d) "Kumbia" (40113) stations within the South sub-region. The linear trends were calculated from the annual data as follows a) Trend = $0.0727x - 126.18$ $r^2 = 0.0053$, b) Trend = $-0.106x + 245.95$ $r^2 = 0.0068$, c) Trend = $-0.014x + 65.47$ $r^2 = 0.0002$ and d) Trend = $-0.024x + 81.01$ $r^2 = 0.0004$. The turquoise line represents the 5 year moving average of annual runoff and the red line represents the 30 year moving average of annual runoff. 100

Figure 37: A time series of annual cattle heat stress for a) "Mounefontein"(40138), b) "Goomeri" (40090), c) "Kingaroy" (40112) and d) "Kumbia" (40113) stations within the South sub-region. The linear trends were calculated from the annual data as follows a) Trend = $0.0130x + 24.21$ $r^2 = 0.0002$, b) Trend = $-0.040x + 116.65$ $r^2 = 0.0096$, c) Trend = $0.047x - 67.73$ $r^2 = 0.0213$ and d) Trend = $0.0394x - 53.93$ $r^2 = 0.0171$. The orange line represents the 5 year moving average of the occurrence of THI values above 80 and the blue line represents the 30 year moving average of occurrence of THI values above 80. 101

Figure 38: Percentage change in annual rainfall per degree of global warming for Queensland, produced by 12 international climate models. 104

Figure 39: Absolute change in annual average temperature per degree of global warming for Queensland, produced by 12 international climate models. 104

LIST OF TABLES

Table1a: An analysis of record length and continuity for each of the stations used for this project. Continuity is expressed as the occurrence of daily data in each decade from 1880 to 2003.....	24
Table1b: An analysis of record length and continuity for additional stations used in the analysis of daily and month rainfall and temperature trends. Continuity is expressed as the occurrence of daily data in each decade from 1880 to 2003.	24
Table 2: A statistical comparison of raw and interpolated rainfall for station 39015 (Bundaberg). While the interpolated data series extends from 1889 to 2003 the Bundaberg raw data only extends to 1989. For this reason all statistical tests were performed on data for the period 1889 to 1989.....	38
Table 3: A statistical comparison of raw and interpolated rainfall for station 39040 (Gin Gin). While the interpolated data series extends from 1889 to 2003 the Gin Gin raw data only extends from 1900 to 2000. For this reason all statistical tests were performed on data for the period 1900 to 2000.	39
Table 4: A statistical comparison of raw and interpolated rainfall for station 39218 (Moolboolaman). While the interpolated data series extends from 1889 to 2003 the Moolboolaman raw data only extends from 1931 to 2002. For this reason all statistical tests were performed on data for the period 1931 to 2002.....	40
Table 5: A statistical comparison of raw and interpolated rainfall for station 39234 (The Cedars). While the interpolated data series extends from 1889 to 2003 the “The Cedars” raw data only extends from 1913 to 2002. For this reason all statistical tests were performed on data for the period 1913 to 2002.....	41
Table 6: A statistical comparison of raw and interpolated rainfall for station 39248 (Tecoma). While the interpolated data series extends from 1889 to 2003 the Tecoma raw data only extends from 1953 to 2002. For this reason all statistical tests were performed on data for the period 1953 to 2002.	42
Table 7: A statistical comparison of raw and interpolated rainfall for station 39057 (Kalpowar). While the interpolated data series extends from 1889 to 2003 the Kalpowar raw data only extends from 1933 to 2002. For this reason all statistical tests were performed on data for the period 1933 to 2002.	43
Table 8: A statistical comparison of raw and interpolated rainfall for station 39129 (Malakof). While the interpolated data series extends from 1889 to 2003 the Malakof raw data only extends from 1932 to 2002. For this reason all statistical tests were performed on data for the period 1932 to 2002.	44
Table 9: A statistical comparison of raw and interpolated rainfall for station 39103 (Bancroft). While the interpolated data series extends from 1889 to 2003 the Bancroft raw data only extends from 1954 to 2002. For this reason all statistical tests were performed on data for the period 1954 to 2002.	45
Table 10: A statistical comparison of raw and interpolated rainfall for station 42059 (Auburn). While the interpolated data series extends from 1889 to 2003 the Bancroft raw data only extends from 1959 to 2002. For this reason all statistical tests were performed on data for the period 1959 to 2002.	46
Table 11: A statistical comparison of raw and interpolated rainfall for station 39039 (Gayndah). While the interpolated data series extends from 1889 to 2003 the Gayndah raw data only extends from 1893 to 2002. For this reason all statistical tests were performed on data for the period 1893 to 2002.	47
Table 12: A statistical comparison of raw and interpolated rainfall for station 39036 (Eidsvold). While the interpolated data series extends from 1889 to 2003 the Eidsvold raw data only extends from 1890 to 2002. For this reason all statistical tests were performed on data for the period 1890 to 2002.	48
Table 13: A statistical comparison of raw and interpolated rainfall for station 40021 (Biggenden). While the interpolated data series extends from 1889 to 2003 the Biggenden raw data only extends from 1899 to 2002. For this reason all statistical tests were performed on data for the period 1899 to 2002.....	48
Table 14: A statistical comparison of raw and interpolated rainfall for station 40138 (Mounefonstein). While the interpolated data series extends from 1889 to 2003 the Mounefonstein raw data only extends from 1949 to 2002. For this reason all statistical tests were performed on data for the period 1949 to 2002.....	49
Table 15: A statistical comparison of raw and interpolated rainfall for station 40090 (Goomeri). While the interpolated data series extends from 1889 to 2003 the Goomer raw data only extends from 1913 to 2002. For this reason all statistical tests were performed on data for the period 1913 to 2002.	50
Table 16: A statistical comparison of raw and interpolated rainfall for station 40112 (Kingaroy). While the interpolated data series extends from 1889 to 2003 the Kingaroy raw data only extends from 1906 to 1999. For this reason all statistical tests were performed on data for the period 1906 to 1999.	51
Table 17: A statistical comparison of raw and interpolated rainfall for station 40113 (Kumbia). While the interpolated data series extends from 1889 to 2003 the Kumbia raw data only extends from 1916 to 2002. For this reason all statistical tests were performed on data for the period 1916 to 2002.	51
Table 18: A statistical comparison of raw and interpolated temperature for station 40112 (Kingaroy). While the interpolated data series extends from 1889 to 2003 the Kingaroy raw data only extends from 1957 to 2002. For this reason all statistical tests were performed on data for the period 1957 to 2002.	56

Table 19: A statistical comparison of raw and interpolated temperature for station 39057 (Kalpowar). While the interpolated data series extends from 1889 to 2003 the Kalpowar raw data only extended from 1962 to 2002. For this reason all statistical tests were performed on data for the period 1962 to 2002.....	57
Table 20: A statistical comparison of raw and interpolated temperature for station 39015 (Bundberg). While the interpolated data series extends from 1889 to 2003 the Bundaberg raw data only extended from 1892 to 2002. For this reason all statistical tests were performed on data for the period 1892 to 2002.....	58
Table 21: A statistical comparison of raw and interpolated temperature for station 39039 (Gayndah). While the interpolated data series extends from 1889 to 2003 the Bundaberg raw data only extended from 1893 to 2002. For this reason all statistical tests were performed on data for the period 1893 to 2002.....	59
Table 22: A comparison of linear trends for different periods for station 39039 (Gayndah).	70
Table 23: A comparison of linear trends for (a) annual maximum number of consecutive wet days, (b) annual wet day persistence, and (c) annual mean wet spell length for two specific time periods 1890 to 2002 and 1949 to 2002 for station 40138 (Mounefontein).	72
Table 24: A comparison of linear trends for (a) annual maximum number of consecutive wet days, and (b) annual wet day persistence for three specific time periods 1890 to 2002, 1913 to 1948 and 1979 to 2002 for station 40090 (Goomeri).	73
Table 25: A summary of linear trends for (a) 80 th percentile rainday amounts for SON, (b) 90 th percentile rainday amounts for SON (c) SON wet spell persistence, and (d) SON mean wet spell length the Kumbia rainfall station.	75
Table 26: Parameter values used in the GRASP model to simulate pasture production, run-off and deep drainage for 14 sites in the Burnett study region.	81
Table 27: Average simulated values of growth, drainage, run-off and heat stress produced by the GRASP model in response to enhanced Greenhouse gas concentrations at 2030 for the Bundaberg Station (39015). Climate Change projections from 12 different General Circulation models have been applied to the GRASP model. Average statistics are presented in the lower portion of the table.	108
Table 28: Average simulated values of growth, drainage, run-off and heat stress produced by the GRASP model in response to enhanced Greenhouse gas concentrations at 2070 for the Bundaberg Station (39015). Climate Change projections from 12 different General Circulation models have been applied to the GRASP model. Average statistics are presented in the lower portion of the table.	109
Table 29: Average simulated values of growth, drainage, run-off and heat stress produced by the GRASP model in response to enhanced Greenhouse gas concentrations at 2030 for the Gin Gin (39040). Climate Change projections from 12 different General Circulation models have been applied to the GRASP model. Average statistics are presented in the lower portion of the table.	110
Table 30: Average simulated values of growth, drainage, run-off and heat stress produced by the GRASP model in response to enhanced Greenhouse gas concentrations at 2070 for the Gin Gin (39040). Climate Change projections from 12 different General Circulation models have been applied to the GRASP model. Average statistics are presented in the lower portion of the table.	111
Table 31: Average simulated values of growth, drainage, run-off and heat stress produced by the GRASP model in response to enhanced Greenhouse gas concentrations at 2030 for the Moolboolaman (39218). Climate Change projections from 12 different General Circulation models have been applied to the GRASP model. Average statistics are presented in the lower portion of the table.	112
Table 32: Average simulated values of growth, drainage, run-off and heat stress produced by the GRASP model in response to enhanced Greenhouse gas concentrations at 2070 for the Moolboolaman (39218). Climate Change projections from 12 different General Circulation models have been applied to the GRASP model. Average statistics are presented in the lower portion of the table.	113
Table 33: Average simulated values of growth, drainage, run-off and heat stress produced by the GRASP model in response to enhanced Greenhouse gas concentrations at 2030 for the "The Cedars" (39234). Climate Change projections from 12 different General Circulation models have been applied to the GRASP model. Average statistics are presented in the lower portion of the table.	114
Table 34: Average simulated values of growth, drainage, run-off and heat stress produced by the GRASP model in response to enhanced Greenhouse gas concentrations at 2070 for the "The Cedars" (39234). Climate Change projections from 12 different General Circulation models have been applied to the GRASP model. Average statistics are presented in the lower portion of the table.	115
Table 35: Average simulated values of growth, drainage, run-off and heat stress produced by the GRASP model in response to enhanced Greenhouse gas concentrations at 2030 for the Tecoma (39248). Climate Change projections from 12 different General Circulation models have been applied to the GRASP model. Average statistics are presented in the lower portion of the table.	116
Table 36: Average simulated values of growth, drainage, run-off and heat stress produced by the GRASP model in response to enhanced Greenhouse gas concentrations at 2070 for the Tecoma (39248). Climate Change	

projections from 12 different General Circulation models have been applied to the GRASP model. Average statistics are presented in the lower portion of the table.	117
Table 37: Average simulated values of growth, drainage, run-off and heat stress produced by the GRASP model in response to enhanced Greenhouse gas concentrations at 2030 for the Kalpowar (39057). Climate Change projections from 12 different General Circulation models have been applied to the GRASP model. Average statistics are presented in the lower portion of the table.	118
Table 38: Average simulated values of growth, drainage, run-off and heat stress produced by the GRASP model in response to enhanced Greenhouse gas concentrations at 2070 for the Kalpowar (39057). Climate Change projections from 12 different General Circulation models have been applied to the GRASP model. Average statistics are presented in the lower portion of the table.	119
Table 39: Average simulated values of growth, drainage, run-off and heat stress produced by the GRASP model in response to enhanced Greenhouse gas concentrations at 2030 for the Malakof (39129). Climate Change projections from 12 different General Circulation models have been applied to the GRASP model. Average statistics are presented in the lower portion of the table.	120
Table 40: Average simulated values of growth, drainage, run-off and heat stress produced by the GRASP model in response to enhanced Greenhouse gas concentrations at 2070 for the Malakof (39129). Climate Change projections from 12 different General Circulation models have been applied to the GRASP model. Average statistics are presented in the lower portion of the table.	121
Table 41: Average simulated values of growth, drainage, run-off and heat stress produced by the GRASP model in response to enhanced Greenhouse gas concentrations at 2030 for the Bancroft (39103). Climate Change projections from 12 different General Circulation models have been applied to the GRASP model. Average statistics are presented in the lower portion of the table.	122
Table 42: Average simulated values of growth, drainage, run-off and heat stress produced by the GRASP model in response to enhanced Greenhouse gas concentrations at 2070 for the Bancroft (39103). Climate Change projections from 12 different General Circulation models have been applied to the GRASP model. Average statistics are presented in the lower portion of the table.	123
Table 43: Average simulated values of growth, drainage, run-off and heat stress produced by the GRASP model in response to enhanced Greenhouse gas concentrations at 2030 for the Auburn (42059). Climate Change projections from 12 different General Circulation models have been applied to the GRASP model. Average statistics are presented in the lower portion of the table.	124
Table 44: Average simulated values of growth, drainage, run-off and heat stress produced by the GRASP model in response to enhanced Greenhouse gas concentrations at 2070 for the Auburn (42059). Climate Change projections from 12 different General Circulation models have been applied to the GRASP model. Average statistics are presented in the lower portion of the table.	125
Table 45: Average simulated values of growth, drainage, run-off and heat stress produced by the GRASP model in response to enhanced Greenhouse gas concentrations at 2030 for the Gayndah (39039). Climate Change projections from 12 different General Circulation models have been applied to the GRASP model. Average statistics are presented in the lower portion of the table.	126
Table 46: Average simulated values of growth, drainage, run-off and heat stress produced by the GRASP model in response to enhanced Greenhouse gas concentrations at 2070 for the Gayndah (39039). Climate Change projections from 12 different General Circulation models have been applied to the GRASP model. Average statistics are presented in the lower portion of the table.	127
Table 47: Average simulated values of growth, drainage, run-off and heat stress produced by the GRASP model in response to enhanced Greenhouse gas concentrations at 2030 for the Eidsvold (39036). Climate Change projections from 12 different General Circulation models have been applied to the GRASP model. Average statistics are presented in the lower portion of the table.	128
Table 48: Average simulated values of growth, drainage, run-off and heat stress produced by the GRASP model in response to enhanced Greenhouse gas concentrations at 2070 for the Eidsvold (39036). Climate Change projections from 12 different General Circulation models have been applied to the GRASP model. Average statistics are presented in the lower portion of the table.	129
Table 49: Average simulated values of growth, drainage, run-off and heat stress produced by the GRASP model in response to enhanced Greenhouse gas concentrations at 2030 for the Biggenden (40021). Climate Change projections from 12 different General Circulation models have been applied to the GRASP model. Average statistics are presented in the lower portion of the table.	130
Table 50: Average simulated values of growth, drainage, run-off and heat stress produced by the GRASP model in response to enhanced Greenhouse gas concentrations at 2070 for the Biggenden (40021). Climate Change projections from 12 different General Circulation models have been applied to the GRASP model. Average statistics are presented in the lower portion of the table.	131
Table 51: Average simulated values of growth, drainage, run-off and heat stress produced by the GRASP model in response to enhanced Greenhouse gas concentrations at 2030 for the Mounefontein (40138). Climate Change	

projections from 12 different General Circulation models have been applied to the GRASP model. Average statistics are presented in the lower portion of the table.	132
Table 52: Average simulated values of growth, drainage, run-off and heat stress produced by the GRASP model in response to enhanced Greenhouse gas concentrations at 2070 for the Mounefontein (40138). Climate Change projections from 12 different General Circulation models have been applied to the GRASP model. Average statistics are presented in the lower portion of the table.	133
Table 53: Average simulated values of growth, drainage, run-off and heat stress produced by the GRASP model in response to enhanced Greenhouse gas concentrations at 2030 for the Goomeri (40090). Climate Change projections from 12 different General Circulation models have been applied to the GRASP model. Average statistics are presented in the lower portion of the table.	134
Table 54: Average simulated values of growth, drainage, run-off and heat stress produced by the GRASP model in response to enhanced Greenhouse gas concentrations at 2070 for the Goomeri (40090). Climate Change projections from 12 different General Circulation models have been applied to the GRASP model. Average statistics are presented in the lower portion of the table.	135
Table 55: Average simulated values of growth, drainage, run-off and heat stress produced by the GRASP model in response to enhanced Greenhouse gas concentrations at 2030 for the Kingaroy (40112). Climate Change projections from 12 different General Circulation models have been applied to the GRASP model. Average statistics are presented in the lower portion of the table.	136
Table 56: Average simulated values of growth, drainage, run-off and heat stress produced by the GRASP model in response to enhanced Greenhouse gas concentrations at 2070 for the Kingaroy (40112). Climate Change projections from 12 different General Circulation models have been applied to the GRASP model. Average statistics are presented in the lower portion of the table.	137
Table 57: Average simulated values of growth, drainage, run-off and heat stress produced by the GRASP model in response to enhanced Greenhouse gas concentrations at 2030 for the Kumbia (40113). Climate Change projections from 12 different General Circulation models have been applied to the GRASP model. Average statistics are presented in the lower portion of the table.	138
Table 58: Average simulated values of growth, drainage, run-off and heat stress produced by the GRASP model in response to enhanced Greenhouse gas concentrations at 2070 for the Kumbia (40113). Climate Change projections from 12 different General Circulation models have been applied to the GRASP model. Average statistics are presented in the lower portion of the table.	139

Background

1. Study region

The study region encompasses several catchments, two bioregions and a wide variety of urban and rural land use types. The coastal plains and ranges of the study region comprise the northern half of the South East Queensland bioregion while the drier western portion of the study region lies within the eastern most portion of the Brigalow bioregion. The study area has been sub-divided into four sub-regions namely North, Central, South and East. These sub-divisions are in-keeping with boundaries set in the 2000 Burnett Catchment Strategy (Figure 1).

On average the study region experiences a sub-tropical climate and receives mainly summer rainfall (70:30). The coastal areas receive a mean rainfall, of approximately 1200mm per year, while the western, northern and southern areas receive approximately 650mm, 750mm and 800mm respectively (Figure 2).

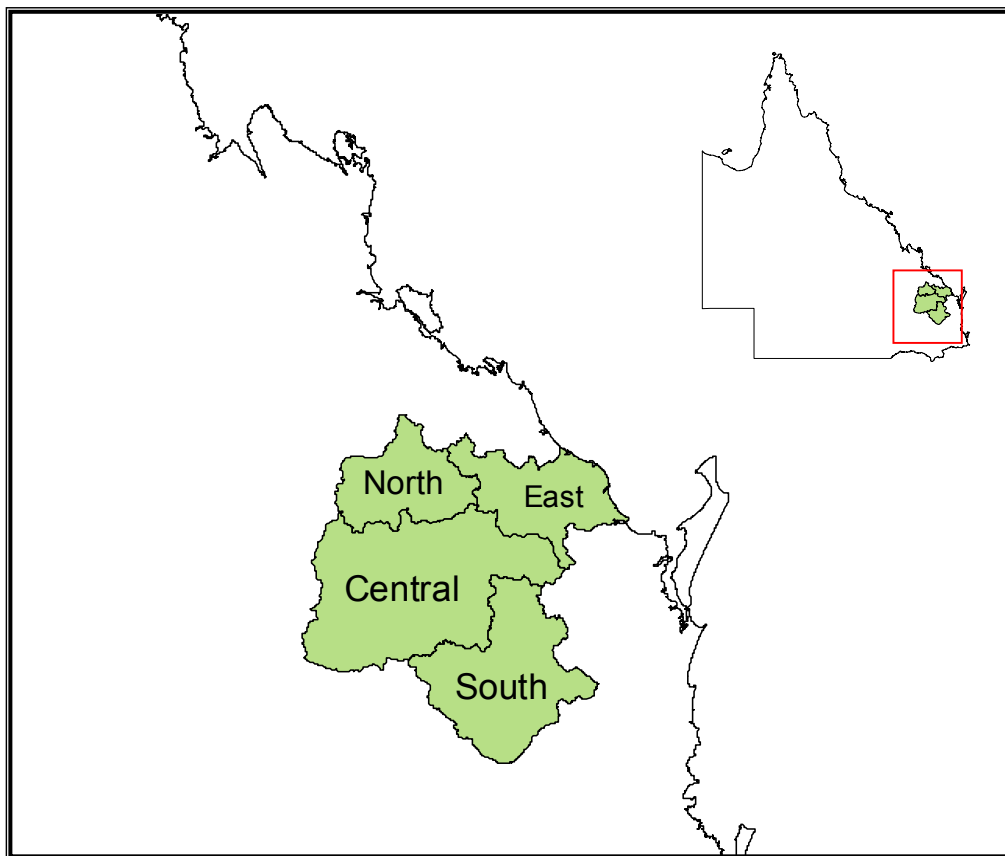


Figure 1: A locality map of the Burnett study area.

Summer rainfall is produced primarily by convective activity in the western inland region, while the coastal areas receive rain from convective activity, monsoonal troughs and tropical cyclones. In winter, rainfall is limited to the South and East sub-regions, although infrequent northwest cloud band activity can produce rain across the majority of the region. In the south the passage of cold fronts produces winter rains whereas in the eastern coastal areas the development of cut-off lows can result in significant winter rainfall (although infrequent).

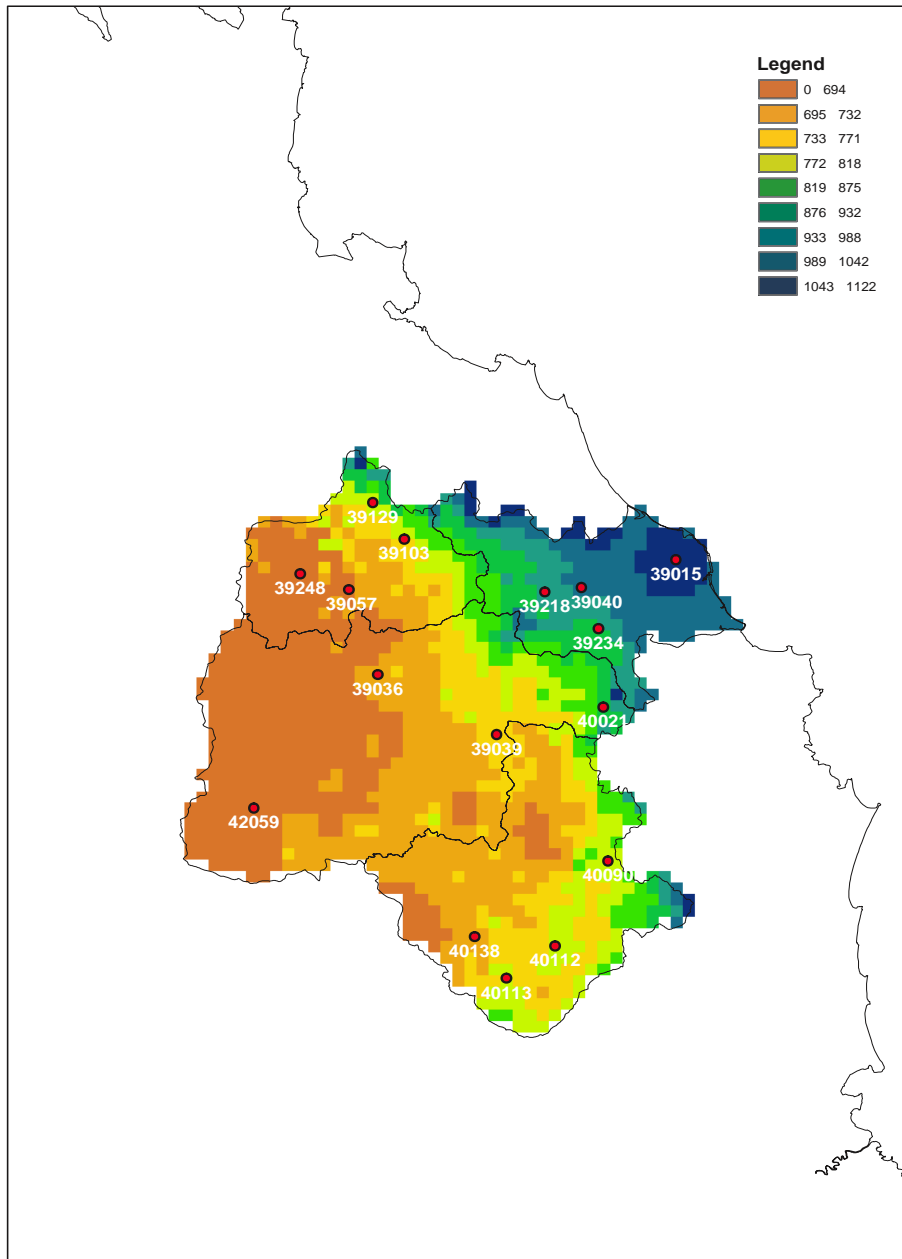


Figure 2: A locality map of the Burnett study region showing long-term average annual rainfall (April to March) for the period 1889 to 2002 and selected climate stations for all four sub-regions.

The principal land use patterns in the study area include grazing (54%), agriculture and other rural use (e.g. intensive livestock production) (21.7%), forestry (18.1%), residential (5%) and National Parks (1.2%) (WBM Oceanics Australia, 1998).

2. Climate station selection and data integrity

The Burnett study region currently contains 241 rainfall stations with only five active stations recording maximum and minimum temperatures.

The under-representation of temperature recording stations is not an issue relevant only to the Burnett Study region but is common to the whole country. "Temperature has always been something of a poor relation in Australian climatology. Rainfall has, historically, been the major

priority in the climatological observing network. This is a natural response to Australia's climate, in which rainfall and its variability have been a critical limiting factor for agriculture, with temperature being of secondary importance (Trewin, 2001:35)"

The greatest difficulty confronting this study was ensuring that the stations chosen were of adequate length and continuity. In order to ensure this occurred two broad approaches were adopted, the first approach was to use data from all stations that met specified criteria of length and completeness of record, and adjust them if necessary to correct for inhomogeneities (Torok, 1996a,b; Torok *et al.*, 2001; Trewin, 2001). The second approach was to use a subset of the data selected on the basis of spatial representativeness, data quality or both. Torok (1996), in his study of long-term Australian temperature data, took the former approach, on the grounds that there were insufficient long-term temperature data available to select only the high-quality stations.

In contrast, Lavery *et al.* (1992), in their study of Australian rainfall trends, had the luxury of being able to be selective over a number of regions with a large number of available records, and use only the highest-quality records from those regions. In this study a station network has been established for the Burnett study region using a combination of both approaches. The station network has been established from a range of baseline climate station data, namely:

- The Torok network of pre-1910 Australian 224 temperature stations;
- The "*Computerising the Australian Climate Archive*" (CLIMARC) network of climate stations;
- The Trewin 2001 station network; and
- The RAINMAN climate station network.

Rainfall stations were selected from these baseline stations based on a number of criteria. These were:

- a. length of record - all rainfall stations chosen had to contain at least 65 years worth of daily rainfall data;
- b. record continuity – all rainfall stations chosen had to contain at least 40 years worth of continuous daily data (Table 1a), and
- c. representativeness – rainfall stations chosen were to provide equivalent representation of both high and low average rainfall conditions within each sub-region identified. This was determined through the spatial interpolation of long-term (1880 to 2002) average annual (April to March) rainfall across the study region (Figure 2).

Baseline temperature recording stations were very sparsely located in the study region limited to only Gayndah and Bundaberg. These stations formed part of both the Torok, CLIMARC and Trewin 2001 baseline datasets. Additional temperature recording stations were chosen for both the North and South sub regions based on most comprehensive record length (Table 1a). Four (4) rainfall stations were selected for each sub-region (Figure 2) across a low to high annual rainfall gradient. In the East sub-region "Bundaberg", "Gin Gin", "Moolboolaman" and "The Cedars" (39015, 39040, 39218, 39234) rainfall stations were selected, with "Bundaberg" representing the area of high rainfall occurrence and "Moolboolaman" representing the area of low rainfall occurrence.

The stations selected for the North sub-region included “Malakof” (39129 - representing the area of high rainfall occurrence), “Bancroft” (39103), “Kalpowar” (39057) and “Tecoma” (39248 – representing the area of low rainfall occurrence). Similarly, in the Central sub-region the rainfall stations selected where:

- “Biggenden” – 40021 (high rainfall occurrence),
- “Gayndah” - 39039,
- “Eidsvold” - 39036, and
- “Auburn” – 42059 (low rainfall occurrence).

The South sub-region included the “Goomeri” (40090), “Kingaroy” (40112), “Kumbia” (40113), and “Mounefontein” (40138) rainfall stations. In this sub-region, “Goomeri” was chosen to represent the area of high rainfall occurrence while “Mounefontein” was chosen to represent the area of low rainfall occurrence.

3. Trend analysis methodology

Trend detection and estimation was undertaken using both simple linear regression (Chock *et al.*, 1982; Kumar and Chock, 1984; Wackter and Bayly, 1987) and more complex statistical analyses such as Kendall's tau test (Hirsch *et al.*, 1982; Hirsch and Slack, 1984; Freas and Sieurin, 1977). In the case of the simple linear regression method, the trend was approximated using least squares fitting techniques (which is defined as finding the straight line such that the squared errors about that line are minimised). This method is most appropriate when the annual summary statistics are normally distributed with a constant variance and was applied to the annual and seasonal time series data.

When analysing the monthly and daily data (reserved for the interpolated data only) the assumption of independent normally distributed errors with the same constant variance was not acceptable. Thus, in order to test for and/or estimate the trend without making such distributional assumptions, a nonparametric method was used. The Kendall's tau test was selected as it represents a nonparametric statistic that can be used to test for trends in monthly and daily climate data (Hirsch *et al.*, 1982). A seasonally adjusted Kendall's tau (Hirsch *et al.*, 1982) allows for different annual means and trends in different calendar months by adding up the 12 Kendall's tau statistics from each month. The Kendall's tau test therefore provided a more robust method of trend analysis resulting from its independent test for significance.

In the case of daily and monthly analysis of the interpolated station data, an additional four climate stations were included. These stations were included primarily to assist in the assessment of daily and monthly rainfall trends, however the Monto (39104) station was included to further substantiate the analysis of maximum and minimum temperature trends (Table 1b).

Table1a: An analysis of record length and continuity for each of the stations used for this project. Continuity is expressed as the occurrence of daily data in each decade from 1880 to 2003.

Station No.	Station Name	Type	Record of daily data for each decade												
			1880s	1890s	1900s	1910s	1920s	1930s	1940s	1950s	1960s	1970s	1980s	1990s	2000s
39015	BUNDABERG (PO)	Rain	1067	3652	3652	3652	3653	3652	3653	3652	3653	3652	3652	181	0
39015	BUNDABERG (PO)	Tmax	0	2794	3645	3646	3649	3651	3649	3650	3646	3621	3621	178	0
39015	BUNDABERG (PO)	Tmin	0	2799	3648	3643	3595	3648	3646	3647	3643	3584	3603	178	0
39036	EIDSVOLD (PO)	Rain	0	3621	3651	3652	3653	3652	3651	3646	3633	3546	3328	3382	1276
39039	GAYNDAH (PO)	Rain	1003	1341	1522	3652	3653	3652	3653	3652	3653	3652	3653	3627	1337
39039	GAYNDAH (PO)	Tmax	0	2302	3431	3624	3633	3648	3653	3652	3646	3652	3644	3651	1332
39039	GAYNDAH (PO)	Tmin	0	2303	3432	3639	3641	3649	3648	3647	3647	3652	3646	3649	1337
39040	GIN GIN (PO)	Rain	0	488	3625	3652	3653	3652	3646	3641	3642	3555	3203	3571	1268
39103	BANCROFT	Rain	0	0	0	0	0	243	397	2221	1552	3629	3650	3619	1308
39129	MALAKOFF	Rain	0	0	0	0	0	1582	1401	1126	3653	3647	3653	3593	1280
39218	MOOLBOOLAMAN	Rain	0	0	0	61	31	1096	1093	852	2284	2257	3013	3621	1306
39234	THE CEDARS	Rain	0	0	0	2678	3530	3409	2861	3132	3651	3646	3645	2523	1308
40021	BIGGENDEN (PO)	Rain	0	444	3652	3559	3653	3651	3648	3645	3635	3470	3282	3544	949
40090	GOOMERI (PO)	Rain	0	0	0	2537	3653	3650	3650	3644	3648	3471	3295	3344	1282
40112	KINGAROY	Rain	0	0	1512	3652	3653	3652	3653	3652	3653	3647	3653	3621	397
40112	KINGAROY	Tmax	0	0	0	0	0	0	0	1092	3644	3558	3640	3631	349
40112	KINGAROY	Tmin	0	0	0	0	0	0	0	1092	3650	3612	3649	3622	350
40113	KUMBIA PO	Rain	0	0	0	1063	1797	3440	3653	3622	3622	3642	3638	3586	1276
40138	MOUNEFONTEIN	Rain	0	0	0	304	397	334	610	3619	3653	3652	3644	3621	1276
39057	KALPOWAR (F)	Rain	0	0	0	0	0	2586	3653	3436	3649	3484	3426	2983	1261
39057	KALPOWAR (F)	Tmax	0	0	0	0	0	0	0	0	2827	1833	2112	0	0
39057	KALPOWAR (F)	Tmin	0	0	0	0	0	0	0	0	2824	1803	2214	0	0
39248	TECOMA	Rain	0	0	0	0	0	120	516	2466	3653	3650	3651	3254	861
42059	AUBURN	Rain	305	0	610	0	216	122	214	609	1643	3470	3572	3604	1146

Table1b: An analysis of record length and continuity for additional stations used in the analysis of daily and month rainfall and temperature trends. Continuity is expressed as the occurrence of daily data in each decade from 1880 to 2003.

Station No.	Station Name	Type	Record of daily data for each decade												
			1880s	1890s	1900s	1910s	1920s	1930s	1940s	1950s	1960s	1970s	1980s	1990s	2000s
39045	GOODNIGHT SCRUB Res 169	Rain	0	0	0	0	0	1584	3653	3480	3285	3551	3478	179	0
39093	WALLAVILLE- MILL St	Rain	0	0	0	2497	3651	3651	3649	3651	3653	3624	3441	3487	1532
39104	MONTO	Rain	0	0	0	0	0	3648	3651	3649	3653	3652	3653	1286	0
39104	MONTO	TMax	0	0	0	0	0	0	0	0	2911	3602	3644	1283	0
39104	MONTO	TMin	0	0	0	0	0	0	0	0	2911	3637	3650	1284	0
40086	GOODGER	Rain	0	0	0	0	2101	3530	3653	3621	3652	3650	3652	2158	350

4. Climate Indices

A simple linear regression analysis was performed on the raw rainfall and temperature data for each of the 16 stations within the Burnett study region. The analyses was repeated on the interpolated data and compared against the raw data to examine differences in trend introduced by the interpolation techniques. The interpolated data was acquired from the SILO climate database (SILO) developed and managed by the Queensland Department of Natural Resources, Mines and Energy.

The SILO database was constructed using observational data collected by the Australian Bureau of Meteorology (Jeffery *et al.*, 2001). The database contains both continuous daily climate records at approximately 4600 locations and interpolated daily climate surfaces across Australia.

The observed climate data at each of the 4600 recording stations in Australia is used in conjunction with interpolated daily climate surfaces and long-term climate surface to produce a continuous daily climate record for each station. Climate records constructed in this manner will be defined as interpolated datasets for the remainder of this report. The interpolated data includes continuous daily time step records of rainfall, maximum and minimum temperature, Class A pan evaporation, solar radiation and vapour pressure for the time period 1 January 1890 till the present (Jeffery *et al.*, 2001; Rayner *et al.*, 2004).

The interpolated climate surfaces are generated using the observed network of recording stations. A thin plate smoothing spline was used to interpolate daily climate variables, other than rainfall, with ordinary kriging and normalisation used to interpolate daily and monthly rainfall (Hutchinson, 1993a; Hutchinson *et al.*, 1993b; Hutchinson *et al.*, 1995; Jeffery *et al.*, 2001). Further details regarding errors, cross validation and production of climate surfaces and patched station data can be obtained from Jeffery *et al.* (2001) and Rayner *et al.* (2004).

The interpolated data was analysed using the software (Statistical and Regional Dynamic Downscaling of Extremes - STARDEX), developed by the US National Climatic Data Centre (NCDC). The software was modified for the purposes of this project in order to expand the trend analysis to calculated climate indices. The most recent version of the software (Version 3.3.0) calculates 57 daily climate indices from both maximum and minimum temperature and rainfall. The daily indices include a range of calculated values such as mean diurnal temperature range, 10th percentile diurnal temperature range, 90th percentile diurnal temperature, mean climatological precipitation (mm/day), mean wet-day persistence and mean dry-day persistence. A more comprehensive list of calculated variables can be found in Appendix A.

Raw Climate Data Analyses

1. Rainfall

The raw data from each of the 16 rainfall stations and 4 temperature stations was analysed using a simple linear regression technique. The annual rainfall time series data exhibited a large degree of variability from site to site, with the linear trends ranging from positive to negative within, as well as across, each sub-region. The four stations within the East sub-region were a=39015 (Bundaberg), b=39040 (Gin Gin), c=39218 (Moolboolaman), d=39234 (The Cedars). Station (a) possessed a relatively long record of rainfall data from 1885 to 2003. The linear trend analysis for this station revealed a positive trend in total annual rainfall, although the trend was not considered statistically significant ($P < 0.05$) (Figure 3a). The three other stations in this region exhibited declining trends in annual rainfall, but each trend explained on average less than 2% of the total annual variability (Figure 3b to d).

The North sub-region was represented by four rainfall stations, namely a= 39248 (Tecoma), b=39057 (Kalpowar), c=39129 (Malakof) and d=39103 (Bancroft). The record length of these stations was shorter than for stations in the East sub-region, with the longest record length only 70 years (station b) (Figure 4b). Three of the four stations (a, b and c) exhibited strong declines in annual rainfall over the period 1930 to 2003 (Figure 4). In each case the station trends were considered statistically significant at the $P \approx 0.01$ level and $P \approx 0.05$ level for stations (a), (b) and (c) respectively. In the case of station (d) the annual rainfall trend exhibited an increase of approximately 27mm per decade, however this was not statistically significant at the 95% confidence interval (Figure 4).

The Central sub-region was represented by four rainfall stations, namely a=42059 (Auburn), b=39039 (Gayndah), c=39036 (Eidsvold) and d=40021 (Biggenden). The stations in this sub-region exhibited relatively long records with little missing data, with the exception of Auburn (45 year rainfall record). Stations (b), (c) and (d) exhibited similar record lengths, however stations (b) and (c) demonstrated a drying trend whilst station (d) revealed an increasing trend in annual rainfall (Figure 5). This highlighted the regional nature of the rainfall trends and substantiates the call for greater spatial resolution of future rainfall change scenarios.

The drying trends exhibited by stations (b) and (c) were both not statistically significant at the 95% confidence interval, as were the positive rainfall trends shown in stations (a) and (d).

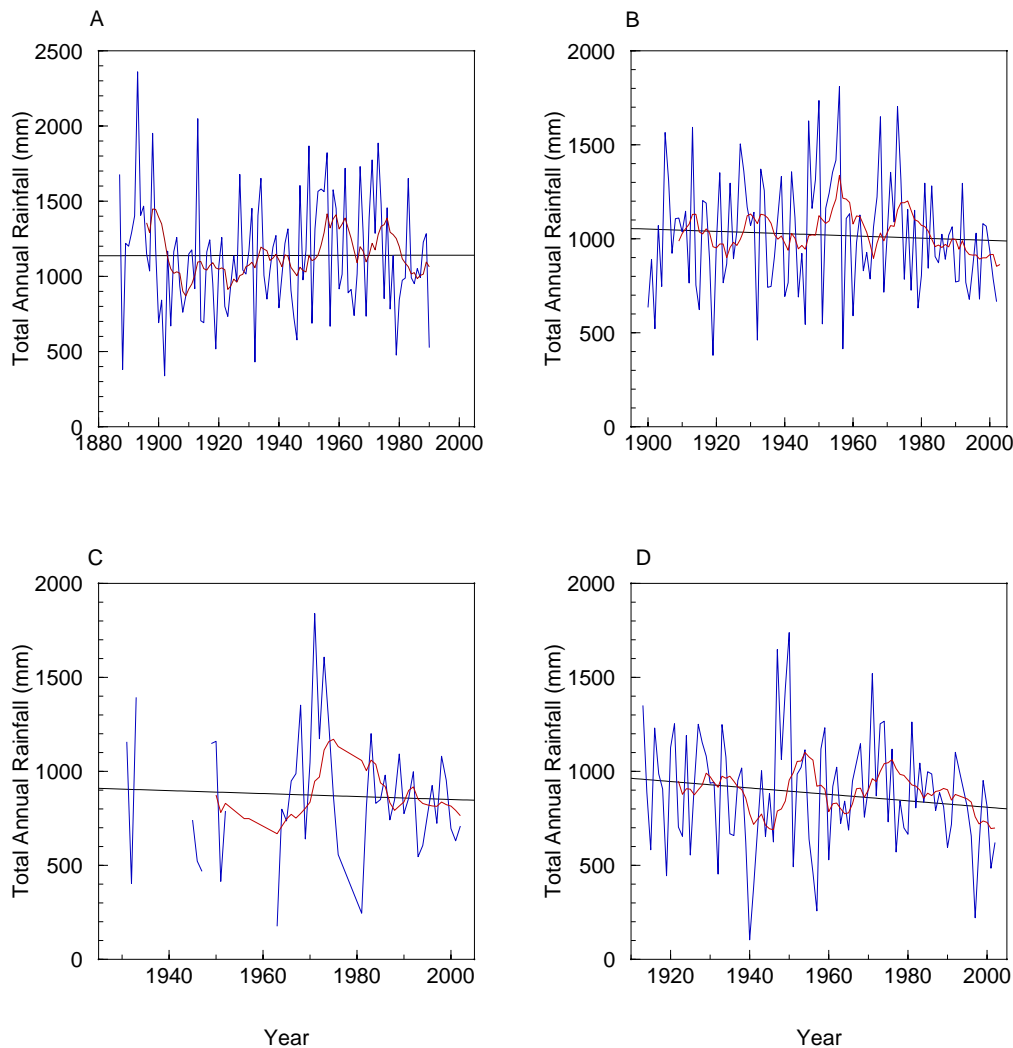


Figure 3: A rainfall time series for a) “Bundaberg”, b) “Gin Gin”, c) “Moolboolaman” and d) “The Cedars” stations within the East sub-region. The linear trends were as follows a) Trend = $0.0292x + 1082.1$ $r^2 = 0.000005$, b) Trend = $-0.6028x + 2196.4$ $r^2 = 0.0035$, c) Trend = $-0.7881x + 2426.1$ $r^2 = 0.0023$ and d) Trend = $-1.7098x + 4228.3$ $r^2 = 0.021$. The smoothed red line represents the 10 year moving average of rainfall.

The four rainfall stations in the South sub-region were: (a) 40138 (Mounefontein), (b) 40090 (Goomeri), (c) 40112 (Kingaroy) and (d) 40113 (Kumbia). As with the other sub-regions the rainfall trends were not consistent between stations. Stations (a) and (b) demonstrated a drying trend (only (a) was statistically significant at the 0.05 level), while stations (c) and (d) revealed positive trends (Figure 6).

A greater consistency in rainfall trends was obtained when partitioning annual rainfall into its seasonal components. In the South sub-region three of the four stations (a, b and d) revealed drying trends in summer rainfall (September to March), while only the “Kingaroy” station demonstrated a non-significant positive trend (not shown). Similarly in winter all stations, except for (“Mounefontein”) revealed positive rainfall trends (not shown). The results of this preliminary analysis would suggest that more meaningful information could be obtained from an analysis of

seasonal and perhaps even daily rainfall variables, however the amount of missing data in the raw climate files made a comprehensive analysis of the raw data not viable.

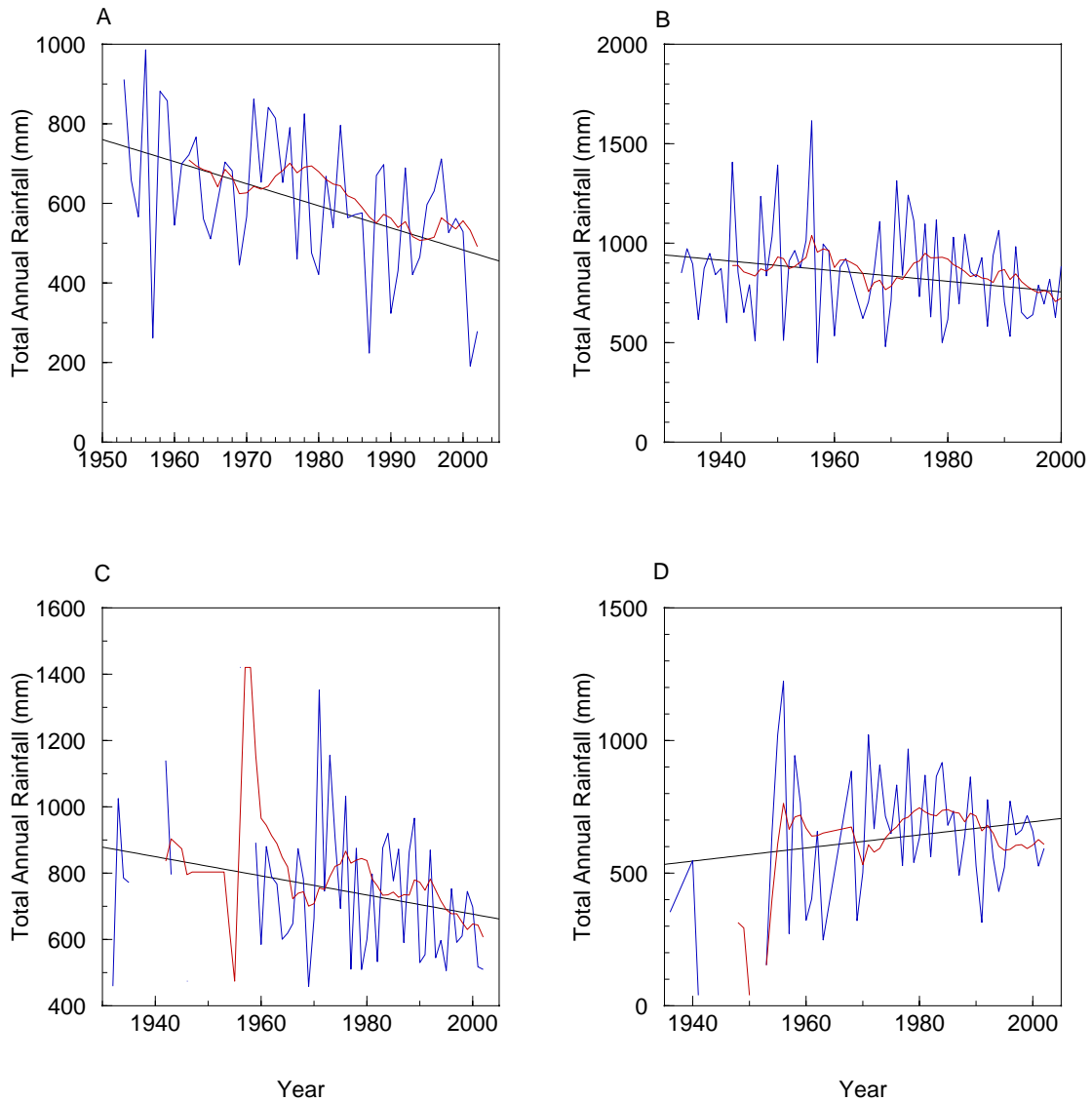


Figure 4: A rainfall time series for a) “Tecoma”, b) “Kalpowar”, c) “Malakof” and d) “Bancroft” stations within the North sub-region. The linear trends were as follows a) Trend = $-5.5504x + 11584.1$ $r^2 = 0.1989$, b) Trend = $-2.6541x + 6063.1$ $r^2 = 0.0487$, c) Trend = $-2.8897x + 6455.5$ $r^2 = 0.0638$ and d) Trend = $2.4682x + 4243.2$ $r^2 = 0.0308$. The smoothed red line represents the 10 year moving average of rainfall.

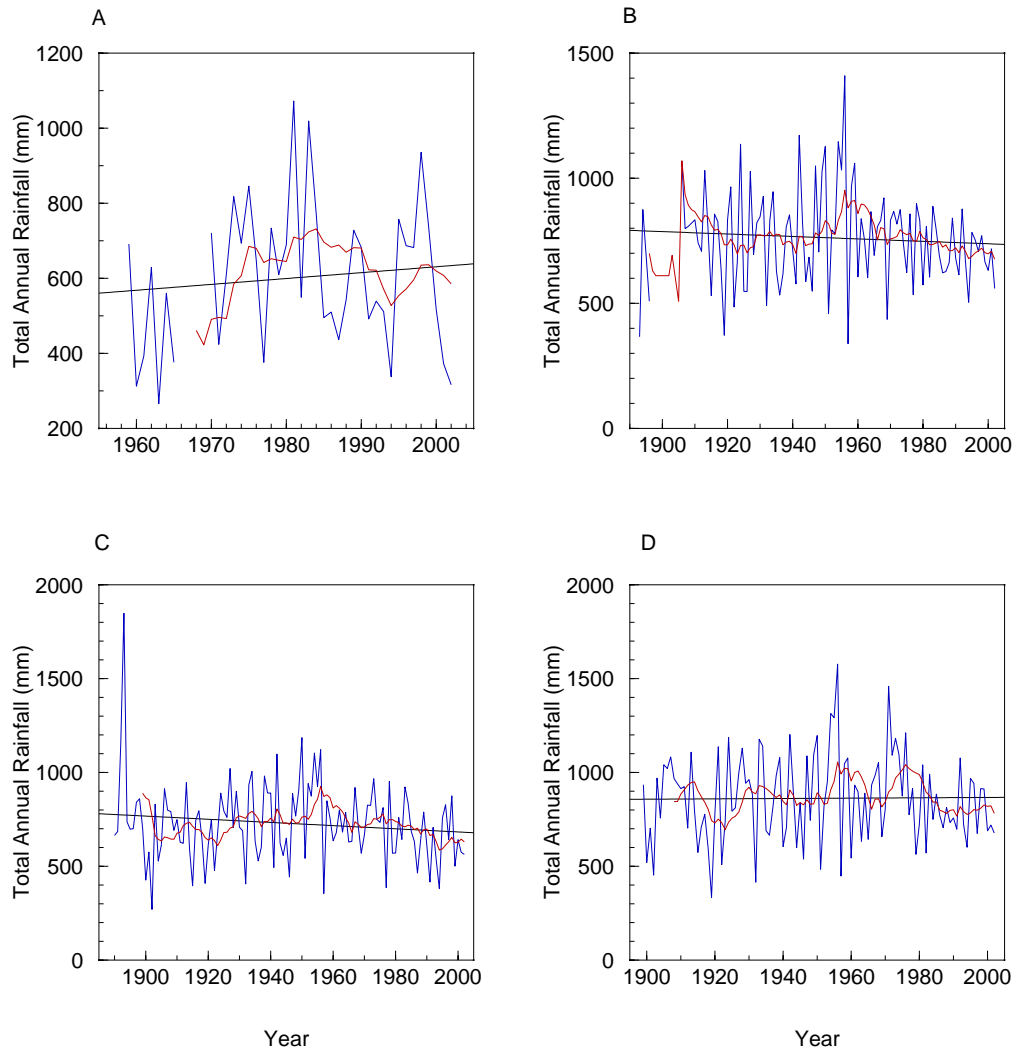


Figure 5: A rainfall time series for a) “Auburn”, b) “Gayndah”, c) “Eidsvold” and d) “Biggenden” stations within the Central sub-region. The linear trends were as follows a) Trend = $1.5635x + 2496.6$ $r^2 = 0.0108$, b) Trend = $-0.486x + 1710.9$ $r^2 = 0.0062$, c) Trend = $-0.8452x + 2373$ $r^2 = 0.0172$ and d) Trend = $0.0934x + 679.55$ $r^2 = 0.0001$. The smoothed red line represents the 10 year moving average of rainfall.

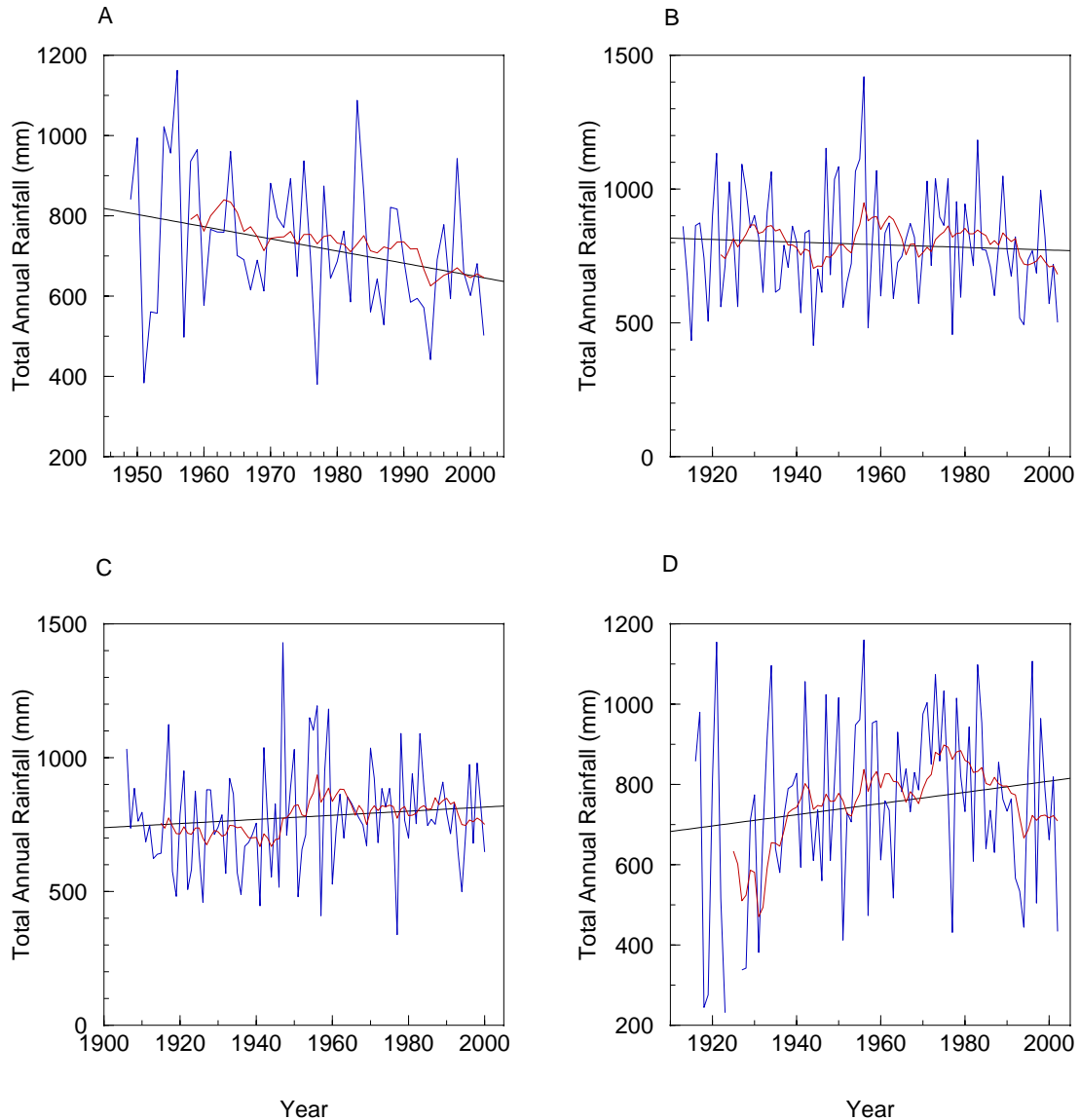


Figure 6: A rainfall time series for a) “Mounefonstein”, b) “Goomeri”, c) “Kingaroy” and d) “Kumbia” stations within the South sub-region. The linear trends were as follows a) Trend = $-3.0358x + 6723.6$ $r^2 = 0.073$, b) Trend = $-0.4919x + 1755.7$ $r^2 = 0.0043$, c) Trend = $0.7694x + 723.71$ $r^2 = 0.0122$ and d) Trend = $1.3942x + 1980.4$ $r^2 = 0.0249$. The smoothed red line represents the 10 year moving average of rainfall.

2. Temperature

Temperature trend analyses were performed on a single temperature recording station in each of the four sub-regions. The South sub-region was represented by station 40112 (Kingaroy - a), the North sub-region by station 39057 (Kalpowar - b), the East sub-region by station 39015 (Bundaberg - c) and the Central sub-region by station 39039 (Gayndah - d). Both the South and North temperature stations had limited records (1957 to 2000 and 1962 to 1989 respectively), while the Central and East had records extending over 99 and 110 years respectively.

A trend analysis was performed on the time series of average maximum and minimum temperatures (Figures 7 and 8), as well as the highest annual maximum daily temperature (Figure 9) and lowest annual minimum daily temperature (Figure 10).

The linear regression analysis of average maximum temperature (Figure 7) revealed that in the South (a) and Central regions (d) average annual maximum temperatures have increased (not statistically significant i.e. $P < 0.05$), while in the North (b) and East (c) regions average annual maximum temperatures have decreased (statistically significant $P \approx 0.001$, $P \approx 0.01$).

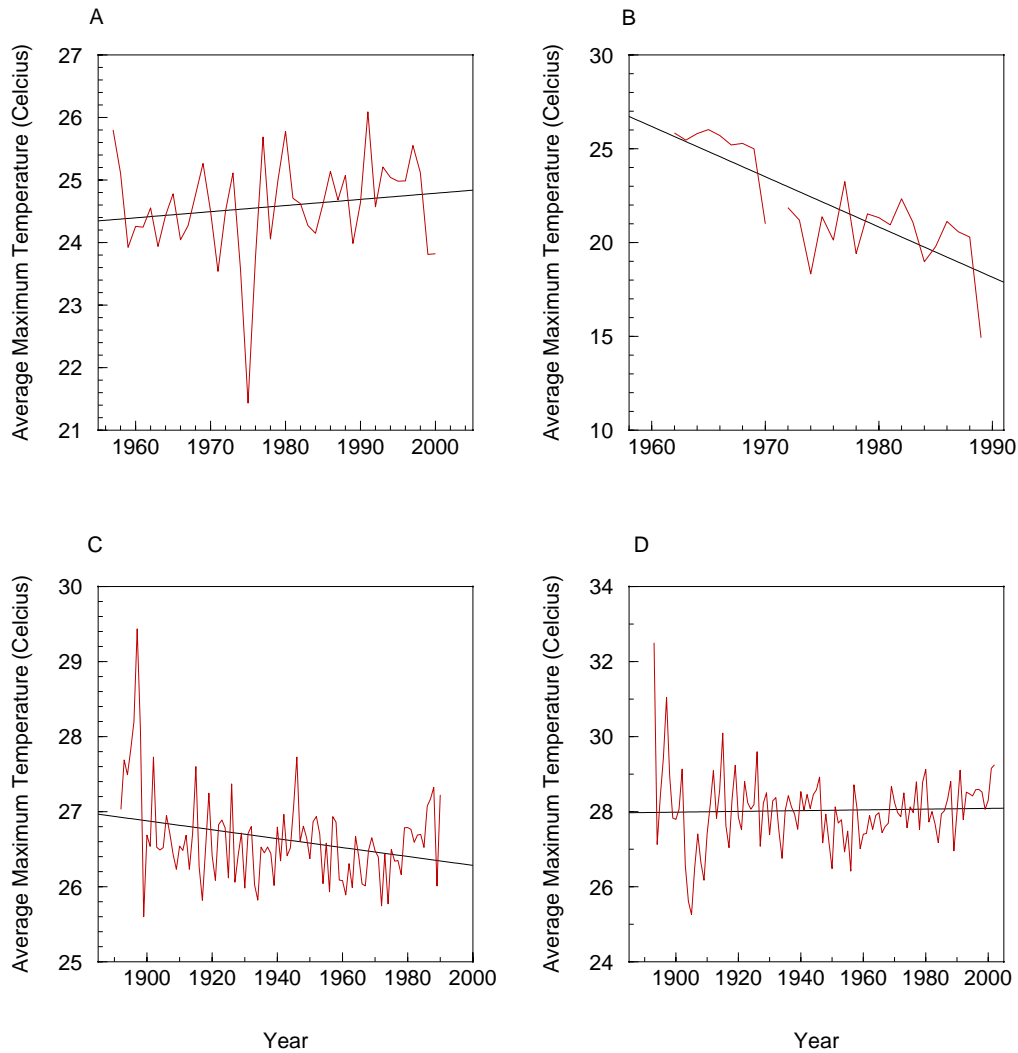


Figure 7: A time series of average annual maximum temperature for a) the South sub-region (40112 - Kingaroy), b) the North sub-region (39057 - Kalpowar), c) the East sub-region (39015 - Bundaberg) and d) the Central sub-region (39039 - Gayndah). The linear trends were as follows a) Trend = $0.0098x + 5.1456$ $r^2 = 0.0256$, b) Trend = $-0.2677x + 550.95$ $r^2 = 0.6442$, c) Trend = $-0.0059x + 38.153$ $r^2 = 0.0847$ and d) Trend = $0.001x + 26.068$ $r^2 = 0.0011$.

In the case of average annual minimum temperatures all sub-regions except for the North demonstrated statistically significant warming trends (Figure 8), that accounted for 31%, 28% and 42% of the total variability demonstrated by the South, East and Central sub-regions respectively. Given the paucity of data for the Kalpowar site (representing the North sub-region), the declining trends in both maximum and minimum temperatures were not considered robust enough to be considered.

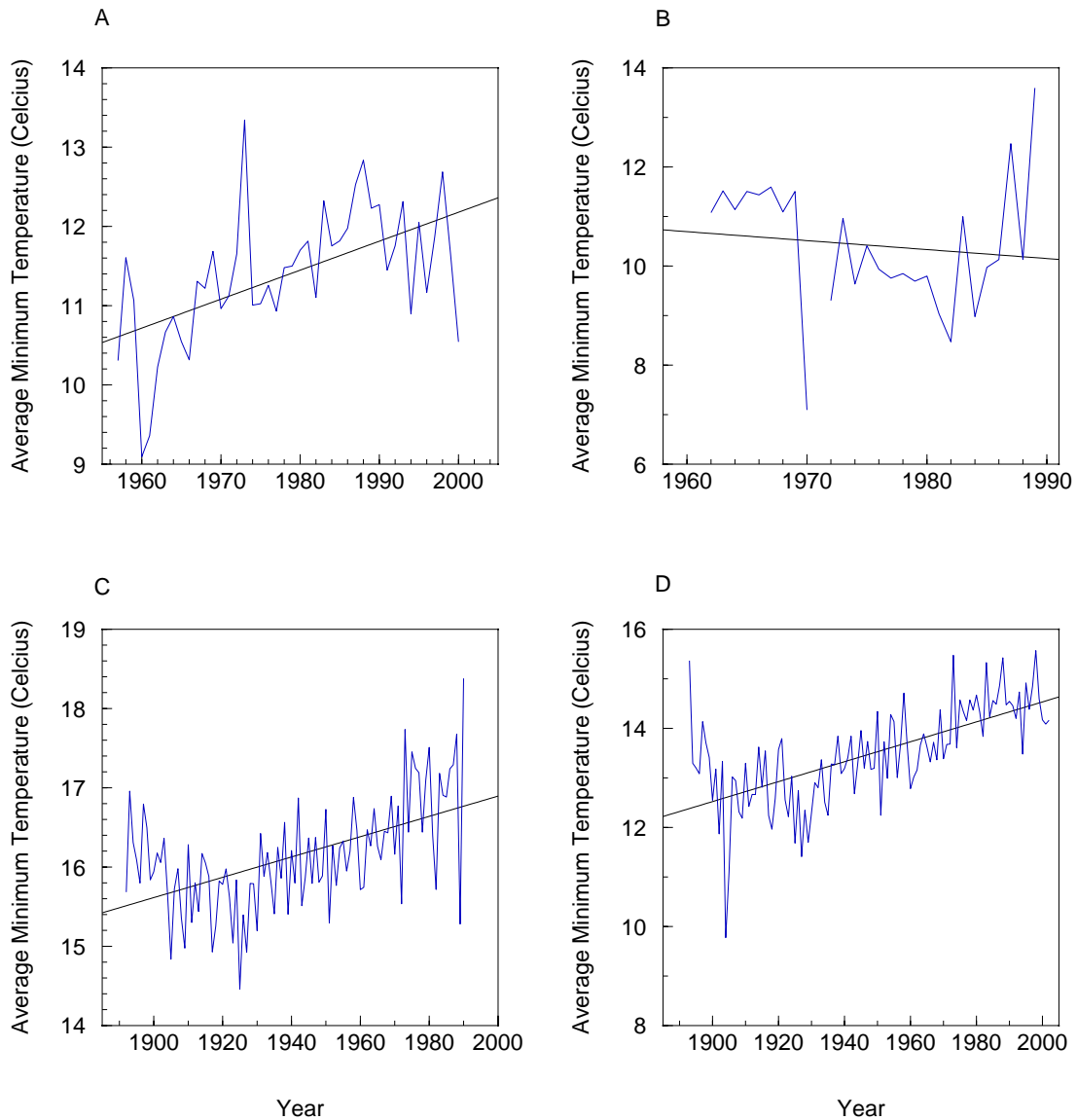


Figure 8: A time series of average annual minimum temperature for a) the South sub-region (40112 - Kingaroy), b) the North sub-region (39057 - Kalpowar), c) the East sub-region (39015 - Bundaberg) and d) the Central sub-region (39039 – Gayndah). The linear trends were as follows a) Trend = $0.0365x - 60.896$ $r^2 = 0.3086$, b) Trend = $-0.0181x + 46.139$ $r^2 = 0.013$, c) Trend = $0.0128x - 8.7306$ $r^2 = 0.2798$ and d) Trend = $0.0201x - 25.701$ $r^2 = 0.4194$.

A trend analysis of the highest annual maximum temperatures revealed that all sub-regions except for the South experienced a downward trend in highest maximum temperatures (Figure 9). The reason for this is unclear but may be revealed through further analyses.

Contrary to the trends exhibited by each sub-region for highest annual maximum temperature, lowest minimum temperatures show greater consistency with the majority stations exhibiting warming (except in the eastern sub-region) (Figure 10). This result is not surprising given the consistent warming trend in average minimum temperatures (Figure 8).

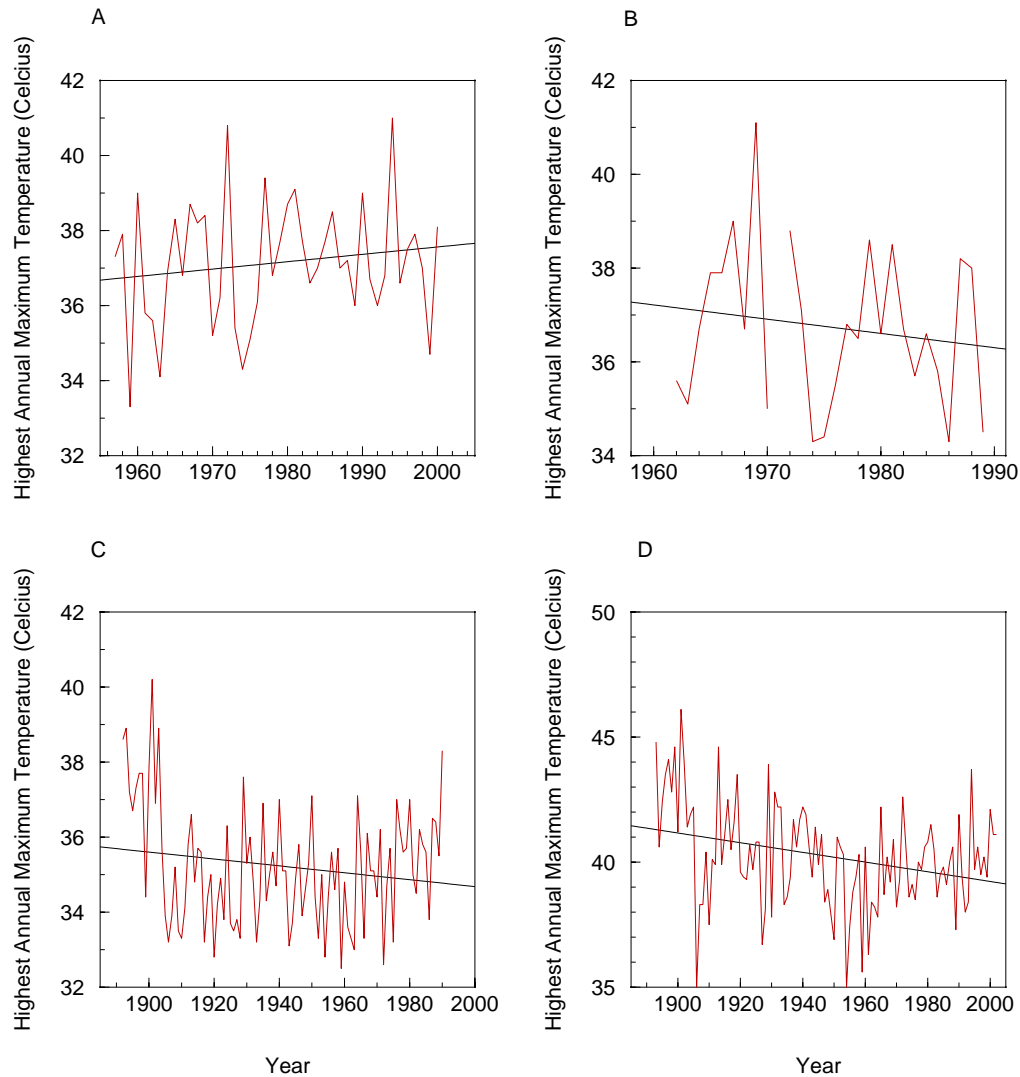


Figure 9: A time series of highest annual maximum temperature for a) the South sub-region (40112 - Kingaroy), b) the North sub-region (39057 - Kalpowar), c) the East sub-region (39015 - Bundaberg) and d) the Central sub-region (39039 - Gayndah). The linear trends were as follows a) Trend = $0.0196x - 1.7203$ $r^2 = 0.0234$, b) Trend = $-0.0304x + 96.758$ $r^2 = 0.0224$, c) Trend = $-0.0092x + 53.074$ $r^2 = 0.0275$ and d) Trend = $-0.0194x + 77.974$ $r^2 = 0.0881$.

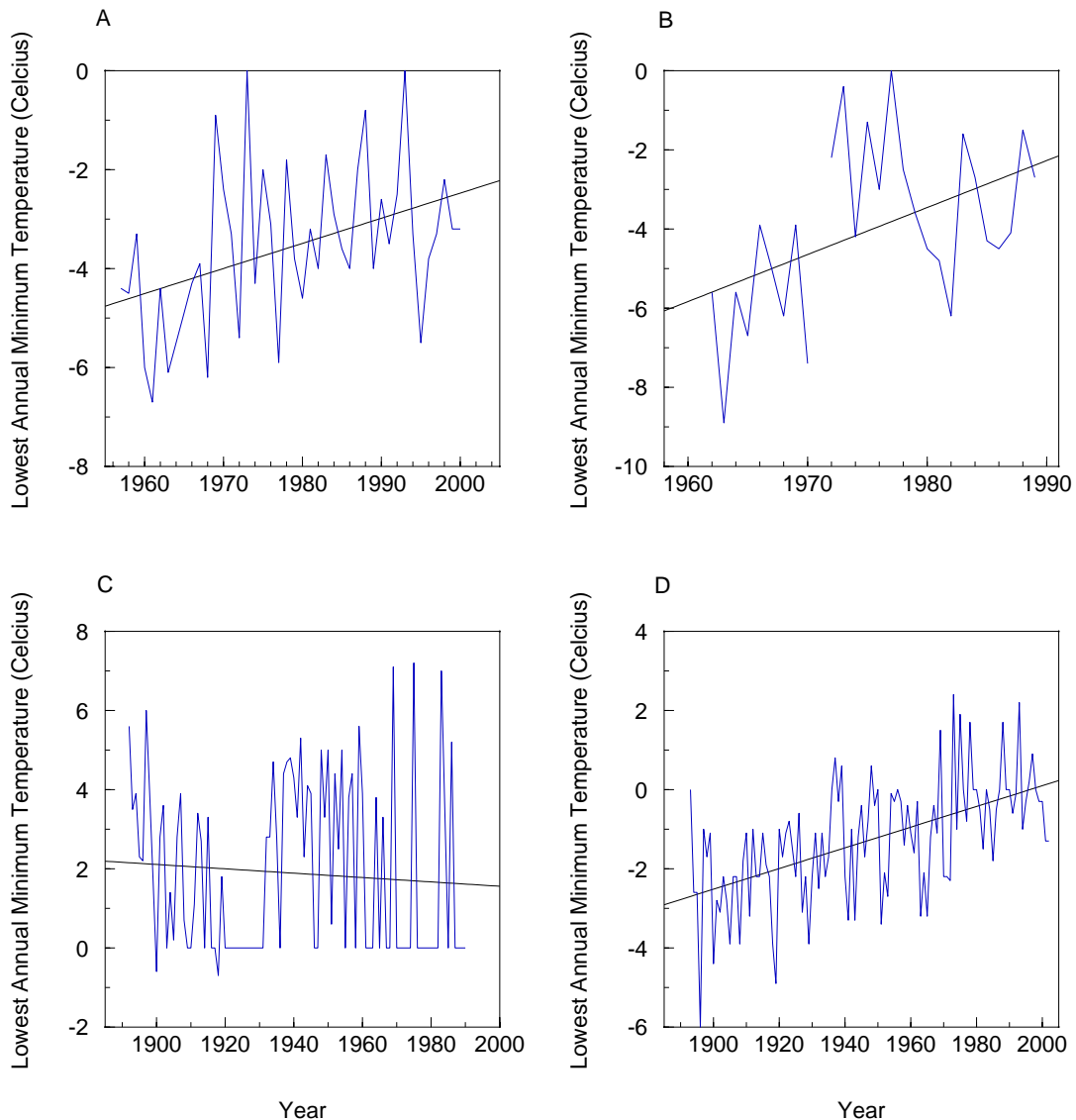


Figure 10: A time series of lowest annual minimum temperature for a) the South sub-region (40112 - Kingaroy), b) the North sub-region (39057 - Kalpowar), c) the East sub-region (39015 - Bundaberg) and d) the Central sub-region (39039 - Gayndah). The linear trends were as follows a) Trend = $0.0508x - 104.04$ $r^2 = 0.1653$, b) Trend = $0.1188x - 238.66$ $r^2 = 0.2155$, c) Trend = $-0.0055x + 12.58$ $r^2 = 0.0053$ and d) Trend = $0.0261x - 52.196$ $r^2 = 0.3085$.

3. Summary of Raw Climate Data Trends

The analysis of raw rainfall and temperature data has revealed a number of important issues regarding climate trends in the Burnett Study region.

These were:

- The annual rainfall trends, based on raw data, demonstrate limited consistency (i.e. stations show increasing and decreasing trends) both within sub-regions and across sub-regions except in the north, and may be of limited use in identifying consistent patterns of change.

- An analysis of seasonal rainfall revealed greater consistency in the direction of summer rainfall change, with all sub-regions showing declining trends or no change.
- The analysis of winter rainfall revealed far less consistency in trends both within and across sub-regions and may account for the lack of consistency in the annual trends.
- The analysis of average minimum temperature trends revealed a consistent warming trend for all but one of the recording stations assessed. The warming trends accounted for between 28 and 42% of the total station variability. Given the very short length of record for the North sub-region recording station (28 years), and the fact that the trend was not statistically significant at the $P=0.05$ level, thus the cooling trend is reported with little confidence.
- Similarly the lowest annual minimum temperatures in all sub-regions except the East have exhibited strong warming trends.
- The analysis of average maximum temperature revealed a less consistent pattern of change between the four sub-regions. The South and Central stations exhibited a warming trend while the East and North sub-region exhibited a cooling trend. Given the short record length for the North station this trend was reported with little confidence. The East station data was however comprehensive, and thus the cooling trend can be reported with some confidence.
- A surprising result from this analysis was the cooling trend exhibited by all four stations for the time series of highest annual maximum temperature. Further investigation using the interpolated climate data is required to determine the validity of the apparent trends.

On the whole the analysis of raw climate data revealed consistent drying trends in summer rainfall over much of the study region as well as warming in minimum temperatures.

Analysis of Interpolated Climate Data

In order to examine the climate trends exhibited by each station and sub-region in a more comprehensive and definitive way the existing raw data must be examined for inconsistencies with missing and erroneous data replaced. This process allows the construction of a more complete time series on which to perform a series of trend analyses. The process of interpolation has been discussed in an earlier section. This discussion described the process by which post 1957 raw climate data is manipulated and missing data in-filled (patched) (Jeffery *et al.*, 2001).

In addition to providing interpolated daily climate data for 1957 to present, new climate surfaces have been developed for the period 1889 to 1956. The new surfaces incorporate data from the “*Computerising the Australian Climate Archive*” (CLIMARC) project using an anomaly-interpolated spline algorithm where data is available or average climatologies where data is not (Rayner *et al.*, 2004). Details regarding this process, as well as error-checking and statistical analyses can be found in Rayner *et al.* (2004).

The interpolated climate data were compared against the raw climate data in order to determine inter-variable correlation and to determine if the interpolated data exhibited the same degree of variability on both annual and seasonal time-scales. Although the interpolated climate data extends from 1889 to present, the comparative analyses were performed on a period comparable with the available length of record at each station.

The length of the raw rainfall record was, in most cases extensive and for this reason the correlation between data sets was extremely good ($r = 0.92$, $P < 0.01$ – averaged across all stations). However in the case of the temperature data the length of raw temperature record was extremely limited except in two cases (i.e. Bundaberg and Gayndah). For this reason the correlation between interpolated and raw temperature data was significantly lower than for temperature datasets ($r = 0.54$, $P < 0.01$).

The inter-variable correlation analyses included a comparison of the variance between individual raw and interpolated station means as described in the F Statistic; an assessment of the correlation between raw and interpolated data expressed by the Pearson Correlation co-efficient (r); a measure of the relationship between the raw and interpolated data ranges (covariance); an assessment of the slope of the “least squares” fit one-to-one linear regression between interpolated and raw data; a measure of the co-efficient of determination (r^2) of the one-to-one regression and assessment of significance (P). In addition the mean, median, standard deviation and linear trends were calculated for each data set to allow for visual comparison.

In instances where the F Statistic was less than one a small difference in the raw and interpolated means existed. This indicated a similar variance in both datasets expressed by the similarity of the means. An accompanying poor significance score for the F Statistic test i.e. $P > 0.05$ indicated an increasing likelihood of exceeding the F value, thus supporting the notion of two highly correlated data sets. The correlation between the two data sets was tested using the Pearson product moment correlation, which reflected the extent of a linear relationship between two data sets. The Covariance measure was used to determine whether the two ranges of data moved together— that is, whether large values of one set were associated with large values of the other (positive covariance), whether small values of one set were associated with large values of the other (negative covariance), or whether values in both sets were unrelated (covariance near zero).

The one-to-one test assessed the liner regression through the raw and interpolated data assuming a zero y intercept. The value expressed in the one-to-one test represented the slope of the liner regression through the interpolated (x) and raw (y) data. A value of one described an almost perfect correlation between data i.e. the x and y data fit extremely well on a one-to-one line. The co-efficient of determination (r^2) provided a measure of how well the liner regression explained the variance between x and y data.

1. Rainfall Correlation Analyses

The rainfall correlation analyses in the East sub-region (Tables 2 to 5) revealed a good fit between raw and interpolated rainfall data, with an average annual correlation co-efficient score of 0.91.

The comparison of Bundaberg (39015) raw and interpolated station data revealed little difference between the interpolated mean, median and standard deviation values (Table 2). The raw data did demonstrate slightly higher standard deviation values, indicating higher variability, although the average difference across the comparison of annual, summer and winter rainfall data was less than 4.5 mm (Table 2).

Table 2: A statistical comparison of raw and interpolated rainfall for station 39015 (Bundaberg). While the interpolated data series extends from 1889 to 2003 the Bundaberg raw data only extends to 1989. For this reason all statistical tests were performed on data for the period 1889 to 1989.

1889 - 1989	ANNUAL	SUMMER	WINTER
MEAN – Interpolated	1148.2	119.6	62.1
MEAN - Raw	1146.9	119.7	61.7
MEDIAN – Interpolated	1130.0	115.8	56.7
MEDIAN - Raw	1137.9	114.6	56.9
STD – Interpolated	362.7	49.1	32.8
STD - Raw	377.0	50.6	33.3
F STATISTIC	0.69967	0.76372	0.8753
SIGNIFICANCE (P)	(0.40)	(0.38)	(0.35)
CORRELATION CO-EFFICIENT (r)	0.99	0.99	0.99
COVARIANCE	134311.52	2439.90	1075.68
ONE-TO-ONE TEST	1.00	1.00	1.00
CO-EFFICIENT OF DETERMINATION (r^2)	0.98	0.98	0.99
SIGNIFICANCE (P)	<0.01	<0.01	<0.01
y= mx + c - Interpolated x ≈ Years	-0.559x + 2232.72 ($r^2 = 0.002$, P = NS)	-0.113x + 338.54 ($r^2 = 0.0045$, P = NS)	-0.017x + 95.70 ($r^2 = 0.0002$, P = NS)
y= mx + c - Raw	0.0272x + 619.30 ($r^2 = 0.0004$, P = NS)	-0.024x + 166.95 ($r^2 = 0.0002$, P = NS)	0.025x + 13.63 ($r^2 = 0.0005$, P = NS)

The F Statistic produced values less than one for annual, summer and winter rainfall comparisons highlighting the similarities in raw and interpolated rainfall variance (Table 2).

Similarly the one-to-one test showed very good agreement between individual data and the linear regression line through the origin i.e. in all cases the slope of the “least squares” fit linear regression was 1 explaining between 98 and 99% of the overall data variability.

In the case of the raw data the linear trends exhibited by the annual and winter rainfall data were in positive directions, however the interpolated data produced a negative or downward trend over the same period (Table 2). In both the winter and the annual case the shift in trend, although in the opposite direction, remained non-significant i.e. not statistically significant at the 95% confidence interval. This does raise concerns regarding linear trend analyses on climate data, with the statistical significance an increasingly important consideration in instances where trend reversals occur.

The Gin Gin station data (39040) exhibited similar results to the Bundaberg station, although in this case the agreement between raw and interpolated data was slightly weaker. In the case of the mean, median and standard deviation, the raw data produced greater values for all periods analysed (Table 3). The F Statistic in all cases was less than one (1), demonstrating highly correlated mean variances across annual, summer and winter rainfall (Table 3).

Table 3: A statistical comparison of raw and interpolated rainfall for station 39040 (Gin Gin). While the interpolated data series extends from 1889 to 2003 the Gin Gin raw data only extends from 1900 to 2000. For this reason all statistical tests were performed on data for the period 1900 to 2000.

1900 – 2002	ANNUAL	SUMMER	WINTER
MEAN – Interpolated	1007.7	107.5	51.7
MEAN – Raw	1020.4	108.8	52.4
MEDIAN – Interpolated	1020.1	100.7	47.8
MEDIAN – Raw	1029.4	102.2	48.3
STD – Interpolated	300.2	36.9	24.8
STD – Raw	305.0	37.4	25.2
F STATISTIC	0.8723	0.8863	0.8544
SIGNIFICANCE (P)	(0.35)	(0.35)	(0.36)
CORRELATION CO-EFFICIENT (r)	1.00	1.00	1.00
COVARIANCE	90577.83	1366.73	618.20
ONE-TO-ONE TEST	1.01	1.01	1.01
CO-EFFICIENT OF DETERMINATION (r ²)	1.00	1.00	1.00
SIGNIFICANCE (P)	<0.01	<0.01	<0.01
y= mx + c - Interpolated x ≈ Years	-0.667x + 2308.63 (R ² = 0.004, P = NS)	-0.086x + 275.72 (R ² = 0.004, P = NS)	-0.051x + 151.24 (R ² = 0.003, P = NS)
y= mx + c – Raw	-0.603x + 2196.41 (R² = 0.004, P = NS)	-0.077x + 258.61 (R² = 0.004, P = NS)	-0.052x + 154.66 (R² = 0.004, P = NS)

The one-to-one test revealed a linear regression slope that slightly over-estimated rainfall at the lower end of the scale and under-estimated rainfall at the higher end of the scale (i.e. the slope of the linear regression through zero is greater than one in all cases (Table 3). Of little surprise was the strongly positive covariance demonstrated by all analyses, particularly in the annual and

summer rainfall (i.e. large values of one set are associated with large values of the other) (Table 3). The linear trend analyses of the interpolated data differed very little from the raw data with regression slopes and intercepts very similar.

The remaining two climate stations namely 39218 (Moolboolaman) and 39234 (The Cedars) demonstrated slightly lower correlations between the raw and interpolated data than the previous two climate stations (Table 4 and 5). In the case of station 39218 (Moolboolaman) the annual mean and median interpolated values were on average 66.5 mm higher than for the raw rainfall. Given the relative closeness of the raw and interpolated summer mean and median values, the results would suggest the greatest differences occurred in the winter period. The raw standard deviation values remained higher than for the interpolated rainfall indicating higher variability in the raw data (Table 4). The one-to-one test revealed that for the most part the annual rainfall values were under-estimated in the interpolated data (i.e. the interpolated data was consistently lower than the corresponding raw annual value) (Table 4). As expected this was consistent in both summer and winter analyses as well.

Table 4: A statistical comparison of raw and interpolated rainfall for station 39218 (Moolboolaman). While the interpolated data series extends from 1889 to 2003 the Moolboolaman raw data only extends from 1931 to 2002. For this reason all statistical tests were performed on data for the period 1931 to 2002.

1931 – 2002	ANNUAL	SUMMER	WINTER
MEAN – Interpolated	938.2	101.2	43.6
MEAN – Raw	870.2	102.2	46.4
MEDIAN – Interpolated	904.2	93.2	38.5
MEDIAN – Raw	839.2	93.0	40.3
STD – Interpolated	320.3	39.8	24.4
STD – Raw	329.8	43.6	27.9
F STATISTIC	0.840	0.5348	0.3731
SIGNIFICANCE (<i>P</i>)	(0.36)	(0.47)	(0.54)
CORRELATION CO-EFFICIENT (<i>r</i>)	0.80	0.89	0.98
COVARIANCE	78315.61	1511.98	681.55
ONE-TO-ONE TEST	0.92	1.02	1.04
CO-EFFICIENT OF DETERMINATION (<i>r</i> ²)	0.63	0.80	0.95
SIGNIFICANCE (<i>P</i>)	<0.01	<0.01	<0.01
y= mx + c - Interpolated <i>x</i> ≈ Years	-2.636x + 6137.72 (<i>R</i> ² = 0.028, <i>P</i> = NS)	-0.421x + 931.17 (<i>R</i> ² = 0.046, <i>P</i> = NS)	0.168x - 288.27 (<i>R</i> ² = 0.020, <i>P</i> = NS)
y= mx + c - Raw	-0.788x + 2426.09 (<i>R</i>² = 0.002, <i>P</i> = NS)	-0.458x + 1006.65 (<i>R</i>² = 0.043, <i>P</i> = NS)	0.067x – 85.30 (<i>R</i>² = 0.002, <i>P</i> = NS)

The direction of the rainfall trend did not change between raw and interpolated rainfall data analysed. The consistently lower interpolated annual rainfall data did serve to strengthen the declining linear rainfall trend (Table 4). Similarly the interpolated summer and winter rainfall produced marginally stronger declines. The stronger trends were still not statistically significant at the 95% confidence interval.

The analysis of rainfall station 32934 (The Cedars) again showed that the interpolated median values were greater in the average annual and winter rainfall cases (Table 5). The summer rainfall comparison however revealed that the interpolated summer mean was lower than the raw summer rainfall mean. Similarly the interpolated median values were also higher in both the annual and winter rainfall periods, with summer values lower.

The average correlation co-efficient value for all rainfall periods considered was higher than for the previous station, suggesting a better correlation between interpolated and raw data. The covariance remained strongly positive for annual, summer and winter rainfall, although again the one-to-one test revealed discrepancies between data. In the case of the annual rainfall the interpolated values were consistently higher than raw rainfall at the lower end of the range and higher than the raw data at the upper end of the range (Table 5).

Table 5: A statistical comparison of raw and interpolated rainfall for station 39234 (The Cedars). While the interpolated data series extends from 1889 to 2003 the “The Cedars” raw data only extends from 1913 to 2002. For this reason all statistical tests were performed on data for the period 1913 to 2002.

1913 - 2002	ANNUAL	SUMMER	WINTER
MEAN – Interpolated	924.7	97.6	47.4
MEAN - Raw	882.5	98.4	48.2
MEDIAN – Interpolated	934.3	93.0	42.8
MEDIAN - Raw	888.5	94.5	41.0
STD – Interpolated	276.8	33.3	21.8
STD - Raw	306.3	34.9	22.5
F STATISTIC	0.349	0.660	0.764
SIGNIFICANCE (P)	(0.56)	(0.42)	(0.38)
CORRELATION CO-EFFICIENT (r)	0.85	0.98	0.96
COVARIANCE	71097.26	1126.28	468.16
ONE-TO-ONE TEST	0.95	1.01	1.01
CO-EFFICIENT OF DETERMINATION (r ²)	0.72	0.96	0.92
SIGNIFICANCE (P)	<0.01	<0.01	<0.01
y= mx + c - Interpolated x ≈ Years	-1.598x + 4052.19 (R ² = 0.022, P = NS)	-0.173x + 436.50 (R ² = 0.018, P = NS)	-0.029x + 104.82 (R ² = 0.001, P = NS)
y= mx + c - Raw	-1.710x + 4228.30 (R² = 0.021, P = NS)	-0.170x + 430.70 (R² = 0.016, P = NS)	-0.060x – 164.67 (R² = 0.005, P = NS)

The same analyses were performed on the North sub-region station data (Table 6 to 9) and again showed a good average correlation between interpolated and observed rainfall data. The average correlation across all four stations was slightly higher than for the East sub-region i.e. 0.95 versus 0.91 although the comparative analyses were performed on shorter time intervals for the North sub-region due to raw rainfall data limitations i.e. an average of 58.25 years of data for each North station versus an average of 85.25 years for each East station analysed.

The examination of mean and median for raw and interpolated rainfall for station 32248 (Tecoma) revealed the interpolated climate data produced consistently higher values for annual, summer and winter rainfall. The standard deviation calculated for annual, summer and winter rainfall remained higher in the raw rainfall data. The F Statistic again demonstrating highly correlated mean variances across annual, summer and winter rainfall. The results for this station were somewhat higher than for the stations in the East region however this remained a function of the period of analysis.

The one-to-one test revealed that at the lower end of the annual rainfall range some large discrepancies occurred between interpolated and raw data. This resulted in a reduction in the slope of the liner regression below the one to one line (Table 6). The time series analyses showed little variation between raw and interpolated rain although the declining trends were slightly weaker in the interpolated data for annual and summer rainfall than for the raw data (Table 6).

Table 6: A statistical comparison of raw and interpolated rainfall for station 39248 (Tecoma). While the interpolated data series extends from 1889 to 2003 the Tecoma raw data only extends from 1953 to 2002. For this reason all statistical tests were performed on data for the period 1953 to 2002.

1953 – 2002	ANNUAL	SUMMER	WINTER
MEAN – Interpolated	631.1	67.1	31.9
MEAN – Raw	607.6	65.4	32.6
MEDIAN – Interpolated	638.8	65.0	30.0
MEDIAN – Raw	601.3	66.2	27.8
STD – Interpolated	164.7	22.6	16.6
STD – Raw	181.4	24.5	20.2
F STATISTIC	0.500	0.582	0.166
SIGNIFICANCE (<i>P</i>)	(0.48)	(0.45)	(0.68)
CORRELATION CO-EFFICIENT (<i>r</i>)	0.94	0.97	0.89
COVARIANCE	27628.26	524.87	291.21
ONE-TO-ONE TEST	0.97	0.98	1.04
CO-EFFICIENT OF DETERMINATION (<i>r</i> ²)	0.89	0.93	0.79
SIGNIFICANCE (<i>P</i>)	<0.01	<0.01	<0.01
y= mx + c - Interpolated <i>x</i> ≈ Years	-4.800x + 10123.41 (<i>R</i> ² = 0.181, <i>P</i> <0.01)	-0.512x + 1079.34 (<i>R</i> ² = 0.109, <i>P</i> <0.05)	-0.119x + 267.54 (<i>R</i> ² = 0.011, <i>P</i> = NS)
y= mx + c - Raw	-5.550x + 11583.64 (<i>R</i>² = 0.199, <i>P</i> <0.01)	-0.548x + 1148.76 (<i>R</i>² = 0.106, <i>P</i> <0.05)	-0.017x + 65.37 (<i>R</i>² = 0.0001, <i>P</i> = NS)

The declining rainfall trend for both interpolated annual and summer rainfall remained statistically significant at the *P*>0.01 and *P*>0.05 levels respectively. The declining interpolated winter rainfall trend was not statistically significant at the 95% confidence interval (Table 6).

The analysis of interpolated and raw rainfall for the Kalpowar rainfall station (39057) revealed strong agreement, with differences between raw and interpolated means, on average less than 5 mm and for median values of less than 2 mm (Table 7). The F Statistic results remained less

than zero for all seasons suggesting highly correlated mean variances. The correlation coefficient remained close to 1 as did the one-to-one test. The linear trend analysis revealed slightly stronger declining trends for the annual and winter interpolated data, with the annual trend statistically significant at the 95% confidence interval (Table 7). The interpolated summer rainfall trend was weaker than for the raw data but was still significant at the 95% confidence interval (Table 7).

Table 7: A statistical comparison of raw and interpolated rainfall for station 39057 (Kalpowar). While the interpolated data series extends from 1889 to 2003 the Kalpowar raw data only extends from 1933 to 2002. For this reason all statistical tests were performed on data for the period 1933 to 2002.

1933 - 2002	ANNUAL	SUMMER	WINTER
MEAN – Interpolated	847.2	90.6	43.8
MEAN - Raw	841.1	92.3	44.1
MEDIAN – Interpolated	843.4	88.0	41.5
MEDIAN - Raw	845.3	89.1	41.1
STD – Interpolated	252.8	28.1	22.3
STD - Raw	244.8	31.3	23.4
F STATISTIC	0.790	0.371	0.951
SIGNIFICANCE (<i>P</i>)	(0.38)	(0.54)	(0.33)
CORRELATION CO-EFFICIENT (<i>r</i>)	0.97	0.96	0.98
COVARIANCE	59186.69	834.18	483.79
ONE-TO-ONE TEST	0.99	1.02	0.99
CO-EFFICIENT OF DETERMINATION (<i>r</i> ²)	0.94	0.92	0.95
SIGNIFICANCE (<i>P</i>)	<0.01	<0.01	<0.01
y= mx + c - Interpolated <i>x</i> ≈ Years	-2.991x + 6732.34 (<i>R</i> ² = 0.06, <i>P</i> <0.05)	-0.371x + 820.98 (<i>R</i> ² = 0.07, <i>P</i> <0.05)	-0.050x + 141.41 (<i>R</i> ² = 0.002, <i>P</i> = NS)
y= mx + c - Raw	-2.654x + 6063.06 (<i>R</i>² = 0.05, <i>P</i> ~0.05)	-0.433x + 944.61 (<i>R</i>² = 0.08, <i>P</i> <0.05)	0.001x – 40.70 (<i>R</i>² = 0.000002, <i>P</i>=NS)

The analysis of the raw and interpolated rainfall for the Malakof rainfall station revealed higher mean annual and summer rainfall values for the interpolated station data (i.e. 19.3 and less than 1 mm respectively), with the interpolated winter mean negligibly less than for the raw rainfall (less than 1 mm) (Table 8).

The Malakof rainfall station was one of the few where the interpolated annual rainfall standard deviation was higher than the raw data suggesting slightly higher annual variability. The F test performed on the summer rainfall produced a very small F value suggest very strong agreement between raw and interpolated summer mean variance (Table 8).

Both the slope and the co-efficient of determination of the interpolated rainfall trends were weaker than for the raw data, with the annual interpolated rainfall trend falling below the 95% confidence interval and the interpolated summer rainfall trend falling from the 99% confidence interval to the 95% confidence interval (Table 8).

Table 8: A statistical comparison of raw and interpolated rainfall for station 39129 (Malakof). While the interpolated data series extends from 1889 to 2003 the Malakof raw data only extends from 1932 to 2002. For this reason all statistical tests were performed on data for the period 1932 to 2002.

1932 - 2002	ANNUAL	SUMMER	WINTER
MEAN – Interpolated	769.7	83.0	38.1
MEAN - Raw	750.4	82.3	39.0
MEDIAN – Interpolated	783.2	78.7	36.0
MEDIAN - Raw	749.1	75.5	36.7
STD – Interpolated	226.8	27.6	20.2
STD - Raw	218.5	39.9	20.1
F STATISTIC	0.788	0.004	0.963
SIGNIFICANCE (<i>P</i>)	(0.38)	(0.95)	(0.33)
CORRELATION CO-EFFICIENT (<i>r</i>)	1.00	0.80	1.00
COVARIANCE	46977.40	914.37	397.25
ONE-TO-ONE TEST	0.99	1.02	1.00
CO-EFFICIENT OF DETERMINATION (<i>r</i> ²)	1.00	0.64	1.00
SIGNIFICANCE (<i>P</i>)	<0.01	<0.01	<0.01
y= mx + c - Interpolated <i>x</i> ≈ Years	-2.077x + 4857.95 (<i>R</i> ² = 0.04, <i>P</i> =NS)	-0.301x + 674.89 (<i>R</i> ² = 0.05, <i>P</i> ~0.05)	0.075x – 109.34 (<i>R</i> ² = 0.01, <i>P</i> = NS)
y= mx + c - Raw	-2.890x + 6455.46 (<i>R</i>² = 0.06, <i>P</i> <0.05)	-0.716x + 1494.42 (<i>R</i>² = 0.12, <i>P</i> <0.01)	0.013x + 13.53 (<i>R</i>² = 0.0002, <i>P</i> =NS)

The comparison of the interpolated and raw rainfall for the Bancroft rainfall station (39103) once again demonstrated an instance where the annual interpolated mean and median values were greater than the raw rainfall data (Table 9). The lower standard deviation calculated for the interpolated annual rainfall data would suggest lower variability about the mean and coupled with the results of the one-to-one test (four large outliers for annual rainfall all with greater higher interpolated values, would suggest that the interpolated rainfall was consistently higher at the lower end of the rainfall range (Table 9).

This point was again demonstrated in the linear trend analyses with the interpolated annual rainfall trend exhibiting a stronger declining trend than in the raw data (i.e. the higher interpolated values occur at the beginning of the time series serving to strengthen the declining trend significantly (Figure 12). The interpolated summer and winter linear trends also exhibit declines although these are slightly weaker than for the raw data (Table 9).

Table 9: A statistical comparison of raw and interpolated rainfall for station 39103 (Bancroft). While the interpolated data series extends from 1889 to 2003 the Bancroft raw data only extends from 1954 to 2002. For this reason all statistical tests were performed on data for the period 1954 to 2002.

1954 - 2002	ANNUAL	SUMMER	WINTER
MEAN – Interpolated	695.6	74.2	34.5
MEAN - Raw	666.4	75.4	34.4
MEDIAN – Interpolated	674.7	74.6	32.6
MEDIAN - Raw	657.0	78.0	31.0
STD – Interpolated	199.5	21.2	19.3
STD - Raw	217.9	22.4	19.5
F STATISTIC	0.562	0.716	0.943
SIGNIFICANCE (<i>P</i>)	(0.46)	(0.40)	(0.33)
CORRELATION CO-EFFICIENT (<i>r</i>)	0.88	0.85	1.00
COVARIANCE	37425.31	400.06	369.80
ONE-TO-ONE TEST	0.96	1.01	1.00
CO-EFFICIENT OF DETERMINATION (<i>r</i> ²)	0.78	0.71	0.99
SIGNIFICANCE (<i>P</i>)	<0.01	<0.01	<0.01
y= mx + c - Interpolated <i>x</i> ≈ Years	-4.528x + 9657.76 (<i>R</i> ² = 0.107, <i>P</i> <0.05)	-0.404x + 873.33 (<i>R</i> ² = 0.075, <i>P</i> ~0.05)	-0.120x + 272.63 (<i>R</i> ² = 0.008, <i>P</i> = NS)
y= mx + c - Raw	-1.728x + 4086.32 (<i>R</i>² = 0.013, <i>P</i> = NS)	-0.471x + 1008.21 (<i>R</i>² = 0.090, <i>P</i> <0.05)	-0.139x + 310.37 (<i>R</i>² = 0.011, <i>P</i> =NS)

The Central sub-region contained a number of rainfall stations with relatively long rainfall records. These stations were chosen to represent the sub-regional changes in rainfall that occurred over time. The rainfall stations, with the exception of Auburn, contained in excess of 100 years of data.

The first rainfall station comparison was performed on the Auburn station (42059). The interpolated data produced greater annual and summer mean and median values and almost equivalent (less than 1mm and 1.5mm lower) winter values (Table 10). The raw standard deviation values for annual, summer and winter rainfall were greater than for the interpolated values, suggesting greater variability in the raw data (Table 10).

The F Statistic as with all other stations analysed produced values less than one, again demonstrating that the interpolated and raw climate data analysed demonstrate equivalent mean variance. The correlation between raw and interpolated annual and summer rainfall was lower than for the comparison of winter rainfall (Table 10). The one-to-one test produced slopes slightly less than 1 (i.e. 0.93 and 0.99 respectively) for both annual and summer rainfall comparisons. The discrepancies between raw and interpolated rainfall at the lower end of the range (i.e. interpolated values greater than raw data) were once again responsible for weakening the linear regression slope (Table 10).

The interpolated linear trend analyses exhibited declining rainfall patterns for annual, summer and winter rainfall (Table 10). The trends were at odds with those calculated from the raw data

although as with the raw trends all the interpolated trends were not significant at the 95% confidence interval.

Table 10: A statistical comparison of raw and interpolated rainfall for station 42059 (Auburn). While the interpolated data series extends from 1889 to 2003 the Bancroft raw data only extends from 1959 to 2002. For this reason all statistical tests were performed on data for the period 1959 to 2002.

1959 - 2002	ANNUAL	SUMMER	WINTER
MEAN – Interpolated	631.5	67.0	32.1
MEAN - Raw	581.5	66.5	32.7
MEDIAN – Interpolated	606.9	64.2	25.2
MEDIAN - Raw	554.6	64.2	23.8
STD – Interpolated	158.3	18.4	21.3
STD - Raw	194.6	21.1	23.2
F STATISTIC	0.179	0.383	0.580
SIGNIFICANCE (P)	(0.64)	(0.52)	(0.43)
CORRELATION CO-EFFICIENT (r)	0.85	0.85	0.98
COVARIANCE	25455.93	323.10	501.67
ONE-TO-ONE TEST	0.93	0.99	1.01
CO-EFFICIENT OF DETERMINATION (r ²)	0.71	0.96	0.95
SIGNIFICANCE (P)	<0.01	<0.01	<0.01
y= mx + c - Interpolated x ≈ Years	-0.833x + 2281.97 (R ² = 0.005, P = NS)	-0.087x + 238.85 (R ² = 0.004, P = NS)	0.079x – 123.81 (R ² = 0.002, P = NS)
y= mx + c - Raw	3.055x – 5469.36 (R² = 0.041, P = NS)	0.034x – 1.58 (R² = 0.0004, P = NS)	0.083x – 132.45 (R² = 0.002, P = NS)

The Gayndah rainfall station (39039) analyses showed very good agreement between means, median and standard deviation values (Table 11). The F statistic once again returned values less than one with poor significance scores. This indicated a similar variance in both datasets expressed by the similarity of the means (Table 11). An accompanying poor significance score for the F Statistic test i.e. $P > 0.05$ indicated a high likelihood of exceeding the F value, thus resulting in a rejection the null hypothesis that the two sets are independent and thus supporting the notion that the two data sets were highly correlated.

Both the correlation and one-to-one test demonstrated good correlation between raw and interpolated values. The one-to-one test identified two significant outliers in both the annual and summer rainfall comparisons where the interpolated data was considerably higher than the raw (i.e. 1470 mm versus 366 mm and 667 mm versus 577 mm for annual rainfall; 59 versus 35 and 93 mm versus 80 mm for summer rainfall). These outliers served to weaken the linear slope below 1 (Table 11).

The linear trend analysis showed stronger declining rainfall for annual, summer and winter rainfall than exhibited by the raw rainfall data. In only one case, namely annual rainfall, did the strengthened interpolated trends prove statistically significant (Table 11).

Table 11: A statistical comparison of raw and interpolated rainfall for station 39039 (Gayndah). While the interpolated data series extends from 1889 to 2003 the Gayndah raw data only extends from 1893 to 2002. For this reason all statistical tests were performed on data for the period 1893 to 2002.

1893 - 2002	ANNUAL	SUMMER	WINTER
MEAN – Interpolated	759.3	81.2	36.4
MEAN – Raw	759.6	82.3	36.7
MEDIAN – Interpolated	775.6	77.6	31.5
MEDIAN - Raw	777.3	79.5	32.2
STD – Interpolated	195.3	22.7	18.4
STD – Raw	190.8	23.7	18.0
F STATISTIC	0.814	0.665	0.855
SIGNIFICANCE (<i>P</i>)	(0.37)	(0.42)	(0.36)
CORRELATION CO-EFFICIENT (<i>r</i>)	0.83	0.99	0.99
COVARIANCE	30621.41	527.93	326.22
ONE-TO-ONE TEST	0.99	1.01	1.00
CO-EFFICIENT OF DETERMINATION (<i>r</i> ²)	0.65	0.98	0.99
SIGNIFICANCE (<i>P</i>)	<0.01	<0.01	<0.01
y= mx + c - Interpolated <i>x</i> ≈ Years	-1.191x + 3082.80 (<i>R</i> ² = 0.033, <i>P</i> < 0.05)	-0.097x + 269.87 (<i>R</i> ² = 0.016, <i>P</i> = NS)	-0.028x + 91.95 (<i>R</i> ² = 0.002, <i>P</i> = NS)
y= mx + c - Raw	-0.362x + 1466.41 (<i>R</i>² = 0.003, <i>P</i> = NS)	-0.073x + 224.11 (<i>R</i>² = 0.008, <i>P</i> = NS)	-0.013x + 62.88 (<i>R</i>² = 0.0005, <i>P</i> = NS)

In the case of the Eidsvold rainfall station, the interpolated rainfall demonstrated slightly lower mean, median and standard deviation values than the raw rainfall (Table 12). The F Statistic test, as with all the other stations analysed, returned values less than one and the correlation analyses returned *r* values of 0.99, 1 and 1 for annual, summer and winter rainfall respectively suggesting an almost perfect correlation (Table 12). Similarly the absence of significant outliers in the comparisons served to return slopes very close to one (1) (Table 12). The interpolated linear trends were slightly stronger in summer and winter rainfall and significantly stronger for annual rainfall (i.e. liner trend went from 'Not Significant' in the raw data to significant at the 99% confidence interval for the interpolated data (Table 12).

In the case of Biggenden rainfall station the agreement between raw and interpolated data was again very good given the extent of the record. The analyses of interpolated rainfall trends revealed increasing annual and summer rainfall and declining winter rainfall (as with the raw data). In each case, however the trends were not statistically significant explaining less than 1% of the overall variability (Table 13).

Table 12: A statistical comparison of raw and interpolated rainfall for station 39036 (Eidsvold). While the interpolated data series extends from 1889 to 2003 the Eidsvold raw data only extends from 1890 to 2002. For this reason all statistical tests were performed on data for the period 1890 to 2002.

1890 - 2002	ANNUAL	SUMMER	WINTER
MEAN – Interpolated	717.2	75.8	37.3
MEAN – Raw	728.2	76.9	37.1
MEDIAN – Interpolated	703.5	73.1	34.2
MEDIAN - Raw	706.8	74.5	33.7
STD – Interpolated	206.9	26.6	18.9
STD – Raw	211.4	26.9	18.4
F STATISTIC	0.819	0.884	0.780
SIGNIFICANCE (P)	(0.37)	(0.35)	(0.38)
CORRELATION CO-EFFICIENT (r)	0.99	1.00	1.00
ONE-TO-ONE TEST	1.02	1.01	1.02
Y= mx + c - Interpolated <i>x ≈ Years</i>	-1.056x + 2773.14 (R ² = 0.028, P < 0.01)	-0.123x + 315.39 (R ² = 0.023, P = NS)	-0.029x + 94.22 (R ² = 0.003, P = NS)
y= mx + c - Raw	-0.845x + 2373.00 (R² = 0.017, P = NS)	-0.110x + 290.08 (R² = 0.018, P = NS)	-0.017x + 70.78 (R² = 0.001, P = NS)

Table 13: A statistical comparison of raw and interpolated rainfall for station 40021 (Biggenden). While the interpolated data series extends from 1889 to 2003 the Biggenden raw data only extends from 1899 to 2002. For this reason all statistical tests were performed on data for the period 1899 to 2002.

1899 - 2002	ANNUAL	SUMMER	WINTER
MEAN – Interpolated	861.0	92.6	42.4
MEAN – Raw	861.8	93.0	42.6
MEDIAN – Interpolated	882.1	90.4	39.0
MEDIAN - Raw	878.2	91.2	39.1
STD – Interpolated	231.0	27.9	20.2
STD – Raw	231.4	28.0	20.3
F STATISTIC	0.987	0.971	0.970
SIGNIFICANCE (P)	(0.37)	(0.42)	(0.36)
CORRELATION CO-EFFICIENT (r)	0.99	1.00	1.00
ONE-TO-ONE TEST	1.00	1.00	1.00
Y= mx + c - Interpolated <i>x ≈ Years</i>	0.028x + 806.25 (R ² = 0.00001, P = NS)	0.015x + 64.05 (R ² = 0.00025, P = NS)	-0.017x + 76.00 (R ² = 0.0006, P = NS)
y= mx + c - Raw	0.093x + 679.55 (R² = 0.00015, P = NS)	0.009x + 76.06 (R² = 0.00009, P = NS)	-0.018x + 78.46 (R² = 0.00075, P = NS)

The comparison of raw and interpolated data for the South sub-region was performed on the rainfall stations of Mounefontein (40138), Goomeri (40090), Kingaroy (40012) and Kumbia (40013). The four stations exhibited declining interpolated rainfall trends, however these trends were not statistically significant at the 95% confidence interval.

The Mounefontein station exhibited closely correlated mean and median values for annual, summer and winter rainfall (Table 14). As with most other stations the interpolated data produced a slightly smaller standard deviation than the raw data, demonstrating a slightly lower variability in the interpolated rainfall. The correlation analyses returned a co-efficient of one for both annual and winter rainfall with summer rainfall returning a correlation co-efficient of 0.99 (Table 14). The one-to-one test similarly returned values of one for both annual and winter rainfall comparisons (Table 14) again demonstrating the high level of correlation between the raw and interpolated rainfall data.

Table 14: A statistical comparison of raw and interpolated rainfall for station 40138 (Mounefontein). While the interpolated data series extends from 1889 to 2003 the Mounefontein raw data only extends from 1949 to 2002. For this reason all statistical tests were performed on data for the period 1949 to 2002.

1949 - 2002	ANNUAL	SUMMER	WINTER
MEAN – Interpolated	723.7	75.5	38.8
MEAN - Raw	725.8	76.0	38.9
MEDIAN – Interpolated	687.5	74.3	30.9
MEDIAN - Raw	690.7	74.2	30.9
STD – Interpolated	174.8	18.1	21.2
STD - Raw	176.7	18.6	21.2
F STATISTIC	0.935	0.844	0.981
SIGNIFICANCE (<i>P</i>)	(0.34)	(0.36)	(0.32)
CORRELATION CO-EFFICIENT (<i>r</i>)	1.00	0.99	1.00
COVARIANCE	30281.53	328.32	441.17
ONE-TO-ONE TEST	1.00	1.01	1.00
CO-EFFICIENT OF DETERMINATION (<i>r</i> ²)	1.00	0.99	1.00
SIGNIFICANCE (<i>P</i>)	<0.01	<0.01	<0.01
y= mx + c - Interpolated <i>x</i> ≈ Years	-2.953x + 6557.99 (<i>R</i> ² = 0.071, <i>P</i> = NS)	-0.303x + 674.55 (<i>R</i> ² = 0.070, <i>P</i> = NS)	-0.136x + 307.07 (<i>R</i> ² = 0.010, <i>P</i> = NS)
y= mx + c - Raw	-3.036x + 6722.99 (<i>R</i>² = 0.073, <i>P</i> = NS)	-0.329x + 726.12 (<i>R</i>² = 0.078, <i>P</i> <0.05)	-0.142x + 320.10 (<i>R</i>² = 0.011, <i>P</i> =NS)

The linear trend analyses returned slightly weaker declining interpolated rainfall trends for annual, summer and winter rainfall, with the summer rainfall trend falling below the 95% confidence interval obtained in the raw summer rainfall analysis (Table 14).

The Goomeri rainfall comparison revealed greater mean, median and standard deviation values than the interpolated data (Table 15). The F Statistic returned values less than zero for annual, summer and winter rainfall comparisons, demonstrating that the interpolated and raw climate data possessed equivalent mean variance. The one-to-one test exhibited very close correlation

between raw and interpolated data, with the co-efficient of determination suggesting no significant outliers and thus the linear regression explained between 98 and 99% of the variability within the two datasets (Table 15).

The linear trend analyses of the interpolated data returned stronger declining trend for both annual and summer rainfall. A marginally weaker positive rainfall trend was returned for the interpolated winter rainfall dataset (Table 15). However the trends were once again below the critical 95% confidence interval and so are considered non-significant.

Table 15: A statistical comparison of raw and interpolated rainfall for station 40090 (Goomeri). While the interpolated data series extends from 1889 to 2003 the Goomer raw data only extends from 1913 to 2002. For this reason all statistical tests were performed on data for the period 1913 to 2002.

1913 – 2002	ANNUAL	SUMMER	WINTER
MEAN – Interpolated	785.3	83.0	40.6
MEAN – Raw	792.8	84.0	41.1
MEDIAN – Interpolated	779.2	81.6	34.7
MEDIAN – Raw	788.6	81.9	35.6
STD – Interpolated	192.1	23.4	19.8
STD – Raw	196.5	24.2	19.8
F STATISTIC	0.829	0.747	0.981
SIGNIFICANCE (<i>P</i>)	(0.36)	(0.39)	(0.32)
CORRELATION CO-EFFICIENT (<i>r</i>)	0.99	0.99	1.00
COVARIANCE	36912.62	555.00	387.18
ONE-TO-ONE TEST	1.01	1.01	1.01
CO-EFFICIENT OF DETERMINATION (<i>r</i> ²)	0.98	0.98	0.99
SIGNIFICANCE (<i>P</i>)	<0.01	<0.01	<0.01
y= mx + c - Interpolated <i>x</i> ≈ Years	-0.781x + 2313.13 (<i>R</i> ² = 0.011, <i>P</i> = NS)	-0.128x + 333.79 (<i>R</i> ² = 0.020, <i>P</i> = NS)	0.019x + 4.26 (<i>R</i> ² = 0.001, <i>P</i> = NS)
y= mx + c - Raw	-0.492x + 1755.67 (<i>R</i>² = 0.004, <i>P</i> = NS)	-0.107x + 293.19 (<i>R</i>² = 0.013, <i>P</i> = NS)	0.032x – 21.04 (<i>R</i>² = 0.002, <i>P</i> = NS)

The remaining stations analysed for the South sub-region were Kingaroy and Kumbia. Both stations contained a relatively long record of 93 and 86 years respectively.

The comparison of raw and interpolated data returned the most highly correlated results for the Kingaroy station with both the correlation co-efficient and one-to-one test returning a value of one for annual, summer and winter rainfall (Table 16). The linear trend analyses showed little difference between the raw and interpolated rainfall data, with declining trends for both annual and summer rainfall and increasing trends for the winter rainfall analyses (Table 16). In both the raw and interpolated summer analyses the trend was significant at the 95% confidence interval.

Table 16: A statistical comparison of raw and interpolated rainfall for station 40112 (Kingaroy). While the interpolated data series extends from 1889 to 2003 the Kingaroy raw data only extends from 1906 to 1999. For this reason all statistical tests were performed on data for the period 1906 to 1999.

1906 – 1999	ANNUAL	SUMMER	WINTER
MEAN – Interpolated	778.2	82.1	40.1
MEAN – Raw	780.3	82.3	40.2
MEDIAN – Interpolated	760.4	81.7	34.2
MEDIAN – Raw	763.7	82.6	34.3
STD – Interpolated	190.4	21.0	19.1
STD – Raw	192.8	21.2	19.2
CORRELATION CO-EFFICIENT (r)	1.00	1.00	1.00
ONE-TO-ONE TEST	1.00	1.00	1.00
CO-EFFICIENT OF DETERMINATION (r ²)	1.00	1.00	1.00
y= mx + c - Interpolated x ≈ Years	-1.806x + 4306.62 (R ² = 0.018, P = NS)	-0.329x + 720.79 (R ² = 0.047, P <0.05)	0.103x – 156.29 (R ² = 0.004, P = NS)
y= mx + c - Raw	-1.842x + 4381.55 (R ² = 0.018, P = NS)	-0.330x + 722.85 (R ² = 0.046, P <0.05)	0.100x – 149.90 (R ² = 0.004, P =NS)

Table 17: A statistical comparison of raw and interpolated rainfall for station 40113 (Kumbia). While the interpolated data series extends from 1889 to 2003 the Kumbia raw data only extends from 1916 to 2002. For this reason all statistical tests were performed on data for the period 1916 to 2002.

1916 – 2002	ANNUAL	SUMMER	WINTER
MEAN – Interpolated	787.1	82.9	41.2
MEAN – Raw	752.5	83.4	41.2
MEDIAN – Interpolated	793.6	81.6	36.9
MEDIAN – Raw	768.8	80.9	37.2
STD – Interpolated	187.5	19.8	20.1
STD – Raw	219.5	20.4	21.1
CORRELATION CO-EFFICIENT (r)	0.85	0.96	0.99
ONE-TO-ONE TEST	0.96	1.00	0.99
CO-EFFICIENT OF DETERMINATION (r ²)	0.71	0.92	0.98
y= mx + c - Interpolated x ≈ Years	-0.234x + 1245.47 (R ² = 0.001, P = NS)	-0.061x + 201.53 (R ² = 0.006, P = NS)	0.027x – 10.98 (R ² = 0.001, P = NS)
y= mx + c - Raw	1.394x – 1980.41 (R ² = 0.025, P = NS)	-0.144x + 366.17 (R ² = 0.029, P <0.05)	0.029x – 14.75 (R ² = 0.001, P =NS)

The Kumbia rainfall station returned lower correlation indices than the Kingaroy station with discrepancies prevalent in summer rainfall. The one-to-one test revealed the presence of a number of significant outliers where interpolated rainfall was higher than raw rainfall (Table 17).

The linear trend analyses showed a shift from a positive linear trend in the raw annual rainfall data to a negative trend in the interpolated data. In both cases the trends were not significant at the 95% confidence interval (Table 17).

The linear trend analyses were repeated for each station, within each sub-region on the entire interpolated record (i.e. 1889 to 2003) in order to consider the effect of additional years (Figure 11). In the case of the East sub region the results were as follows:

- A. 39015 (Bundaberg) – $y = -1.841x + 46898.31$ ($r^2 = 0.029$, $P = \text{NS}$)
- B. 39040 (Gin Gin) – $y = -1.647x + 4234.89$ ($r^2 = 0.032$, $P = \text{NS}$)
- C. 39218 (Moolboolaman) – $y = -1.862x + 4579.31$ ($r^2 = 0.042$, $P < 0.05$)
- D. 39234 (The Cedars) – $y = -2.162x + 5154.14$ ($r^2 = 0.062$, $P < 0.01$)

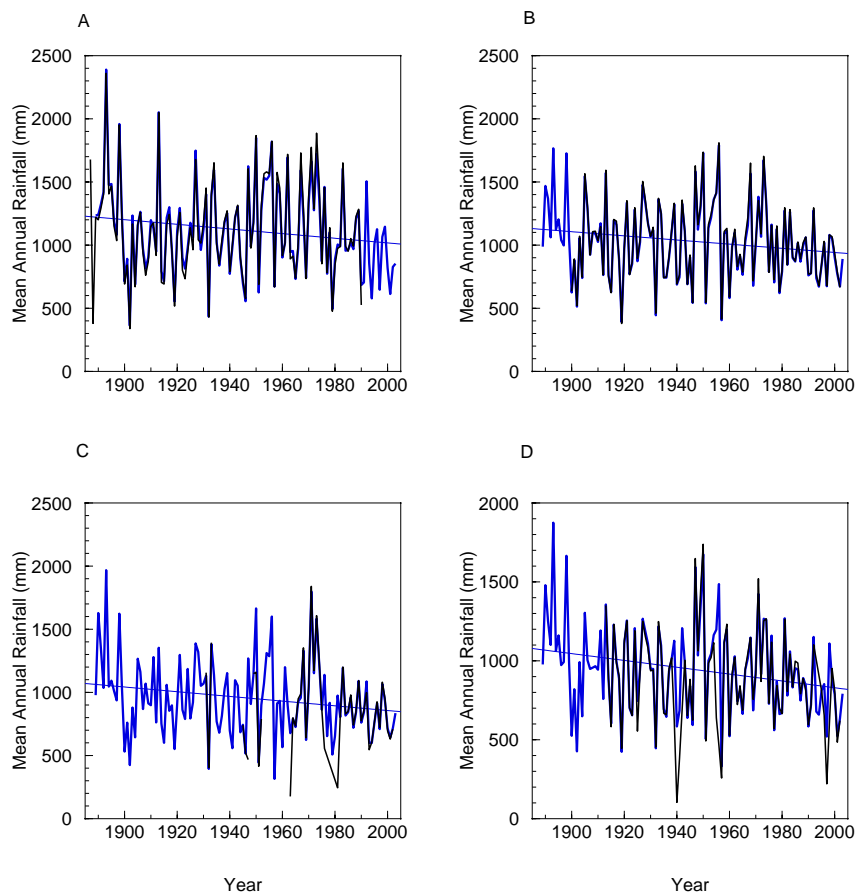


Figure 11: Raw annual rainfall (dark blue) and interpolated (light blue) annual rainfall time series data for the a) Bundaberg b) Gin Gin c) Moolboolaman and d) The Cedars rainfall stations. The straight line represents the linear regression for the interpolated annual rainfall series from 1889 to 2003.

The linear trend analysis performed on the interpolated rainfall data for each station in the North sub-region (Figure 12) produced the following results:

- A. 39248 (Tecoma) – $y = -1.213x + 3010.51$ ($r^2 = 0.048$, $P < 0.05$)
- B. 39057 (Kalpowar) – $y = -1.421x + 3623.03$ ($r^2 = 0.18$, $P < 0.05$)
- C. 39129 (Malakof) – $y = -2.047x + 4790.37$ ($r^2 = 0.078$, $P < 0.01$)
- D. 39103 (Bancroft) – $y = -2.126x + 4008.19$ ($r^2 = 0.308$, $P < 0.01$)

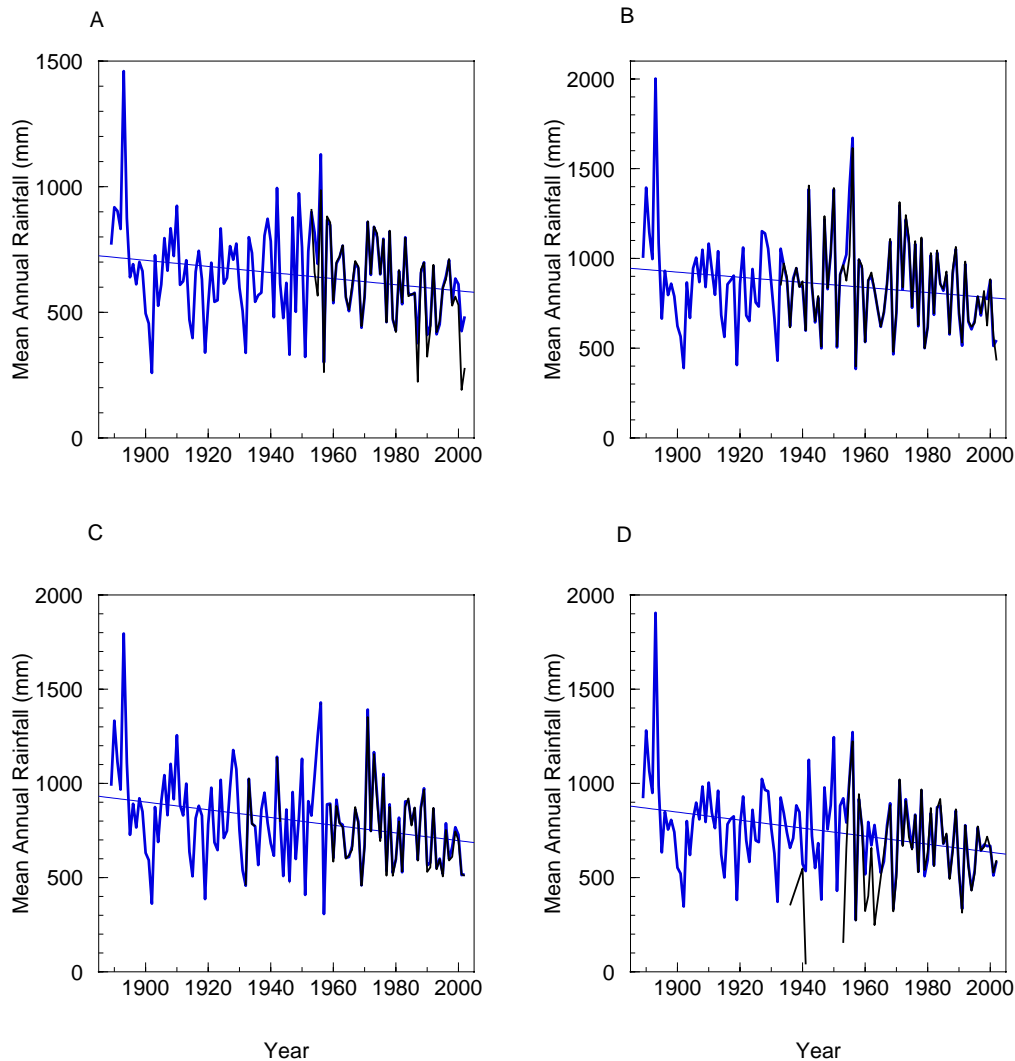


Figure 12: Raw annual rainfall (dark blue) and interpolated (light blue) annual rainfall time series data for the a) Tecoma b) Kalpowar c) Malakof and d) Bancroft rainfall stations. The straight line represents the linear regression for the interpolated annual rainfall series from 1889 to 2003.

The linear trend analysis performed on the interpolated rainfall data for each station in the Central sub-region (Figure 13) produced the following results:

- A. 42059 (Auburn) – $y = -1.173x + 2964.54$ ($r^2 = 0.037$, $P < 0.05$)
- B. 39039 (Gayndah) – $y = -0.974x + 2653.08$ ($r^2 = 0.028$, $P < 0.05$)
- C. 39036 (Eidsvold) – $y = -1.071x + 2801.32$ ($r^2 = 0.031$, $P = \text{NS}$)
- D. 40021 (Biggenden) – $y = -1.211x + 3241.24$ ($r^2 = 0.026$, $P = \text{NS}$)

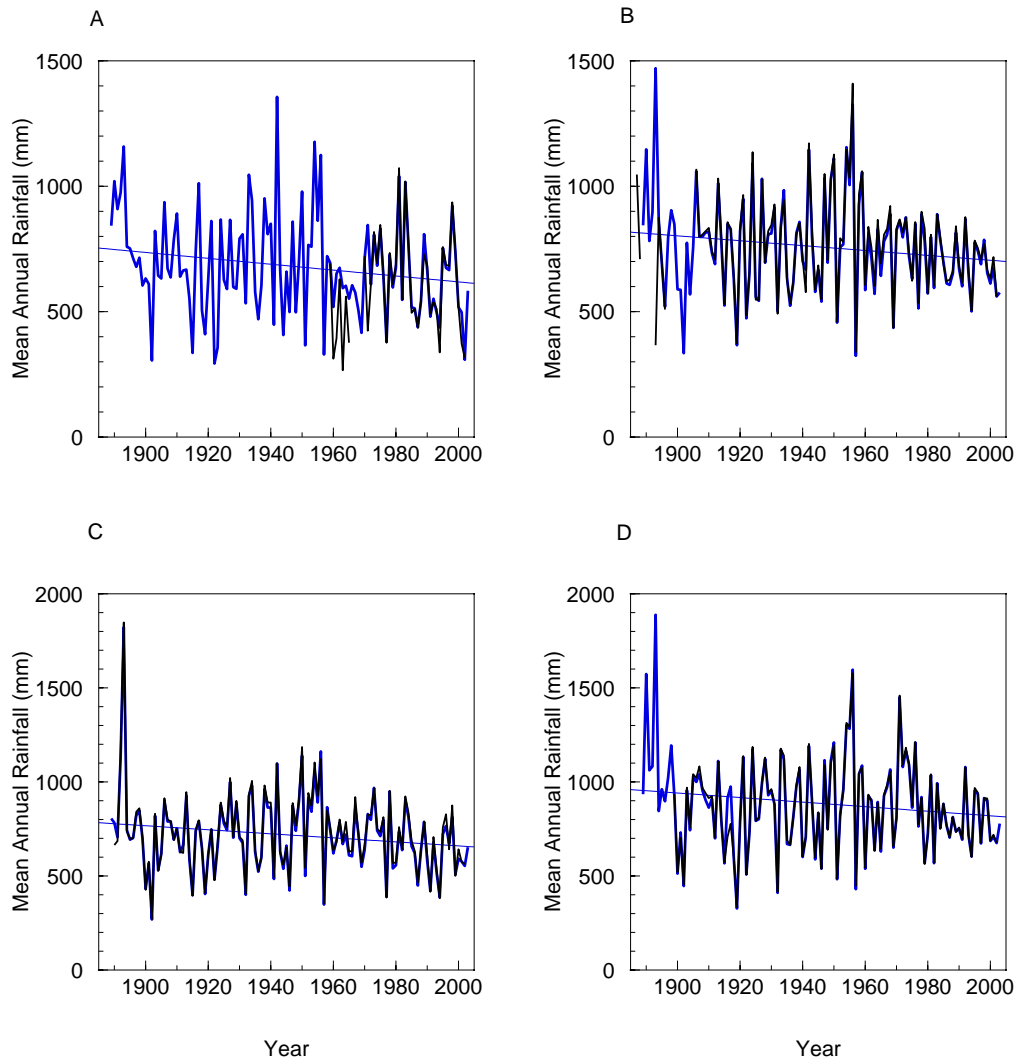


Figure 13: Raw annual rainfall (dark blue) and interpolated (light blue) annual rainfall time series data for the a) 42059 (Auburn), b) 39039 (Gayndah), c) 39036 (Eidsvold) and d) 40021 (Biggenden) rainfall stations. The straight line represents the linear regression for the interpolated annual rainfall series from 1889 to 2003.

The linear trend analysis performed on the interpolated rainfall data for each station in the South sub-region (Figure 14) produced the following results:

- A. 40138 (Mounefontein) – $y = -0.701x + 2094.69$ ($r^2 = 0.015$, $P = \text{NS}$)
- B. 40090 (Goomeri) – $y = -1.293x + 3316.51$ ($r^2 = 0.043$, $P < 0.05$)
- C. 40112 (Kingaroy) – $y = -0.258x + 1280.34$ ($r^2 = 0.002$, $P = \text{NS}$)
- D. 40113 (Kumbia) – $y = -0.400x + 1566.64$ ($r^2 = 0.005$, $P = \text{NS}$)

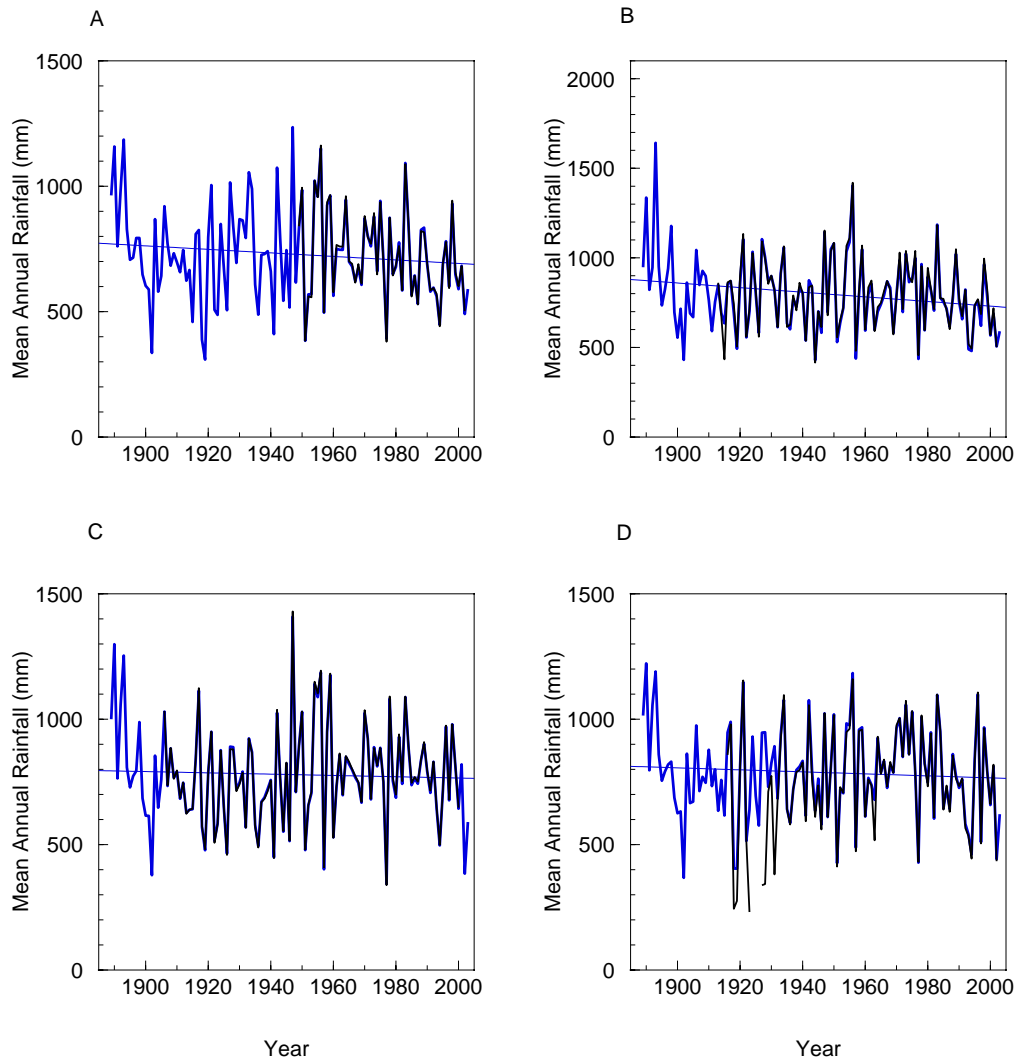


Figure 14: Raw annual rainfall (dark blue) and interpolated (light blue) annual rainfall time series data for the a) 40138 (Mounefontein, b) 40090 (Goomeri), c) 40112 (Kingaroy), and d) 40113 (Kumbia) rainfall stations. The straight line represents the linear regression for the interpolated annual rainfall series from 1889 to 2003.

2. Temperature Correlation Analysis

A number of statistical analyses were employed to assess the correlation between raw and interpolated temperature. These included the calculation of the correlation co-efficient, the one-to-one test, and an assessment of covariance. The mean, median and standard deviation values were again presented in order to allow a comparison between raw and interpolated data. Similarly the linear trend equations were presented for both interpolated and raw data to allow for comparisons to be drawn. The results revealed an important limitation of the interpolated data particularly when data was scarce. The comparison of observed and interpolated Kalpowar station data revealed poor correlation due to the interpolated data resembling a more coastal environment due to the influence of the Bundaberg station.

The comparison of raw and interpolated data for the Kingaroy station revealed strong agreement mean and median values for maximum, minimum, highest maximum and lowest minimum temperatures (Table 18). As with most of the interpolated rainfall station data, the interpolated temperature data exhibited marginally lower variability than the raw data. The correlation co-efficient values exhibited a strong mean correlation although maximum temperatures showed a slightly weaker relationship (Table 18). The one-to-one test revealed discrepancies between interpolated and raw maximum and minimum temperatures at the lower end of the temperature scale. In the case of the lowest minimum temperature comparison, two outliers (i.e. greater observed values) served to enhance the regression line beyond the ideal slope of 1 (Table 18).

Table 18: A statistical comparison of raw and interpolated temperature for station 40112 (Kingaroy). While the interpolated data series extends from 1889 to 2003 the Kingaroy raw data only extends from 1957 to 2002. For this reason all statistical tests were performed on data for the period 1957 to 2002.

1957 – 2002	TMAX	TMIN	MAX_TMAX	MIN_TMIN
MEAN – Interpolated	24.9	11.7	37.2	-3.1
MEAN - Raw	24.6	11.4	37.1	-3.6
MEDIAN – Interpolated	24.8	11.7	37.0	-3.0
MEDIAN - Raw	24.6	11.5	37.0	-3.6
STD – Interpolated	0.6	0.7	1.6	1.6
STD - Raw	0.8	0.8	1.6	1.6
CORRELATION CO-EFFICIENT (r)	0.78	0.96	0.98	0.96
COVARIANCE	0.34	0.53	2.54	2.41
ONE-TO-ONE TEST	0.99	0.98	1.00	1.12
CO-EFFICIENT OF DETERMINATION (r ²)	0.60	0.89	0.96	0.90
SIGNIFICANCE (P)	<0.01	<0.01	<0.01	<0.01
y= mx + c - Interpolated x ≈ Years	0.0116x + 2.01 (R ² = 0.06, P = NS)	0.0284x – 44.57 (R ² = 0.29, P <0.01)	0.0172x + 3.18 (R ² = 0.01, P = NS)	0.0422x – 86.53 (R ² = 0.12, P <0.05)
y= mx + c - Raw	0.0098x + 5.14 (R ² = 0.02, P = NS)	0.0365x – 60.90 (R ² = 0.31, P <0.01)	0.0196x – 1.72 (R ² = 0.02, P = NS)	0.0508x – 104.04 (R ² = 0.17, P <0.01)

The covariance statistic showed that although the raw and interpolated ranges moved together (i.e. positive covariance) the values were relatively small. While this was primarily a function of the unit of measure the statistic did demonstrate that the covariance was lower for temperature than for rainfall for the stations analysed (Table 18). The comparison of raw and interpolated

temperature data for the Kalpowar climate station revealed very poor agreement between data sets (Table 19). The correlation co-efficient statistic demonstrated almost no relationship between raw and interpolated data. Similarly the one-to-one test and measure of covariance highlighted the poor correlation between data sets.

The linear trend analysis demonstrated poor agreement with both maximum and minimum temperature trend diametrically opposed (Table 19). Given the poor correlation between the raw and interpolated data a judgement was required as to which dataset would be used in the simulation experiments. Given the interpolated data provided both a longer time series and contained a regional signal (i.e. the interpolations were based on stations in the vicinity) it was decided to use the interpolated data.

Table 19: A statistical comparison of raw and interpolated temperature for station 39057 (Kalpowar). While the interpolated data series extends from 1889 to 2003 the Kalpowar raw data only extended from 1962 to 2002. For this reason all statistical tests were performed on data for the period 1962 to 2002.

1962 – 2002	TMAX	TMIN	MAX_TMAX	MIN_TMIN
MEAN – Interpolated	25.8	13.6	36.5	-1.0
MEAN - Raw	22.0	10.4	36.7	-4.0
MEDIAN – Interpolated	25.8	13.6	36.5	-0.5
MEDIAN - Raw	21.3	10.1	36.7	-4.1
STD – Interpolated	0.5	0.5	1.6	1.7
STD - Raw	2.8	1.3	1.7	2.1
CORRELATION CO-EFFICIENT (r)	0.17	0.09	0.90	0.65
COVARIANCE	0.23	0.06	2.36	2.33
ONE-TO-ONE TEST	0.85	0.77	1.01	1.60
CO-EFFICIENT OF DETERMINATION (r^2)	0.03	-0.04	0.81	-1.22
SIGNIFICANCE (P)	NSS	NSS	<0.01	NSS
y= mx + c - Interpolated $x \approx \text{Years}$	0.0111x + 3.89 ($R^2 = 0.03$, $P = \text{NS}$)	0.0350x – 55.50 ($R^2 = 0.31$, $P < 0.01$)	-0.0042x + 44.90 ($R^2 = 0.0005$, $P = \text{NS}$)	0.0516x – 102.93 ($R^2 = 0.06$, $P = \text{NS}$)
y= mx + c - Raw	-0.02677x + 550.95 ($R^2 = 0.64$, $P < 0.01$)	-0.0181x + 46.14 ($R^2 = 0.01$, $P = \text{NS}$)	-0.0304x + 96.76 ($R^2 = 0.02$, $P = \text{NS}$)	0.1188x – 238.66 ($R^2 = 0.22$, $P < 0.05$)

The length of temperature record for the Bundaberg climate station served to produce a very strong agreement between raw and interpolated temperature data (Table 20). The mean and median temperature values exhibited less than 0.2°C differences for maximum, minimum and highest maximum temperatures. The lowest minimum temperatures exhibited greater differences of 2.3 and 3.4 °C for mean and median values respectively (Table 20).

The one-to-one analysis showed that the large differences in mean and median values were a function of higher interpolated values than contained in the raw data (i.e. 10 outliers where the interpolated data was at least one standard deviation greater than the raw data).

The linear trend analysis revealed a weakening of the declining trend in maximum temperature as well as the positive trend in minimum temperature. While the trend in interpolated maximum temperature was not statistically significant at the 95% confidence interval, the trends in

interpolated minimum, highest maximum and lowest minimum were significant at the 99% and 95% confidence intervals.

Table 20: A statistical comparison of raw and interpolated temperature for station 39015 (Bundberg). While the interpolated data series extends from 1889 to 2003 the Bundaberg raw data only extended from 1892 to 2002. For this reason all statistical tests were performed on data for the period 1892 to 2002.

1892 – 2002	TMAX	TMIN	MAX_TMAX	MIN_TMIN
MEAN – Interpolated	26.7	16.3	35.2	4.2
MEAN - Raw	26.6	16.1	35.2	1.9
MEDIAN – Interpolated	26.7	16.2	35.0	4.0
MEDIAN - Raw	26.5	16.1	35.1	0.6
STD – Interpolated	0.5	0.7	1.4	1.3
STD - Raw	0.6	0.7	1.6	2.2
CORRELATION CO-EFFICIENT (r)	0.76	0.86	0.77	0.33
COVARIANCE	0.21	0.41	1.66	0.97
ONE-TO-ONE TEST	0.9989	0.9881	1.0018	0.4522
CO-EFFICIENT OF DETERMINATION (r ²)	0.57	0.72	0.58	0.11
SIGNIFICANCE (P)	<0.01	<0.01	<0.01	<0.01
y= mx + c - Interpolated x ≈ Years	-0.0014x + 29.43 (R ² = 0.01, P = NS)	0.0170x – 16.64 (R ² = 0.50, P <0.01)	-0.0109x + 56.25 (R ² = 0.05, P <0.05)	0.0264x – 47.07 (R ² = 0.32, P <0.05)
y= mx + c - Raw	-0.0059x + 38.15 (R² = 0.08, P<0.01)	0.0128x – 8.73 (R² = 0.28, P<0.01)	-0.0092x + 53.07 (R² = 0.03, P =NS)	-0.0055x + 12.58 (R² = 0.01, P =NS)

The comparison of raw and interpolated temperature data for the Gayndah station again revealed relatively strong agreement between the two datasets as the extent of the raw record was in excess of 100 years (Table 21). The mean and median values showed slightly greater variation than for the Bundaberg and Kingaroy stations indicating a slightly weaker correlation between raw and interpolated data (Table 21). The raw data exhibited greater standard deviation values for all the temperature variables analysed suggesting, once again that the raw data exhibited greater within sample variability.

The correlation coefficient statistic and one-to-one analysis showed a weaker agreement between data than for the Bundaberg and Kingaroy stations, with the one-to-one test revealing a number of outliers in the comparison of minimum temperature. In the case of the minimum temperature comparison the outliers were made up of greater interpolated values compared with the raw (Table 21). These findings suggest that the interpolation procedure employed in the derivation of the data sets does not capture the lower extremes in temperature. This conclusion has also been made in the Rayner *et al.*, 2004 report and further suggests that upper extremes will be affected in the same way due to the smoothing introduced by the interpolation technique.

In the case of the linear trend analysis the interpolated minimum temperature data demonstrated a slight reduction of the warming trend although this trend remained significant at the 95% confidence interval.

Table 21: A statistical comparison of raw and interpolated temperature for station 39039 (Gayndah). While the interpolated data series extends from 1889 to 2003 the Bundaberg raw data only extended from 1893 to 2002. For this reason all statistical tests were performed on data for the period 1893 to 2002.

1893 - 2002	TMAX	TMIN	MAX_TMAX	MIN_TMIN
MEAN – Interpolated	27.9	13.6	39.0	-0.6
MEAN - Raw	28.0	13.5	40.2	-1.3
MEDIAN – Interpolated	27.9	13.5	39.0	-0.5
MEDIAN - Raw	28.0	13.4	40.3	-1.1
STD – Interpolated	0.6	0.7	1.7	1.3
STD - Raw	1.0	1.0	2.1	1.5
CORRELATION CO-EFFICIENT (r)	0.68	0.88	0.73	0.78
COVARIANCE	0.39	0.60	2.57	1.49
ONE-TO-ONE TEST	1.00	0.99	1.03	1.14
CO-EFFICIENT OF DETERMINATION (r ²)	0.44	0.71	0.52	0.43
SIGNIFICANCE (P)	<0.01	<0.01	<0.01	<0.01
y= mx + c - Interpolated x ≈ Years	-0.0009x + 29.7 (R ² = 0.002, P = NS)	0.0135x – 12.71 (R ² = 0.39, P <0.01)	0.0130x + 13.70 (R ² = 0.06, P <0.01)	0.0067x – 13.57 (R ² = 0.03, P = NS)
y= mx + c – Raw	0.0010x + 26.07 (R ² = 0.001, P = NS)	0.0201x – 25.70 (R ² = 0.42, P <0.01)	-0.0194x + 77.97 (R ² = 0.09, P <0.01)	0.0261x – 52.20 (R ² = 0.31, P <0.01)

The linear trend analyses for maximum and minimum temperature were repeated for each station, within each sub-region on the entire interpolated record (i.e. 1889 to 2003) in order to consider the effect of additional years on the overall trend (Figure 15). In the case of the case of average annual maximum temperature the results were as follows (Figure 15):

- A. 40112 (Kingaroy) – $y = 0.0005x + 24.06$ ($r^2 = 0.001$, $P = NS$)
- B. 39057 (Kalpowar) – $y = 0.0028x + 20.55$ ($r^2 = 0.021$, $P = NS$)
- C. 39015 (Bundaberg) – $y = 0.0014x + 23.91$ ($r^2 = 0.008$, $P = NS$)
- D. 39039 (Gayndah) – $y = 0.0003x + 27.29$ ($r^2 = 0.0003$, $P = NS$)

In the case of the case of average annual minimum temperature the results were as follows (Figure 16):

- A. 40112 (Kingaroy) – $y = 0.0117x - 11.60$ ($r^2 = 0.284$, $P <0.01$)
- B. 39057 (Kalpowar) – $y = 0.0213x - 28.76$ ($r^2 = 0.50$, $P <0.01$)
- C. 39015 (Bundaberg) – $y = 0.0143x - 11.45$ ($r^2 = 0.453$, $P <0.01$)
- D. 39039 (Gayndah) – $y = 0.0112x - 8.28$ ($r^2 = 0.287$, $P <0.01$)

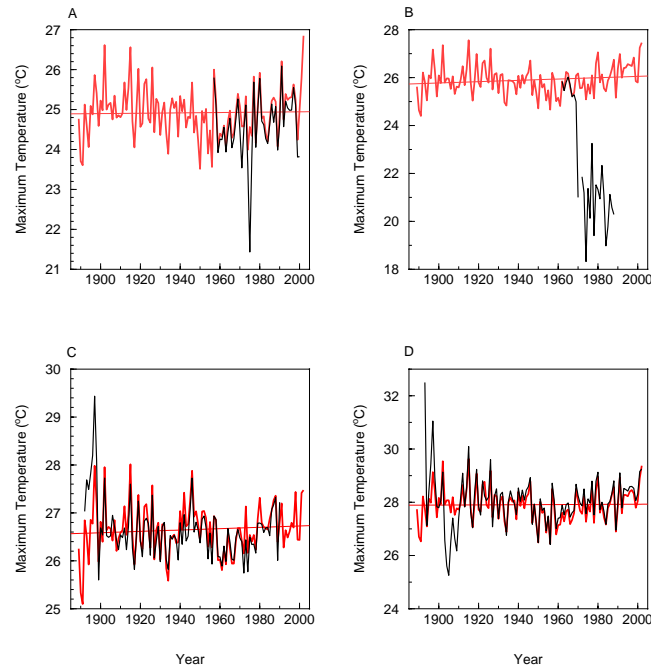


Figure 15: A time series of average annual maximum temperature for a) the South sub-region (40112 - Kingaroy), b) the North sub-region (39057 - Kalpowar), c) the East sub-region (39015 - Bundaberg) and d) the Central sub-region (39039 – Gayndah). The red line represents the interpolated data and the black line represents the raw data.

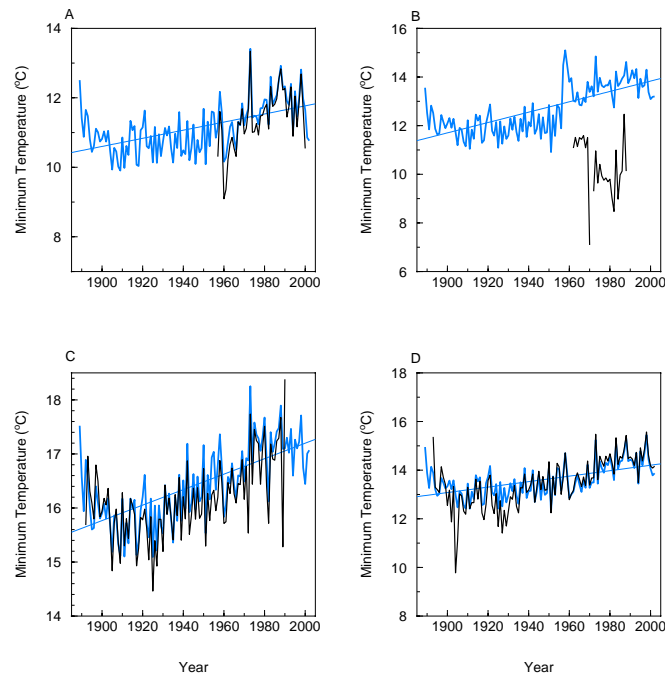


Figure 16: A time series of average annual minimum temperature for a) the South sub-region (40112 - Kingaroy), b) the North sub-region (39057 - Kalpowar), c) the East sub-region (39015 - Bundaberg) and d) the Central sub-region (39039 – Gayndah). The blue line represents the interpolated data and the black line represents the raw data.

3. Summary of Interpolated and Raw Climate Data Comparisons

The analysis of raw rainfall and temperature data revealed a number of important issues regarding data integrity in the Burnett Study region.

These were:

- The raw and interpolated rainfall data showed strong agreement across all stations (except Moolboolaman, The Cedars, Aurburn, Gayndah and Kumbia) exhibiting correlation coefficient values above 0.92. In the case of the stations listed above the correlation coefficient values ranged from 0.82 to 0.88. The strong correlation with raw rainfall station data provided some confidence in the use of the interpolated data in the subsequent biophysical modelling.
- The raw and interpolated temperature data revealed weaker agreement with maximum temperature data consistently lower than minimum, highest maximum and lowest minimum temperature comparisons.
- The linear trend analyses performed on the interpolated rainfall data varied little against the raw data except in 6 out of 48 cases. In each of the cases neither the raw nor interpolated linear rainfall trend were statistically significant. This suggested that the interpolated rainfall station data was suitable for trend analyses if the limitations of the data are recognised.
- The linear trend analyses performed on the interpolated temperature data showed greater variation with 5 out of 15 cases where the raw and interpolated trends were opposed. In 3 of the 5 cases the change in the trends were statistically significant. This would suggest that the interpolated temperature data for this region should be used with extreme caution in any type of trend analyses.
- An examination of the entire interpolated rainfall data time series revealed consistent declining annual rainfall trends across all stations, with seven stations returning declining trends below the 95% confidence interval. This would suggest that the trends were strongly influenced by intra-seasonal climate variability (substantiated by summer and winter linear trend analyses). The examination of daily statistics for different three-month windows, presented in the following section, provide more insight into the nature of the trends.
- An examination of the entire interpolated temperature data time series revealed consistent warming trends in both average maximum and minimum temperatures. The maximum temperature trends were however all below the 95% confidence interval. These results corresponded well with the official Bureau of Meteorology trend analyses, which showed minimum temperatures warming far more rapidly than maximum temperatures.

To re-iterate, both the raw and interpolated climate data revealed consistent drying trends in summer rainfall over much of the study region as well as warming in minimum temperatures. The agreement between interpolated and raw data was such as to allow the interpolated data to be examined further for daily statistical trends and to utilise as the base climate files for use in the biophysical modelling discussed in subsequent sections.

Linear Trend Analysis of Extreme and Daily Climate Indices

The interpolated data was used to calculate extreme and daily climate indices for the period 1890 to 2002. These indices included 95th percentile diurnal temperature range, wet day persistence, dry day persistence, and greatest annual 10-day rainfall period. A more comprehensive list of all climate indices can be found in Appendix A. The climate indices and linear trend analysis was performed using the Statistical and Regional Dynamic Downscaling of Extremes software (STARDEX 3.3.0). The software was originally developed by the US National Climatic Data Centre (NCDC) and included about 20 climate indices. A further 20 indices were added by Malcolm Haylock from the Australian Bureau of Meteorology in 2000. Further indices were added by Colin Harpham of King's College London, after receiving the code from the European Climate Assessment (ECA), relating to wet and dry spells.

Given the results from the comparisons of raw and interpolated temperature data, particularly in the North sub-region, it was decided that an additional station be chosen to represent possible trends in temperature (Figure 17). An additional station was included for each of the other sub-regions in order to ensure that the station selection within each sub-region would adequately capture the inherent variability (Figure 17).

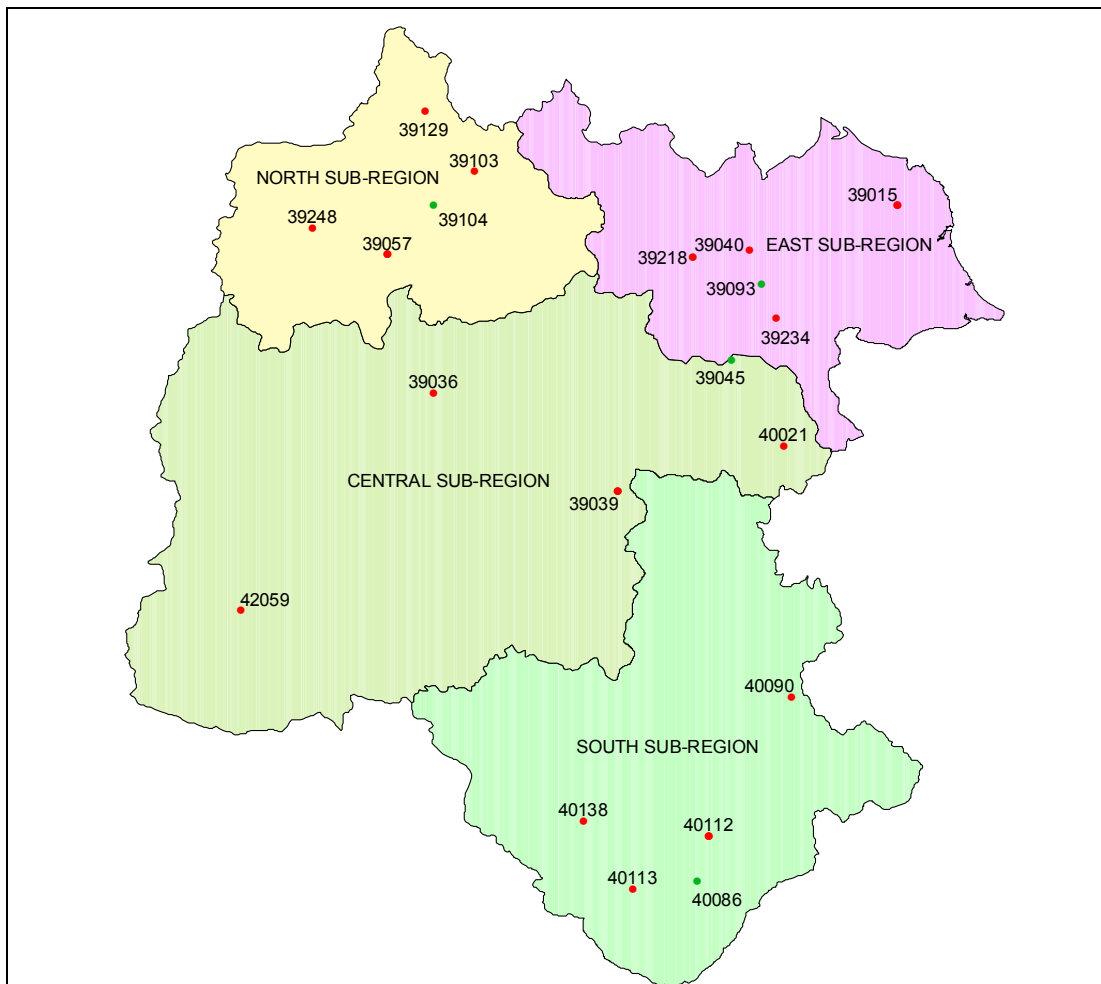


Figure 17: A locality map of the Burnett study area showing both the original climate station selection (highlighted in red) and the additional sites (highlighted in green) for all four sub-regions.

1. **Linear Trend Analysis of Climate Indices for the East Sub-Region**

The analysis of the Bundaberg climate station revealed statistically significant trends in both temperature and rainfall indices. Statistically significant positive trends were found in mean maximum temperatures during the March to May (MAM) and June to August (JJA) periods, explaining only approximately four and five percent of the overall time series variability in each case ($y=0.0042x + 19.0523$, $r^2=0.04$ $P=0.03$; $y=0.0047x + 13.326$, $r^2=0.05$ $P=0.03$). This would explain why the linear trend analysis of the mean annual maximum temperature time series returned a “non-significant” positive trend.

The minimum temperatures exhibited statistically significant positive trends for all three-month periods analysed with the JJA and September to November (SON) periods exhibiting the greatest warming (i.e. $y=0.0183x - 24.62$, $r^2=0.28$ $P=0.001$; $y=0.0143x - 11.401$, $r^2=0.31$ $P=0.001$). In response to the strong warming trend in minimum temperatures and weaker warming trends in maximum temperatures, diurnal temperature ranges across each of the three-month periods exhibited statistically significant declines.

In addition to the declining diurnal temperature range, the 90th percentile heat wave duration for the periods December to February (DJF), SON exhibited a declining trend as a result of longer duration heat waves in the earlier part of the record ($y= -0.0318x + 65.731$, $r^2=0.09$ $P=0.0007$ for DJF and $y= -0.0291x + 54.6551$, $r^2=0.10$ $P=0.0017$ for SON). Similarly the analysis of cold wave duration also revealed statistically declining trends over the MAM and JJA ($y= -0.0133x + 26.64$, $r^2=0.03$ $P=0.018$ for MAM and $y= -0.0246x + 49.1317$, $r^2=0.05$ $P=0.0008$ for JJA).

The linear trend analysis of the Bundaberg rainfall indices suggested that the declining annual rainfall trend was produced by declines in large daily falls (i.e. above the 60th percentile), with little difference in daily rainfall below the 60th percentile. The declining trend in the 60th, 80th, 90th and 95th percentile of rainfall amounts occurred predominantly in the DJF three-month period:

1. $y= -0.0362x + 80.975$, $r^2=0.06$ $P=0.0018$ for DJF;
2. $y= -0.0687x + 156.334$, $r^2=0.05$ $P=0.0107$ for DJF;
3. $y= -0.1453x + 320.459$, $r^2=0.07$ $P=0.0105$ for DJF; and
4. $y= -0.2255x + 494.759$, $r^2=0.07$ $P=0.0116$ for DJF.

The declining annual trend was also a function of a decline in the maximum number of consecutive wet days and mean wet-day persistence, with declining trends again significant for the DJF period.

In the case of the Gin Gin climate station the production of the climate indices and subsequent linear trend analyses revealed fewer statistically significant temperature indices trends. In this case no maximum temperature indices produced significant linear trends, and only annual and SON mean minimum temperature produced warming trends of $y= 0.0143x - 12.813$, $r^2=0.46$ $P=0.0001$ and $y= 0.0134x - 10.9092$, $r^2=0.28$ $P=0.0001$ respectively.

As in the case of the Bundaberg climate station, the Gin Gin station demonstrated statistically significant declining trends in mean diurnal temperature range across all three-month periods analysed as well as across the year as a whole.

1. $y= -0.0128x + 35.29$, $r^2=0.25$ $P=0.0001$ for DJF;
2. $y= -0.0127x + 35.98$, $r^2=0.12$ $P=0.0001$ for MAM;

3. $y = -0.0105x + 33.63$, $r^2=0.08$ $P=0.005$ for JJA;
4. $y = -0.0165x + 44.59$, $r^2=0.27$ $P=0.0001$ for SON; and
5. $y = -0.0128x + 36.72$, $r^2=0.27$ $P=0.0001$ for the annual daily average.

This would support the general observation that daily minimum temperatures are increasing more rapidly than daily maximum temperatures and hence leading to a reduction in mean diurnal temperature range (Pittock *et al.*, 2004).

The Gin Gin climate station also demonstrated a statistically significant increase in the percentage days where maximum temperature was above the long-term 90th percentile (i.e. extreme temperature events) for the JJA period as well as a decline in the percentage number of days where minimum temperatures were below the long-term 10th percentile threshold (declining trends determined for all periods analysed).

The rainfall indices for the Gin Gin climate station revealed a similar behaviour to the Bundaberg station with statistically significant declines in heavier rains (i.e. the 50th, 60th, 90th, 95th percentile rains). For the most part the declining trends were limited to the DJF period except in the case of the 95th percentile rain events where both annual and DJF periods produced statistically significant declining trends. The linear trends were as follows:

1. $y = -0.0294x + 65.74$, $r^2=0.05$ $P=0.0265$ for 50th percentile rainday amounts in DJF;
2. $y = -0.0298x + 69.23$, $r^2=0.04$ $P=0.0134$ for 60th percentile rainday amounts in DJF;
3. $y = -0.0976x + 225.82$, $r^2=0.05$ $P=0.0317$ for 90th percentile rainday amounts in DJF;
4. $y = -0.2126x + 464.78$, $r^2=0.07$ $P=0.0069$ for 95th percentile rainday amounts in DJF; and
5. $y = -0.0986x + 237.78$, $r^2=0.05$ $P=0.0324$ for 95th percentile rainday amounts for the annual daily average.

The decline in percentile rainday amounts were also accompanied with declines in greatest 3, 5 and 10 day total rainfall in the DJF, supporting the hypothesis that the declining annual rainfall trends experienced over the period 1890 to 2002 were a function of declining late summer extreme rains.

The Moolboolaman climate station possessed an extensive rainfall time series (1890 to 2002) but had made no measurement of daily temperatures. For this reason the temperature trends exhibited by this station (produced from the interpolated data) were not reported.

The analysis of rainfall indices for the Moolboolaman climate station revealed that while annual average rainfall (Figure 11c) and the annual average daily rainfall (i.e. $y = -0.0052x + 12.73$, $r^2=0.04$ $P=0.032$) had demonstrated a statistically significant decline for the period 1890 to 2002, the SON period demonstrated statistically significant increasing trends in 80th and 90th and 95th percentile rainday amounts:

1. $y = 0.0537x - 90.01$, $r^2=0.09$ $P=0.0027$ for 80th percentile rainday amounts in SON;
2. $y = 0.1012x - 175.33$, $r^2=0.15$ $P=0.0001$ for 90th percentile rainday amounts in SON; and
3. $y = 0.1372x - 239.07$, $r^2=0.07$ $P=0.0003$ for 95th percentile rain rainday amounts in SON.

While SON 80th, 90th and 95th percentile rainday amounts demonstrated increasing trends the DJF, MAM and annual average periods demonstrated a decline in the maximum number of consecutive wet days:

1. $y = -0.0336x + 72.86$, $r^2=0.08$ $P=0.0001$ for maximum number of consecutive wet days in DJF;
2. $y = -0.0105x + 25.81$, $r^2=0.02$ $P=0.0341$ for maximum number of consecutive wet days in MAM; and
3. $y = -0.0317x + 69.96$, $r^2=0.08$ $P=0.0001$ for maximum number of consecutive wet days annually.

In addition to the decline in the maximum consecutive wet days, the length of wet spells also demonstrated statistically significant declining trends across all periods analysed. This would suggest that in this Moolboolaman region rainfall has become more infrequent (i.e. decreasing wet spell lengths $y = -0.0046x + 11.09$, $r^2 = 0.18$ $P = 0.0001$ and increasing dry spell lengths $y = 0.0077x - 7.33$, $r^2 = 0.02$ $P = 0.0218$), although when it does occur it has been more intense.

The “The Cedars” climate station did differ from the previous climate stations, as it did not demonstrate any statistically significant trends (increasing or decreasing) for extreme rainday amounts. The climate station did however return statistically significant declining trends for wet spell persistence, mean wet spell length and greatest 3, 5 and 10-day total rainfall over the DJF period.

1. $y = -0.0012x + 2.87$, $r^2 = 0.11$ $P = 0.0002$ for wet spell persistence in DJF;
2. $y = -0.0064x + 14.93$, $r^2 = 0.09$ $P = 0.0002$ for mean wet spell length in DJF;
3. $y = -0.5553x + 1204.15$, $r^2 = 0.05$ $P = 0.0179$ for greatest 3-day total rainfall in DJF;
4. $y = -0.7173x + 1540.59$, $r^2 = 0.06$ $P = 0.0039$ for greatest 5-day total rainfall in DJF
5. $y = -0.9221x + 1974.96$, $r^2 = 0.08$ $P = 0.0183$ for greatest 10-day total rainfall in DJF consecutive wet days annually.

This result would suggest that in the “The Cedars region rainfall declines resulted from increasing infrequency of rain with no compensating effect on intensity.

The additional station chosen for the eastern sub-region was climate station 39093 (Wallaville). The DJF three-month period was the only period to demonstrate statistically significant declining trends in both average daily rainfall and for extreme rainfall (i.e. 90th and 95th). The declines in this three-month period were strong enough to influence the annual period of analysis as well and result in a statistically significant declining annual trend. Similarly both wet spell persistence and mean wet spell length also demonstrated declining trends for the DJF period.

2. **Linear Trend Analysis of Climate Indices for the North Sub-Region**

The linear trend analysis was first performed on the Tecoma climate station. The analysis revealed that maximum temperatures demonstrated a statistically significant warming trend only for the JJA period (i.e. $y = 0.005x + 12.48$, $r^2 = 0.04$ $P = 0.0324$). Minimum temperatures demonstrated statistically significant warming trends for all periods analysed with the greatest rate of warming found in the JJA three-month period:

1. $y = 0.010x - 0.76$, $r^2 = 0.19$ $P = 0.0001$ for DJF;
2. $y = 0.017x - 20.40$ $r^2 = 0.22$ $P = 0.0001$ for MAM;
3. $y = 0.019x - 31.22$, $r^2 = 0.19$ $P = 0.0001$ for JJA;
4. $y = 0.015x - 16.66$, $r^2 = 0.26$ $P = 0.0001$ for SON; and
5. $y = 0.015x - 17.23$, $r^2 = 0.36$ $P = 0.0001$ for the annual daily average.

As was demonstrated for the Bundaberg climate station in the East sub-region, mean diurnal temperature range showed statistically significant declining trends across all the periods analysed. The temperature extremes (i.e. warm and cold extremes) also demonstrated statistically significant trends, these included declining trends in the 10th percentile maximum temperature during the DJF and SON period as well as a warming trend in the 90th percentile maximum temperatures in the JJA period.

Statistically significant warming trends were revealed in both the 10th and 90th percentile minimum temperatures across all analysis periods. This would indicate that while there appeared to be a relative cooling in the lower percentile summer (DJF and SON) maximum temperatures the lower and upper percentile minimum temperatures showed consistent warming across all analysis periods.

Consistent with the warming of mean maximum temperatures demonstrated in the JJA period was a statistically significant increase in the duration of the 90th percentile heat wave duration (i.e. $y = 0.014x - 24.90$, $r^2 = 0.04$ $P = 0.0036$ for the JJA period). Further analysis of the indices did reveal that the extensive heat 90th percentile heat wave duration in 2001 (i.e. 13 days, highest on record) would have strongly influenced on the trend.

The linear trend analysis of the rainfall indices for Tecoma demonstrated statistically significant positive trends in percentile rainday amounts for the 20th, 40th, 50th, 60th, 80th, 90th and 95th percentiles. This increase appeared to take place in a stepwise manner after 1950 and could thus be some function of the interpolation process. However if this were indeed some function of the interpolation process it would be likely to have produced greater annual average values as well. The linear trend analysis of the annual average rainday amounts did not reveal this stepwise characteristic and thus the increase in percentile rainday amounts would appear not to be an arithmetic function of interpolation.

While the Tecoma climate station demonstrated an increase in percentile rainday amounts, the linear trend analysis revealed a concomitant increase in the maximum number of consecutive dry days across all analysis periods except for JJA:

1. $y = 0.062x - 102.58$, $r^2 = 0.07$ $P = 0.0014$ for DJF;
2. $y = 0.109x - 180.88$ $r^2 = 0.06$ $P = 0.0016$ for MAM;
3. $y = 0.071x - 111.93$ $r^2 = 0.05$ $P = 0.0096$ for SON; and
4. $y = 0.103x - 151.34$, $r^2 = 0.03$ $P = 0.0141$ for the annual average values.

The Tecoma climate station also demonstrated statistically significant declining trends in mean wet-day persistence and wet spell length as well as increasing trends in dry spell persistence and dry-spell length across all analysis periods.

The Tecoma climate station thus demonstrated statistically significant warming of minimum temperatures as well as declines in frequency of rain. The climate station did however reveal that while annual average rainfall had declined annual rainfall intensity (rain per rainday) and rainday amounts had increased (i.e. $y = 0.020x - 34.06$ $r^2=0.06$ $P=0.0006$ for annual average rainfall intensity).

The Kalpowar climate station temperature indices revealed statistically significant linear warming trends. In the case of mean maximum temperature, both MAM and JJA demonstrated significant warming trends, although most of the warming appears to have occurred over the last 20 years (i.e. $y = 0.006x + 13.36$ $r^2=0.07$ $P=0.0173$ for MAM and $y = 0.005x + 10.25$ $r^2=0.05$ $P=0.0148$).

In the case of mean minimum temperatures statistically significant warming trends were determined for all analysis periods, however given the poor relationship between the raw and interpolated temperatures and the stepwise characteristic of the time series data (i.e. post 1957 minimum temperatures significantly higher than pre 1957 temperatures) it was impossible to determine the validity of the trends exhibited by the temperature indices.

The Kalpowar raw and interpolated rainfall demonstrated strong correlation over the analysis period 1933 to 2002 and hence more confidence could be placed on the resultant linear trend analyses of the derived rainfall indices. The measures of wet spell persistence and mean wet spell length, as well as dry spell persistence and mean dry spell length demonstrated statistically significant declining and increasing trends respectively across all analysis periods. The annual indices returned the following trends:

1. $y = -0.001x + 3.25$, $r^2=0.28$ $P=0.0001$ for annual wet spell persistence;
2. $y = -0.006x + 13.61$, $r^2=0.17$ $P=0.0001$ for annual mean wet spell length;
3. $y = 0.001x - 0.33$, $r^2=0.06$ $P=0.0172$ for annual dry spell persistence; and
4. $y = 0.010x - 13.59$, $r^2=0.03$ $P=0.0192$ for annual mean dry spell length.

The results from this climate station were ambiguous regarding temperature trends but returned a statistically significant declining trend in annual rainfall. This would appear to be the function of increasing infrequency of rainfall events.

The derivation of climate indices and subsequent linear trend analyses for the Malakof climate station revealed statistically significant increases in heavier rains (i.e. the 50th, 60th, 90th, 95th percentile rains). The 50th and 60th percentile rainday amounts demonstrate statistically significant increasing trends across all analysis periods except for JJA. The 80th, 90th and 95th percentile rainday amounts exhibited significant increasing trends for the periods MAM and SON. The extent of increase in these two periods produced significant increasing trends in the annual average 90th and 95th percentile rainday amounts as well. The annual linear trends were as follows:

1. $y = 0.013x - 19.61$, $r^2=0.08$ $P=0.0001$ for the annual 50th percentile rainday amount;
2. $y = 0.018x - 27.37$, $r^2=0.08$ $P=0.0001$ for the annual 60th percentile rainday amount;
3. $y = 0.036x - 54.09$, $r^2=0.09$ $P=0.0001$ for the annual 80th percentile rainday amount;
4. $y = 0.047x - 67.86$, $r^2=0.05$ $P=0.0009$ for the annual 90th percentile rainday amount; and
5. $y = 0.047x - 56.59$, $r^2=0.01$ $P=0.0127$ for the annual 95th percentile rainday amount.

The measures of wet spell persistence and mean wet spell length, as well as dry spell persistence and mean dry spell length demonstrated statistically significant declining and increasing trends respectively across all analysis periods. The annual indices returned the following trends:

1. $y = -0.001x + 2.86$, $r^2=0.20$ $P=0.0001$ for annual wet spell persistence;
2. $y = -0.005x + 12.51$, $r^2=0.20$ $P=0.0001$ for annual mean wet spell length;
3. $y = 0.0004x + 0.02$, $r^2=0.24$ $P=0.0001$ for annual dry spell persistence; and
4. $y = 0.025x - 39.87$, $r^2=0.20$ $P=0.0001$ for annual mean dry spell length.

The declining annual trend for the Malakof climate station appears to be the product of less frequent rains, although the rains that do occur have become more intense.

The Bancroft climate station once again exhibited the stepwise increase in both maximum and minimum temperatures post 1957. For this reason the linear temperature trend analyses were not reported.

The Bancroft climate station did exhibit statistically significant trends in average daily rainfall for both the DJF and JJA period (i.e. $y = -0.014x + 31.21$, $r^2=0.06$ $P=0.036$ for DJF and $y = -0.006x + 11.99$, $r^2=0.05$ $P=0.0275$ for the JJA). The extent of decline in DJF rainday amounts was large enough to influence the annual average rainday linear trend (i.e. $y = -0.006x + 13.26$, $r^2=0.09$ $P=0.0012$) and produce a declining trend.

The decline in rainday amounts in the DJF period also occurred with an increase in the maximum number of consecutive dry days (i.e. $y = 0.036x - 53.71$, $r^2=0.03$ $P=0.0053$), dry spell persistence (i.e. $y = 0.001x - 0.99$, $r^2=0.19$ $P=0.0001$) and mean dry spell length (i.e. $y = 0.018x - 30.11$, $r^2=0.11$ $P=0.0001$).

The Bancroft climate station also demonstrated statistically significant increasing trends in daily rainfall intensity, thus as with many of the stations already analysed, Bancroft's rainfall declines are accompanied by increases in daily rainfall intensity across all periods analysed.

The additional climate station considered for this sub-region was Monto (39104). This station contained rainfall records for the period 1930 to 2002 and temperature data for the period 1960 to 2002. Unfortunately, given the poor station density in this region this climate station also

demonstrated the stepwise increase in temperature post 1957. Therefore, as with the other stations for this region, the temperature trend analyses were not reported.

The Monto climate station exhibited a statistically significant declining trend in average annual and average annual daily rainfall (i.e. $y = -0.004x + 9.38$, $r^2=0.04$ $P=0.0222$ for average annual daily rainfall). The rainfall indices indicated that the declines were once again the function of change in rainfall frequency (i.e. declines in maximum number of consecutive wet days, wet spell persistence and mean wet spell length).

3. Linear Trend Analysis of Climate Indices for the Central Sub-Region

The first climate station analysed for the central sub-region was Auburn (42059). As the central sub-region contained a climate station with a particularly long time series of temperature information (i.e. Gayndah - 1893 to 2002) the transition from observed to synthetic (CLIMARC) surface data was relatively smooth. This was not the case for the North sub-region where the transition between observed and synthetic data was quite pronounced (i.e. stepwise characteristic for all temperature indices time series data.).

The maximum and minimum temperature time series data exhibited statistically significant linear warming trends across the entire record (i.e. 1890 to 2002). The maximum temperatures exhibited a statistically significant warming trend for the JJA three-month period. An examination of the time series data revealed that most of the warming occurred post 1960 (i.e. $y = 0.007x + 7.85$, $r^2 = 0.06$ $P=0.0063$ for the entire record versus $y = 0.024x - 26.85$, $r^2 = 0.11$ $P<0.05$ for the period 1960 to 2002). The minimum temperature displayed statistically significant warming trends across all periods analysed, with most significant warming again post 1960. The 90th percentile minimum temperatures also demonstrated statistically significant warming trends across all analysis periods analysed:

1. $y = 0.012x - 2.63$, $r^2=0.22$ $P=0.0001$ for DJF;
2. $y = 0.011x - 3.89$ $r^2=0.13$ $P=0.0001$ for MAM;
3. $y = 0.018x - 24.03$, $r^2=0.17$ $P=0.0001$ for JJA;
4. $y = 0.011x - 2.73$, $r^2=0.16$ $P=0.0001$ for SON; and
5. $y = 0.012x - 4.24$, $r^2=0.37$ $P=0.0001$ for the annual daily average

As a result of the significant minimum temperature warming trends across all analysis periods and the limited warming trend exhibited by maximum temperatures for the JJA period, mean diurnal temperature ranges demonstrated statistically significant declining trends across all analysis periods.

The rainfall indices generated for this climate station revealed declining trends in daily rainfall amounts in the JJA period and across the year as a whole (i.e. annual daily average rainday amount). The linear trends for the JJA and annual period were:

6. $y = -0.004x + 9.83$, $r^2=0.04$ $P=0.0213$ for DJF; and
7. $y = -0.003x + 7.80$ $r^2=0.03$ $P=0.0252$ for the annual average daily rainday amount.

A further examination of the rainfall data revealed a stepwise change in many of the indices consistent with the shift between interpolated and observed data (i.e. 1959 to 2002) for this reason the remaining linear trend analyses were not reported.

The Gayndah climate station (39039) contained an extensive record of both temperature and rainfall (1893 to 2002), for this reason the linear trend analyses were considered a more robust indication of longer-term changes in climate. The temperature indices demonstrated statistically significant warming trends in JJA maximum temperatures (i.e. $y = 0.005x + 12.98$ $r^2=0.04$ $P=0.025$) as well as minimum temperature for all periods analysed. The greatest rate of warming was demonstrated in the MAM and JJA periods, consistent with the warming in maximum temperatures. The linear trends were as follows:

1. $y = 0.008x + 3.97$, $r^2=0.14$ $P=0.0213$ for DJF
2. $y = 0.015x - 14.80$, $r^2=0.19$ $P=0.0213$ for MAM
3. $y = 0.015x - 22.22$, $r^2=0.15$ $P=0.0213$ for JJA
4. $y = 0.011x - 7.66$, $r^2=0.20$ $P=0.0213$ for SON; and
5. $y = 0.002x - 10.14$, $r^2=0.34$ $P=0.0213$ for annual average daily values.

As with all the other climate stations analysed, Gayndah demonstrated a decline in diurnal temperature range consistent with the more rapid warming demonstrated by the minimum temperature data. The 90th percentile maximum temperature exhibited both a statistically significant warming trend in MAM and JJA periods although the MAM warming was most pronounced over the period 1985 to 2002. The 90th percentile heat wave duration also produced a warming trend in the JJA period (i.e. $y = 0.011x - 19.16$ $r^2=0.04$ $P=0.031$), however an examination of the time series data revealed that the warming trend was the product of the 2001 heat wave duration of 10 days. This value of 10 days was approximately 5 standard deviations from the long-term mean thus representing an extreme individual value.

In terms of daily rainfall amounts the Gayndah station did not return statistically significant trends for any of the analysis periods. The climate station did however demonstrate statistically significant positive trends in annual 80th and 90th percentile rainday amounts, however these trends were the product of low rainday amounts in 1902 (i.e. 90th percentile rainday amount of 10.86mm) and 1904 (i.e. 90th percentile rainday amount of 14.3mm) as well as large rainday amounts in 2001 (i.e. 90th percentile rainday amount of 36.01 mm).

Both the wet spell persistence and mean wet spell length demonstrated statistically significant declining trends both in the DJF period and annually for the period 1890 to 2002, however the most marked declines occurred over the period 1960 to 2002 with the comparison of results shown in Table 22

Table 22: A comparison of linear trends for different periods for station 39039 (Gayndah).

		1890 to 2002	1960 to 2002
Slope	DJF	-0.001	-0.004
	ANN	-0.001	-0.003
Intercept	DJF	2.61	8.76
	ANN	2.55	5.52
Co-efficient of determination (r^2)	DJF	0.09	0.13
	ANN	0.19	0.14

The analysis of the Gayndah climate station would suggest that while warming trends in minimum temperature could be confidently identified, changes in daily rainfall indices were more difficult to determine. The time series data did suggest declines in wet spell persistence and mean length, however much of the signal was produced but significant declines post 1965.

The Eidsvold climate station possessed an extensive rainfall time series (1890 to 2002) but had not recorded daily temperature. For this reason the temperature trends exhibited by this station were not reported.

The trend analyses of derived rainfall indices have been reported given the extensive rainfall record length. The rainfall data showed no statistically significant trends in average daily rainfall but did demonstrate statistically significant declining trends in 20th, 40th, 50th and 60th percentile rainday amounts for the DJF period. The declining trends were expressed as follows:

1. $y = -0.009x + 19.39$, $r^2=0.07$ $P=0.0011$ for the DJF 20th percentile rainday amount;
2. $y = -0.021x + 46.35$, $r^2=0.10$ $P=0.0016$ for the DJF 40th percentile rainday amount;
3. $y = -0.027x + 59.04$, $r^2=0.08$ $P=0.0014$ for the DJF 50th percentile rainday amount;
and
4. $y = -0.031x + 71.38$, $r^2=0.07$ $P=0.0062$ for the DJF 60th percentile rainday amount.

In conjunction with a decline in DJF lower percentile rainday amounts was a decline in rainfall intensity for the same period (i.e. $y = -0.029x + 68.85$, $r^2=0.05$ $P=0.0154$).

This climate station also exhibited trends contrary to some of the other stations analysed by demonstrating an increase in JJA wet spell persistence and mean wet spell length (i.e. $y = 0.001x - 1.20$, $r^2=0.03$ $P=0.0159$ for JJA wet spell persistence and $y = 0.002x - 2.95$, $r^2=0.03$ $P=0.0098$ for JJA mean wet spell length). This would suggest that in the Eidsvold area daily rainfall amounts have declined although the persistence or length of those events has become slightly longer. The existence of the opposing trends would go some way to explaining why the Eidsvold climate stations did not return a statistically significant change in average daily rainfall.

The Biggenden (40021) and additional “Goodnight Scrubs” (39045) climate stations were again stations not recording daily temperatures and for this reason trends exhibited by the interpolated temperature data were not reported.

The Biggenden rainfall indices produced relatively equivocal results with very few statistically significant trends returned. The climate station did show an increase in SON extreme daily rainfall (i.e. 95th percentile rainday amount = $0.001x - 135.81$ $r^2=0.08$ $P=0.0122$). In addition the climate station demonstrated a statistically significant decline in DJF wet spell persistence and mean wet spell length (i.e. $y = -0.001x + 2.20$ $r^2=0.06$ $P=0.0096$ for wet spell persistence and $y = -0.004x + 9.96$ $r^2=0.05$ $P=0.0134$ for mean wet spell).

The “Goodnight Scrubs” climate station also returned very few statistically significant trends for the derived rainfall indices but did demonstrate a decline in DJF consecutive wet days (i.e. $y = -0.0306x + 66.50$, $r^2=0.10$ $P=0.0004$), annual average wet spell length (i.e. $y = -0.004x + 10.22$, $r^2=0.22$ $P=0.0001$), but an increase in annual average dry spell length (i.e. $y = 0.008x - 7.60$, $r^2=0.03$ $P=0.0261$).

This would indicate that while the Biggenden and “Goodnight Scrubs” climate stations did not demonstrate strong trends in rainfall change a consistent pattern of decline in the frequency of rainday (e.g. declines in wet spell length or persistence or increases in dry spell length or persistence).

4. **Linear Trend Analysis of Climate Indices for the South Sub-Region**

The South sub-region was represented by the Mounefontein (40138), Goomeri (40090), Kingaroy (40112), Kumbia (40113) and Goodger (40086) climate stations. The Kingaroy station was the only station in this sub-region that reported daily temperatures all the remaining stations recorded only rainfall. While interpolated temperature data was available for each station and used in the linear trend analyses the results were not reported.

The Mounefontein climate station contained the shortest rainfall record of all five stations used to represent the South sub-region (i.e. 1949 to 2002). For this reason the entire interpolated record (1890 to 2002) was compared against the observed record (1949 to 2002) in order to highlight any differences.

The trend comparisons revealed that in all cases only small difference between the slope and intercept existed (Table 23). The comparison also revealed that the 1949 to 2002 period exhibited more variability than the 1890 to 2002 period as the co-efficient of determination was lower in all cases for the shorter time period.

The linear trend analysis revealed statistically significant declining trends in consecutive wet days, wet spell persistence and mean wet spell length across all analysis periods. The trends would appear for the most part to be the product of the 1949 to 2002 period given the close correlation (i.e. $r = 0.99984$) across both time periods.

Table 23: A comparison of linear trends for (a) annual maximum number of consecutive wet days, (b) annual wet day persistence, and (c) annual mean wet spell length for two specific time periods 1890 to 2002 and 1949 to 2002 for station 40138 (Mounefontein).

		1890 to 2002	1949 to 2002
Slope:	(a)	-0.033	-0.029
	(b)	-0.002	-0.002
	(c)	-0.006	-0.005
Intercept:	(a)	70.99	62.09
	(b)	3.46	3.73
	(c)	12.74	11.36
Co-efficient of Determination (r^2):	(a)	0.23	0.06
	(b)	0.35	0.12
	(c)	0.34	0.11

The Goomeri climate station raw rainfall record extended from 1913 to 2002 and thus very little interpolated data was required to expand the time series back to 1890. While the linear trend analysis of annual rainfall returned a statistically significant ($P < 0.05$) declining trend (Figure 14), the analysis of daily rainday amounts did not.

The rainfall indices did return statistically significant declining trends in both maximum number of consecutive wet days and wet spell persistence in the DJF period (i.e. $y = -0.030x + 65.18$ $r^2 = 0.10$ $P = 0.0003$ for maximum number of consecutive wet days and $y = -0.001x + 2.35$ $r^2 = 0.06$ $P = 0.0045$ for wet spell persistence).

The annual average maximum number of consecutive wet days and wet spell persistence also demonstrated statistically significant declining trends, however a closer examination of the time series data revealed that the declines occurred in two distinct periods.

The first period occurred from 1913 to 1948. This was interspersed by a period of recovery from 1950 to 1978 and then a quite steep decline from 1980 to present.

The second period of declining wet spell persistence and consecutive wet days superseded the declines experienced during the 1913 to 1948 period (Table 24).

Table 24: A comparison of linear trends for (a) annual maximum number of consecutive wet days, and (b) annual wet day persistence for three specific time periods 1890 to 2002, 1913 to 1948 and 1979 to 2002 for station 40090 (Goomeri).

		1890 to 2002	1913 to 1948	1979 to 2002
Slope:	(a)	-0.025	-0.024	-0.053
	(b)	-0.001	-0.00005	-0.005
Intercept:	(a)	56.18	52.00	111.33
	(b)	2.02	0.54	11.17
Co-efficient of Determination (r^2):	(a)	0.10	0.02	0.03
	(b)	0.11	<1%	0.25

The Kingaroy climate station had recorded temperature data for the period 1957 to 2002 and rainfall data for the period 1906 to 2002. The linear trend analyses can thus be reported for both temperature and rainfall although in most cases warming trends did not become apparent until the post 1957 period.

The temperature indices for the Kingaroy climate station returned statistically significant warming trends for JJA maximum temperatures as well as for minimum temperatures across all analysis periods.

1. $y = 0.006x + 8.15$, $r^2=0.06$ $P=0.0143$ for JJA maximum temperatures;
2. $y = 0.009x - 0.82$, $r^2=0.17$ $P=0.0001$ for DJF minimum temperatures;
3. $y = 0.016x - 19.45$, $r^2=0.21$ $P=0.0001$ for MAM minimum temperatures;
4. $y = 0.014x - 23.64$, $r^2=0.14$ $P=0.0002$ for JJA minimum temperatures;
5. $y = 0.011x - 10.47$, $r^2=0.19$ $P=0.0001$ for JJA minimum temperatures; and
6. $y = 0.013x - 13.49$, $r^2=0.33$ $P=0.0001$ for JJA minimum temperatures.

As with all the other temperature reporting stations, the more rapid warming exhibited by the minimum temperatures produced an overall decline the diurnal temperature range across all periods analysed. The warming trend appeared to be the result of an increase in both the 90th percentile maximum temperatures, for the JJA period and an increase in 90th percentile minimum temperatures for all periods analysed. The Kingaroy station also demonstrated statistically significant declines in the 10th percentile cold wave duration for the MAM period and annually. The linear trends were as follows:

1. $y = -0.014x + 29.81$, $r^2=0.05$ $P=0.0065$ for MAM 10th percentile cold wave duration; and
2. $y = -0.010x + 24.69$, $r^2=0.03$ $P=0.014$ for annual 10th percentile cold wave duration.

The poor co-efficient of determination scores demonstrated by the cold wave duration indices resulted from a number of years were extremely dry conditions and thus low night-time minimum temperatures occurred. The years, namely 1965, 1969, 1977, 1997 were associated with El Niño events that produced widespread rainfall deficits over Queensland.

The rainfall indices for the Kingaroy climate station returned few definitive trends. Of most interest was the apparent increase in 80th, 90th and 95th percentile rainday amounts for the SON period. The linear trend analysis returned the following trends:

1. $y = 0.026x - 36.01$, $r^2=0.03$ $P=0.032$ for SON 80th percentile rainday amounts;
2. $y = 0.046x - 67.42$, $r^2=0.04$ $P=0.037$ for SON 90th percentile rainday amounts; and
3. $y = 0.070x - 107.68$, $r^2=0.05$ $P=0.018$ for SON 95th percentile rainday amounts.

The increasing trend in extreme rainday amounts was accompanied by statistically significant declines in annual wet spell persistence and mean wet spell length (i.e. $y = -0.001x + 1.55$, $r^2=0.06$ $P=0.0229$ for wet spell persistence and $y = -0.002x + 6.46$, $r^2=0.09$ $P=0.022$). This would suggest that while extreme rainday amounts are increasing the duration of events are declining.

The Kumbia (40013) rainfall recording station (40013) demonstrated statistically significant increases in DJF and SON extreme rainfall (i.e. 80th, 90th and 95th percentile rainday amounts). However both sites also return statistically significant declining trends in wet spell persistence and mean wet spell length. The characteristic of increasing extreme daily amounts and declining wet spell persistence would appear to be common across all stations analysed for this project. The rainfall trends for Kumbia are summarised in Table 25.

Table 25: A summary of linear trends for (a) 80th percentile rainday amounts for SON, (b) 90th percentile rainday amounts for SON (c) SON wet spell persistence, and (d) SON mean wet spell length the Kumbia rainfall station.

		KUMBIA
Slope:	(a)	0.032
	(b)	0.054
	(c)	-0.001
	(d)	-0.005
Intercept:	(a)	-44.50
	(b)	-83.43
	(c)	3.04
	(d)	10.71
Co-efficient of Determination (r^2):	(a)	0.08
	(b)	0.06
	(c)	0.11
	(d)	0.14

The Goodger rainfall station provided less definitive trends in rainfall indices even though it's record extended from 1924 to 2002. The station demonstrated statistically significant declines in DJF and MAM consecutive wet days as well as declines in MAM wet spell persistence and mean wet spell length.

5. Summary of linear trend analyses of Interpolated Climate Data

The linear trend analysis of interpolated rainfall and temperature data revealed a number of important issues regarding the possible contemporary impacts of anthropogenic climate change in the Burnett Study region.

These were:

- The interpolated temperature station data for each sub-region showed consistent warming trends. The maximum temperatures in the North, Central and South sub-regions exhibited strongest warming trends in the winter months (JJA). The East sub-region did not reveal any statistically significant warming trends in average maximum temperatures but did exhibit warming trends in extreme maximum temperature events.
- Interpolated minimum temperatures demonstrated greater rates of warming than for maximum temperatures, with most station data exhibiting warming trend across the entire year. As a result of the more rapid and extensive warming in minimum temperatures all temperature recording stations returned statistically significant declines in diurnal temperature range.

- In terms of rainfall changes, all sub-regions exhibited declining rainfall trends although most of these trends were not revealed in changes in average rainday amounts but through measures of extreme rainfall and wet spell persistence.
- Most of the stations in the East sub-region demonstrated statistically significant declines in extreme rainday amounts i.e. 60th, 80th, 90th and 95th percentile for the DJF period. In addition declines in maximum number of consecutive wet days, wet spell persistence and mean wet spell length all exhibited declines in the DJF and in some cases the MAM period. One station, namely Moolboolaman exhibited contrary trends in extreme 80th and 90th percentile rainfall for the SON period.
- The majority of stations in the North sub-region demonstrated statistically significant increasing trends in extreme percentile (i.e. 60th, 80th, 90th and 95th percentile) rainday amounts across all seasons with most significant increases found in the SON period. In addition stations in this sub-region also exhibited increasing trends in maximum consecutive dry days as well as declines in wet spell persistence across all periods. The Bancroft station was one of the few to exhibit statistically significant declines in average rainday amounts for the DJF period.
- The stations in the Central sub-region returned more equivocal trend results from the examination of daily rainfall. For the most part stations demonstrated a mix of increases in lower percentile rainfall i.e. 20th to 50th as well as extremes i.e. 80th to 95th percentile rainday amounts. Consistent to all but one station was a decline in wet spell persistence and mean wet spell length for the summer rainfall period (i.e. DJF and SON). In this region three of the five stations analysed did return statistically significant declines in average daily rainfall for both the JJA and annually.
- The South sub-region, as with the Central sub-region returned few statistically significant rainfall trends. Consistent across all stations were the declines in mean wet spell length and wet spell persistence, for the most part, during the DJF period. Two of the five stations (i.e. Kingaroy and Kumbia) returned statistically significant increases in extreme daily rainfall amounts (i.e. 80th, 90th and 95th percentiles) for the SON period.

In summary all temperature recording stations demonstrating consistent warming trends in minimum temperature with fewer stations returning warming trends in maximum temperature. Rainfall declines indicated across the majority of the study area have been the result of changes in wet spell persistence and mean wet spell length.

The North, Central and South regions did share some similarities in terms of increases in daily rainfall intensity, a feature not shared by the East sub region. This would suggest that in the North, Central and South sub-regions rainfall intensity has been increasing although the frequency and the duration of events have declined.

This would suggest that rainfall is becoming slightly less effective for growth in the more inland regions as it becomes heavier and less frequent. This issue is examined in the following section which analyses the trends in pasture production, runoff, deep drainage and heat stress.

Linear Trend Analysis of Simulated Biophysical Data for the Burnett Study Region

An objective of this research project was to consider the impact of historical climate trends on the biophysical environment by analysing climate related changes in pasture production, runoff and deep drainage and bovine heat stress. In order to achieve this objective the biophysical impacts of historical climate variability and change must be considered within a modelling framework given the extremely short record of observational data.

The impacts of historical climate variability and change have been assessed on native pasture production, deep drainage, runoff using the pasture production model GRASP (Littleboy and McKeon, 1997). The description that follows has been reproduced from a number of previous reports and represents a composite of the most relevant features and functionality of the model.

The GRASP model can be described as a 'pasture growth' model, which combines a soil water model and a model of above-ground dry-matter flow. It has been built for specific objectives relating to grazing management of Australian rangelands, such as:

- (1) objective assessment of drought and degradation risk in near-real time (Carter *et al.*, 2000);
- (2) simulation of grazing management options including seasonal forecasting (Ash *et al.*, 2000, McKeon *et al.*, 2000, Stafford Smith *et al.*, 2000);
- (3) assessment of safe carrying capacity (Johnston *et al.* 1996, Hall *et al.*, 1998);
- (4) evaluation of impact of climate change and CO₂ increase (Hall *et al.*, 1998, Howden *et al.* 1999);
- (5) reconstruction of historical degradation episodes (Carter *et al.*, 2000; McKeon and Hall 2002); and
- (6) analysis of historical droughts (Stafford Smith and McKeon 1998)

GRASP has been developed incrementally since 1978 in parallel with application studies and field trials. Thus the model has been under constant critique/review in terms of development, parameterisation, validation and usefulness to client needs. The GRASP model is currently being developed to address issues of seedling establishment, grazing land degradation, fire risk and catchment runoff and erosion. The model has been comprehensively described in earlier publications such as Littleboy and McKeon (1997), and a critique of model limitations is given in Day *et al.*, 1997 and Howden *et al.* 1998.

The GRASP model is an empirical model that links known empirical relationships between plant growth and water use with known empirical relationships between plant growth and growth indices (Littleboy and McKeon 1997).

The soil water balance in GRASP simulates, on a daily time step, the processes of soil evaporation, pasture transpiration (Rickert and McKeon 1982), tree transpiration (Scanlan and *et al.*, 1994), run-off, and through drainage. Four soil layers are simulated on a daily time step (0-10cm, 10-50cm, 50-100cm, >100cm) using inputs of rainfall and class A pan evaporation. Soil evaporation occurs from top 50cm, grass transpiration from top 100cm and tree transpiration from all four layers. Initially an empirical runoff model has been used (Scanlan *et al.*, 1996) with run-off calculated as a function of surface cover, rainfall intensity and soil water deficit.

The soil water balance in GRASP simulates separately the processes of soil evaporation, pasture transpiration (Rickert and McKeon 1982), tree transpiration, runoff and through drainage. Rainfall is partitioned into runoff and infiltration using an empirical relationship derived from ground cover, daily rainfall, rainfall intensity and soil water deficit, which have been derived from experimental measurements by Scanlan *et al.*, 1994. The equation takes the form of:

$$\text{Runoff} = \text{cover_term} \times (\text{rain} - (\text{rainfall_intensity}/110) \times \text{soil water_deficit})$$

where runoff is a daily runoff (mm), the cover_term is calculated from standing biomass and litter; rainfall_intensity is the maximum rainfall intensity in a 15 min period for the day (mm/h); and soil water_deficit is the deficit of the top two soil layers (mm).

Validation of model runoff against measured stream flow provides a check the model water balance, a number of such validation experiments have occurred against gauging stations and against independent methods of assessing runoff such as those derived by Zhang *et al.* 2001 using vapour pressure deficit.

A more standard hydrological approach (curve numbers linked to cover) has also been implemented, but has not been used for the purposes of this project in order to allow runoff to change in response to rainfall intensity under future climate conditions (Yee Yet *et al.*, 1999).

The above-ground pasture processes of growth, senescence of green tissue, detachment of standing dead matter, litter decomposition, animal trampling and consumption are modelled at a daily time step. Five pasture dry matter pools are represented: green leaf; green stem; standing dead leaf; standing dead stem; and surface pasture litter. Plant growth is calculated as a function of solar radiation interception, air temperature, VPD, soil moisture or grass transpiration, and available nitrogen. Growth parameters can be changed for different CO₂ concentrations, thus allowing potential CO₂ fertilisation effects to be explored. Daily climate data are used as inputs and surfaces of daily climate data (Jeffrey *et al.*, 2000) have been developed to support application of the model at a national level (Carter *et al.*, 2000).

Nitrogen uptake is calculated as a function of transpiration accumulated from the start of the growing season in each year. Potential annual nitrogen uptake is a key parameter as nitrogen limits pasture growth in wetter years (Mott *et al.*, 1992, 1985, 1981; McKeon *et al.*, 1990). Parameters have been derived from data collected in field studies (>100 sites) specifically designed to measure as many of the functional parameters (e.g. peak nitrogen yield) as possible (McKeon *et al.*, 1990; Day *et al.*, 1997). Calibration of parameters using field data is usually restricted to a limited number of parameters (e.g. above-ground transpiration efficiency, nitrogen uptake per mm of transpiration, potential regrowth rate after defoliation or burning).

Spatial versions of the model have allowed parameterisation using (1) extensive ground truthing measurements of above-ground standing dry matter (>200,000 observations in Queensland, Hassett *et al.*, 2000; >330,000 Australia wide, Hall *et al.*, 2001); and (2) time series of remotely sensed green cover (NDVI, Carter *et al.*, 2000, 2002). Animal production (annual steer live weight, wool cut) is calculated at an annual time step from simulated variables such as % utilisation, number of green or growing days (Hall *et al.*, 1998; McKeon *et al.*, 2000). For the purposes of this project the point scale version of the GRASP model (Littleboy and McKeon, 1997) has been used and bench marked against the spatial version described by Hall *et al.*, 2001.

The various feedback effects of grazing on pastures have been considered through sub-model simulation of:

- (1) perennial grass basal cover which drives potential regrowth rate;
- (2) pasture composition which changes species parameters (e.g. nitrogen use efficiency, detachment rates);
- (3) effects of grazing on plant functioning (water and nitrogen uptake); and
- (4) soil loss affecting available water range and nutrient availability.

However, in the case of the experiment described in this report, the pasture composition has been linked empirically to climate in order to simulate potential changes resulting from enhanced greenhouse gas concentrations and associated climate change.

The Temperature-Humidity Index (THI) has been shown to be a robust predictor of heat stress in cattle, being related to reduced liveweight gain in beef cattle, conception and mortality rates as well as being used to investigate distribution of beef cattle varieties in Africa and Australia. The THI has minimal input requirements and has been used in a variety of environments, making it suitable for assessment proposed. THI uses inputs of maximum temperature and dewpoint. These variables are anticipated to change substantially over the next decades to centuries due to global warming with changes likely over the past several decades

THI is calculated from Johnson *et al.* (1963) as:

$$\text{THI} = T_{\text{max}} + (0.36 * T_{\text{dewpoint}}) + 41.2$$

where T_{max} is daily maximum dry bulb temperature (°C) and T_{dewpoint} is daily dewpoint temperature (°C). Thermal stress is likely to occur in beef cattle when daily THI exceeds a value of 80 (based on previous studies), and days in the historical climate data set where this occurred will be identified.

The possible effect of increased CO₂ on tree/grass interactions is not considered in this report. The assumption made is that the 'effective' tree density will be maintained. Similarly, the impacts of grazing animals were not considered in the simulation experiments in order to produce results consistent with changes in climate only. Grazing pressure was assumed constant at thirty percent of the total standing dry matter (TSDM).

The model experiments were set up in such a way as to isolate the climate impacts on pasture production, deep drainage and runoff. This was achieved by running the GRASP model with a set of average pasture growth parameters for each climate station. The average pasture growth parameters are based on observed data collected from 74 sites throughout Queensland (Day *et al.*, 1997) using a methodology specifically designed to obtain a minimum dataset for model parameterisation (McKeon *et al.*, 1990; Philip and Day, 1997). In addition average soils parameters were for each climate stations and tree, grazing and fire interactions were not considered.

The average GRASP parameters were used in the simulation experiments are summarised in Table 26. The large range demonstrated by individual parameters highlights the diversity of production in Queensland due to varying soils, pasture types, and background climate.

While running an average parameter set for each of the climate station may not capture the regional production signal it was considered the most appropriate experiment design to all comparisons between stations.

The soil water model in GRASP was designed to simulate evapotranspiration, soil moisture and run-off with validation primarily from observations of soil moisture. Thus the calculation of deep drainage is regarded as indicative so that the relative effects of climate trends can be assessed. Accurate assessment of deep drainage for salinity hazard/risk calculations requires models which concentrate on this relatively small component of the soil water balance more accurately than GRASP.

Observed class A pan evaporation, solar radiation and vapour pressure data were limited (i.e. not available before 1957 or 1970 for evaporation) and for this reason the change in these particular variables both historically and as part of the climate change projections were estimated from regression analyses with maximum temperature.

1. Simulations of historical pasture production, deep drainage, runoff and cattle heat stress for the East sub-region

The simulation of historical pasture production, deep drainage, runoff and cattle heat stress was undertaken for each of the four representative climate stations within the sub-region. The results were then analysed using an annual, 5-year and 10-year moving average in order to identify any longer-term cyclic behaviour in each of the parameters investigated.

An analysis of the simulated pasture production for each of the four climate stations revealed a declining trend common across all the stations (Figure 18). The average annual pasture production for the East sub-region was simulated at 3090 kg of TSDM/ha. As with the long-term rainfall trend analyses for this sub-region, the declining trends in pasture production were not statistically significant at $P < 0.05$. The 5-year and 10-year moving averages exhibited extended periods of below average growth during the period 1920 to 1940 with above average growth in the periods 1900 to 1910, the mid 50s the 70s and early 80s (Figure 18). Declines in pasture production have been apparent in the 10-year running mean since the early 90s with most pronounced declines exhibited by the “The Cedars” climate station situated in the driest part of the sub-region (Figure 18 d).

Table 26: Parameter values used in the GRASP model to simulate pasture production, run-off and deep drainage for 14 sites in the Burnett study region.

GRASP parameters used in the Simulation Study	Mean	Range
SLkgSc Soil loss (kg/ha/year) calculated as a function of runoff and a concentration of sediment in runoff derived from Scanlan and McIvor (1993).	702	1767-252
Grass Transpiration Pasture transpiration (mm/year) calculated from the soil water balance model using a dynamic green cover.	280	613 - 81
Tsdm Total above-ground standing dry matter (kg/ha) at the date of capturing information calculated from the model which includes the flows of dry matter: pasture growth, senescence, detachment and consumption.	1743	2330 - 583
Nuptak Nitrogen uptake by the pasture since the start of the growing season at the date of capturing information.	16	20 - 9
%basal Grass basal cover (percentage) calculated each year as a function of evapo-transpiration over the previous two years.	2.93	4.39 - 1.42
hd/skm Stocking rate (head per square km) calculated each year at the end of the growing season to eat a proportion of total standing dry matter over the next year.	22.5	30.5 - 6.7
%util Percentage utilisation of pasture growth calculated as average consumption by livestock divided by average pasture growth.	26.2	28.1 - 22.9
%peren Percent desirable perennial grasses in the pasture calculated each year from the pasture composition model of Ash <i>et al.</i> (2000).	89	90 - 88
%gidys Percentage of days in the year that the pasture growth index exceeds 0.05. The pasture growth index is calculated each day from climate indices.	72	90 - 55
Min_TS Nitrogen mineralisation index calculated as a function of temperature and soil water (days). The mineralisation index is calculated each day as a function of temperature and soil water and is accumulated each year.	65.4	83.2 - 44.3
%burns Percentage of years that the pasture was burnt. The value is calculated from the decision rule where pasture burning occurs each year. Only a proportion of the pasture is burnt.	76.7	100 - 20

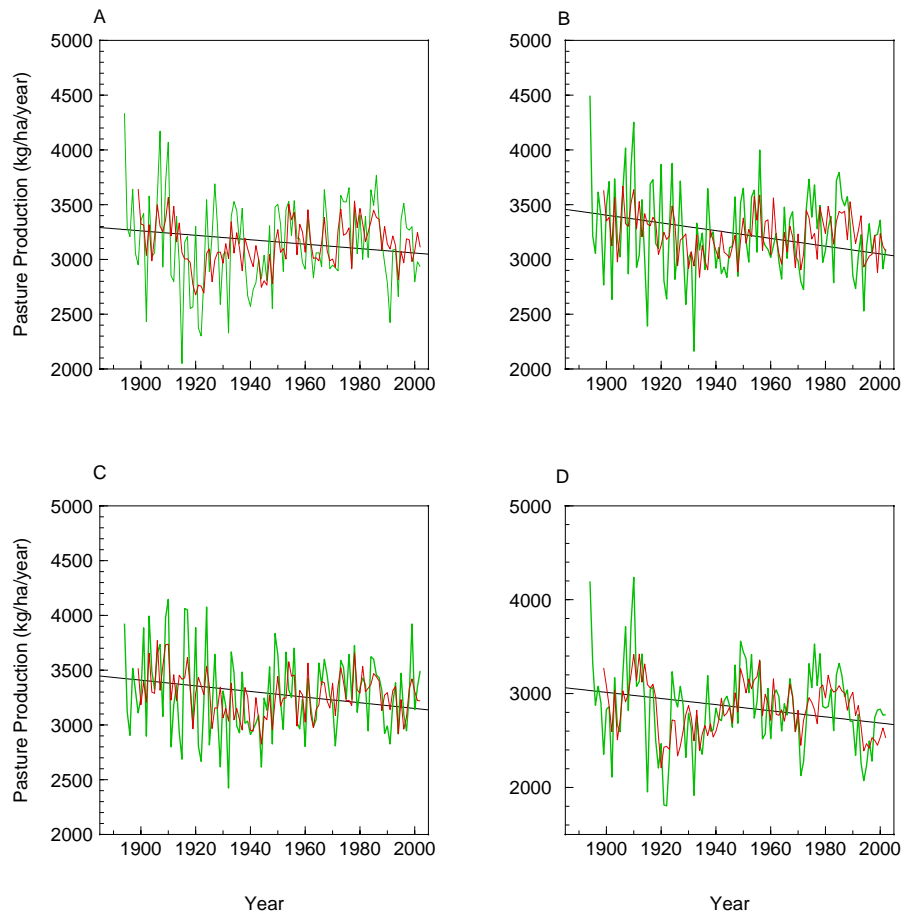


Figure 18: A time series of annual pasture production for a) “Bundaberg”(39015), b) “Gin Gin” (39040), c) “Moolboolaman” (39218) and d) “The Cedars” (39234) stations within the East sub-region. The linear trends were calculated from the annual data as follows a) Trend = $-2.025x + 7108.64$ $r^2 = 0.0016$, b) Trend = $-3.540x + 10129.48$ $r^2 = 0.0041$, c) Trend = $-2.576x + 8303.08$ $r^2 = 0.0021$ and d) Trend = $-3.2688x + 9222.44$ $r^2 = 0.0049$. The smoothed green line represents the 5 year moving average of pasture production and the smoothed red line represents the 10 year moving average of pasture production.

A simple calculation of ‘safe’ stocking rate was made from each pasture production time series in order to determine the possible change in the number of cattle that could run at each site. The safe stocking rate was calculated using the following equation:

$$\text{‘Safe’ Stocking Rate} = (\text{Percent Utilisation} \times \text{Pasture Growth}) / \text{Average Animal Intake};$$

where percent utilisation was fixed at 20% (0.20) and average animal intake was fixed at 2700 kg per year. The resultant ‘safe’ stocking rate time series data, for each station, was assessed on an annual, 5-year and 30-year moving window in order to identify any cyclic behaviour in the record. The 30-year moving average period was used in order to replicate the timeframe on which objective ‘safe’ grazing capacities for south-west Queensland were calculated and thus provide some measure for how objective safe carry capacity may change in the Burnett Study region in response to enhanced greenhouse gas concentrations.

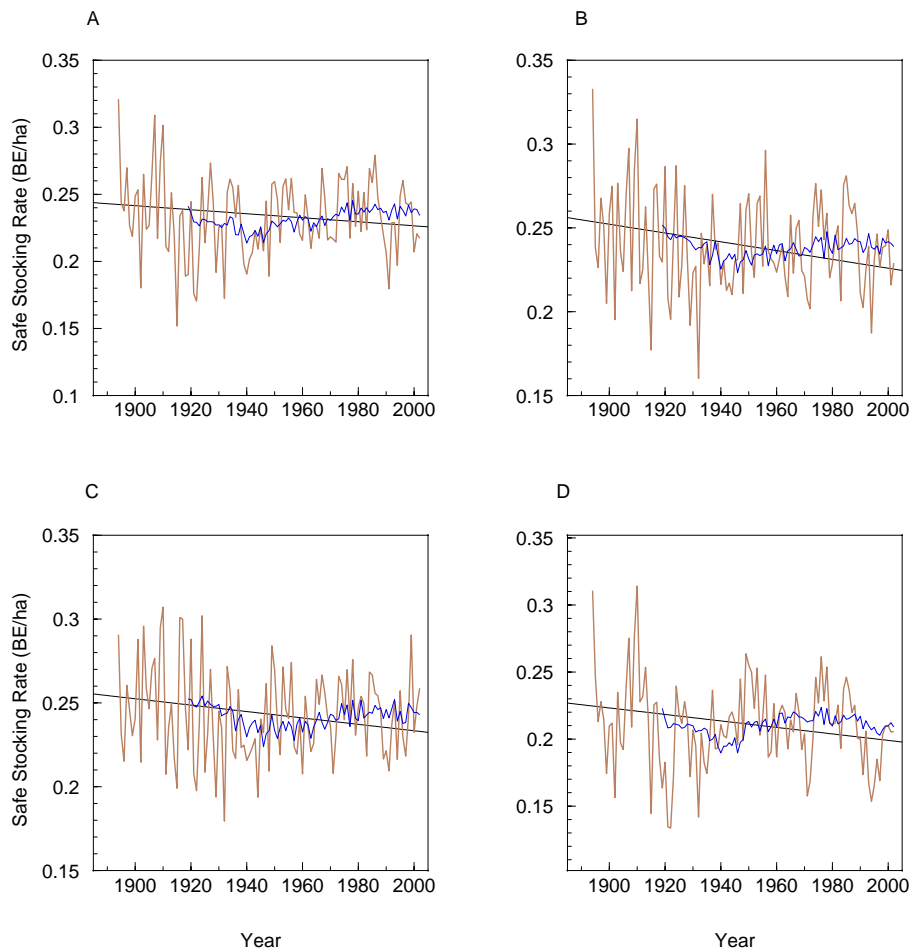


Figure 19: A time series of annual ‘safe’ stocking rate for a) “Bundaberg”(39015), b) “Gin Gin” (39040), c) “Moolboolaman” (39218) and d) “The Cedars” (39234) stations within the East sub-region. The linear trends were calculated from the annual data as follows a) Trend = $-0.0002x + 0.53$ $r^2 = 0.0016$, b) Trend = $-0.0003x + 0.75$ $r^2 = 0.0041$, c) Trend = $-0.0002x + 0.62$ $r^2 = 0.0021$ and d) Trend = $-0.0002x + 0.68$ $r^2 = 0.0049$. The smoothed brown line represents the 5-year moving average of ‘Safe’ Stocking rate and the smoothed blue line represents the 30-year moving average of pasture production.

As in the case of annual rainfall and pasture production time series data, the linear trend analysis of ‘safe’ stocking rate for all four climate stations exhibited declining trends for the period 1890 to 2002 (Figure 19). In each case the declining trends were not statistically significant at the 95% confidence interval (Figure 19). The wet 70s contributed strongly to the 30-year moving average of ‘safe’ stocking rate with each time series indicating more favourable stocking rates post 1970 than in the earlier part of the simulated time series. The “The Cedars” climate station demonstrated declines in the 30-year moving average of ‘safe’ stocking rate post 1990 reflecting a significant decline in rainfall for this period.

The linear trend analysis of simulated annual drainage time series returned declining trends across all four climate stations (Figure 20). The declining trend was significant in only one case - for the Moolboolaman station (Figure 20). The 30-year running mean of simulated drainage for each climate station demonstrated large drainage values during the 70s consistent with above average rainfall for the same period and also highlighted that drainage is highly episodic.

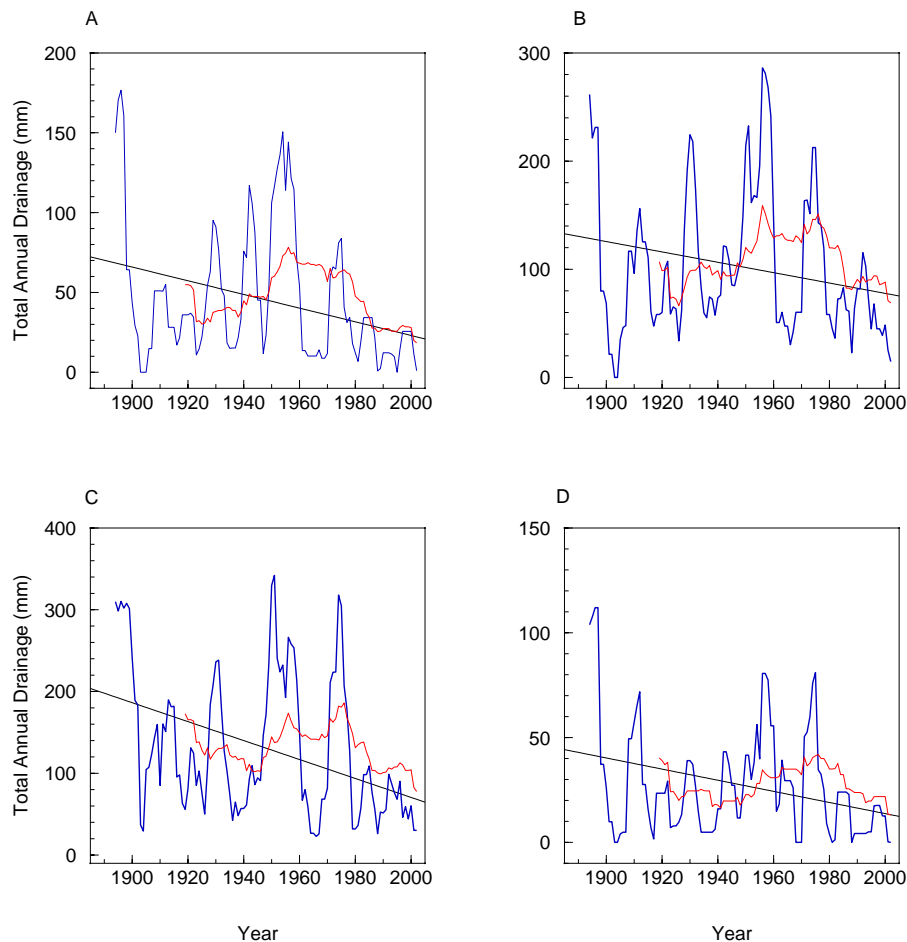


Figure 20: A time series of annual drainage for a) “Bundaberg”(39015), b) “Gin Gin” (39040), c) “Moolboolaman” (39218) and d) “The Cedars” (39234) stations within the East sub-region. The linear trends were calculated from the annual data as follows a) Trend = $-0.429x + 880.10$ $r^2 = 0.031$, b) Trend = $-0.479x + 1036.19$ $r^2 = 0.012$, c) Trend = $-1.158x + 2386.90$ $r^2 = 0.051$ and d) Trend = $-0.0266x + 544.71$ $r^2 = 0.021$. The smoothed blue line represents the 5-year moving average of drainage and the smoothed red line represents the 30-year moving average of drainage.

The 30-year running mean of simulated drainage showed a marked decline across all stations since the early 1980s (Figure 20). This is reflected in the annual data as well as the 5-year running mean for all four stations. The 30-year moving average of drainage for the period up to and including 2002 was the lowest on record at the Bundaberg, Moolboolaman and “The Cedars” stations (Figure 20), with the Gin Gin station demonstrating lower 30-year periods up to and including 1925 (Figure 20b).

The linear trend analysis of the simulated runoff data exhibited both negative (declining) and positive (increasing) trends (Figure 21). This was due to the interaction of both available cover and rainfall intensity in the calculation of runoff. In the case of the Bundaberg, Gin Gin and Moolboolaman stations the linear trend analyses returned declining trends that were not significant at the 95% confidence interval (Figure 21). The “The Cedars” climate station did however return a positive linear trend for the equivalent period 1890 to 2002, produced primarily due to low runoff values at the beginning of the record (common to all East sub-region stations) and consistently higher values later in the record (Figure 21).

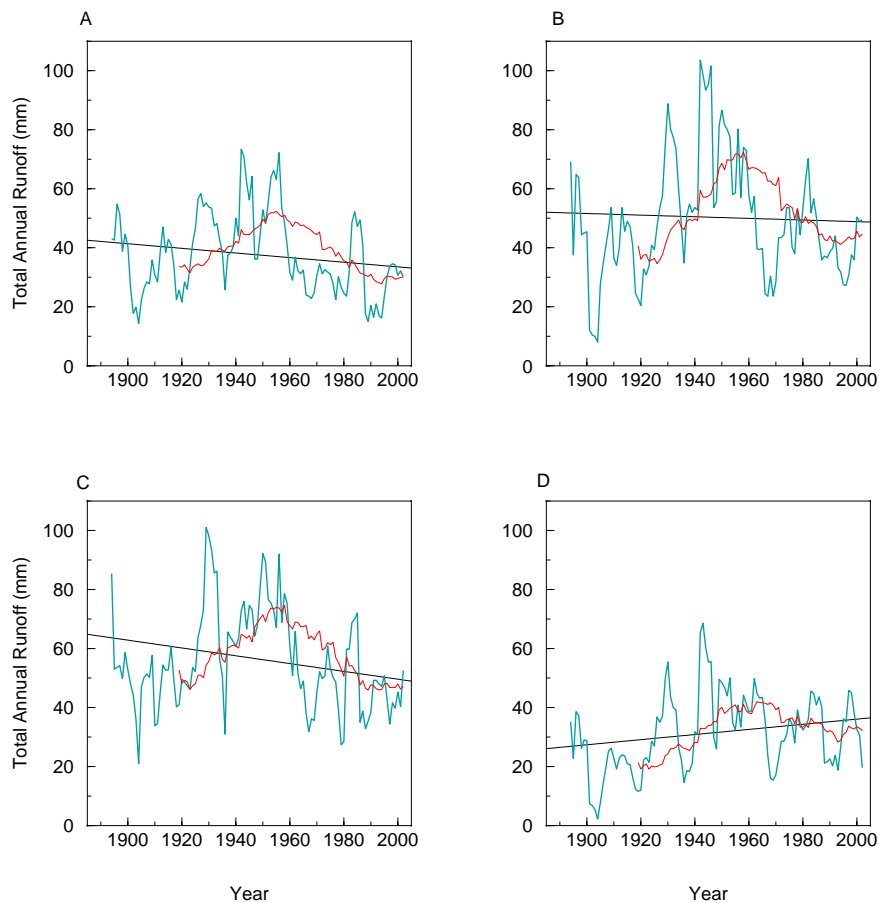


Figure 21: A time series of annual runoff for a) “Bundaberg”(39015), b) “Gin Gin” (39040), c) “Moolboolaman” (39218) and d) “The Cedars” (39234) stations within the East sub-region. The linear trends were calculated from the annual data as follows a) Trend = $-0.078x + 190.36$ $r^2 = 0.0071$, b) Trend = $-0.028x + 104.12$ $r^2 = 0.0003$, c) Trend = $-0.132x + 314.28$ $r^2 = 0.0089$ and d) Trend = $0.087x - 137.73$ $r^2 = 0.0081$. The smoothed turquoise line represents the 5-year moving average of runoff and the smoothed red line represents the 30-year moving average of runoff.

Both the 5-year and 30-year time series data demonstrated declines in runoff since the 1960s with the 30-year period up to and include 2002 (i.e. 1973 to 2002) close to the lowest on record for both the Bundaberg and Moolboolaman stations (Figure 21).

The heat stress index across all four of the East sub-region stations exhibited declining trends for the period 1890 to 2002 (Figure 22). This was a function of the complex interaction between maximum temperature and moisture availability (represented by dewpoint temperature) used to calculate the index. At the beginning of the record maximum temperatures were significantly higher than the long-term mean for all four stations (greater than one standard deviation from the long-term mean). These above average maximum temperatures were associated with anomalously high annual rainfall thus producing the highest THI values for the entire record (Figure 22). Lower than average maximum temperatures in the late 1960s and early 70s were the result of extended periods of above average rainfall and thus while the dewpoint temperatures were relatively high the maximum temperatures were low and occurrence of THI above 80 was the lowest on record. The linear trend analysis of the annual THI data, while producing declining trends for the period 1890 to 2002, returned only one instance where the trend was statistically significant at the 95% confidence level (i.e. Bundaberg). In all cases the 30-year running mean has demonstrated an upturn in THI since the late 1970s (Figure 22)

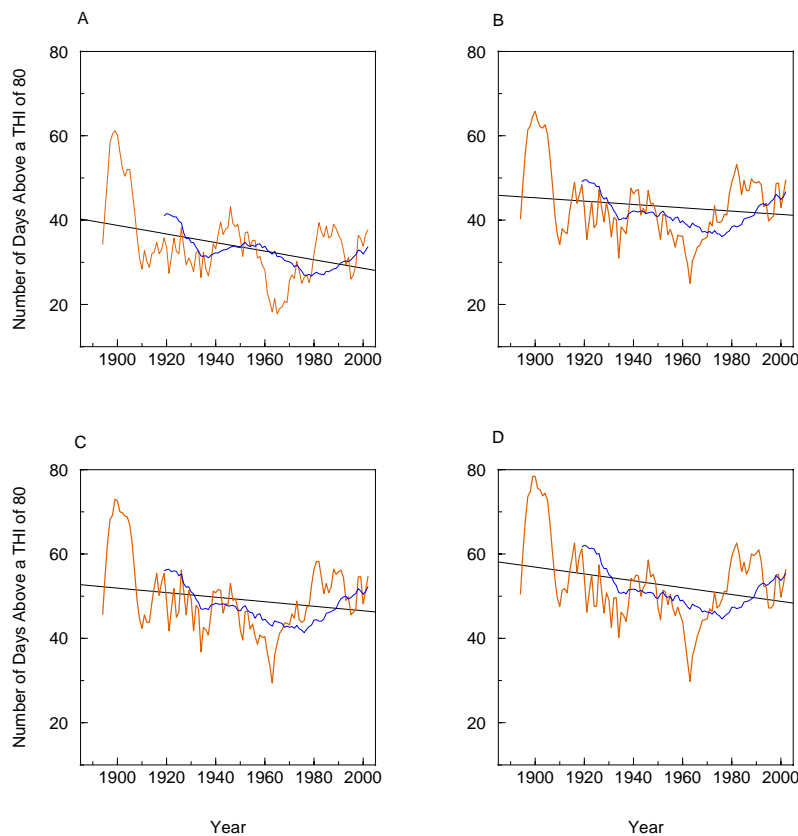


Figure 22: A time series of annual cattle heat stress for a) “Bundaberg”(39015), b) “Gin Gin” (39040), c) “Moolboolaman” (39218) and d) “The Cedars” (39234) stations within the East sub-region. The linear trends were calculated from the annual data as follows a) Trend = $-0.102x + 232.07$ $r^2 = 0.054$, b) Trend = $-0.039x + 120.33$ $r^2 = 0.0071$, c) Trend = $-0.054x + 154.18$ $r^2 = 0.0121$ and d) Trend = $-0.081x + 211.19$ $r^2 = 0.0257$. The smoothed orange line represents the 5-year moving average of THI days above 80 and the smoothed blue line represents the 30-year moving average of THI days above 80.

2. Simulations of historical pasture production, deep drainage, runoff and cattle heat stress for the North sub-region

Simulated annual pasture production for each of the four climate stations used for the North sub-region demonstrated a decline over the period 1890 to 2002 (Figure 23). The declining trends demonstrated by each of the four climate stations were not statistically significant at the 95% confidence interval. The 5-year and 10-year running means of pasture production demonstrated higher than average values at the beginning of the record (i.e. pre 1910) with and extend period of lower than average production across most of the sites from 1920 to 1950 (with the exception of Malakof, where simulated pasture production recovered over the 10-year period centred on 1920) (Figure 23). Both the Kalpowar and Bancroft stations demonstrated increases in 10-year running mean pasture production values for the early 1980s due to the influence of the wet 1970s on the running mean. The Tecoma and Malakof climate stations did not demonstrate this feature even though favourable rains fell at both stations during this time.

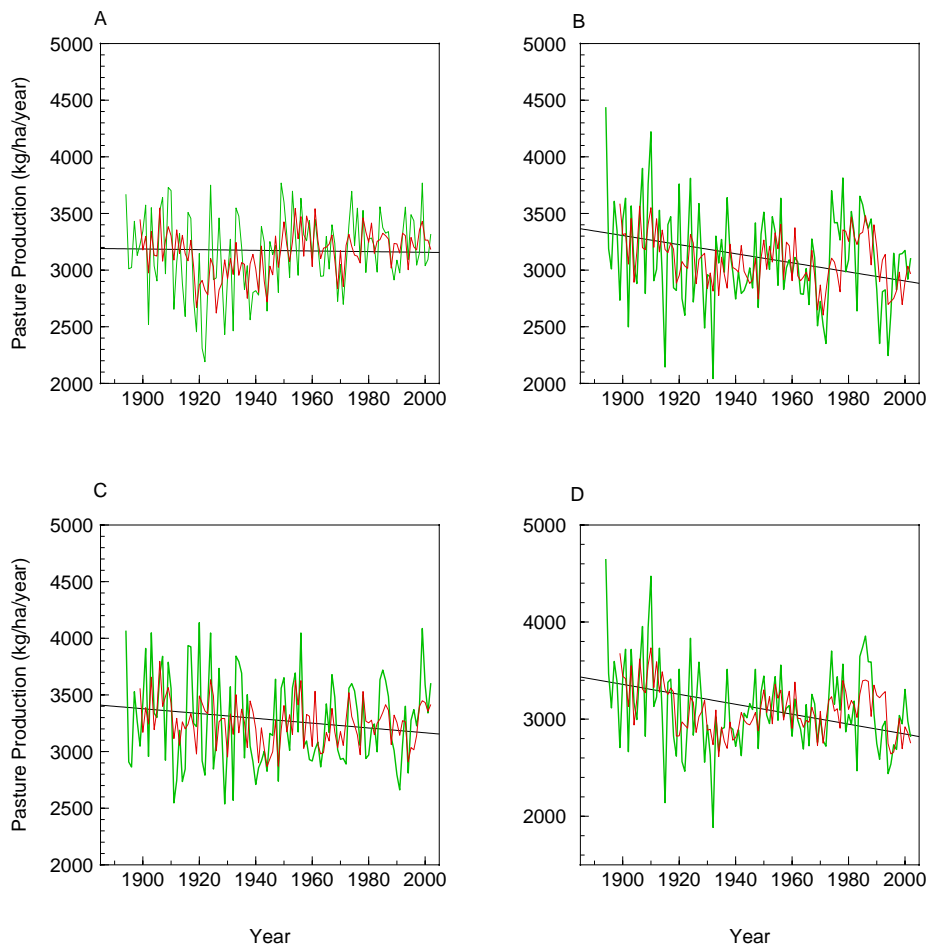


Figure 23: A time series of annual pasture production for a) “Tecoma”(39248), b) “Kalpowar” (39057), c) “Malakof” (39129) and d) “Bancroft” (39103) stations within the North sub-region. The linear trends were calculated from the annual data as follows a) Trend = $-0.288x + 3722.22$ $r^2 = 0.00004$, b) Trend = $-4.015x + 10932.89$ $r^2 = 0.0056$, c) Trend = $-2.124x + 7413.67$ $r^2 = 0.0015$ and d) Trend = $-5.114x + 13074.88$ $r^2 = 0.0094$. The green line represents the 5 year moving average of pasture production and the red line represents the 10 year moving average of pasture production.

The simulated ‘safe’ carrying capacity values calculated for each of the four climate stations exhibited declining trends for the period 1890 to 2002 (Figure 24). In all cases the trends were not statistically significant at the 95% confidence interval, with no trend evident for the Tecoma climate station (Figure 24).

The long-term changes in stocking rate, represented by the 30-year running mean, revealed higher carrying capacities pre-1960 than any other time in the record due to anomalously high pasture production during this period (Figure 24). The Tecoma station, unlike the other three did demonstrate improved carry capacities post-1960 due to poor pasture productivity during the 1910 to 1940 period (Figure 23 and 24 a).

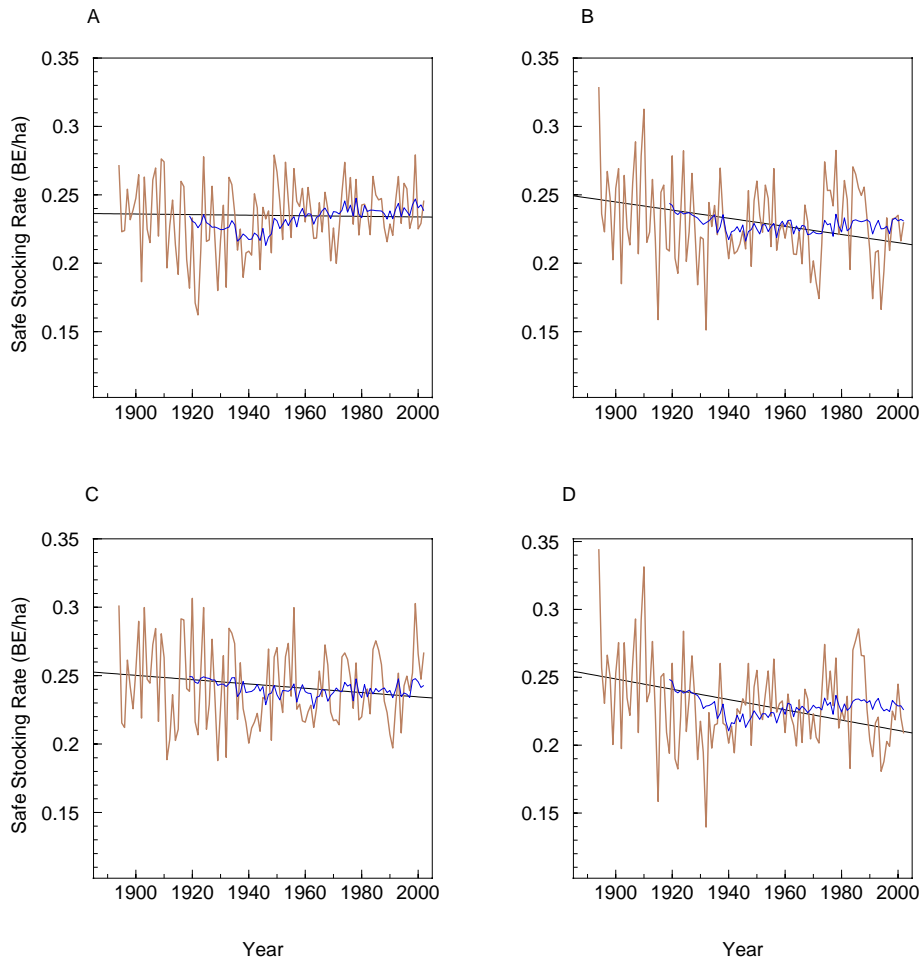


Figure 24: A time series of ‘Safe’ Stocking Rate for a) “Tecoma”(39248), b) “Kalpowar” (39057), c) “Malakof” (39129) and d) “Bancroft” (39103) stations within the North sub-region. The linear trends were calculated from the annual data as follows a) Trend = $-0.288x + 3722.22$ $r^2 = 0.00004$, b) Trend = $-4.015x + 10932.89$ $r^2 = 0.0056$, c) Trend = $-2.124x + 7413.67$ $r^2 = 0.0015$ and d) Trend = $-5.114x + 13074.88$ $r^2 = 0.0094$. The smoothed brown line represents the 5 year moving average of ‘safe’ stocking rate and the smoothed blue line represents the 10 year moving average of ‘safe’ carrying capacity.

The simulated drainage time series data for all four climate stations exhibited more defined linear trends than either the simulated pasture or calculated ‘safe’ stocking rate data (Figure 25). The simulated drainage data, for each of the four climate stations, demonstrated declining trends, although only the Kalpowar climate station (Figure 25 b) returned a statistically significant trend (i.e. $P < 0.05$) (Figure 25). All the climate stations within the North sub-region exhibited the lowest 5 year running mean of drainage for the period up to and including 2002 (Figure 25). The

lowest mean drainage values for the 5 year period 1998 to 2002 are consistent with low rainfall for this period (Figure 12).

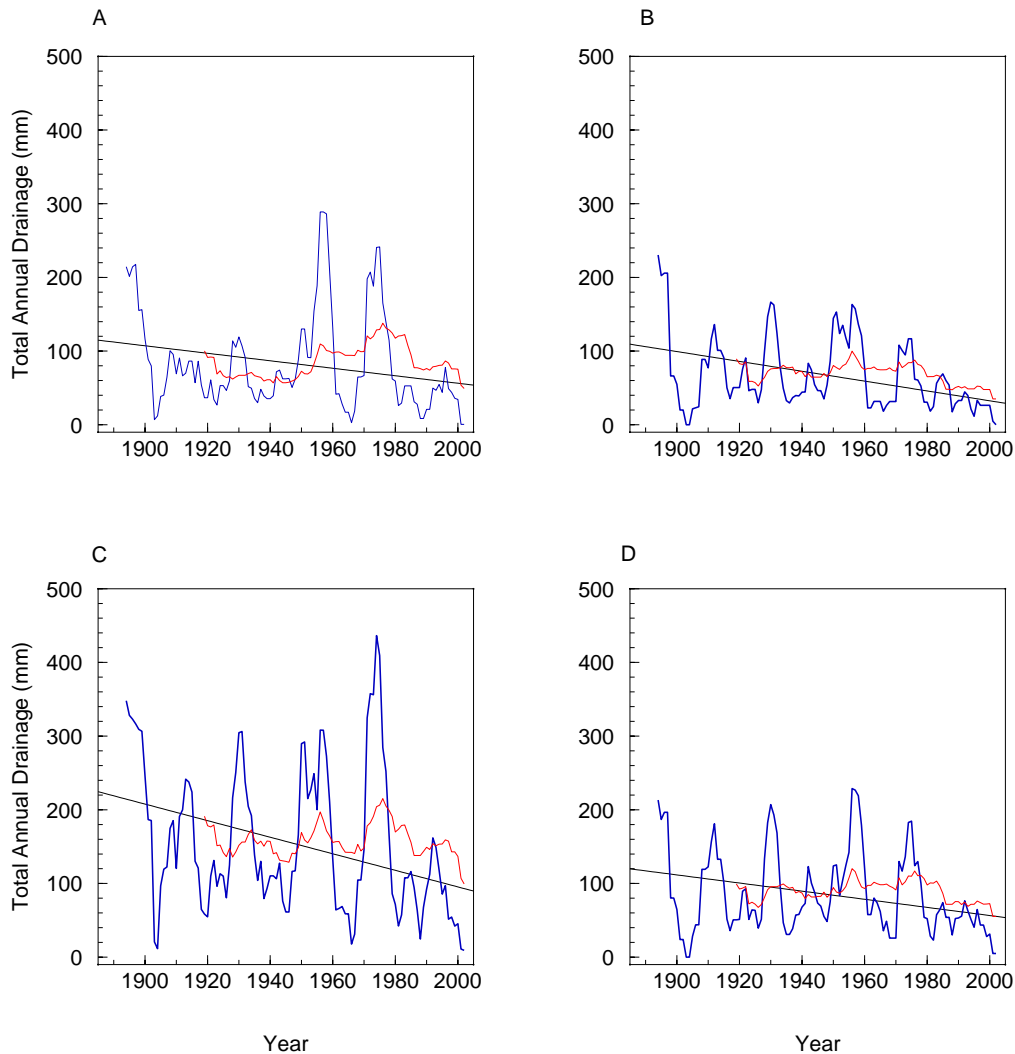


Figure 25: A time series of simulated drainage for a) “Tecoma”(39248), b) “Kalpowar” (39057), c) “Malakof” (39129) and d) “Bancroft” (39103) stations within the North sub-region. The linear trends were calculated from the annual data as follows a) Trend = $-0.508x + 1073.18$ $r^2 = 0.0168$, b) Trend = $-0.668x + 1368.48$ $r^2 = 0.0393$, c) Trend = $-1.124x + 2343.08$ $r^2 = 0.0360$ and d) Trend = $-0.551x + 1158.60$ $r^2 = 0.0216$. The smoothed blue line represents the 5 year moving average of drainage and the smoothed red line represents the 30 year moving average of drainage.

The annual runoff time series data, for each of the four climate stations, simulated using the GRASP model again returned declining linear trends (Figure 26). As was the case with some of the other biophysical indices the annual trends were not statistically significant at the 95% confidence interval. The 5 year moving average runoff values exhibited some longer-term cyclic behaviour with lower runoff values in the early part of the simulated record (i.e. 1900 to 1930), 1960s and late 1990s (Figure 26), and greater than average runoff during the late 1890s, 1940 to 1960 period and mid 1980s (Figure 26). The 30 year running mean highlighted the wet periods of the 1930s to 1960s and showed a return to runoff values similar to those found at the beginning of the record (Figure 26).

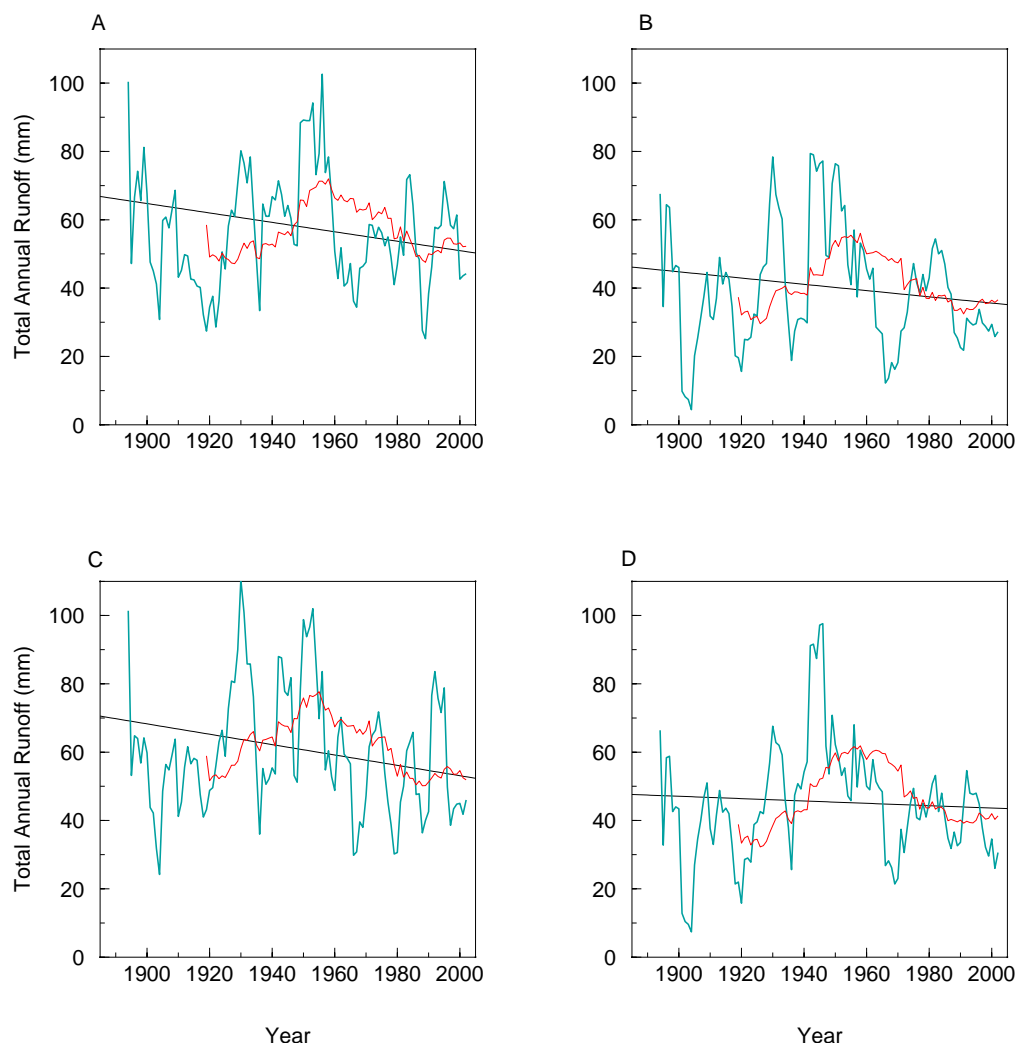


Figure 26: A time series of simulated runoff for a) “Tecoma”(39248), b) “Kalpowar” (39057), c) “Malakof” (39129) and d) “Bancroft” (39103) stations within the North sub-region. The linear trends were calculated from the annual data as follows a) Trend = $-0.138x + 326.81$ $r^2 = 0.0086$, b) Trend = $-0.091x + 218.60$ $r^2 = 0.0046$, c) Trend = $-0.152x + 356.62$ $r^2 = 0.0102$ and d) Trend = $-0.034x + 112.63$ $r^2 = 0.0007$. The smoothed turquoise line represents the 5 year moving average of runoff and the smoothed red line represents the 30 year moving average of runoff.

While the majority of biophysical indicators demonstrated declining trends in the North sub-region, the simulated cattle heat stress indices across three (Kalpowar, Malakof and Bancroft) of the four climate stations exhibited an increasing trend (Figure 27). The general pattern of the 5 year running mean values is similar to those produced for the East sub-region (Figure 22). The significant difference between to two regions was the extent of anomalously warm conditions in the early part of the record, with the North sub-region exhibiting slightly lower maximum temperature conditions at that time.

Three of the four climate stations exhibited a lower average incidence of THI values above 80, than for the East sub-region. The Tecoma climate station demonstrated a frequency of occurrence of THI values above 80 significantly higher than for the other three climate stations and also slightly greater than experienced in the East sub-region.

Both the 5 year and 30 year running mean values exhibited a decline in the occurrence of THI above 80 during the period 1920 to 1970, with the more recent record i.e. 1960 to present revealing strong increases to a frequency of occurrence more comparable to the early part of the record (i.e. 1890 to 1915) (Figure 27).

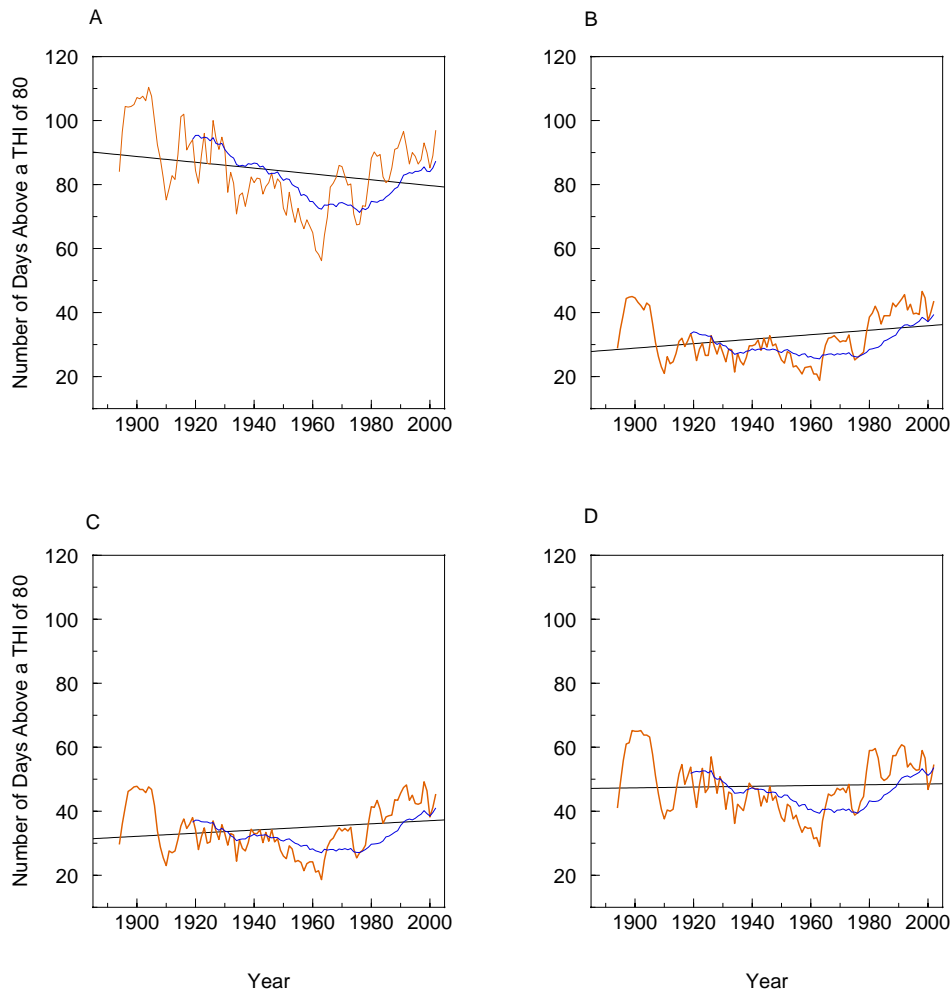


Figure 27: A time series of simulated annual cattle heat stress for a) “Tecoma”(39248), b) “Kalpowar” (39057), c) “Malakof” (39129) and d) “Bancroft” (39103) stations within the North sub-region. The linear trends were calculated from the annual data as follows a) Trend = $-0.091x + 261.52$ $r^2 = 0.0217$, b) Trend = $0.070x - 104.09$ $r^2 = 0.0296$, c) Trend = $0.049x - 60.78$ $r^2 = 0.0130$ and d) Trend = $0.012x - 24.25$ $r^2 = 0.0006$. The smoothed orange line represents the 5 year moving average of days with THI above 80 and the smoothed blue line represents the 30 year moving average of days with THI above 80.

3. ***Simulations of historical pasture production, deep drainage, runoff and cattle heat stress for the Central sub-region***

Given the low average annual rainfall and high average annual maximum and minimum temperatures in this sub-region simulated pasture production and hence ‘safe’ stocking rate were lower than for both the East and North sub-regions.

The average annual pasture production across all four climate stations was equivalent to 2776 kg TSDM/ha, with the average ‘safe’ stocking rate at 0.21 BE/ha.

Simulated pasture production in the Central sub-region is unusual compared to the other sub-regions, given that the climate station located in the driest area has return a increasing trend in annual production values (Figure 28) even though the linear trend analysis of annual rainfall returned a statistically significant declining trend for the period 1890 to 2002. While the annual trend was positive for the Auburn climate this trend was not statistically significant at the 95% confidence interval and was primarily the function of above average pasture production in two discreet periods namely the late 1950s and early 1960s and the 1970s (Figure 28).

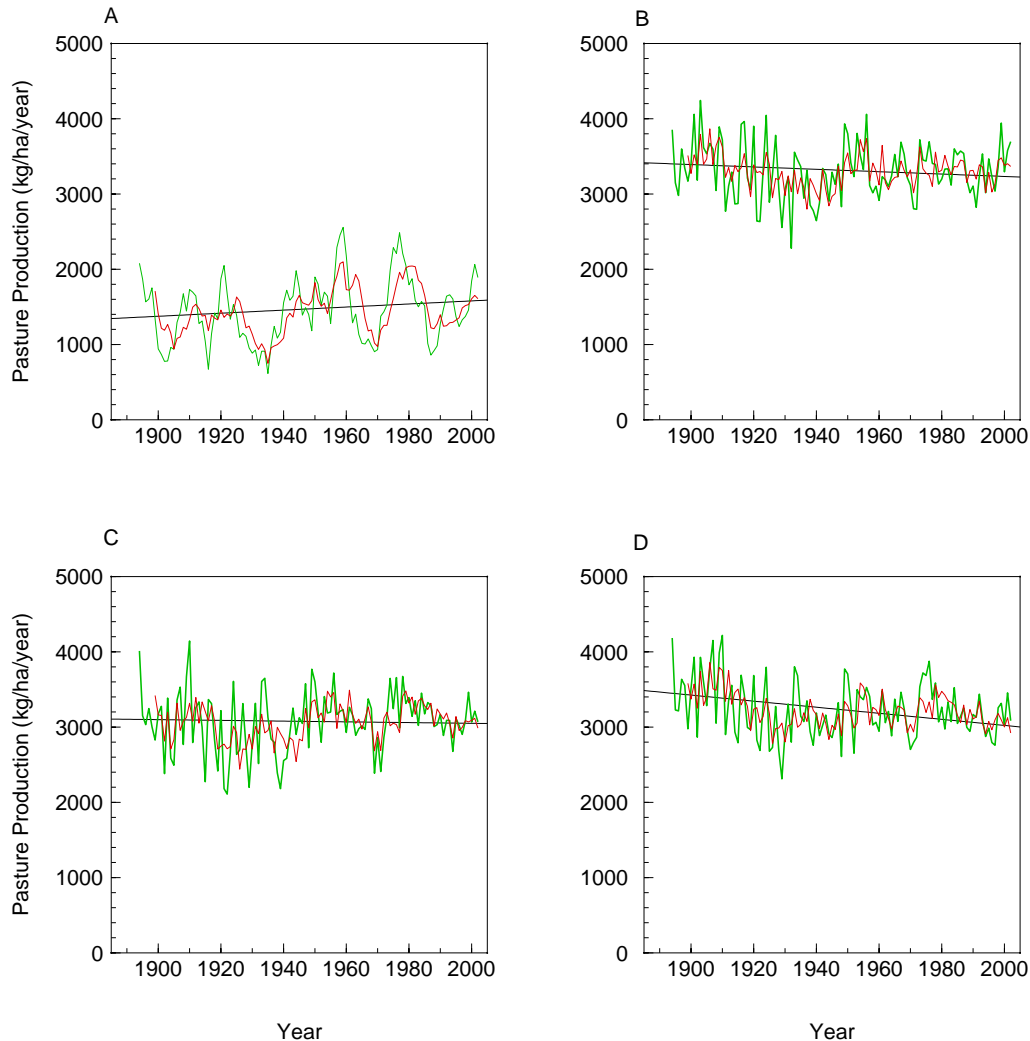


Figure 28: A time series of annual pasture production for a) “Auburn”(42059), b) “Gayndah” (39039), c) “Eidsvold” (39036) and d) “Biggenden” (40021) stations within the Central sub-region. The linear trends were calculated from the annual data as follows a) Trend = $2.042x - 2505.84$ $r^2 = 0.0051$, b) Trend = $-1.578x + 6388.56$ $r^2 = 0.001$, c) Trend = $-0.489x + 4026.79$ $r^2 = 0.0001$ and d) Trend = $-4.029x + 11079.08$ $r^2 = 0.0063$. The smoothed green line represents the 5 year moving average of pasture production and the smoothed red line represents the 10 year moving average of pasture production.

The calculation of ‘safe’ carrying capacity from the simulated pasture production values returned similar trends to those calculated from the annual pasture production values (Figure 29). The Auburn climate station demonstrated a ‘non-significant’ positive trend in-keeping with the simulated pasture values. Similarly, the remaining three climate stations returned declining trends although these again were not statistically significant at the 95% confidence interval (Figure 29). The 30 year running mean of ‘safe’ stocking rate exhibited a break-point at

approximately 1970. Before 1970 ‘safe’ stocking rates were slightly lower than 30 year running mean rates post 1970.

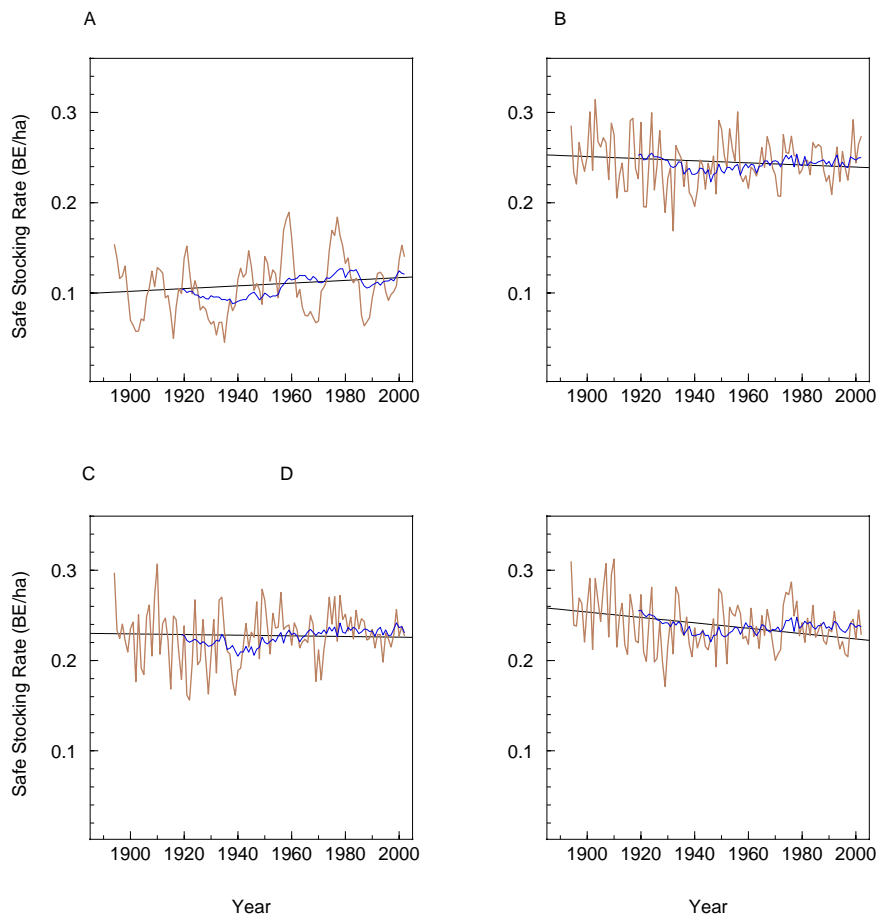


Figure 29: A time series of annual ‘safe’ stocking rate for a) “Auburn”(42059), b) “Gayndah” (39039), c) “Eidsvold” (39036) and d) “Biggenden” (40021) stations within the Central sub-region. The linear trends were calculated from the annual data as follows a) Trend = $0.00015x - 0.19$ $r^2 = 0.0051$, b) Trend = $-0.0001x + 0.47$ $r^2 = 0.00087$, c) Trend = $-0.00004x + 0.30$ $r^2 = 0.0001$ and d) Trend = $-0.0003x + 0.82$ $r^2 = 0.0064$. The smoothed brown line represents the 5 year moving average of ‘safe’ stocking rate and the smoothed blue line represents the 10 year moving average of ‘safe’ stocking rate.

The linear trend analysis of simulated drainage for this sub-region returned declining trends for each of the four climate stations (Figure 30). In each case the climate station trends were not statistically significant at the 95% confidence interval. The Gayndah climate station returned a declining trend approaching statistical significance while the remaining three stations were marginal (Figure 30). The 30 year running mean of deep drainage exhibited the lowest values for the period up to and including 2002 for all stations except Auburn, with this site returning the highest drainage value for the 30 year period up to and including 2002 (Figure 30). This finding was consistent with the simulated pasture production values and calculated ‘safe’ stocking rates produced for the Auburn station.

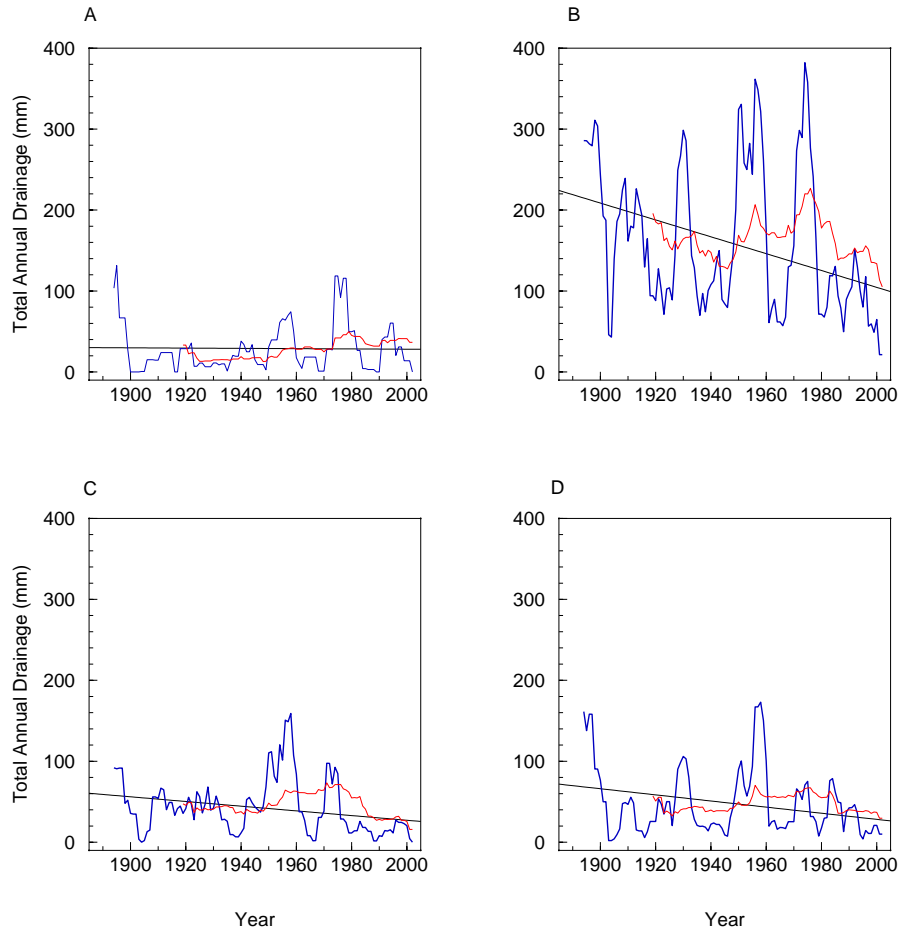


Figure 30: A time series of annual deep drainage for a) “Auburn”(42059), b) “Gayndah” (39039), c) “Eidsvold” (39036) and d) “Biggenden” (40021) stations within the Central sub-region. The linear trends were calculated from the annual data as follows a) Trend = $-0.017x + 62.18$ $r^2 = 0.0001$, b) Trend = $-1.041x + 2186.54$ $r^2 = 0.0355$, c) Trend = $-0.290x + 607.31$ $r^2 = 0.0169$ and d) Trend = $-0.379x + 785.29$ $r^2 = 0.0203$. The blue line represents the 5 year moving average of deep drainage and the red line represents the 10 year moving average of deep annual drainage.

The linear trend analysis of simulated runoff for the Central sub-region returned declining trends for all stations except Auburn (Figure 31). Once again all trends calculated from the annual data were not statistically significant at the 95% confidence interval. The 5 year running mean of runoff revealed a marked change for the Gayndah, Eidsvold and Biggenden climate stations after the early 1960s with runoff consistently lower than previous simulated (Figure 31). The results for these three stations would suggest that the interaction of rainfall and cover have resulted in the exceedence of a threshold for runoff. The 30 year running mean runoff value at 2002 for the three climate stations was lower or comparable to the lowest values simulated in the earlier part of the record (Figure 31).

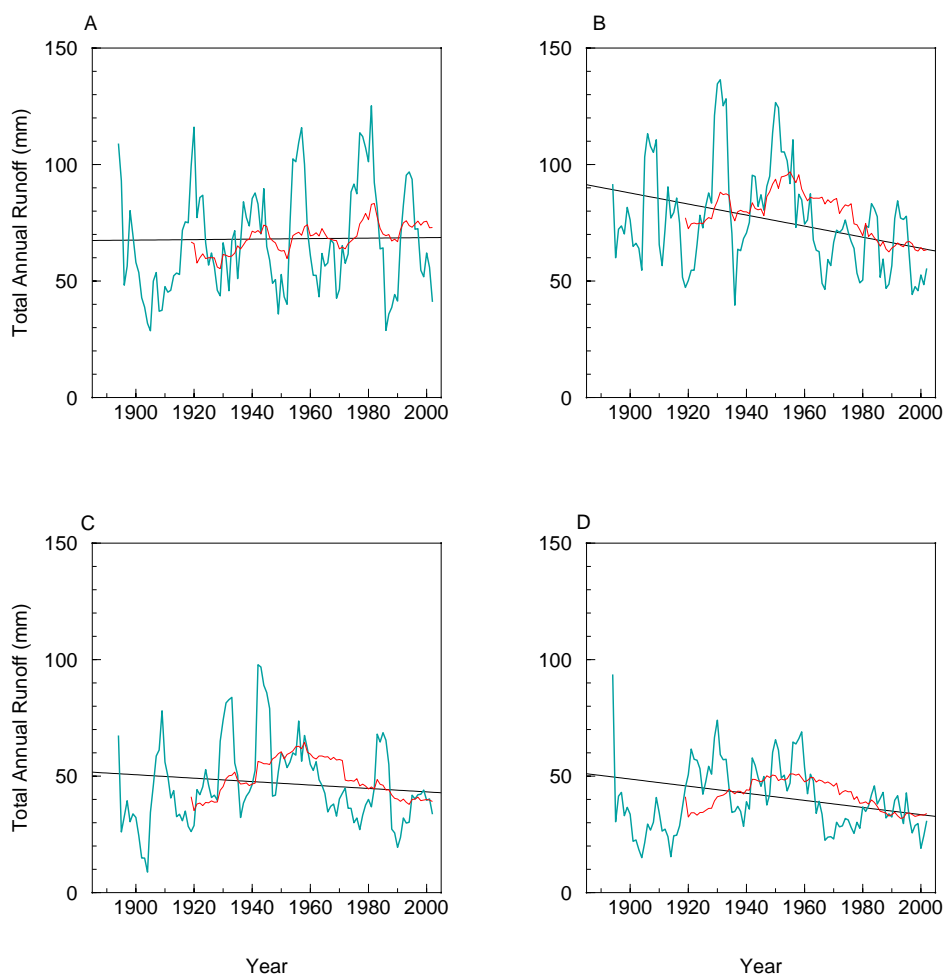


Figure 31: A time series of annual deep drainage for a) “Auburn”(42059), b) “Gayndah” (39039), c) “Eidsvold” (39036) and d) “Biggenden” (40021) stations within the Central sub-region. The linear trends were calculated from the annual data as follows a) Trend = $0.00064x + 47.33$ $r^2 = 0.00004$, b) Trend = $-0.237x + 538.24$ $r^2 = 0.0196$, c) Trend = $-0.074x + 190.33$ $r^2 = 0.0032$ and d) Trend = $-0.153x + 338.65$ $r^2 = 0.0157$. The turquoise line represents the 5 year moving average of annual runoff and the red line represents the 10 year moving average of annual runoff.

The linear trend analysis of the cattle heat stress index across all four of the Central sub-region stations exhibited declining trends for the period 1890 to 2002 (Figure 32). This was a function of the complex interaction between maximum temperature and moisture availability (represented by dewpoint temperature) used to calculate the index. At the beginning of the record maximum temperatures were significantly higher than the long-term mean for all four stations (greater than one standard deviation from the long-term mean). These above average maximum temperatures were associated with anomalously high annual rainfall thus producing the highest THI values for the entire record (Figure 32). Lower than average maximum temperatures in the late 1960s and early 70s were the result of extended periods of above average rainfall and thus while the dewpoint temperatures were relatively high the maximum temperatures were low and thus the occurrence of THI above 80 was the lowest on record. The linear trend analysis of the annual THI data, while producing declining trends for the period 1890 to 2002, returned no instances where the trend was statistically significant at the 95% confidence level. In all cases the 30-year running mean has demonstrated an upturn in THI since the late 1970s consistent with observed warming in both maximum and minimum temperatures (Figure 32)

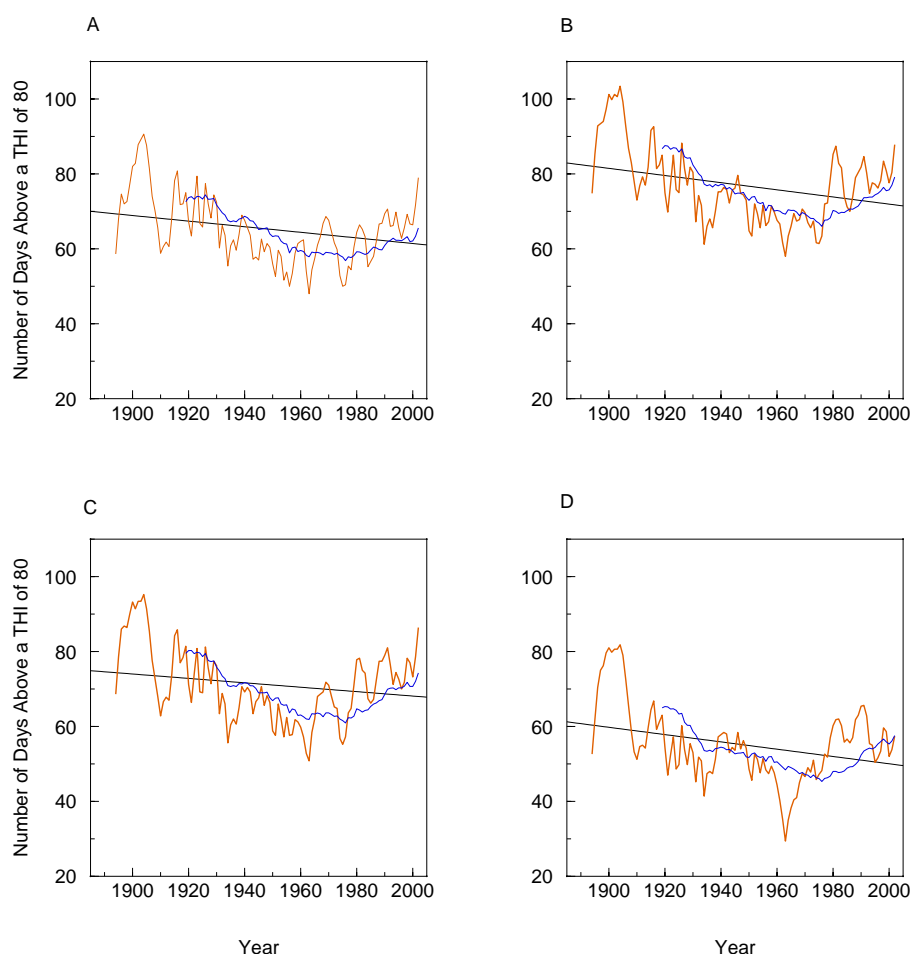


Figure 32: A time series of annual cattle heat stress for a) “Auburn”(42059), b) “Gayndah” (39039), c) “Eidsvold” (39036) and d) “Biggenden” (40021) stations within the Central sub-region. The linear trends were calculated from the annual data as follows a) Trend = $-0.075x + 210.85$ $r^2 = 0.0181$, b) Trend = $-0.096x + 263.00$ $r^2 = 0.028$, c) Trend = $-0.059x + 185.83$ $r^2 = 0.0104$ and d) Trend = $-0.097x + 244.70$ $r^2 = 0.0343$. The orange line represents the 5 year moving average of total number of days where THI was above 80 and the blue line represents the 10 year moving average of total number of days where THI was above 80.

4. Simulations of historical pasture production, deep drainage, runoff and cattle heat stress for the South sub-region

An analysis of the simulated pasture production in the South sub-region revealed a declining trend common across all the stations (Figure 33). The average annual pasture production for the South sub-region was simulated at 3216 kg of TSDM/ha. This would suggest slightly better production in this sub-region than any of the others and would thus result in a higher average ‘safe’ stocking rate as well.

As with the other sub-regions, the linear trend analysis of simulated pasture production while returning declining annual trends, failed to produce any that were statistically significant at the 95% confidence interval. The 5-year and 10-year moving averages exhibited extended periods of below average growth during the 1920 to 1940 with above average growth in the periods 1900 to 1910 and the 70s and early 80s (Figure 33). Declines in pasture production were apparent in the 10-year running mean since the early 90s with most pronounced declines exhibited by the Mounefontein climate station situated in the driest part of the sub-region (Figure 33 a).

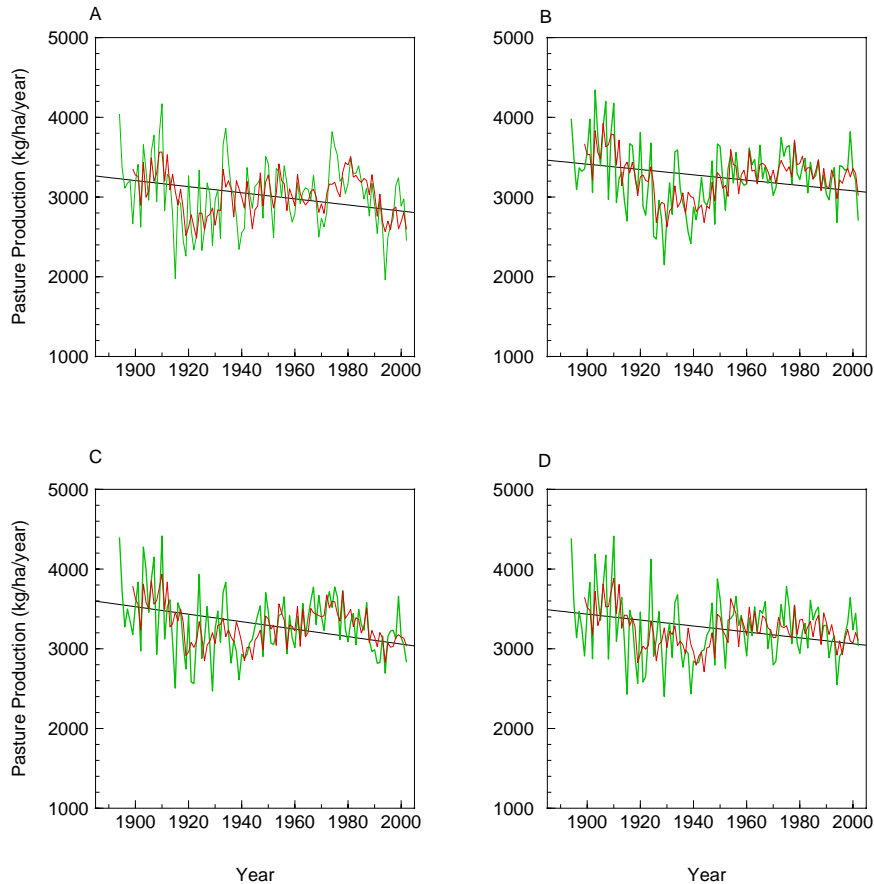


Figure 33: A time series of annual pasture production for a) “Mounefontein”(40138), b) “Goomeri” (40090), c) “Kingaroy” (40112) and d) “Kumbia” (40113) stations within the South sub-region. The linear trends were calculated from the annual data as follows a) Trend = $-3.818x + 10460.60$ $r^2 = 0.006$, b) Trend = $-3.342x + 9761.54$ $r^2 = 0.005$, c) Trend = $-4.685x + 12427.75$ $r^2 = 0.0084$ and d) Trend = $-3.715x + 10492.98$ $r^2 = 0.005$. The green line represents the 5 year moving average of pasture production and the red line represents the 10 year moving average of pasture production.

As the ‘safe’ stocking rates were calculated as a function of simulated pasture production the trend results were similar to those in Figure 33 (Figure 34). In each case the declining trends returned were not statistically significant at the 95% confidence interval. The wet 70s contributed strongly to the 30 year moving average of ‘safe’ stocking rate with each time series indicating more favourable stocking rates post 1970 than in the earlier part of the simulated time series.

The 5 year moving average of ‘safe stocking rate also revealed a consistent period of low ‘safe’ stocking rate between the early 1920s and early 1950s consistent with relatively low rainfall for that period. The 5 year moving average of ‘safe’ stocking rates also highlighted the recent declines since the early 1990s, again consistent with observed rainfall declines.

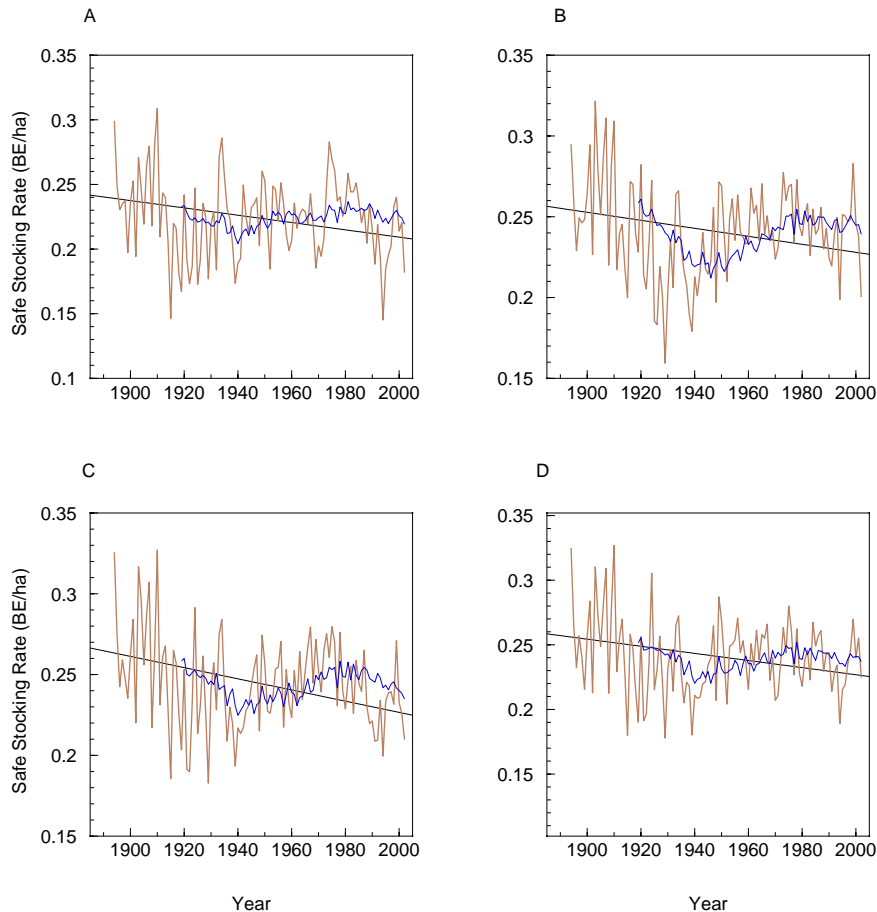


Figure 34: A time series of annual 'safe' stocking rate for a) "Mounefontein"(40138), b) "Goomei" (40090), c) "Kingaroy" (40112) and d) "Kumbia" (40113) stations within the South sub-region. The linear trends were calculated from the annual data as follows a) Trend = $-0.0003x + 0.77$ $r^2 = 0.0062$, b) Trend = $-0.0002x + 0.72$ $r^2 = 0.0046$, c) Trend = $-0.0003x + 0.92$ $r^2 = 0.00839$ and d) Trend = $-0.0003x + 0.78$ $r^2 = 0.00496$. The brown line represents the 5 year moving average of annual 'safe' stocking rate and the blue line represents the 30 year moving average of annual 'safe' stocking rate.

The linear trend analysis of simulated drainage for this sub-region returned declining trends for each of the four climate stations (Figure 35). In each case the climate station trends were not statistically significant at the 95% confidence interval.

Both the 5 year and 30 year moving average of deep drainage provided important insights into the effect that rainfall variability can have on processes such as drainage and runoff. The 5 year moving average of drainage showed a well defined peak during the mid 1950s. This peak in drainage was consistent with above average rainfall across most of Queensland during 1950, and 1954 to 1957 period (Figure 35). The 30 year moving average values also showed relatively consistent above average drainage conditions for the period 1960 to 1990, reflecting both the wet 1950s and wet 1970s. Since the early 1990s the 30 year moving average of drainage began to decline in response to lower than average rainfall.

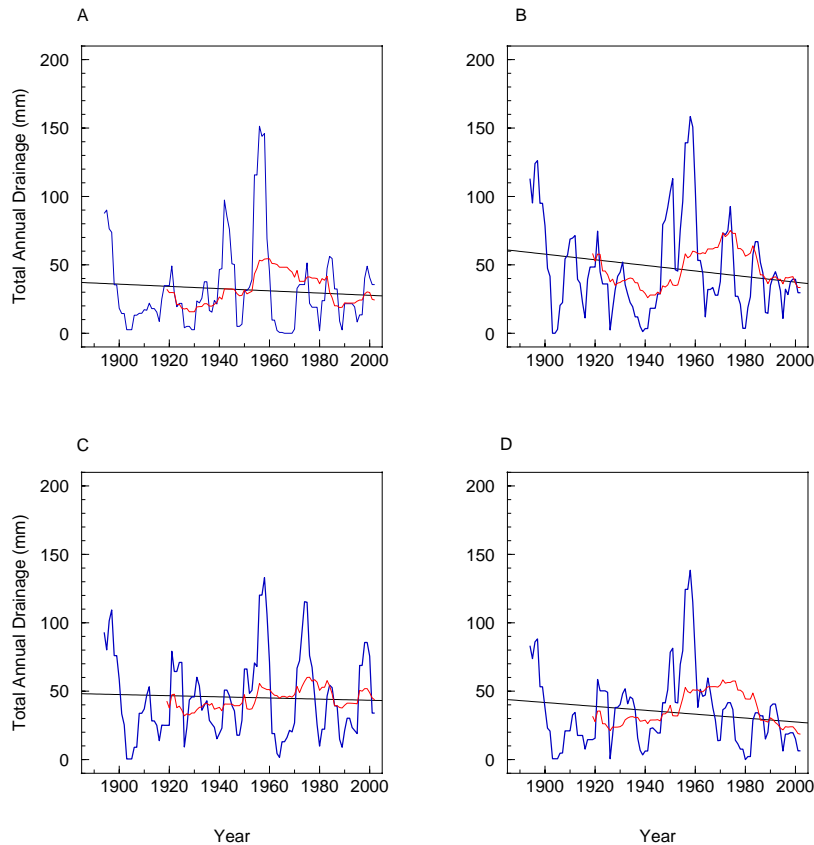


Figure 35: A time series of annual deep drainage for a) “Mounefontein”(40138), b) “Goomeri” (40090), c) “Kingaroy” (40112) and d) “Kumbia” (40113) stations within the South sub-region. The linear trends were calculated from the annual data as follows a) Trend = $-0.082x + 190.76$ $r^2 = 0.0019$, b) Trend = $-0.205x + 446.89$ $r^2 = 0.0085$, c) Trend = $-0.0042x + 126.79$ $r^2 = 0.0004$ and d) Trend = $-0.142x + 311.92$ $r^2 = 0.0065$. The blue line represents the 5 year moving average of annual deep drainage and the red line represents the 30 year moving average of annual deep drainage.

The linear trend analysis of simulated runoff for the South sub-region returned declining trends for all stations except Mounefontein (Figure 36). Once again all trends calculated from the annual data were not statistically significant at the 95% confidence interval and explained less than 1% of the time series variability.

The 5 year running mean of runoff revealed a marked change for the Goomeri, Kingaroy and Kumbia climate stations after the early 1960s with runoff consistently lower than previous simulated (Figure 36). The results for these three stations would suggest that the interaction of rainfall and cover have resulted in the exceedence of a threshold for runoff.

The 30 year moving average of runoff clearly reflected the dry 1900 to 1920 period as well as the wet 1940s and 1950s (Figure 36).

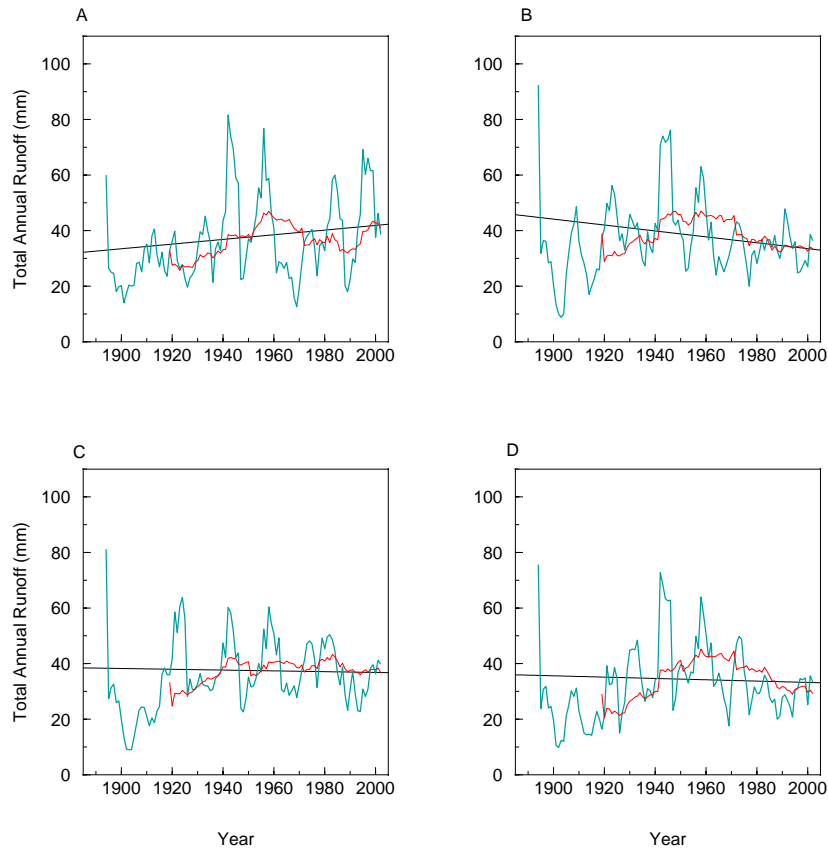


Figure 36: A time series of annual runoff for a) “Mounefontein”(40138), b) “Goomeri” (40090), c) “Kingaroy” (40112) and d) “Kumbia” (40113) stations within the South sub-region. The linear trends were calculated from the annual data as follows a) Trend = $0.0727x - 126.18$ $r^2 = 0.0053$, b) Trend = $-0.106x + 245.95$ $r^2 = 0.0068$, c) Trend = $-0.014x + 65.47$ $r^2 = 0.0002$ and d) Trend = $-0.024x + 81.01$ $r^2 = 0.0004$. The turquoise line represents the 5 year moving average of annual runoff and the red line represents the 30 year moving average of annual runoff.

The linear trend analysis of the cattle heat stress for the South Sub-region revealed both positive and negative trends for the period 1890 to 2002 (Figure 37). Three of the four climate stations (i.e. Goomeri, Kingaroy and Kumbia) returned positive trends in the occurrence of heat stress (Figure 37). This was a function of their locality in the drier portion of the sub-region.

The South sub-region, as with all the others, exhibited an anomalously high (greater than one standard deviation from the mean) frequency of occurrence for THI above 80 although this was not enough to return statistically significant linear trends for any station (Figure 37).

In all cases the 30-year running mean demonstrated an upturn in THI since the late 1970s consistent with observed warming in both maximum and minimum temperatures (Figure 37). This was particularly pronounced for the driest climate station (Goomeri).

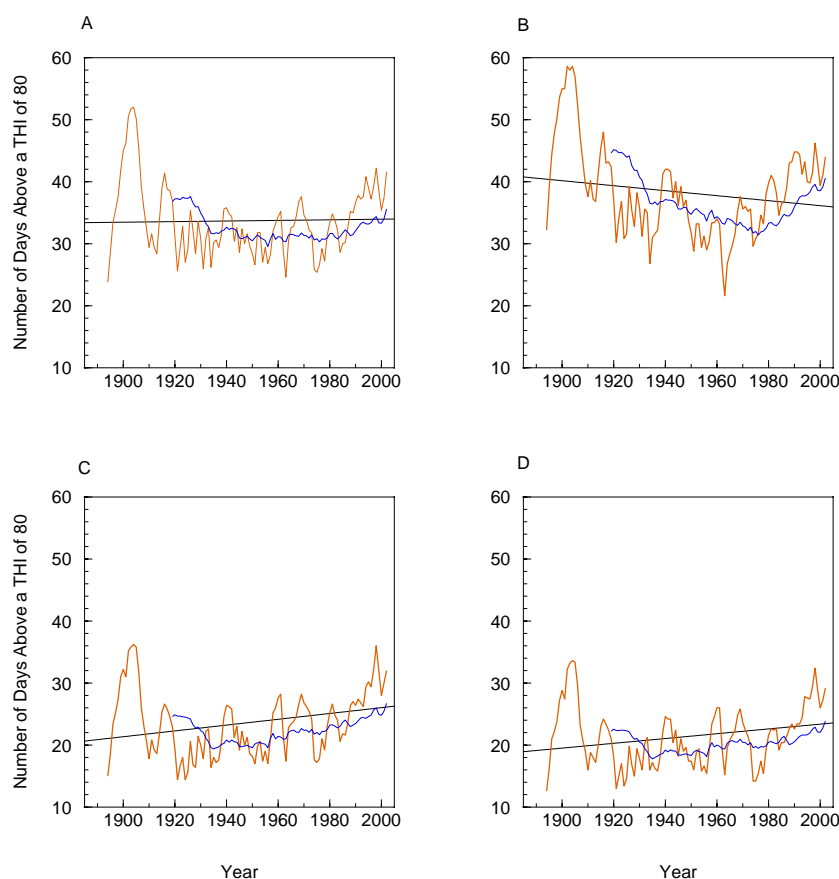


Figure 37: A time series of annual cattle heat stress for a) “Mounefontein”(40138), b) “Goomeri” (40090), c) “Kingaroy” (40112) and d) “Kumbia” (40113) stations within the South sub-region. The linear trends were calculated from the annual data as follows a) Trend = $0.0130x + 24.21$ $r^2 = 0.0002$, b) Trend = $-0.040x + 116.65$ $r^2 = 0.0096$, c) Trend = $0.047x - 67.73$ $r^2 = 0.0213$ and d) Trend = $0.0394x - 53.93$ $r^2 = 0.0171$. The orange line represents the 5 year moving average of the occurrence of THI values above 80 and the blue line represents the 30 year moving average of occurrence of THI values above 80.

5. Summary of the results from simulations of historical pasture production, deep drainage, runoff and cattle heat stress for the Burnett study region.

The simulation studies revealed a number of important issues regarding the contemporary impacts of both natural variability and anthropogenic climate change on biophysical indicators such as pasture production, deep drainage, runoff and cattle heat stress.

These were:

- The simulation of annual pasture production, revealed consistent declining trends across all stations and sub-regions except for the driest station in the central sub-region (Auburn). While the simulation results returned a consistent declining trend in pasture production for the study region, there was no instance where the linear trends were statistically significant or explained more than 1% of the production variability.
- Similarly the simulation of deep drainage returned no instances where drainage increased although both the Central and South sub-regions returned almost no linear trends for the period 1890 to 2002. While the simulation results returned a consistent declining trend in

deep drainage for the study region, there was no instance where the linear trends were statistically significant or explained more than 1% of the production variability.

- The simulated runoff data returned three instances where positive trends occurred. These instances occurred in the East, Central and South sub-regions in predominantly drier locations. Again, while the simulation results returned, for the most part, declines in runoff for the study region, there was no instance where the linear trends were statistically significant or explained more than 1% of the production variability. In some cases the trends were approaching statistical significance with P close to 0.10.
- The simulation of the occurrence of THI above 80 returned a predominantly negative trend across the Study region. The North and South sub-regions did demonstrate instance where positive trends were returned. However the linear trends for all sub-regions were below the 95% confidence limit. The declining trend was driven predominantly by a declining trend in atmospheric moisture in this region.
- While the linear trend analysis for the entire period did not indicate significant long-term changes, the 5, 10, and 30 year moving averages revealed the existence of important short and longer-term variability. Most notable were above average conditions in the late 1960s and 1970s consistent with above average rainfall and below average conditions since the early 1990s, consistent with anomalously low rainfall.
- The small net changes produced by the simulation studies is the function of the opposing effects that increasing temperature may have on pasture production. Projected increase in temperature can increase pasture production during spring as the pastures may be better placed to use the spring rainfall if conditions are warmer. Increasing temperature can also decrease pasture production by increasing potential evapo-transpiration and producing higher vapour pressure deficits.

In summary all the biophysical indicators simulated in this project returned linear trends below the 95% confidence interval with these trends explain less than 1% of the internal data variability. Whilst the models rely on rainfall and temperature to formulate the values analysed for this project the interaction of temperature and rainfall, often serves to weaken the direction of change.

On the whole the Burnett study region exhibited consistent declines in pasture, deep drainage and runoff although a number of instance occurred where climate stations returned positive trends for these particular indices. In all instances these trends were not statistically significant at the 95% confidence interval and explained less than 1% of the data variability.

Simulated Change in Pasture Production, Run-off, Drainage and Heat Stress in Response to Global Warming

At present projections of future changes in rainfall and temperature, for Queensland, are available as absolute values or percentage change from a climatological base period (1990 to 1999), with these projections developed from a full range of probable future greenhouse gas emission scenarios. Future emissions are the product of complex interacting systems driven by population change, socioeconomic development, and technological change; all of which are highly uncertain, especially when extended as far as the year 2100 (Pittock, 2004).

The interaction of population change, socio-economic development and technological change in terms of the effects on future greenhouse gas concentrations were considered by an international panel of specialists and published in a Special Report on Emission Scenarios (SRES) in 2000 (Nakicenovic and Swart 2000). Thirty-five SRES scenarios were developed for the report based on four different “storylines” of population, technological, and economic development at both regional and global scales. The resultant accumulated emissions by 2100, expressed in units of thousands of millions of tonnes of carbon equivalent (GtC), range from a low of 770 GtC to approximately 2540 GtC (Nakicenovic and Swart 2000). This equates to carbon dioxide concentrations at 2100 from 540 to 970 ppmv (Nakicenovic and Swart 2000).

The global warming response produced by this range of future emission scenarios is large with temperatures increases by 2100 of between 1.4 and 5.8 °C above the 1990 to 1999 base (IPCC 2001). In order to capture the full range of uncertainty when developing future climate change scenarios one must not only consider the uncertainty regarding future emissions but also uncertainty due to difference between climate models.

In order to fully consider these two elements of uncertainty for the purposes of this project the entire SRES emission scenario range and the resultant simulation output from a number of climate models were considered.

The full range of SRES scenarios were used to initialise twelve climate models, which in turn produced global and regional scenarios of changes in temperature and rainfall. The twelve climate models used to determine the patterns of climate change for the Australian region consist of both coarse and fine resolution models. Typically, there are significant differences between models with regard to climate changes simulated at the regional scale, particularly for precipitation. For this reason the models used underwent a number of quality control tests. These were:

1. The model must have adequate model documentation;
2. The model must be initialised from a observed increase in greenhouse forcing through the twentieth century (a ‘warm start’ simulation); and
3. The models must be able to replicate the average climatic conditions for the Australian region in terms of seasonal mean temperature, precipitation and mean sea level pressure.

The climate response from each model was calculated at each grid point in terms of local temperature change (or percent rainfall change) per degree of global warming (Whetton, 2001). This was done by linearly regressing the local seasonal mean temperature (or rainfall) against global average temperature and taking the slope of the relationship at each grid point as the estimated response. The grid point values were then mapped to obtain the pattern of model response (Whetton, 2001) (Figure 38 and 39).

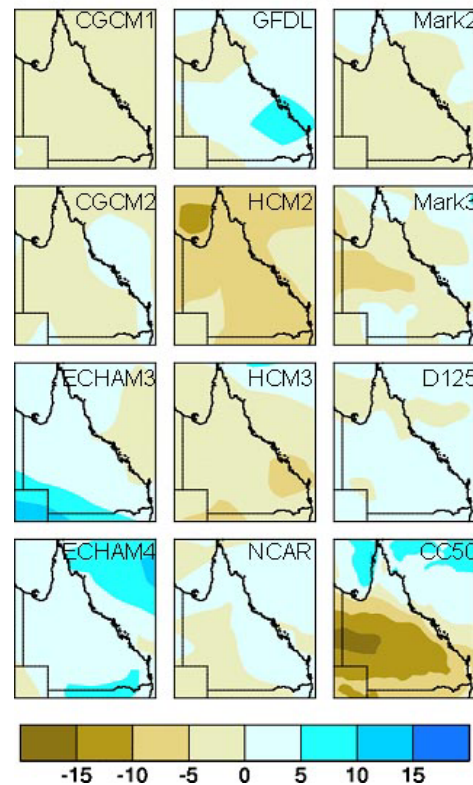


Figure 38: Percentage change in annual rainfall per degree of global warming for Queensland, produced by 12 international climate models.

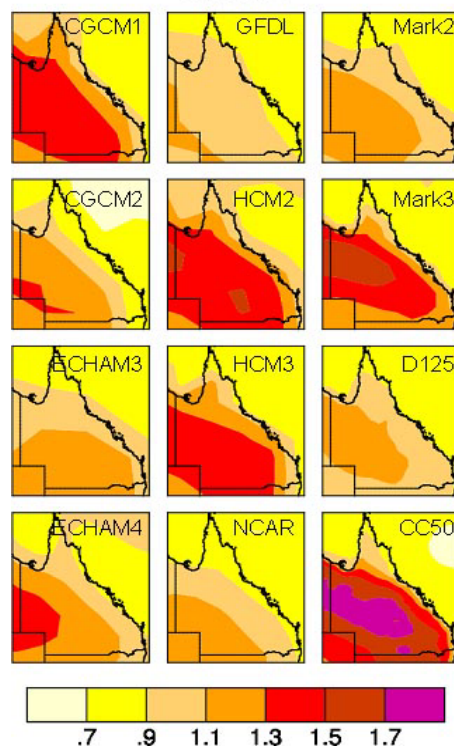


Figure 39: Absolute change in annual average temperature per degree of global warming for Queensland, produced by 12 international climate models.

The seasonal and annual response patterns from each of the twelve climate models were interpolated onto a common 5° by 5° grid map (Figure 38 and 39).

In order for the individual climate simulations to be used in a modeling experiment the change in both temperature and rainfall per degree in global warming was converted to an absolute change by prescribing an amount of global warming. In the case of this project a global average temperature increase was prescribed for a 2030 and 2070 period based on the mid-point of the range 0.3 to 2.0°C for 2030 (i.e. 0.85°C) and 0.7 to 5.8°C for 2070 (i.e. 2.55°C) (IPCC 2001).

However, in order to use the scenarios of absolute temperature and percentage rainfall change at 2030 and 2070, in a biophysical modeling framework, the scenarios of change were incorporated into the historical climate record in order to produce a daily time series. The method for producing the daily climate change files was modified from earlier work by Crimp *et al.*, (2002).

The historical daily rainfall record for the period 1900 to 2002 was used to modify all remaining climate variables required to simulate pasture production (i.e. maximum and minimum temperature, evaporation, vapour pressure and solar radiation). The historical daily rainfall record was used as a template for identifying both 'rain' and 'non-rain' affected days throughout the record in order to develop daily climatologies for 'rain' and 'non-rain' days temperature, vapour pressure, solar radiation and evaporation. These calculations were undertaken as follows:

1. a day was classified as 'rain' affected if rainfall occurred on (a) the previous day, (b) day of record, or (c) next day; otherwise the day was classified as a 'dry' day. For solar radiation, only the day of occurrence and day preceding rainfall were classified as 'rain-affected';
2. for each calendar day, a seven day running mean was calculated using the calendar date as the mid point. This latter procedure provided some smoothing but was required given limited number of rain days in some seasons;
3. The seven day running means were then created, with the averaging being grouped on 'rain' and 'non-rain' affected days; and
4. the sequence of 'rain' and 'non-rain' affected days was then used to assign the relevant average seven day running mean value back into the long-term record.

Using the above procedure a 102-year daily record of temperature, vapour pressure, evaporation and solar radiation can be calculated using the prescribed variability contained in the rainfall record. While this process assumes no change in future 'within-season' and daily rainfall variability, GCMs limited ability to adequately simulate daily rainfall variability made this an appropriate compromise.

At this point the 2030 and 2070 average temperature change and percentage rainfall change projections from the 12 climate models were added to the 'baseline' climate data. The baseline maximum and minimum temperatures were changed using a linear regression equation developed from the historical relationships. The slopes of the maximum and minimum temperature regression lines were compared at each location in order to determine how to apportion the projected change in average temperature. In the case where both historical maximum and minimum temperatures records returned positive linear trends the slope of each trend line was used to apportion the projected average temperature change. In the case where trends were divergent, i.e. maximum temperatures decreasing and minimum temperatures increasing projected average temperature change was apportioned by applying half of the average temperature change to both maximum and minimum temperature.

Future projections of change in evaporation, VPD and solar radiation were not available for this project so these parameters were modified based on regression relationships with maximum temperature. Correlations between annual average maximum temperature and other climate variables at the national scale were: $r = 0.78$ (evaporation), $r = 0.69$ (radiation) and $r = 0.57$ (vapour pressure). At the State resolution correlations between annual average maximum temperature and remaining climate variables were $r = 0.76$ (evaporation), $r = 0.67$ (radiation) and $r = 0.61$ (vapour pressure).

The 'baseline' rainfall record was modified by applying the projected change directly to the daily rainfall amounts. In other words a 20% reduction in projected rainfall would be accounted for by reducing daily values by 20%.

The process above served to produce a climate data set of 102 years with either no change ('baseline') or a 2030 or 2070 change applied. The climate data was used by the GRASP model to produce a 102 year times series of pasture, production, deep drainage and runoff. The simulation included the 'CO₂ fertilisation effect' by modifying the radiation use efficiency and transpiration efficiency setting in the model in response to changes in CO₂ concentration (Crimp *et al.*, 2002). The time series of simulated data was averaged in order to provide a discrete value for each variable at 2030 and 2070.

Simulated pasture growth integrates the impacts of changes in rainfall, temperature, solar radiation, humidity, evaporative demand and CO₂ concentration. Biological processes have mostly non-linear responses to climate variables. For example in the case of temperature effects on plant growth there is a lower temperature below which growth cannot occur, an optimal temperature which promotes maximum growth and a supra-optimal temperature above which is too hot for growth to occur. Climate variables also can have opposing effects on the processes of plant water use and growth. For example increasing daytime temperature can increase evaporative demand and vapour pressure deficit reducing pasture water use efficiency. In contrast increasing daytime temperatures are likely to increase photosynthesis where temperatures are currently limiting (e.g. quite frequently for C₄ tropical grasses in south east Queensland, McKeon *et al.*, 1988, McKeon *et al.*, 1998b).

Native pasture growth in south-east Queensland can also be limited by nitrogen (and to a lesser extent phosphorus) (McKeon *et al.*, 1998a). Thus the maximum response to "favourable" climate changes can be limited by nutrient availability. In the following studies nutrient availability has been assumed to be unaffected by climate change scenarios (e.g. Hall *et al.* 1998).

The general effects of CO₂ on pasture growth and water use parameters are as suggested by Howden *et al.*, 1998, Hall *et al.*, 1998 and Howden *et al.*, 1999. Increasing CO₂ concentration is assumed to result in a slower rate of water use, and increased transpiration and radiation use efficiencies.

The impact of CO₂ increase has differing effects for drier and wetter scenarios where pasture production is low for climatic reasons than the benefits of CO₂ are likely to be expressed. However in the case where nutrients are likely to limit growth then little advantage is likely from the effects of CO₂ concentration. Thus the major benefit of increasing CO₂ is likely to be in the dryer rainfall scenarios.

1. Climate Change Projections for the East sub-region

The model simulation results for each station within the sub-region have been summarised in the tables that follow. The projected global annual average temperature increase of 0.85°C by 2030 resulted in a warming in the East sub-region of between 0.68 and 1.02°C (above the 1990 to 1999 climatological base) and 6.38% to –6.38% change in rainfall (based on the range of outputs from the twelve climate models).

By 2070 the projected increase in global temperature of 2.55°C (above the 1990 to 1999 climatological base) resulted in a warming in the East sub-region of between 2.04 and 3.06°C (above the 1990 to 1999 climatological base) and 19.13% to –19.13% change in rainfall.

The combined effect of projected warming and projected rainfall change on pasture production, deep drainage, runoff and heat stress for each of the four climate stations was simulated using the GRASP model and modified historical climate record (as described above). Of the twelve climate models used 7 projected declining rainfall for this sub-region while 5 projected rainfall increases. The resultant impacts on the simulated pasture production, deep drainage and runoff values were thus both positive and negative.

The impact of climate change scenarios was summarised in percentage terms for annual pasture growth, drainage and runoff. However in the case of each stress indices the base climate indicated zero heat stress days for several locations as would be expected in a favourable climate such as coastal or elevated regions. Thus the analysis of heat stress days is reported in terms of absolute number of days rather than percentage increase.

The climate change simulations for Bundaberg climate station (39015) revealed seven instances were annual pasture growth declined (in response to projected rainfall declines) and five instances were pasture production increased (Table 27). Given the equally probable range of rainfall increase and decrease and temperature increase of between 0.68 and 1.02°C by 2030, little mean change in pasture production was produced (i.e. 0.1% - Table 27). The simulated response from deep drainage and runoff was more definitive with mean changes of –5.3 and –1.9% respectively.

The determination of the climate change impact on heat stress revealed an important limitation in the current methodology used to produce daily climate change time series data. The production of daily climatologies served to smooth the occurrence of extreme temperature conditions and hence reduce the frequency of THI days above 80 (Table 27). In the case of the Bundaberg climate station the scaling process resulted in the occurrence of zero days above a THI of 80.

It is difficult at this stage to assess the implications of an increase in heat stress days. Environments which would be regarded as “benign” (i.e. zero or a low number of heat stress days) may in fact be relatively more impacted by a small increase in heat stress days than environments where the base climate already has a moderate occurrence of heat stress and hence some adaptation of management or choice of cattle breeds has already occurred.

The projected changes in THI above 80 thus represent a conservative estimate of future change in the frequency of occurrence.

By 2070 the simulated change in pasture production, deep drainage, runoff and heat stress for the Bundaberg climate station increased in response to higher temperatures and greater rainfall

change. Pasture production was shown to decline by 1%, with this decline largely offset by the large project increases in rainfall simulated by the CSIRO Mark 2 model. Both deep drainage and runoff were shown to decline by 13 and 6% respectively (Table 28). In the case of THI days above 80, while the base simulation showed zero occurrences of days above a THI of 80, the average annual occurrence by 2070 increased to 68 days.

Table 27: Average simulated values of growth, drainage, run-off and heat stress produced by the GRASP model in response to enhanced Greenhouse gas concentrations at 2030 for the Bundaberg Station (39015). Climate Change projections from 12 different General Circulation models have been applied to the GRASP model. Average statistics are presented in the lower portion of the table.

2030	Annual Growth (kg/ha)	Annual Drainage (mm)	Annual Run-Off (mm)	Heat Stress Index (Days)
BASE	3137	37	35	0
CGCM1	3131	33	34	0
GFDL	3229	50	38	0
Mark2	3131	33	34	0
CGCM2	3182	42	36	0
HCM2	3075	27	32	1
Mark3	3134	33	34	1
ECHAM3	3131	33	34	0
HCM3	3070	27	32	0
D125	3181	41	36	0
ECHAM4	3181	41	36	0
NCAR	3182	42	36	0
CC50	3075	27	32	1
Aggregated Statistics of Mean Percentage Change across all Scenarios (Heat Stress Index results presented as days not percentages)				
MEAN	0.1%	-5.3%	-1.9%	0.2
MEDIAN	-0.2%	-10.6%	-3.1%	0
STANDARD DEVIATION	1.6%	18.3%	5.4%	0.4
MAXIMUM	2.9%	31.7%	8.2%	1
MINIMUM	-2.2%	-28.8%	-9.3%	0

Table 28: Average simulated values of growth, drainage, run-off and heat stress produced by the GRASP model in response to enhanced Greenhouse gas concentrations at 2070 for the Bundaberg Station (39015). Climate Change projections from 12 different General Circulation models have been applied to the GRASP model. Average statistics are presented in the lower portion of the table.

2070	Annual Growth (kg/ha)	Annual Drainage (mm)	Annual Run-Off (mm)	Heat Stress Index (Days)
BASE	3137	37	35	0
CGCM1	3137	37	35	0
GFDL	3095	25	31	79
Mark2	3387	75	44	54
CGCM2	3095	25	31	79
HCM2	3258	48	38	54
Mark3	2828	11	25	91
ECHAM3	3095	25	31	91
HCM3	3095	25	31	79
D125	2839	12	25	79
ECHAM4	3259	46	38	79
NCAR	3259	46	38	79
CC50	3258	48	38	54
Aggregated Statistics of Mean Percentage Change across all Scenarios (Heat Stress Index results presented as days not percentages)				
MEAN	-1.0%	-12.8%	-5.7%	68
MEDIAN	-1.3	-31.7%	-10.3%	79
STANDARD DEVIATION	5.8%	49.7%	16.8%	25.2
MAXIMUM	8.0%	100%	25.8%	91
MINIMUM	-9.8%	-69.2%	-27.8%	0

The Gin Gin climate station revealed a small mean annual increase in pasture production of 0.2% by 2030, although deep drainage and runoff again showed declines of approximately 4 and 2% respectively (Table 29). The change in the frequency of THI days above 80 was larger for this location with an average increase from 2 to 12.8 days (Table 29).

The CO₂ fertilisation effect was evident when reviewing the maximum and minimum changes in pasture production. For an increase of 2% and 0.8°C for rainfall and temperature respectively, an increase in pasture production of 1.4% was simulated. However, for the same increase in temperature but 2% decline in annual rainfall produced no decline in pasture production occurred. This common result would suggest that the CO₂ fertilisation effect served to mitigate pasture productivity losses (Table 29).

By 2070 mean annual pasture production was projected to decline by 0.3%, with deep drainage and runoff declining by approximately 11 and 7% respectively (Table 30). The projected change in the frequency of days with THI above 80 showed an increase from the baseline of 2 to a mean of 83 days per year (Table 30).

Table 29: Average simulated values of growth, drainage, run-off and heat stress produced by the GRASP model in response to enhanced Greenhouse gas concentrations at 2030 for the Gin Gin (39040). Climate Change projections from 12 different General Circulation models have been applied to the GRASP model. Average statistics are presented in the lower portion of the table.

2030	Annual Growth (kg/ha)	Annual Drainage (mm)	Annual Run-Off (mm)	Heat Stress Index (Days)
BASE	3212	88	48	2
CGCM1	3212	81	46	12
GFDL	3287	107	51	11
Mark2	3212	81	46	12
CGCM2	3251	94	49	11
HCM2	3165	70	43	16
Mark3	3215	81	46	16
ECHAM3	3212	81	46	12
HCM3	3163	70	43	12
D125	3250	93	49	12
ECHAM4	3250	93	49	12
NCAR	3251	94	49	11
CC50	3165	70	43	16
Aggregated Statistics of Mean Percentage Change across all Scenarios (Heat Stress Index results presented as days not percentages)				
MEAN	0.2%	-4.0%	-2.3%	12.7
MEDIAN	No Change	-7.4%	-3.8%	12
STANDARD DEVIATION	1.2%	12.6%	5.1%	2.01
MAXIMUM	2.4%	21.5%	6.8%	16
MINIMUM	-1.5%	-20.2%	-9.1%	11

Table 30: Average simulated values of growth, drainage, run-off and heat stress produced by the GRASP model in response to enhanced Greenhouse gas concentrations at 2070 for the Gin Gin (39040). Climate Change projections from 12 different General Circulation models have been applied to the GRASP model. Average statistics are presented in the lower portion of the table.

2070	Annual Growth (kg/ha)	Annual Drainage (mm)	Annual Run-Off (mm)	Heat Stress Index (Days)
BASE	3212	88	48	2
CGCM1	3191	68	43	86
GFDL	3435	146	57	64
Mark2	3191	68	43	86
CGCM2	3320	105	50	64
HCM2	2987	40	35	98
Mark3	3198	67	43	98
ECHAM3	3191	68	43	86
HCM3	2980	41	36	86
D125	3324	102	51	86
ECHAM4	3324	102	51	86
NCAR	3320	105	50	64
CC50	2987	40	35	98
Aggregated Statistics of Mean Percentage Change across all Scenarios (Heat Stress Index results presented as days not percentages)				
MEAN	-0.3%	-10.6%	-6.7%	83.5
MEDIAN	-0.7%	-22.3%	-10.6%	86
STANDARD DEVIATION	4.5%	35.6%	14.3%	12.8
MAXIMUM	7.0%	65.7%	19.7%	98
MINIMUM	-7.2%	-53.7%	-25.8%	64

The projected 2030 changes in pasture production for the Moolboolaman climate station ranged from a 2.8% increase to a 1.8% decline (Table 31). The mean change in pasture production was thus very small (i.e. 0.05%).

The projected 2030 changes in deep drainage for the Moolboolaman climate station ranged from plus or minus 20% (Table 31). The mean change in deep drainage was approximately -4%. Similarly the projected changes in runoff ranged from a 7.3% to -6.7%, with a small mean annual decline of approximately 1% (Table 31).

The projected changes in the frequency of days above a THI of 80 for Moolboolaman more than doubled. Increasing from 11 to 26 days (Table 31).

Table 31: Average simulated values of growth, drainage, run-off and heat stress produced by the GRASP model in response to enhanced Greenhouse gas concentrations at 2030 for the Moolboolaman (39218). Climate Change projections from 12 different General Circulation models have been applied to the GRASP model. Average statistics are presented in the lower portion of the table.

2030	Annual Growth (kg/ha)	Annual Drainage (mm)	Annual Run-Off (mm)	Heat Stress Index (Days)
BASE	3251	116	54	11
CGCM1	3245	107	53	26
GFDL	3330	139	58	17
Mark2	3245	107	53	26
CGCM2	3287	123	56	17
HCM2	3196	92	51	35
Mark3	3248	106	53	35
ECHAM3	3245	107	53	26
HCM3	3192	93	51	26
D125	3286	121	56	26
ECHAM4	3286	121	56	26
NCAR	3287	123	56	17
CC50	3196	92	51	35
Aggregated Statistics of Mean Percentage Change across all Scenarios (Heat Stress Index results presented as days not percentages)				
MEAN	0.05%	-4.3%	-1.0%	26
MEDIAN	-0.2%	-7.5%	-2.0%	26
STANDARD DEVIATION	1.3%	12.1%	4.4%	6.6
MAXIMUM	2.4%	19.8%	7.3%	35
MINIMUM	-1.8%	-20.1%	-6.7%	17

The projected 2070 changes in pasture production for the Moolboolaman climate station ranged from 6.7% to –5.8% (Table 32). This again demonstrated the impact that CO₂ fertilisation may have in mitigating the effects of rainfall decline. The mean change in annual pasture production was very small with a 0.1% decline averaged across all projections.

The projected 2070 changes in deep drainage for the Moolboolaman climate station ranged from 62.9 to –52.5% (Table 32). The mean change in deep drainage was approximately –10.8% by 2070 (skewed strongly towards declines i.e. median at –22.0%) with projected changes in annual mean runoff of –3.8% (Table 32).

The projected changes in the frequency of days above a THI of 80 for Moolboolaman were large increasing from an average of 11 days to 92.8 days a year.

Table 32: Average simulated values of growth, drainage, run-off and heat stress produced by the GRASP model in response to enhanced Greenhouse gas concentrations at 2070 for the Moolboolaman (39218). Climate Change projections from 12 different General Circulation models have been applied to the GRASP model. Average statistics are presented in the lower portion of the table.

2070	Annual Growth (kg/ha)	Annual Drainage (mm)	Annual Run-Off (mm)	Heat Stress Index (Days)
BASE	3251	116	54	11
CGCM1	3223	90	50	95
GFDL	3467	189	66	75
Mark2	3223	90	50	95
CGCM2	3359	136	58	75
HCM2	3061	55	43	106
Mark3	3225	88	51	106
ECHAM3	3223	90	50	95
HCM3	3063	56	43	95
D125	3362	133	58	95
ECHAM4	3362	133	58	95
NCAR	3359	136	58	75
CC50	3061	55	43	106
Aggregated Statistics of Mean Percentage Change across all Scenarios (Heat Stress Index results presented as days not percentages)				
MEAN	-0.1%	-10.8%	-3.8%	92.8
MEDIAN	-0.8%	-22.0%	-7.3%	95
STANDARD DEVIATION	4.0%	34.3%	12.9%	11.7
MAXIMUM	6.7%	62.9%	20.7%	106
MINIMUM	-5.8%	-52.5%	-20.7%	75

The “The Cedars” climate station demonstrated a significant increase in the frequency of THI days above 80 in both 2030 and 2070 (Table 33 and 34). In the 2030 case THI days above 80 increase from a control or base amount of 3 to an average across all twelve climate models of 45 (Table 33). By 2070 the average simulated incidence of THI average across all twelve models was 101 days (Table 34).

Annual pasture production for the “The Cedars” climate stations showed small average declines in 2030 of 0.7% with a range of change from 3.9% to –4.4% (Table 33). This simulated response would suggest the absence of a CO₂ fertilisation effect. As with the other stations, both deep drainage and runoff revealed greater declines by 2030 of 5.9% and 3.8% respectively (Table 33). In both cases while positive changes were simulated by 5 of the 12 models the median values suggested predominance towards declines (i.e. median values –11.9% and –4.9% respectively).

Table 33: Average simulated values of growth, drainage, run-off and heat stress produced by the GRASP model in response to enhanced Greenhouse gas concentrations at 2030 for the “The Cedars” (39234). Climate Change projections from 12 different General Circulation models have been applied to the GRASP model. Average statistics are presented in the lower portion of the table.

2030	Annual Growth (kg/ha)	Annual Drainage (mm)	Annual Run-Off (mm)	Heat Stress Index (Days)
BASE	2828	21	29	3
CGCM1	2795	18	28	44
GFDL	2938	28	31	37
Mark2	2795	18	28	44
CGCM2	2872	23	29	37
HCM2	2707	15	25	54
Mark3	2799	18	27	54
ECHAM3	2795	18	28	44
HCM3	2704	15	26	44
D125	2866	23	29	44
ECHAM4	2866	23	29	44
NCAR	2872	23	29	37
CC50	2707	15	25	54
Aggregated Statistics of Mean Percentage Change across all Scenarios (Heat Stress Index results presented as days not percentages)				
MEAN	-0.7%	-5.9%	-3.8%	44.8
MEDIAN	-1.1%	-11.9%	-4.9%	44
STANDARD DEVIATION	2.6%	18.6%	6%	6.3
MAXIMUM	3.9%	32.2%	7.4%	54
MINIMUM	-4.4%	-28.8%	-12.3%	37

By 2070 the “The Cedars” climate station simulated declines in pasture production, deep drainage and runoff of 3.5%, 11.6% and 10.1% respectively. Again simulation results revealed predominance of declines with median values reflecting stronger declines (i.e. -4%, -32.2% and -14.8% change respectively) (Table 34).

This climate station did not demonstrate as pronounced a CO₂ fertilisation effect as the other three climate stations in this sub-region with the equivalent 2070 positive and negative changes in rainfall producing pasture production values 10.4% and -18.1% change respectively (Table 34). This may possibly be a result of a low baseline rainfall resulting in a lower average pasture growth at this location allowing greater expression of sensitivity to the climate change scenarios.

Table 34: Average simulated values of growth, drainage, run-off and heat stress produced by the GRASP model in response to enhanced Greenhouse gas concentrations at 2070 for the “The Cedars” (39234). Climate Change projections from 12 different General Circulation models have been applied to the GRASP model. Average statistics are presented in the lower portion of the table.

2070	Annual Growth (kg/ha)	Annual Drainage (mm)	Annual Run-Off (mm)	Heat Stress Index (Days)
BASE	2828	21	29	3
CGCM1	2715	14	25	103
GFDL	3123	44	37	87
Mark2	2715	14	25	103
CGCM2	2958	27	31	87
HCM2	2317	6	18	110
Mark3	2717	14	25	110
ECHAM3	2715	14	25	103
HCM3	2321	7	18	103
D125	2951	26	31	103
ECHAM4	2951	26	31	103
NCAR	2958	27	31	87
CC50	2317	6	18	110
Aggregated Statistics of Mean Percentage Change across all Scenarios (Heat Stress Index results presented as days not percentages)				
MEAN	-3.5%	-11.6%	-10.1%	100.8
MEDIAN	-4.0%	-32.2%	-14.8%	103
STANDARD DEVIATION	9.5%	51.4%	19.3%	8.8
MAXIMUM	10.4%	108.5%	25.9%	110
MINIMUM	-18.1%	-67.8%	-35.8%	87

2. Climate Change Projections for the North sub-region

The projected global annual average temperature increase of 0.85°C by 2030 resulted in a warming in the North sub-region of between 0.68 and 1.19°C (above the 1990 to 1999 climatological base) and 6.38% to –6.38% change in rainfall (based on the range of outputs from the twelve climate models).

By 2070 the projected increase in global temperature of 2.55°C (above the 1990 to 1999 climatological base) resulted in a warming in the North sub-region of between 2.04 and 3.57°C (above the 1990 to 1999 climatological base) and 19.25% to –19.25% change in rainfall. Of the twelve climate models used in the experiment seven projected declining rainfall for this sub-region while 5 projected rainfall increases. The resultant impact on the simulated pasture production, deep drainage and runoff values was thus both positive and negative.

The climate change simulations for Tecoma climate station (39248) revealed seven instances where annual pasture growth declined (in response to projected rainfall declines) and five

instances were pasture production increased (Table 35). Given the equally probable range of rainfall increase and decrease and temperature increase of between 0.68 and 1.02°C by 2030 little mean change in pasture production was produced (i.e. 0.2% increase by 2030 - Table 35). The simulated response from deep drainage and runoff was more definitive with mean changes of -4.1% and -1.6% respectively (Table 35).

Table 35: Average simulated values of growth, drainage, run-off and heat stress produced by the GRASP model in response to enhanced Greenhouse gas concentrations at 2030 for the Tecoma (39248). Climate Change projections from 12 different General Circulation models have been applied to the GRASP model. Average statistics are presented in the lower portion of the table.

2030	Annual Growth (kg/ha)	Annual Drainage (mm)	Annual Run-Off (mm)	Heat Stress Index (Days)
BASE	3142	70	56	81
CGCM1	3141	65	55	106
GFDL	3223	87	60	103
Mark2	3137	65	55	104
CGCM2	3142	66	55	103
HCM2	3087	55	52	108
Mark3	3141	65	55	106
ECHAM3	3183	74	58	106
HCM3	3087	55	52	106
D125	3179	75	58	104
ECHAM4	3179	75	58	104
NCAR	3179	75	58	104
CC50	3087	55	52	108
Aggregated Statistics of Mean Percentage Change across all Scenarios				
(Heat Stress Index results presented as days not percentages)				
MEAN	0.2%	-4.1%	-1.6%	105.2
MEDIAN	No Change	-7.2%	-3.2%	105
STANDARD DEVIATION	1.4%	13.4%	4.5%	1.8
MAXIMUM	2.6%	23.2%	6.4%	108
MINIMUM	-1.8%	-21.6%	-7.7%	103

By 2070 simulated pasture production pasture revealed declines of approximately 1% with the twelve model scenarios producing a range of pasture production change of between 7% and -11% (Table 36).

Similarly both deep drainage and runoff exhibited declines of 10% and 6% respectively, with simulation results across the twelve scenarios ranging from 75% to -56% and 19% to -26% respectively (Table 36).

The projected change in frequency of THI days above 80 exhibited increases from a base value of 81 days to an average of 136 days (Table 36).

Table 36: Average simulated values of growth, drainage, run-off and heat stress produced by the GRASP model in response to enhanced Greenhouse gas concentrations at 2070 for the Tecoma (39248). Climate Change projections from 12 different General Circulation models have been applied to the GRASP model. Average statistics are presented in the lower portion of the table.

2070	Annual Growth (kg/ha)	Annual Drainage (mm)	Annual Run-Off (mm)	Heat Stress Index (Days)
BASE	3142	70	56	81
CGCM1	3113	54	51	142
GFDL	3353	123	67	122
Mark2	3110	55	51	131
CGCM2	3115	56	51	122
HCM2	2809	31	42	146
Mark3	3113	54	51	142
ECHAM3	3260	82	60	142
HCM3	2845	32	42	142
D125	3256	84	60	131
ECHAM4	3256	84	60	131
NCAR	3256	84	60	131
CC50	2809	31	42	146
Aggregated Statistics of Mean Percentage Change across all Scenarios (Heat Stress Index results presented as days not percentages)				
MEAN	-1.1%	-9.9%	-5.9%	135.7
MEDIAN	-0.9%	-21.6%	-9.0%	136.5
STANDARD DEVIATION	5.8%	37.9%	14.2%	8.7
MAXIMUM	6.7%	74.2%	19.2%	146
MINIMUM	-10.6%	-55.7%	-26.3%	122

The Kalpowar climate station revealed almost no change in mean pasture production across all twelve climate model scenarios (i.e. 0.1% increase for 2030) although the range between scenarios was from 2.6% to -2% (Table 37). Once again the pasture production simulations returned positive average production in 5 instances and negative pasture production values in 7 instances, consistent with the range of rainfall projections present in the sample of twelve climate models (Table 37).

As with all other previous simulations both deep drainage and runoff exhibited declines of -4% and -2% respectively with results more aligned to a declining trend i.e. median values of -7% and -3% respectively (Table 37).

As discussed previously, the production of daily climatologies served to smooth the occurrence of extreme temperature conditions and hence reduce the frequency of THI days above 80. In the case of the Kalpowar climate station the scaling process resulted in the occurrence of zero days above a THI of 80 in the base case (Table 37). The climate model projections of increased temperature in the range 2.04 to 3.57°C resulted in an increase of on average 1.3 days across all twelve climate model scenarios. While the process of daily climatology production resulted in

a smoothing of extreme temperature events, the results would suggest a limited occurrence of heat stress in this location.

Table 37: Average simulated values of growth, drainage, run-off and heat stress produced by the GRASP model in response to enhanced Greenhouse gas concentrations at 2030 for the Kalpowar (39057). Climate Change projections from 12 different General Circulation models have been applied to the GRASP model. Average statistics are presented in the lower portion of the table.

2030	Annual Growth (kg/ha)	Annual Drainage (mm)	Annual Run-Off (mm)	Heat Stress Index (Days)
BASE	3057	54	39	0
CGCM1	3047	50	38	2
GFDL	3136	68	42	0
Mark2	3056	50	37	1
CGCM2	3055	51	37	0
HCM2	2998	42	35	2
Mark3	3047	50	38	2
ECHAM3	3088	58	40	2
HCM3	2996	42	35	2
D125	3097	58	40	1
ECHAM4	3097	58	40	1
NCAR	3097	58	40	1
CC50	2998	42	35	2
Aggregated Statistics of Mean Percentage Change across all Scenarios				
(Heat Stress Index results presented as days not percentages)				
MEAN	0.1%	-4.2%	-2.2%	1.3
MEDIAN	-0.1%	-7.3%	-2.8%	1.5
STANDARD DEVIATION	1.4%	14.2%	5.2%	0.8
MAXIMUM	2.6%	24.7%	7.4%	2
MINIMUM	-2.0%	-22.7%	-9.3%	0

By 2070 the simulated average pasture production for all twelve scenarios was of the order of -1.6% (Table 38). The median value of -1.3% suggested a slight positive bias in production values resulting from the GFDL model projections of large annual rainfall increases by 2070 (Table 38).

The deep drainage and runoff simulations again demonstrated greater change, with mean change in deep drainage of -11.5% and in runoff of -5.8%. In this case the simulations were more aligned with decline, as the median values were -24% and -10.2% respectively (Table 38).

The occurrence of days with THI above 80 revealed large increases of between 13 and 64 days, with a mean value of 36 days (Table 38).

Table 38: Average simulated values of growth, drainage, run-off and heat stress produced by the GRASP model in response to enhanced Greenhouse gas concentrations at 2070 for the Kalpowar (39057). Climate Change projections from 12 different General Circulation models have been applied to the GRASP model. Average statistics are presented in the lower portion of the table.

2070	Annual Growth (kg/ha)	Annual Drainage (mm)	Annual Run-Off (mm)	Heat Stress Index (Days)
BASE	3057	54	39	0
CGCM1	3008	40	35	41
GFDL	3279	97	48	13
Mark2	3017	41	35	29
CGCM2	3026	43	34	13
HCM2	2698	22	29	64
Mark3	3008	40	35	41
ECHAM3	3157	63	42	41
HCM3	2729	23	29	41
D125	3159	64	42	29
ECHAM4	3159	64	42	29
NCAR	3159	64	42	29
CC50	2698	22	29	64
Aggregated Statistics of Mean Percentage Change across all Scenarios (Heat Stress Index results presented as days not percentages)				
MEAN	-1.6%	-11.5%	-5.8%	36.2
MEDIAN	-1.3%	-24.0%	-10.2%	35
STANDARD DEVIATION	6.2%	39.9%	14.8%	16.3
MAXIMUM	7.2%	78.7%	22.2%	64
MINIMUM	-11.7%	-59.3%	-25.0%	13

The Malakof climate station exhibited relatively modest changes in 2030 for the simulated values of pasture production, deep drainage and runoff. In terms of pasture production, small gains and losses in production were simulated in response to both positive and negative rainfall change projections. On average (across all scenarios), pasture production increased by 0.3%, with the median value showing no overall change (Table 39).

The deep drainage simulations produced, on average across all twelve scenarios, a change of – 4.1% (Table 39). Similarly runoff declined, on average, by 1.1%, although the median would suggest predominance of negative values (Table 39).

Heat stress in 2030 was simulated to increase, on average, by more than 100% from a base case of 1 day to 4 days by 2030 (Table 39).

Table 39: Average simulated values of growth, drainage, run-off and heat stress produced by the GRASP model in response to enhanced Greenhouse gas concentrations at 2030 for the Malakof (39129). Climate Change projections from 12 different General Circulation models have been applied to the GRASP model. Average statistics are presented in the lower portion of the table.

2030	Annual Growth (kg/ha)	Annual Drainage (mm)	Annual Run-Off (mm)	Heat Stress Index (Days)
BASE	3223	136	60	1
CGCM1	3220	126	59	5
GFDL	3298	163	64	2
Mark2	3226	128	59	2
CGCM2	3222	128	59	2
HCM2	3187	110	57	6
Mark3	3220	126	59	5
ECHAM3	3256	142	62	5
HCM3	3183	111	57	5
D125	3264	144	62	2
ECHAM4	3264	144	62	2
NCAR	3264	144	62	2
CC50	3187	110	57	6
Aggregated Statistics of Mean Percentage Change across all Scenarios (Heat Stress Index results presented as days not percentages)				
MEAN	0.3%	-4.1%	-1.1%	3.7
MEDIAN	No Change	-6.4%	-1.8%	3.5
STANDARD DEVIATION	1.1%	11.7%	3.8%	1.8
MAXIMUM	2.3%	19.2%	6.0%	6
MINIMUM	-1.2%	-19.5%	-6.0%	2

The projected 2070 changes in pasture production for the Malakof climate station ranged from 6.2% to –5.0% (Table 40). This again demonstrated the impact CO₂ fertilisation may have in mitigating the effects of rainfall decline. The mean change in annual pasture production was very small with a 0.2% increase in production simulated.

The projected 2070 changes in deep drainage for the Malakof climate station ranged from 58.7% to –51.5% (Table 40). The mean change in deep drainage was approximately –11.2% by 2070 (skewed strongly towards declines i.e. median at –20.8%) with projected changes in annual mean runoff of –3.8% (Table 40).

The projected changes in the frequency of days above a THI of 80 for Malakof were large with a greater than 100% increase in THI 80 days (i.e. from 1 in the base case to a mean of 44.8 days).

Table 40: Average simulated values of growth, drainage, run-off and heat stress produced by the GRASP model in response to enhanced Greenhouse gas concentrations at 2070 for the Malakof (39129). Climate Change projections from 12 different General Circulation models have been applied to the GRASP model. Average statistics are presented in the lower portion of the table.

2070	Annual Growth (kg/ha)	Annual Drainage (mm)	Annual Run-Off (mm)	Heat Stress Index (Days)
BASE	3223	136	60	1
CGCM1	3213	106	56	56
GFDL	3422	217	71	16
Mark2	3212	108	56	36
CGCM2	3209	111	56	16
HCM2	3061	66	48	69
Mark3	3213	106	56	56
ECHAM3	3327	153	65	56
HCM3	3067	68	48	56
D125	3327	156	65	36
ECHAM4	3327	156	65	36
NCAR	3327	156	65	36
CC50	3061	66	48	69
Aggregated Statistics of Mean Percentage Change across all Scenarios (Heat Stress Index results presented as days not percentages)				
MEAN	0.2%	-11.2%	-3.8%	44.8
MEDIAN	-0.3%	-20.8%	-6.6%	46
STANDARD DEVIATION	3.6%	32.4%	12.2%	18.2
MAXIMUM	6.2%	58.7%	18.0%	69
MINIMUM	-5.0%	-51.5%	-20.4%	16

The Bancroft climate station revealed changes in pasture production of between 2.9% and –3.0% for 2030. Mean pasture production for all twelve climate change model scenarios was a modest –0.2% change (Table 41).

The simulated 2030 deep drainage values ranged from an annual average of 55mm to 85mm (Table 41). The mean projected change across all climate change scenarios was –4.6% (Table 41).

The simulated runoff values at 2030 ranged from an annual average of 40mm to 46mm, representing a change of between 6.7% and –8.3% (Table 41). The mean projected change across all climate change scenarios was –1.9% change (Table 41).

Simulated heat stress for the Bancroft climate station exhibited greater than 100% increase in the frequency of days with THI above 80 for a base case of 3 days to a 2030 case of 22 days (Table 41).

Table 41: Average simulated values of growth, drainage, run-off and heat stress produced by the GRASP model in response to enhanced Greenhouse gas concentrations at 2030 for the Bancroft (39103). Climate Change projections from 12 different General Circulation models have been applied to the GRASP model. Average statistics are presented in the lower portion of the table.

2030	Annual Growth (kg/ha)	Annual Drainage (mm)	Annual Run-Off (mm)	Heat Stress Index (Days)
BASE	3087	70	43	3
CGCM1	3068	64	42	24
GFDL	3175	85	46	11
Mark2	3079	65	42	18
CGCM2	3080	65	42	11
HCM2	2997	55	40	34
Mark3	3068	64	42	24
ECHAM3	3121	73	44	24
HCM3	2996	55	40	24
D125	3131	74	44	18
ECHAM4	3131	74	44	18
NCAR	3131	74	44	18
CC50	2997	55	40	34
Aggregated Statistics of Mean Percentage Change across all Scenarios (Heat Stress Index results presented as days not percentages)				
MEAN	-0.2%	-4.6%	-1.9%	21.5
MEDIAN	-0.3%	-7.3%	-2.5%	21
STANDARD DEVIATION	1.9%	13.1%	4.6%	7.4
MAXIMUM	2.9%	21.8%	6.7%	34
MINIMUM	-3.0%	-21.8%	-8.3%	11

By 2070 the simulated range of annual pasture production was between 2711kg TDSM/ha and 3324kg TDSM/ha representing a possible change of between 7.7% and –12.2% (Table 42). The mean pasture production across all twelve climate change scenarios showed a decline of 2% (Table 42).

Both the deep drainage and runoff values indicated declines of the order of 11.9% and 5.1% respectively (Table 42). Simulated heat stress across all twelve climate change scenarios increased from a base case of 3 days to 85.5 days per year (Table 42).

Table 42: Average simulated values of growth, drainage, run-off and heat stress produced by the GRASP model in response to enhanced Greenhouse gas concentrations at 2070 for the Bancroft (39103). Climate Change projections from 12 different General Circulation models have been applied to the GRASP model. Average statistics are presented in the lower portion of the table.

2070	Annual Growth (kg/ha)	Annual Drainage (mm)	Annual Run-Off (mm)	Heat Stress Index (Days)
BASE	3087	70	43	3
CGCM1	3004	52	40	96
GFDL	3324	120	52	58
Mark2	3016	54	39	78
CGCM2	3029	55	39	58
HCM2	2711	30	34	107
Mark3	3004	52	40	96
ECHAM3	3198	80	46	96
HCM3	2738	31	33	96
D125	3201	81	46	78
ECHAM4	3201	81	46	78
NCAR	3201	81	46	78
CC50	2711	30	34	107
Aggregated Statistics of Mean Percentage Change across all Scenarios (Heat Stress Index results presented as days not percentages)				
MEAN	-2.0%	-11.9%	-5.1%	85.5
MEDIAN	-2.3%	-23.3%	-8.3%	87
STANDARD DEVIATION	6.6%	37.3%	13.0%	16.8
MAXIMUM	7.7%	71.5%	19.2%	107
MINIMUM	-12.2%	-57.0%	-22.5%	58

3. Climate Change Projections for the Central sub-region

The projected global annual average temperature increase of 0.85°C by 2030 resulted in a warming in the Central sub-region of between 0.68 and 1.19°C (above the 1990 to 1999 climatological base) and 6.38% to –6.38% change in rainfall (based on the range of outputs from the twelve climate models).

By 2070 the projected increase in global temperature of 2.55°C (above the 1990 to 1999 climatological base) resulted in a warming in the Central sub-region of between 2.04 and 3.57°C (above the 1990 to 1999 climatological base) and 19.25% to –19.25% change in rainfall. Of the twelve climate models used in the experiment 7 projected declining rainfall for this sub-region while 5 projected rainfall increases. The resultant impact on the simulated pasture production, deep drainage and runoff values was thus both positive and negative.

The climate change simulations for Auburn climate station (42059) revealed seven instances where annual pasture growth declined (in response to projected rainfall declines) and five

instances where pasture production increased (Table 43). Given the equally probable range of rainfall increase and decrease and temperature increase of between 0.68 and 1.02°C by 2030 little mean change in pasture production was produced (i.e. 1.2% decline by 2030 - Table 43).

Table 43: Average simulated values of growth, drainage, run-off and heat stress produced by the GRASP model in response to enhanced Greenhouse gas concentrations at 2030 for the Auburn (42059). Climate Change projections from 12 different General Circulation models have been applied to the GRASP model. Average statistics are presented in the lower portion of the table.

2030	Annual Growth (kg/ha)	Annual Drainage (mm)	Annual Run-Off (mm)	Heat Stress Index (Days)
BASE	1361	24	67	52
CGCM1	1329	23	63	72
GFDL	1492	31	73	60
Mark2	1340	23	63	65
CGCM2	1351	23	63	60
HCM2	1237	18	59	77
Mark3	1324	23	63	77
ECHAM3	1397	26	68	72
HCM3	1241	18	59	72
D125	1405	27	68	65
ECHAM4	1405	27	68	65
NCAR	1405	27	68	65
CC50	1237	18	59	77
Aggregated Statistics of Mean Percentage Change across all Scenarios (Heat Stress Index results presented as days not percentages)				
MEAN	-1.2%	-3.2%	-3.5%	68.9
MEDIAN	-1.5%	-5.9%	-5.4%	68.5
STANDARD DEVIATION	5.6%	15.3%	6.5%	6.4
MAXIMUM	9.6%	27.9%	8.7%	77
MINIMUM	-9.1%	-23.5%	-12.0%	60

By 2070 the simulated pasture production had declined by 4.5% with values ranging between 1726kg TDSM/ha and 993kg TDSM/ha (Table 44).

Simulated deep drainage and runoff declined by a further 8.4% and 10.3% respectively by 2070. For the first time (compared with either the East of North sub-region) the magnitude of simulated runoff was greater than for deep drainage (Table 43 and 44), with the change in runoff greater than the change in deep drainage.

The Auburn climate station also revealed further increases in heat stress consistent with the projected increase in temperature of 2.04 and 3.57°C by 2070. On average an increase from a base of 52 days to 107 days was simulated by 2070 (Table 44).

Table 44: Average simulated values of growth, drainage, run-off and heat stress produced by the GRASP model in response to enhanced Greenhouse gas concentrations at 2070 for the Auburn (42059). Climate Change projections from 12 different General Circulation models have been applied to the GRASP model. Average statistics are presented in the lower portion of the table.

2070	Annual Growth (kg/ha)	Annual Drainage (mm)	Annual Run-Off (mm)	Heat Stress Index (Days)
BASE	1361	24	67	52
CGCM1	1242	18	57	110
GFDL	1726	47	83	90
Mark2	1264	19	56	103
CGCM2	1291	20	56	90
HCM2	993	9	43	119
Mark3	1211	17	57	119
ECHAM3	1466	31	70	110
HCM3	1015	9	44	110
D125	1485	31	70	103
ECHAM4	1485	31	70	103
NCAR	1485	31	70	103
CC50	993	9	43	119
Aggregated Statistics of Mean Percentage Change across all Scenarios (Heat Stress Index results presented as days not percentages)				
MEAN	-4.5%	-8.4%	-10.3%	106.6
MEDIAN	-7.1%	-22.1%	-14.7%	106.5
STANDARD DEVIATION	16.4%	45.9%	18.1%	9.9
MAXIMUM	26.8%	91.2%	23.9%	119
MINIMUM	-27.0%	-63.2%	-34.8%	90

The Gayndah climate station demonstrated modest changes in simulated pasture production for the 2030 period. Changes in pasture production ranged from 2% to –1.5%, with all twelve climate change scenarios producing an aggregated change in production of only 0.1% (Table 45)

Simulated change in deep drainage and runoff was, as for every other climate station analysed, greater than the change in simulated pasture production. In this case both deep drainage and runoff declined by 4% and 1.9% respectively (Table 45).

The Gayndah baseline climatology demonstrated a heat stress occurrence of approximately 67 days per year. With a projected warming of between 0.68 and 1.19°C the occurrence of Heat Stress increased to approximately 98 days per year, thus representing an increase of 46% (Table 45).

Table 45: Average simulated values of growth, drainage, run-off and heat stress produced by the GRASP model in response to enhanced Greenhouse gas concentrations at 2030 for the Gayndah (39039). Climate Change projections from 12 different General Circulation models have been applied to the GRASP model. Average statistics are presented in the lower portion of the table.

2030	Annual Growth (kg/ha)	Annual Drainage (mm)	Annual Run-Off (mm)	Heat Stress Index (Days)
BASE	3287	141	75	67
CGCM1	3287	130	73	100
GFDL	3351	169	79	86
Mark2	3281	131	73	96
CGCM2	3285	132	73	86
HCM2	3239	113	70	107
Mark3	3286	129	73	107
ECHAM3	3323	148	76	100
HCM3	3239	114	70	100
D125	3317	149	76	96
ECHAM4	3317	149	76	96
NCAR	3317	149	76	96
CC50	3239	113	70	107
Aggregated Statistics of Mean Percentage Change across all Scenarios (Heat Stress Index results presented as days not percentages)				
MEAN	0.1%	-4.0%	-1.9%	98.1
MEDIAN	No Change	-6.7%	-2.9%	98
STANDARD DEVIATION	1.1%	12.1%	3.7%	7.1
MAXIMUM	2.0%	20.2%	4.8%	107
MINIMUM	-1.5%	-19.9%	-7.2%	86

By 2070 simulated pasture production values had increased by 9.6% although values did range from 19.2% to -0.8% across all twelve climate change scenarios. The increase in pasture production simulated by 2070 was uncharacteristic with all other sub-regions returning pasture production declines for this period. A closer inspection of the data revealed that the climate shifts produced by applying the climate change scenarios was sufficient to alter the date at which nitrogen is reset. In the original simulation the change in temperature and rainfall resulted in Nitrogen being reset in August instead of September as with all other sites. By fixing the Nitrogen reset date in September average pasture production declined by a modest 0.3%. (not shown). This result highlights the complexity of the modelling biophysical processes and the resultant “surprises” that can eventuate due to particular interactions of rainfall and temperature.

Even though pasture production was shown, on average, to increase both simulated deep drainage and runoff showed declines. These declines were of the order of 8.8% and 13.4% respectively (Table 46).

Once again the occurrence of heat stress conditions further increased in response to projected regional warming. An 86% increase in the frequency of THI days above 80 was simulated across for all twelve climate change scenarios, representing a increase from 67 to 128 days a year by 2070 (Table 46).

Table 46: Average simulated values of growth, drainage, run-off and heat stress produced by the GRASP model in response to enhanced Greenhouse gas concentrations at 2070 for the Gayndah (39039). Climate Change projections from 12 different General Circulation models have been applied to the GRASP model. Average statistics are presented in the lower portion of the table.

2070	Annual Growth (kg/ha)	Annual Drainage (mm)	Annual Run-Off (mm)	Heat Stress Index (Days)
BASE	3287	141	75	67
CGCM1	3709	113	61	129
GFDL	3465	229	88	116
Mark2	3262	111	69	123
CGCM2	3261	114	69	116
HCM2	3358	69	54	141
Mark3	3679	111	62	141
ECHAM3	3916	166	69	129
HCM3	3406	71	53	129
D125	3905	168	69	123
ECHAM4	3905	168	69	123
NCAR	3905	168	69	123
CC50	3358	69	54	141
Aggregated Statistics of Mean Percentage Change across all Scenarios				
(Heat Stress Index results presented as days not percentages)				
MEAN	9.6%	-8.8%	-13.4%	127.8
MEDIAN	5.4%	-19.4%	-8.7%	126
STANDARD DEVIATION	7.9%	34.1%	12.0%	9.0
MAXIMUM	19.2%	62.0%	16.4%	141
MINIMUM	-0.8%	-51.2%	-29.0%	116

The Eidsvold climate station revealed changes in pasture production of between 3.3% and -3.8% for 2030. Mean pasture production across all twelve climate change model scenarios was a modest -0.4% change (Table 47).

The simulated deep drainage values in 2030 ranged from an annual average of 23mm to 43mm, representing a change of between 32.6% and -27% (Table 47). The mean projected change across all climate change scenarios was -4.3% (Table 47).

The simulated runoff values in 2030 ranged from an annual average of 40mm to 50mm, representing a change of between 9.4% and -11.8% (Table 47). The mean projected change across all climate change scenarios was -2.8% change (Table 47).

Simulated heat stress for the Eidsvold climate station exhibited an increase from 58 to 87 days a year by 2030 (Table 47).

Table 47: Average simulated values of growth, drainage, run-off and heat stress produced by the GRASP model in response to enhanced Greenhouse gas concentrations at 2030 for the Eidsvold (39036). Climate Change projections from 12 different General Circulation models have been applied to the GRASP model. Average statistics are presented in the lower portion of the table.

2030	Annual Growth (kg/ha)	Annual Drainage (mm)	Annual Run-Off (mm)	Heat Stress Index (Days)
BASE	3039	32	46	58
CGCM1	3018	29	44	90
GFDL	3139	43	50	77
Mark2	3016	29	44	82
CGCM2	3027	29	44	77
HCM2	2924	23	41	96
Mark3	3013	28	44	96
ECHAM3	3089	35	47	90
HCM3	2933	24	40	90
D125	3084	35	47	82
ECHAM4	3084	35	47	82
NCAR	3084	35	47	82
CC50	2924	23	41	96
Aggregated Statistics of Mean Percentage Change across all Scenarios				
(Heat Stress Index results presented as days not percentages)				
MEAN	-0.4%	-4.3%	-2.8%	86.7
MEDIAN	-0.7%	-9.0%	-3.9%	86
STANDARD DEVIATION	2.3%	17.8%	6.4%	7.2
MAXIMUM	3.3%	32.6%	9.4%	96
MINIMUM	-3.8%	-27.0%	-11.8%	77

By 2070 the simulated pasture production had declined by 3.8% with values ranging between 3287kg TDSM/ha and 2477kg TDSM/ha (Table 48).

Simulated deep drainage and runoff declined by 10% and 7.7% respectively by 2070, with greater changes in simulated runoff than deep drainage (Table 47 and 48).

The Eidsvold climate station also revealed further increases in heat stress consistent with the projected increase in temperature of 2.04 and 3.57°C by 2070. On average an increase from a base value of 58 to 120 days was simulated by 2070.

Table 48: Average simulated values of growth, drainage, run-off and heat stress produced by the GRASP model in response to enhanced Greenhouse gas concentrations at 2070 for the Eidsvold (39036). Climate Change projections from 12 different General Circulation models have been applied to the GRASP model. Average statistics are presented in the lower portion of the table.

2070	Annual Growth (kg/ha)	Annual Drainage (mm)	Annual Run-Off (mm)	Heat Stress Index (Days)
BASE	3039	32	46	58
CGCM1	2916	23	40	120
GFDL	3287	67	57	107
Mark2	2923	23	40	115
CGCM2	2947	24	40	107
HCM2	2477	10	32	135
Mark3	2875	22	40	135
ECHAM3	3161	40	49	120
HCM3	2526	10	32	120
D125	3160	41	49	115
ECHAM4	3160	41	49	115
NCAR	3160	41	49	115
CC50	2477	10	32	135
Aggregated Statistics of Mean Percentage Change across all Scenarios (Heat Stress Index results presented as days not percentages)				
MEAN	-3.8%	-10.0%	-7.7%	119.9
MEDIAN	-3.8%	-28.1%	-11.8%	117.5
STANDARD DEVIATION	9.1%	50.6%	17.3%	10.1
MAXIMUM	8.1%	>100%	24.4%	135
MINIMUM	-18.5%	-67.4%	-30.7%	107

The Biggended climate station simulations revealed an average change in pasture production of -0.1% by 2030 (Table 49). Both the simulated deep drainage and runoff values showed declines of 5.5% and 2.4% respectively (Table 49). Simulated heat stress increased by over 100% with the base value increasing from 9 to 52 (Table 49).

Table 49: Average simulated values of growth, drainage, run-off and heat stress produced by the GRASP model in response to enhanced Greenhouse gas concentrations at 2030 for the Biggenden (40021). Climate Change projections from 12 different General Circulation models have been applied to the GRASP model. Average statistics are presented in the lower portion of the table.

2030	Annual Growth (kg/ha)	Annual Drainage (mm)	Annual Run-Off (mm)	Heat Stress Index (Days)
BASE	3205	37	40	9
CGCM1	3198	33	38	55
GFDL	3291	49	43	42
Mark2	3193	33	38	51
CGCM2	3194	34	38	42
HCM2	3116	27	36	58
Mark3	3187	32	38	58
ECHAM3	3252	40	41	55
HCM3	3133	27	36	55
D125	3246	40	41	51
ECHAM4	3246	40	41	51
NCAR	3246	40	41	51
CC50	3116	27	36	58
Aggregated Statistics of Mean Percentage Change across all Scenarios (Heat Stress Index results presented as days not percentages)				
MEAN	-0.1%	-5.5%	-2.4%	52.3
MEDIAN	-0.3%	-9.7%	-3.6%	53
STANDARD DEVIATION	1.7%	17.7%	6.0%	5.6
MAXIMUM	2.7%	31.1%	9.1%	58
MINIMUM	-2.8%	-28.2%	-10.0%	42

By 2070 the average simulated pasture production had declined by 2.0% with values ranging between 3440kg TDSM\ha and 2793kg TDSM\ha (Table 50).

Simulated deep drainage and runoff declined by a further 13% and 6.3% respectively.

The Biggenden climate station also revealed further increases in heat stress consistent with the projected increase in temperature of 2.04 and 3.57°C by 2070. On average, the base heat stress index increased from 9 days 107 days (Table 50).

Table 50: Average simulated values of growth, drainage, run-off and heat stress produced by the GRASP model in response to enhanced Greenhouse gas concentrations at 2070 for the Biggenden (40021). Climate Change projections from 12 different General Circulation models have been applied to the GRASP model. Average statistics are presented in the lower portion of the table.

2070	Annual Growth (kg/ha)	Annual Drainage (mm)	Annual Run-Off (mm)	Heat Stress Index (Days)
BASE	3205	37	40	9
CGCM1	3138	25	35	115
GFDL	3440	75	51	88
Mark2	3140	26	35	101
CGCM2	3141	27	35	88
HCM2	2793	12	28	120
Mark3	3112	24	36	120
ECHAM3	3320	45	43	115
HCM3	2843	12	27	115
D125	3320	46	44	101
ECHAM4	3320	46	44	101
NCAR	3320	46	44	101
CC50	2793	12	28	120
Aggregated Statistics of Mean Percentage Change across all Scenarios (Heat Stress Index results presented as days not percentages)				
MEAN	-2.0%	-13.1%	-6.3%	107.1
MEDIAN	-2.0%	-30.1%	-11.8%	108
STANDARD DEVIATION	6.7%	48.7%	18.3%	11.9
MAXIMUM	7.3%	>100%	27.3%	120
MINIMUM	-12.8%	-68.0%	-30.9%	88

4. Climate Change Projections for the South sub-region

The projected global annual average temperature increase of 0.85°C by 2030 resulted in a warming in the South sub-region of between 0.68 and 1.19°C (above the 1990 to 1999 climatological base) and 6.38% to –6.38% change in rainfall (based on the range of outputs from the twelve climate models).

By 2070 the projected increase in global temperature of 2.55°C (above the 1990 to 1999 climatological base) resulted in a warming in the South sub-region of between 2.04 and 3.57°C (above the 1990 to 1999 climatological base) and 19.25% to –19.25% change in rainfall. Of the twelve climate models used in the experiment 7 projected declining rainfall for this sub-region while 5 projected rainfall increases. The resultant impact on the simulated pasture production, deep drainage and runoff values was thus both positive and negative.

The climate change simulations for the Mounefontein climate station (40138) revealed seven instances where annual pasture growth declined (in response to projected rainfall declines) and five instances where pasture production increased (Table 51). Given the equally probable range of rainfall increase and decrease and temperature increase of between 0.68 and 1.02°C by 2030

little mean change in pasture production was produced (i.e. 0.1% increase by 2030 - Table 51). The simulated response from deep drainage and runoff was equally small with mean changes of -1.0% and -0.9% respectively (Table 51).

The limitation of the production methodologies for daily climatologies was once again highlighted with the Mounefontein climate station exhibiting zero occurrences of THI days above 80 (Table 51). The projected change in the number of days where THI was above 80 did show a marginal increase from 0 to 1 day (Table 51).

Table 51: Average simulated values of growth, drainage, run-off and heat stress produced by the GRASP model in response to enhanced Greenhouse gas concentrations at 2030 for the Mounefontein (40138). Climate Change projections from 12 different General Circulation models have been applied to the GRASP model. Average statistics are presented in the lower portion of the table.

2030	Annual Growth (kg/ha)	Annual Drainage (mm)	Annual Run-Off (mm)	Heat Stress Index (Days)
BASE	2958	23	35	0
CGCM1	2932	21	33	1
GFDL	3060	31	39	0
Mark2	2932	21	33	1
CGCM2	2998	26	36	0
HCM2	2855	16	31	1
Mark3	2935	20	33	1
ECHAM3	2997	25	36	1
HCM3	2932	21	33	1
D125	2997	25	36	1
ECHAM4	3060	31	39	1
NCAR	2997	25	36	1
CC50	2842	16	31	3
Aggregated Statistics of Mean Percentage Change across all Scenarios (Heat Stress Index results presented as days not percentages)				
MEAN	0.1%	-1.0%	-0.9%	1
MEDIAN	-0.8%	-10.8%	-4.1%	1
STANDARD DEVIATION	2.3%	20.5%	7.0%	0.7
MAXIMUM	3.5%	33.8%	10.3%	3
MINIMUM	-3.9%	-30.8%	-11.3%	0

By 2070 the Mounefontein climate station exhibited a mean change in annual pasture production of -1.7%, with the median value of -4.0% showing the predominance of declining production scenarios (Table 52).

In this instance mean deep drainage was shown to increase by 0.8% although the median was strongly negative (i.e. 33.8% decline). The runoff simulations showed a 2.8% decline across all twelve of the climate change simulations. Heat stress increased consistently with projected

regional warming from a base of 0 occurrence of heat stress to a mean of 22 days a year simulated by all twelve models (Table 52).

Table 52: Average simulated values of growth, drainage, run-off and heat stress produced by the GRASP model in response to enhanced Greenhouse gas concentrations at 2070 for the Mounefontein (40138). Climate Change projections from 12 different General Circulation models have been applied to the GRASP model. Average statistics are presented in the lower portion of the table.

2070	Annual Growth (kg/ha)	Annual Drainage (mm)	Annual Run-Off (mm)	Heat Stress Index (Days)
BASE	2958	23	35	0
CGCM1	2839	15	31	16
GFDL	3225	51	45	10
Mark2	2839	15	31	16
CGCM2	3074	30	38	10
HCM2	2460	6	23	39
Mark3	2835	15	31	39
ECHAM3	3063	29	38	16
HCM3	2839	15	31	16
D125	3063	29	38	16
ECHAM4	3224	49	45	16
NCAR	3063	29	38	16
CC50	2411	6	23	56
Aggregated Statistics of Mean Percentage Change across all Scenarios				
(Heat Stress Index results presented as days not percentages)				
MEAN	-1.7%	0.8%	-2.8%	22.2
MEDIAN	-4.0%	-33.8%	-12.4%	16
STANDARD DEVIATION	8.6%	60.8%	20.3%	14.4
MAXIMUM	9.0%	>100%	28.9%	56
MINIMUM	-18.5%	-73.8%	-34.0%	10

The climate change simulations for the Goomeri climate station (40090) as with all the other stations, revealed seven instances where annual pasture growth declined (in response to projected rainfall declines) and five instances where pasture production increased (Table 53). Given the equally probable range of rainfall increase and decrease and temperature increase of between 0.68 and 1.02°C by 2030 little mean change in pasture production was produced (i.e. 0.1% increase by 2030 - Table 53). The simulated response from deep drainage and runoff was equally small with mean changes of -1.5% and 0.2% respectively (Table 53).

The limitation of the production methodologies for daily climatologies was once again highlighted with the Goomeri climate station exhibiting zero occurrence of THI days above 80 in the baseline simulation (Table 53). The projected change in the number of days where THI was above 80 did show a marginal increase from 0 to 4.5 days (Table 53).

Table 53: Average simulated values of growth, drainage, run-off and heat stress produced by the GRASP model in response to enhanced Greenhouse gas concentrations at 2030 for the Goomeri (40090). Climate Change projections from 12 different General Circulation models have been applied to the GRASP model. Average statistics are presented in the lower portion of the table.

2030	Annual Growth (kg/ha)	Annual Drainage (mm)	Annual Run-Off (mm)	Heat Stress Index (Days)
BASE	3233	36	37	0
CGCM1	3209	32	36	4
GFDL	3327	48	41	3
Mark2	3209	32	36	4
CGCM2	3277	40	38	3
HCM2	3138	26	34	5
Mark3	3210	32	36	5
ECHAM3	3266	39	39	4
HCM3	3209	32	36	4
D125	3266	39	39	4
ECHAM4	3319	47	41	4
NCAR	3266	39	39	4
CC50	3142	25	34	10
Aggregated Statistics of Mean Percentage Change across all Scenarios (Heat Stress Index results presented as days not percentages)				
MEAN	0.1%	-1.5%	0.2%	4.5
MEDIAN	-0.7%	-10.9%	-2.9%	4
STANDARD DEVIATION	1.8%	19.2%	6.2%	1.8
MAXIMUM	2.9%	31.7%	10.7%	10
MINIMUM	-2.9%	-29.7%	-8.7%	3

By 2070 the Goomeri climate station exhibited a mean change in annual pasture production of –0.9%, with the median value of –2.6% showing the predominance of declining production scenarios for this location (Table 54).

In this instance mean runoff was shown to increase by 0.3% although the median was strongly negative (i.e. 8.7% decline). The deep drainage simulations show an average 1.6% decline for all twelve of the climate change simulations. Heat stress again increased consistently with projected regional warming (i.e. and increase from 0 to 48 days) (Table 54).

Table 54: Average simulated values of growth, drainage, run-off and heat stress produced by the GRASP model in response to enhanced Greenhouse gas concentrations at 2070 for the Goomeri (40090). Climate Change projections from 12 different General Circulation models have been applied to the GRASP model. Average statistics are presented in the lower portion of the table.

2070	Annual Growth (kg/ha)	Annual Drainage (mm)	Annual Run-Off (mm)	Heat Stress Index (Days)
BASE	3233	36	37	0
CGCM1	3147	24	33	47
GFDL	3470	74	48	23
Mark2	3147	24	33	47
CGCM2	3342	47	41	23
HCM2	2836	10	27	60
Mark3	3136	24	34	60
ECHAM3	3332	44	42	47
HCM3	3147	24	33	47
D125	3332	44	42	47
ECHAM4	3462	71	49	47
NCAR	3332	44	42	47
CC50	2814	9	27	77
Aggregated Statistics of Mean Percentage Change across all Scenarios (Heat Stress Index results presented as days not percentages)				
MEAN	-0.9%	-1.6%	0.3%	47.6
MEDIAN	-2.6%	-32.7%	-8.7%	47
STANDARD DEVIATION	6.4%	56.3%	19.0%	14.7
MAXIMUM	7.3%	>100%	31.1%	77
MINIMUM	-12.9%	-74.3%	-27.2%	23

The Kingaroy climate station, as with all other stations in the Burnett study again exhibited marginal changes in mean annual pasture production. In this case the Kingaroy climate station exhibited a 0.4% increase in average annual production across the twelve climate change scenario's for 2030 (Table 55). The simulated response from deep drainage and runoff was also reasonable small with mean changes of -1.4% and -0.8% respectively (Table 55).

The Kingaroy climate station exhibited no increase in the occurrence of days with THI above 80 for 2030 (Table 55).

Table 55: Average simulated values of growth, drainage, run-off and heat stress produced by the GRASP model in response to enhanced Greenhouse gas concentrations at 2030 for the Kingaroy (40112). Climate Change projections from 12 different General Circulation models have been applied to the GRASP model. Average statistics are presented in the lower portion of the table.

2030	Annual Growth (kg/ha)	Annual Drainage (mm)	Annual Run-Off (mm)	Heat Stress Index (Days)
BASE	3251	33	35	0
CGCM1	3241	29	34	0
GFDL	3335	44	39	0
Mark2	3241	29	34	0
CGCM2	3290	36	36	0
HCM2	3184	23	31	0
Mark3	3242	28	34	0
ECHAM3	3292	36	36	0
HCM3	3241	29	34	0
D125	3292	36	36	0
ECHAM4	3338	44	39	0
NCAR	3292	36	36	0
CC50	3179	22	31	0
Aggregated Statistics of Mean Percentage Change across all Scenarios (Heat Stress Index results presented as days not percentages)				
MEAN	0.4%	-1.4%	-0.8%	0
MEDIAN	-0.3%	-11.0%	-4.1%	0
STANDARD DEVIATION	1.5%	20.9%	6.9%	0
MAXIMUM	2.7%	34.1%	10.2%	0
MINIMUM	-2.2%	-33.0%	-11.2%	0

By 2070 the simulated changes in pasture production, deep drainage, runoff and heat stress for the Kingaroy climate station increased only marginally in response to higher temperatures and greater rainfall change.

Pasture production was shown to increase by 0.2%, with this increase largely the product of a single model simulation (Table 56).

Both deep drainage and runoff were shown to decline by 0.3 and 1.9% respectively (Table 56).

In the case of THI days above 80, while the base simulation showed zero occurrences of days above the 80, the average annual occurrence by 2070 increased to 4 days.

Table 56: Average simulated values of growth, drainage, run-off and heat stress produced by the GRASP model in response to enhanced Greenhouse gas concentrations at 2070 for the Kingaroy (40112). Climate Change projections from 12 different General Circulation models have been applied to the GRASP model. Average statistics are presented in the lower portion of the table.

2070	Annual Growth (kg/ha)	Annual Drainage (mm)	Annual Run-Off (mm)	Heat Stress Index (Days)
BASE	3251	33	35	0
CGCM1	3202	21	31	3
GFDL	3498	71	47	1
Mark2	3202	21	31	3
CGCM2	3357	43	39	1
HCM2	2971	8	23	4
Mark3	3201	20	31	4
ECHAM3	3356	41	39	3
HCM3	3202	21	31	3
D125	3356	41	39	3
ECHAM4	3490	68	47	3
NCAR	3356	41	39	3
CC50	2954	8	23	13
Aggregated Statistics of Mean Percentage Change across all Scenarios (Heat Stress Index results presented as days not percentages)				
MEAN	0.2%	-0.3%	-1.9%	3.7
MEDIAN	-1.5%	-35.2%	-12.2%	3
STANDARD DEVIATION	5.2%	61.0%	21.6%	3.1
MAXIMUM	7.6%	>100%	32.7%	13
MINIMUM	-9.1%	-75.8%	-34.7%	1

The climate change simulations for the Kumbia climate station (40113) revealed seven instances where annual pasture growth declined (in response to projected rainfall declines) and five instances where pasture production increased (Table 57).

Given the equally probable range of rainfall increase and decrease and temperature increase of between 0.68 and 1.02°C by 2030 little mean change in pasture production was produced (i.e. 0.2% increase by 2030 - Table 57).

The simulated response from deep drainage and runoff was more definitive with mean changes of -1.3% and -0.2% respectively (Table 57).

The Kumbia climate station exhibited no increase in the occurrence of days with THI above 80 (Table 57).

Table 57: Average simulated values of growth, drainage, run-off and heat stress produced by the GRASP model in response to enhanced Greenhouse gas concentrations at 2030 for the Kumbia (40113). Climate Change projections from 12 different General Circulation models have been applied to the GRASP model. Average statistics are presented in the lower portion of the table.

2030	Annual Growth (kg/ha)	Annual Drainage (mm)	Annual Run-Off (mm)	Heat Stress Index (Days)
BASE	3182	24	32	0
CGCM1	3167	21	31	0
GFDL	3272	34	35	0
Mark2	3167	21	31	0
CGCM2	3220	27	33	0
HCM2	3099	16	29	0
Mark3	3163	21	31	0
ECHAM3	3222	27	33	0
HCM3	3167	21	31	0
D125	3222	27	33	0
ECHAM4	3275	34	35	0
NCAR	3222	27	33	0
CC50	3096	16	29	0
Aggregated Statistics of Mean Percentage Change across all Scenarios (Heat Stress Index results presented as days not percentages)				
MEAN	0.2%	-1.3%	-0.2%	0
MEDIAN	-0.5%	-13.2%	-3.4%	0
STANDARD DEVIATION	1.8%	23.6%	6.4%	0
MAXIMUM	2.9%	38.2%	10.1%	0
MINIMUM	-2.7%	-35.3%	-10.1%	0

By 2070 the Kumbia climate station simulated declines in pasture production and runoff of 0.8%, and 1% respectively. The simulation of deep drainage showed an increase of 2.2% by 2070, made up largely by a single climate change model scenario (Table 58).

Again simulation results revealed predominance of declines with median values reflecting stronger declines (i.e. 2.5%, 36.8% and 9% declines respectively) (Table 58).

This climate station did not demonstrate as pronounced a CO₂ fertilisation effect as the other three climate stations in this sub-region with the equivalent positive and negative changes in rainfall producing pasture production values 7.4% and -13.2% change respectively (Table 58).

Table 58: Average simulated values of growth, drainage, run-off and heat stress produced by the GRASP model in response to enhanced Greenhouse gas concentrations at 2070 for the Kumbia (40113). Climate Change projections from 12 different General Circulation models have been applied to the GRASP model. Average statistics are presented in the lower portion of the table.

2070	Annual Growth (kg/ha)	Annual Drainage (mm)	Annual Run-Off (mm)	Heat Stress Index (Days)
BASE	3182	24	32	0
CGCM1	3102	15	29	1
GFDL	3418	57	42	0
Mark2	3102	15	29	1
CGCM2	3291	33	35	0
HCM2	2802	5	22	2
Mark3	3091	14	29	2
ECHAM3	3288	31	35	1
HCM3	3102	15	29	1
D125	3288	31	35	1
ECHAM4	3413	55	42	1
NCAR	3288	31	35	1
CC50	2763	5	22	6
Aggregated Statistics of Mean Percentage Change across all Scenarios (Heat Stress Index results presented as days not percentages)				
MEAN	-0.8%	2.2%	-1.0%	1.4
MEDIAN	-2.5%	-36.8%	-9.0%	1
STANDARD DEVIATION	6.4%	67.3%	19.6%	1.6
MAXIMUM	7.4%	>100%	30.3%	6
MINIMUM	-13.2%	-77.9%	-31.5%	0

5. Summary of the results from climate change simulations of pasture production, deep drainage, runoff and cattle heat stress for the Burnett study region.

The simulation studies revealed a number of important issues regarding the possible future changes in pasture production, deep drainage, runoff and cattle heat stress in response to enhanced concentrations of greenhouse gases.

These were:

- Given the coarse resolution of the twelve climate models; scenarios of temperature and rainfall change produced from individual models varied little from one sub-region to another.

- While inter-model differences were large when considering the range of possible future rainfall scenarios i.e. $\pm 6\%$ by 2030 and $\pm 19\%$ by 2070 (in response to 0.85 and 2.55°C of global warming), the range of possible future temperature change was relatively small.
- On the whole changes in pasture production for 2030 were marginal with most climate stations producing less than 1% change. In almost all instances except for the Gayndah climate station location, 2070 pasture production exhibited declines. In this case mean 2070 pasture production was shown to rise by approximately 10%.
- Drainage and runoff demonstrated a consistent pattern of decline across the East, North and Central sub-regions, with the South sub-region demonstrating both increases and decreases. The runoff values highlighted the water-limiting environment of both the South and Central sub-regions with runoff and deep drainage relatively small compared to the wetter North and East sub-regions.
- The determination of the climate change impact on heat stress revealed an important limitation in the current methodology used to produce daily climate change time series data. The production of daily climatologies served to smooth the occurrence of extreme temperature conditions and hence reduce the frequency of THI days above 80.
- The occurrence of zero THI days above 80 was limited primarily to the South sub-region due to relatively cooler conditions. The central region demonstrated a significant increase in the occurrence of heat stress as did the North and East sub-regions.

In summary the climate change simulations of pasture production, deep drainage and runoff indicated marginal change in pasture productivity averaged across all 12 climate models representing climate change in the Burnett region. However, the range of response between scenarios was large indicating the complexity of temperature and rainfall responses. The simulations did reveal that although no large changes in pasture production occurred, in most cases, the changes suggested the predominance of declining productivity. Mean changes in deep drainage and runoff were, for the most part, negative with 2070 changes posing serious risk if realised. While no large changes in pasture productivity were revealed the incidence of heat stress was shown to increase across all sub-regions, with the Central and North sub-regions most pronounced. This added stress on cattle may be a significant factor for the grazing industry to adapt to in future.

Discussion and Conclusions

Analyses of national climate variability have revealed that climatic events (e.g. drought, flood and extreme temperature events) are increasingly falling outside the long-term historical experience as a consequence of anthropogenic climate change. As current agricultural practices have been strongly shaped by existing climate conditions, predicted changes in climate, resulting from enhanced greenhouse gas concentrations, may result in loss of productivity and environmental degradation.

The research undertaken in this project set out to provide a detailed climatic analysis quantifying trends of key climate variables in the Burnett study region. This included an analysis of climatic trends in terms of their potential impacts on natural resource management issues such as deep drainage and run-off, pasture productivity/condition and heat stress in cattle. The documentation of the potential impact of future climate scenarios may have on both the natural resource and grazing productivity was also required and represents the bulk of the following discussion.

The report has achieved all these aims and has summarised, in detail, the results at the end of each section. It has demonstrated that the Burnett Study region is characterised by large spatial and temporal climate variability. The analysis of historical records for this region has demonstrated the importance of this variability in determining both industry reliability and economic returns within the agricultural sector.

History has revealed that the grazing industry is intrinsically linked to natural climate variability and thus adapting to the range of climate change impacts identified in this project will represent an additional component of the property management process. While diversification of on-farm production and the use of seasonal climate forecasting have served to mitigate the economic impact of recent climate events on production (to a limited degree), longer-term climatic variations on decadal and multi-decadal timescales have yet to be considered (Crimp *et al.*, 2002). One view is that by adopting methods to track year to year climate variability effectively, climate change over decades to centuries will automatically be accommodated (Gifford *et al.* 1996). However increases in heat stress for the majority of the Burnett study region by 2070 may pose to great a negative impact to adapt to, thus necessitating some form of industry restructuring in the North, Central and East sub-region.

Current pastoral management problems in this region include undesirable grass species, woody weed infestation, soil erosion, animal nutrition, health and to a lesser degree salinisation and soil acidification. However many of these problems may become more of a challenge in the future and will require further technological advances to resolve.

While property scale adaptation is an option to resolving or mitigating future climate change impacts changing existing property management practices will require: (1) confidence that climate change can be separated from the naturally high year-to-year climate variability inherent in these production systems; (2) the motivation to change based on the perceived risk and opportunities of climate change, (3) establishment and implementation of applicable new technologies and demonstration of their benefits; (4) buffering against establishment failure of new practices during less favourable climate periods; and (5) alteration of transport and market infrastructure to support altered production.

The analysis of the raw historical climate data revealed a high degree of variability between stations and over time. The analysis of raw summer rainfall revealed generally consistent declining trends for most stations, although the linear trends for rainfall explained a very small percentage of the overall variability.

The comparison of the raw and interpolated climate data revealed strong agreement across all stations (except Moolboolaman, The Cedars, Aurburn, Gayndah and Kumbia) exhibiting correlation co-efficient values above 0.92. In the case of the stations listed above the correlation

co-efficient values ranged from 0.82 to 0.88. The strong correlation with raw rainfall station data provided a high degree of confidence in the use of the interpolated data in the subsequent biophysical modelling.

The linear trend analyses performed on the interpolated rainfall data varied little against the raw data except in 6 out of 48 cases. In each of the cases neither the raw or interpolated linear rainfall trend was statistically significant. This would suggest that the interpolated rainfall station data was suitable for trend analyses if the limitations of the data were recognised.

The linear trend analyses performed on the interpolated temperature data showed greater variation with 5 out of 15 cases where the raw and interpolated trends were opposed. In 3 of the 5 cases the change in the trends were statistically significant. This would suggest that the interpolated temperature data for this region should be used with extreme caution in any type of trend analyses.

An examination of the entire interpolated rainfall data time series revealed consistent declining annual rainfall trends across all stations, with seven stations returning declining trends below the 95% confidence interval. This would suggest that the trends are strongly influenced by intra-seasonal climate variability (substantiated by summer and winter linear trend analyses). The examination of daily statistics for different three-month windows, presented in the following section, will provide more insight into the nature of the trends.

An examination of the entire interpolated temperature data time series revealed consistent warming trends in both average maximum and minimum temperatures. The maximum temperature trends were however all below the 95% confidence interval. These results correspond well with the official Bureau of Meteorology trend analyses, which show annual average minimum temperatures warming 30% more rapidly than maximum temperatures.

The simulation of annual pasture production, revealed consistent declining trends across all stations and sub-regions except for the driest station in the central sub-region (Auburn). While the simulation results returned a consistent declining trend in pasture production for the study region, there was no instance where the linear trends were statistically significant or explained more than 1% of the production variability. However this should be considered a conservative estimate of change given that the impacts of grazing animals were not considered in the simulation experiments in order to produce results consistent with changes in climate only. Grazing pressure was assumed constant at thirty percent of the total standing dry matter (TSDM). If the impacts of stock had been considered it is the authors view that the decline in pasture production would have been greater.

Similarly the simulation of deep drainage returned no instance where drainage increased although both the Central and South sub-regions returned almost no linear trends for the period 1890 to 2002. While the simulation results returned a consistent declining trend in deep drainage for the study region, there was no instance where the linear trends were statistically significant or explained more than 1% of the production variability.

The simulated runoff data returned three instances where positive trends occurred. These instances occurred in the East, Central and South sub-regions in predominantly drier locations. Again, while the simulation results returned for the most part declines in runoff for the study region, there was no instance where the linear trends were statistically significant or explained

more than 1% of the production variability. In some cases the trends were approaching statistical significance with P close to 0.10.

The simulation of the occurrence of THI above 80 returned a predominantly negative trend across the Study region. The North and South sub-regions did demonstrate instances where positive trends were returned. However the linear trends for all sub-regions were below the 95% confidence limit. The declining trends were considered to be the product of extremely high heat stress occurrence at the beginning of the record.

The climate change experiments were limited to a degree by the coarse resolution of the twelve climate models. As a result the scenarios of temperature and rainfall change produced from individual models varied little from one sub-region to another. While inter-model differences were large when considering the range of possible future rainfall scenarios i.e. $\pm 6\%$ by 2030 and $\pm 19\%$ by 2070 (in response to 0.85 and 2.55°C of global warming), the range of possible future temperature change was relatively small.

On the whole changes in pasture production for 2030 were marginal with most climate stations producing less than 1% change. In almost all instances except for the Gayndah climate station, 2070 pasture production exhibited declines. In this case mean 2070 pasture production was shown to rise in response to a simulated lengthening of the growing season (i.e. one month earlier than all other sites). The re-analysis of this station with a the growing season set to the same period as all other stations produced pasture growth trends similar to all stations analysed (i.e. average decline of 0.3% by 2070).

Projected changes in deep drainage were on average greater for than pasture production with a relatively consistent pattern of decline across the majority of stations. In the South sub-region stations showed a number of instances where deep drainage in 2030 increased. Similarly runoff demonstrated a consistent pattern of decline across the East, North and Central sub-regions, with the South sub-region demonstrating both increases and decreases. Runoff and deep drainage values in the South and Central region illustrated how water limited these environments were, with values significantly lower than in the North and East sub-regions.

Previously simulation studies have suggested that increasing CO₂ was likely to lead to increased drainage as a result of higher soil moisture values resulting from slower transpiration rates. However, simulated drainage in GRASP is an episodic process occurring only when rainfall occurs on a soil water profile near field capacity and there is high surface cover reducing runoff. Thus the reduction in drainage is likely to be the result of lower soil water levels and higher potentially evaporative demand. Further explanation will require detailed analysis of daily simulations.

The determination of the climate change impact on heat stress revealed an important limitation in the current methodology used to produce daily climate change time series data. The production of daily climatologies served to smooth the occurrence of extreme temperature conditions and hence reduce the frequency of heat stress. The occurrence of no heat stress days was limited primarily to the South sub-region due to relatively cooler conditions. All regions demonstrated a significant increase in the occurrence of heat stress by 2030.

A number of caveats exist with regard to the interpretation of these simulation results. These relate to a variety of issues ranging from the uncertainty of the climate change scenarios to the

representation of pasture model parameters such as soils and available nitrogen and are summarised as follows:

- the climate change scenarios have been determined from a range of possible future greenhouse gas emissions each considered equally plausible. The resultant range of projected change in global temperature is large but was reduced for the purposes of this study to a 2030 and 2070 mean value;
- the climate change scenarios used for the study are based on average annual changes in rainfall and temperature. The future climate of Australia will include shifts in both regional and seasonal variability, a feature yet to be considered;
- the mechanisms of change in rainfall, i.e. number of raindays and/or amount of rain per day were not identified in the scenarios so the projected day-to-day variability in rainfall for the next 100 years was assumed to be the same as the last 100 years;
- changes in other important climatic elements such as humidity, VPD, solar radiation, potential evaporation demand are not available from the model simulations but are calculated as a function of the historical relationship between maximum temperature and all the other elements;
- in terms of the pasture growth model, input parameters such as soils, relief, tree cover and pasture species composition have been simplified in order to allow a comparative analyses to be made;
- plant species response to interaction of climate change and CO₂ has only been studied for a few combinations of species and environments, so expert knowledge was applied to the modelling study in order to account for general changes; and
- the long-term changes in soil organic matter and nitrogen availability as a result of climate change are unknown and hence current values in the model were used.

In the discussion that follows the authors provide a brief review of the potential impacts that may face the Burnett Study region, based on the results of the climate change experiments discussed in the previous section and assess the grazing industries adaptive capacity by reviewing current property management options, costs and related benefits.

Possible impacts on the Burnett's Grazing Industry

The key management issue of concern for the grazing industry relates to animal production attributes such as liveweight gain of cattle and sheep, wool growth of sheep, flock/herd reproduction/mortality and milk production in dairy cattle. Previous research has already linked cattle growth to the availability of young, digestible plant material (Mannetje, 1974; Ash *et al.*, 1982; McLennan *et al.*, 1988; Howden *et al.*, 1999), which in turn is strongly influenced by the occurrence and duration of suitable climatic conditions for plant growth (McKeon *et al.*, 1990, McKeon *et al.*, 1993; Hall *et al.*, 1998). Thus the primary driver of change in the grazing industry will be related climate induced change to the growing period of pastures and/or pasture composition (Hall *et al.*, 1998; McKeon and Hall, 2002).

As the major management issues for the grazing industry currently relate to (1) pasture productivity, (2) herbage quality (3), pests, diseases and weeds, (4) botanical changes in native pasture species, (5) soil erosion and (6) animal husbandry and health (Hall *et al.*, 2000), the remaining discussion will deal with these six management issues.

Impacts on Pasture Productivity and Possible Adaptation Measures

Increases in CO₂ concentration, maximum and minimum temperatures, and changes in rainfall were the main driving force for pasture productivity changes. The climate change scenarios used to initialise the GRASP model were based on conservative estimates of projected global temperature increase i.e. 0.85°C by 2030 and 2.55°C by 2070, resulting in regional increase in temperature for the Burnett study region of between 0.68 and 1.02°C and 2.04 to 3.06°C by 2070 (above the 1990 to 1999 climatological base). The scenarios of rainfall change were 6.38% to –6.38% in 2030 and 19.13% to –19.13% by 2070 (based on the range of outputs from the twelve climate models).

Even though both positive and negative changes in rainfall were projected for the Burnett Study region, and the CO₂ fertilisation effect was considered, the average simulated pasture production still demonstrated small declines (less than 1%) in productivity by 2030 (although productivity changes were highly variable between stations). By 2070 declines in pasture production of up to 4.5 % were demonstrated by most stations.

Thus opportunities to improve pasture productivity will be limited with the maintenance of current productivity levels a greater challenge in the future. Some options available to maintain or enhance current forage production may include: (1) sowing new pastures which are better adapted to higher temperatures, water constraints and changes in soil fertility; and/or (2) providing additional nitrogen through use of sown legumes (Lodge *et al.*, 1984, Walker and Weston 1990). However introducing new pasture species is likely to be considered a controversial strategy given the possible impacts on regional biodiversity.

The greater utilisation of strategic spelling, responsively changing stocking rates based on seasonal climate forecasting and sustainable constant stocking may allow pastures some opportunity to recover from seasons of low rainfall thus preventing or mitigating resource degradation under warmer, more variable rainfall conditions. However this type of strategic spelling should be practised in conjunction with sowing new pastures and legumes in order to realise any large benefits (Hodgkinson and Tongway 2000).

The approach of responsively changing stocking rate or adopting a constant conservative stocking rate is likely to be successful in an environment where there is a high probability of extended droughts of more than 1 year (McKeon and Hall 2002). These particular adaptation measures would require a comprehensive record of annual growth and determination of long-term growth trends to formally calculate the 'safe carrying capacity' of a particular region.

Impacts on Herbage Quality and possible amelioration options

Three major aspects affecting herbage quality for feed are (1) energy supply, (2) protein (N) content, and (3) digestibility. While this project did not attempt to model these aspects a number of other research projects have assessed the impact of climate change on herbage quality. The research indicates that increased levels of CO₂ result in decreases leaf N-content, increases non-structural carbohydrate, but causes little change in digestibility (Lilley *et al.* 2001b). Warmer conditions tend to significantly decrease non-structural carbohydrate concentrations while slightly reducing leaf N-content. Reducing the N-input to a pasture (Peyraud and Astigarraga 1998), or increasing the atmospheric CO₂ concentration (Lilley *et al.*, 2001b), was shown to reduce the herbage protein although this was compensated for by an increase in the non-structural carbohydrates

The breeding cultivars having high non-structural carbohydrate levels may represent a viable adaptation option although any efforts to improve pasture would be limited by cost and scale of the individual grazing enterprise.

Impacts on Pests, Diseases and Weeds and Possible Adaptation Measures

Historically the grazing industry has demonstrated some degree of vulnerability to pests, disease and weed infestation although it is not clear if the Burnett study region is any more or less prone to these problems (McLeod, 1995; Sutherst, 1990; Sutherst *et al.*, 1996, White *et al.*, 2003)). McLeod (1995) estimated that cattle ticks cost the northern tropical beef cattle industry \$41 million annually in control measures and \$91 million in productivity losses.

The major risk to the grazing industry from climate change relates to the potential change in the distribution of pests, diseases and weeds. In some cases the change may be gradual and go undetected until episodic events trigger widespread outbreaks

Under conditions of lower rainfall and warmer temperatures (such as projected for the Burnett region), the resultant reduction in pasture productivity and drier conditions would limit the use of fire as a management tool (Burrows *et al.*, 2002).

Current methods for controlling pests and disease in the grazing industry include:

- applications of pesticide and chemicals to respond to outbreaks;
- biological weed control;
- vaccinations to enhance resistance to existing pests and disease; and
- selection of tick resistant (*Bos indicus*) cattle in the northern Australia (White *et al.*, 2004).

These measures have proved useful in controlling pests and disease in response to natural climate variability and will continue to do so under project climate change. The increasing costs and resistance to chemical sprays may make this form of strategic adaptation more problematic in the future although technological advance may counter this trend.

A second adaptation method involves the development of improved predictive tools and indicators that will allow more effective control and eradication conditions to be identified.

Impacts on Species Change in Native Pasture and Possible Adaptation Measures

The species composition of native pastures changes in response to variability in rainfall (quantity and timing) and to changes in grazing pressure (McKeon and Hall, 2002) and is also expected in response to changes in atmospheric CO₂ concentration (Warwick *et al.*, 1998, Chakraborty *et al.*, 1998). Increases in atmospheric CO₂ concentration are likely to result in increases in water use efficiency and growth rates of plants (Gifford, 1988; Howden *et al.*, 1998; 1999). The magnitude of these changes is possibly greater for C₃ than for C₄ species (Kimball *et al.*, 1993; Poorter, 1993; Campbell *et al.*, 1997). Thus increases in CO₂ concentrations are likely to increase the competitive advantages of C₃ shrubs (woody weeds) over the C₄ grasses resulting in changes in pasture composition and quality.

Developments in chemical control have provided some technical solutions in controlling regrowth of woody weeds and botanical composition of pastures, and may prove to be an effective management tool in regions where pasture production may be reduced (Scanlan, 1988).

An additional adaptation option remains the conservative management of grazing pressure. By reducing grazing pressure on native pastures, periods of vulnerability through degradation and hence susceptibility to invasion may be reduced.

Impacts on Soil Erosion, Runoff and Deep Drainage and Possible Adaptation Measures

The historical climate trends demonstrated by the Burnett Study region, revealed a reduction in rainfall, but increased incidence of extreme events (i.e. increase in the 80th to 95th percentile rainfall amounts). This, coupled with the slight reduction in pasture production by 2070 may result in greater susceptibility to soil erosion. The impact the simulated declines in both deep drainage and runoff will have for the Burnett study region is unclear at this time and would require further investigation.

Impacts on Animal Husbandry and Health and Possible Adaptation Options

Animal health, as with the other management issues listed above, is intrinsically linked to the exploitation of animal behaviour or traits that provides some form of adaptation to existing climate conditions. The current upward trend in Australia's animal numbers is not only a function of demand but also the result of the continued improvement in animal attributes, especially drought resistance in sheep and cattle, pests and diseases resilience.

The potential impacts of climate change on animal health and husbandry will as a result of both direct and indirect effects. The direct effects will be as a result of changes in drought extent and increased temperature. The indirect impacts of climate change will be experienced through international market forces where prices for meat and wool are strongly influenced by production of overseas competitors (including world grain production) (White, 1972; Herne 1998).

The simulation of the historical occurrence of heat stress returned a predominantly negative trend across the Burnett Study region. The North and South sub-regions did demonstrate instance where positive trends were returned. However the linear trends for all sub-regions were below the 95% confidence limit. The anomalously high THI values at the beginning of the time series across all stations may well be an artificial feature of the interpolation process. However, the results do correspond with work by Hall *et al.*, 1998 and Howden *et al.*, 1999, which suggested significant increases in heat stress since 1957. In all cases, the longer-term simulation studies performed for this project show a return of heat stress frequencies similar to those experienced in the 1890 to 1910 period, although the occurrence of heat stress in this earlier part of the record may be a function of poor data.

The climate change experiments showed a significant increase in the occurrence of heat stress by 2030 and most certainly by 2070. Adaptation to heat stress for the extensive grazing industry will be very difficult although the planting of shade trees and increased frequency of watering points may offset stress to some degree. For the intensive grazing industry such as feedlots and dairying, shading and spraying may represent viable adaptation options.

The discussion above would suggest that some adaptation options do exist to offset project changes in both temperature and rainfall. Managing grazing to cope with climate variability, grass and vegetation thickening, disease and soil erosion have been the focus of efforts to-date. With these issues remaining important management options in the future.

References

- Ash, A.J., O'Reagain, P.J., McKeon, G.M. and Stafford Smith, M. (2000). Managing climate variability in grazing enterprises: A case study of Dalrymple Shire, north-eastern Australia. In *'Applications of Seasonal Climate Forecasting in Agricultural and Natural Ecosystems - the Australian Experience'*. (Eds G. Hammer, N. Nicholls and C. Mitchell.) Kluwer Academic Press: Netherlands. p 253-270.
- Ash, A.J., Prinsen, J.H., Myles, D.J. and Hendricksen, R.E. (1982). Short-term effects of burning native pasture in spring on herbage and animal production in south-east Queensland. *Proceedings of the Australian Society of Animal Production* **14**, 377-80.
- Burrows, W.H., Henry, B.K., Back, P.V., Hoffman, M.B., Tait, L.J., Anderson, E.R., Menke, N., Danaher, T., Carter, J.O. and McKeon, G.M. (2002). Growth and carbon stock change in eucalypt woodlands in north-east Australia: ecological and greenhouse sink implications. *Global Change Biology* **8**: 769-784.
- Carter, J.O., Bruget, D., Hall, W.B. and Collett, L. (2002) Using satellite data to calibrate a continental scale model of pasture production. In: *Proceedings 11th Australasian Remote Sensing and Photogrammetry Association Conference*, Brisbane, Queensland, Australia September 2002. p. 831-840.
- Carter, J.O., Hall, W.B., Brook, K.D., McKeon, G.M., Day, K.A. and Paull, C.J. (2000). Aussie GRASS: Australian grassland and rangeland assessment by spatial simulation. In *'Applications of Seasonal Climate Forecasting in Agricultural and Natural Ecosystems - the Australian Experience'*. (Eds G. Hammer, N. Nicholls and C. Mitchell.) Kluwer Academic Press: Netherlands.
- Chakraborty, S., G.M. Murray, P.A. Magarey, T. Yonow, R. O'Brien, B.J. Croft, M.J. Barbarbetti, K. Sivasithamparam, K.M. Old, M.J. Dudzinski, R.W. Suthert, D.L. Penrose, C. Archer and R.W. Emmett, 1998: Potential impact of climate change on plant diseases of economic significance to Australia. *Australasian Plant Pathology*, **27**, 15-35.
- Chock, D. P., Kumar, S. and Herrmann, R.W. (1982). An analysis of trends in oxidant air quality in the South Coast Air Basin of California. *Atmospheric Environment*, **16**(11): 2615 - 2624.
- Crimp, S.J., Flood, N.R., Carter, J.O., Conroy, J.P. and McKeon, G.M. (2002). Evaluation of the Potential Impacts of Climate Change On Native Pasture Production – *Implications for livestock carrying capacity*: Final Report for the Australian Greenhouse Office, 60pp. 2002
- Crimp, S.J., McKeon, G., Day, K.A. and Howden, S.M. (2000). Climate Change: Future Implications for Queensland's Rangeland Region. In: *"Learning from history: preventing land and pasture degradation under climate change"*. Eds. G.M. McKeon and W. Hall. Final Report to the AGO.
- Crimp, S.J., McKeon, G.M., Hall, W.B., Howden, S.M., Stone, R.C. and Jones, D.A. (1999) Climate change in Queensland's grazing lands: approaches and climatic trends. In: D. Elridge and D. Freudenberger (eds) *People and Rangelands: Building the Future. Proceedings VIth International Rangelands Congress*, July 1999, Townsville, Australia. p. 36-38.
- Day, K.A., McKeon, G.M. and Carter, J.O. (1997). *Evaluating the risks of pasture and land degradation in native pasture in Queensland*. Final Project Report for Rural Industries and Research Development Corporation project DAQ124A, 119 pp.

- Evans, D.R., Humphreys, M.O. and Williams, T.A. (1996) Forage yield and quality interactions between white clover and contrasting ryegrass varieties in grazed swards. *J of Agricultural Science* **126**, 295-299.
- Freas, W. A., and Sieurin, E. (1977). "A Nonparametric Calibration Procedure for Multi- Source Urban Air Pollution Dispersion Models". *Fifth Conference on Probability and Statistics in Atmospheric Sciences*, American Meteorological Society, Las Vegas, Nevada.
- Gifford RM, Campbell BD, Howden SM (1996) Option for adapting agriculture to climate change: Australian and New Zealand examples. Pp399-416 in *Greenhouse: Coping with Climate Change*. Eds WJ Bouma, GI Pearman, MR Manning. CSIRO Publishing, Collingwood, Australia.
- Hall, W.B., McKeon, G.M., Carter, J.O., Day, K.A., Howden, S.M., Scanlan, J.C., Johnston, P.W. and Burrows, W.H. (1998). Climate change and Queensland's grazing lands: II. An assessment of the impact on animal production from native pastures. *Rangeland Journal*, **20**: 174-202
- Hall, W.B., Bruget, D., Carter, J.O., McKeon, G.M., Yee Yet, J.S., Peacock, A., Hasset, R.C. and Brook, K.D. (2001). *Australian Grassland and Rangeland Assessment by Spatial Simulation (Aussie GRASS)* QNR9 Final Report for Climate Variability in Agriculture Program, April 2001.
- Herne, B. (1998). U.S. Cattle cycle is the key to rising prices. *Brigaletter* **32** (August), 1-2.
- Hirsch, R. M., and Slack, J.R. (1984). A nonparametric trend test for seasonal data with serial dependence. *Water Resources Research*, **20**(6): 727 - 732.
- Hirsch, R. M., Slack, R.M and Smith, R.A. (1982). Techniques of trend analysis for monthly water quality data. *Water Resources Research*, **18**(1): 107 – 121.
- Howden, S.M., Walker, L., McKeon, G.M., Hall, W.B., Ghannoum, O., Day, K.A., Conroy, J.P., Carter, J.O. and Ash, A.J. (1998). Simulation of changes in CO₂ and climate on native pasture growth. Final report for the Rural Industries Research and Development Corporation: Evaluation of the impact of climate change on northern Australian grazing industries (DAQ 139A), 141pp.
- Howden, S.M., McKeon, G.M., Walker, L., Carter, J.O., Conroy, J.P., Day, K.A., Hall, W.B., Ash, A.J. and Ghannoum, O. (1999). Global change impacts on native pastures in south-east Queensland, Australia. *Environmental Modelling and Software* **14**, 307-16
- Hutchinson, M.F. (1993a). On thin plate splines and kriging. *Computing and Science in Statistics*, vol. 25, Tarter, M.E., Lock, M.D. (eds), Interface Foundation of North America, Berkeley, p. 55-62.
- Hutchinson, M.F. (1995). Interpolating mean rainfall using thin plate smoothing splines. *International Journal of Geographical Information Systems*, **9**: 385-403.
- Hutchinson, M.F., Richardson, C.W. and Dyke, P.T. (1993b). Normalisation of rainfall across different time steps. *Management of Irrigation and Drainage Systems*, vol. 9. *Irrigation and Drainage Division*, ASCE, US Department of Agriculture, p. 432-439.
- Jeffrey, S.J., Carter, J.O., Moodie, K.B. and Beswick, A.R. (2001). Using spatial interpolation to construct a comprehensive archive of Australian climate data. *Environmental Modelling and Software*, **16**: 309-30.

- Johnston, P.W., McKeon, G.M. and Day, K.A. (1996a). Objective 'safe' grazing capacities for south-west Queensland, Australia: Development of a model for individual properties. *Rangeland Journal*, **18**: 224-58.
- Kirschbaum, M.U.F. (1999). Modelling forest growth and carbon storage in response to increasing CO₂ and temperature. *Tellus*: **51B**, 5, 871-888.
- Kirschbaum, M.U.F. (2004). Direct and indirect climate change effects on photosynthesis. *Plant Biology* (Accepted).
- Kumar, S., and Chock, D.P. (1984). An update on oxidant trends in the South Coast Air Basin of California. *Atmospheric Environment*, **18**(10): 2131 - 2134.
- Lavery, B., Kariko, A. and Nicholls, N. 1992. A historical rainfall data set for Australia. *Australian Meteorological Magazine*, **40**: 33-39.
- Littleboy, M. and McKeon, G.M. (1997). Subroutine GRASP: Grass Production Model. Documentation of the Maroola Version of Subroutine GRASP. Appendix 2 of Evaluating the risks of pasture and land degradation in native pasture in Queensland. Final Project Report for Rural Industries and Research Development Corporation project DAQ124A, 76 pp.
- Lodge, G.M., Whalley, R.D.B. and Robinson, G.C. (1984). Temperate Rangelands in Management of Australia's Rangelands. Eds G.N. Harrington, A.D. Wilson and M.D. Young. CSIRO Melbourne, p. 317-332
- Mannetje, L.'t. (1974). Relations between pasture attributes and liveweight gains on a subtropical pasture. Proceedings of the XII International Grassland Congress, Volume 3, Moscow, pp. 299-304.
- McKeon, G.M., Howden, S.M., Abel, N.O.J. and King, J.M. (1993). Climate change: adapting tropical and sub-tropical grasslands. *Proceedings of 17th International Grassland Congress*, Palmerston North, New Zealand, p1181-90
- McKeon, G.M., Howden, S.M., Silburn, D.M., Carter, J.O., Clewett, J.F., Hammer, G.L., Johnston, P.W., Lloyd, P.L., Mott, J.J., Walker, B., Weston, E.J. and Willcocks, J.R. (1988). The effect of Climate Change on Crop and Pastoral Production in Queensland. In Pearman, G.I. (ed). *Greenhouse, Planning for Climate Change*. CSIRO Division of Atmospheric Physics, Melbourne. pp. 546-63
- McKeon, G.M., Day, K.A., Howden, S.M., Mott, J.J., Orr, D.M., Scattini, W.J. and Weston, E.J. (1990). Management of pastoral production in northern Australian savannas. *Journal of Biogeography*, **17**: 255-72.
- McKeon, G.M., Carter, J.O., Day, K.A., Hall, W.B. and Howden, S.M. (1998a). Evaluation of the impact of climate change in northern Australian grazing industries. Final report on DAQ139A to RIRDC.
- McKeon, G.M., Hall, W.B., Crimp, S.J. and Howden, S.M., Stone, R.C. and Jones, D.A. (1998b). Climate Change and Queensland's grazing lands: I. Approaches and Climatic Trends. *The Rangeland Journal*. **20**: 151-76

- McKeon, G.M., Ash, A.J., Hall, W.B. and Stafford Smith M. (2000). Simulation of grazing strategies for beef production in north-east Queensland. 'Applications of Seasonal Climate Forecasting in Agricultural and Natural Ecosystems - the Australian Experience'. (Eds G. Hammer, N. Nicholls and C. Mitchell.) Kluwer Academic Press: Netherlands. p. 227-252.
- McKeon and Hall 2002 (Eds) (2002). Can Seasonal Climate Forecasting Prevent Land and Pasture Degradation in Australia's Grazing Lands? Technical Report for Climate Variability in Agriculture Program (QNR 14), May 2002.
- McLennan, S.R., Hendricksen, R.E., Beale, I.F., Winks, L., Miller, C.P. and Quirk, M.F. (1988). The nutritive value of native pastures to Queensland. In 'Native Pastures in Queensland: The Resources and their Management'. (Eds W.H. Burrows, J.C. Scanlan and M.T. Rutherford.) pp. 125-60. (Queensland Department of Primary Industries: Brisbane).
- McLeod, R.S. (1995). Costs of major parasites to the Australian livestock industries. *International Journal of Parasitology* **25**, 1363-7.
- Mott, J.J., Ludlow, M.M., Richards, J.H. and Parsons, A.D. (1992). Effects of moisture supply in the dry season and subsequent defoliation on persistence of the savanna grasses *Themeda triandra*, *Heteropogon contortus*, and *Panicum maximum*. *Australian Journal of Agricultural Research*, **43**: 241–60.
- Mott, J.J., Tothill, J.C. and Weston, E.J. (1981). Animal production for the native woodlands and grasslands of northern Australia. *Journal of the Australian Institute of Agricultural Science*, **47**: 132–41.
- Mott, J.J., Williams, J., Andrew, M.H. and Gillison, A.N. (1985). Australian savanna ecosystems. In *Ecology and Management of the Worlds Savannas* (Eds J.C. Tothill and J.J. Mott.) pp. 56–82. Australian Academy of Science, Canberra.
- Nakicenovic, N. and Swart, S. (2000). *Emissions Scenarios*. A Special Report of Working Group III of the Intergovernmental Panel on Climate Change. Cambridge University Press, Cambridge, UK and New York, USA, 599 pp.
- Owens, J.S. Silburn, D.M., McKeon, G.M., Carroll, C., Willcocks, J. and deVoil, R. (2003). Cover-runoff equations to improve simulation of runoff in pasture growth models. *Australian Journal of Soil Research*, **41**:1467-1488.
- Philp, M.W. and Day, K.A. (1997) Swiftsynd methodology: A methodology for measuring a minimum data set for calibrating pasture and soil parameters of the pasture growth model GRASP. Appendix 3 of evaluating the risks of pasture and land degradation in native pasture in Queensland. Final Report for Rural Industries and Research Development Corporation project DAQ124A. Queensland Department of Natural Resources, Brisbane.
- Pittock, B. (2004). Climate Change: An Australian Guide to the Science and Potential Impacts. Australian Greenhouse Office. 239pp.
- Rayner, D. Moodie, K, Beswick, A, Clarckson, N and Hutchinson, R. (2004). New Australian daily historical climate surfaces using CLIMARC. Queensland Department of Natural Resources, Mines and Energy Internal Report, 82pp.
- Rickert, K.G. and McKeon, G.M. (1982). Soil water balance model: WATSUP. *Proceedings of the Australian Society for Animal Production*, **14**: 198-200.

- Scanlan, J.C., Pressland, A.J. and Myles, D.J. (1996). Runoff and soil movement on mid-slopes in north-east Queensland grazed woodlands. *Rangeland Journal*, **18**: 33–46.
- Scanlan, J.C., McKeon, G.M., Day, K.A., Mott, J.J. and Hinton, A.W. (1994). Estimating safe carrying capacities of extensive cattle grazing properties within tropical, semi-arid woodlands of north-eastern Australia. *Rangeland Journal*, **16**: 64–76.
- Stafford Smith, M. and McKeon, G.M. (1998). Assessing the historical frequency of drought events on rangelands grazing properties: case studies. *Agricultural Systems*, **57**: 271-299.
- Stafford Smith, M., Buxton, R., McKeon, G. and Ash, A. (2000). Seasonal climate forecasting and the management of rangelands: Do production benefits translate into enterprise profits. In: *'Applications of Seasonal Climate Forecasting in Agricultural and Natural Ecosystems - the Australian Experience'*. (Eds G. Hammer, N. Nicholls and C. Mitchell.) Kluwer Academic Press: Netherlands. p. 271-289.
- Sutherst, R.W. (1990). Impact of climate change on pests and diseases in Australia. *Search* **21**, 230-2.
- Sutherst, R.W., Yonow, T., Chakraborty, S., O'Donnell, C. and White, N. (1996). A generic approach to defining impacts of climate change on pests, weeds and diseases in Australia. In *'Greenhouse: Coping with Climate Change'*. (Eds W.J. Bouma, G.I. Pearman and M.R. Manning) pp. 281-307. (CSIRO: Melbourne.).
- Torok, S.J. 1996a. *The development of a high quality historical temperature database for Australia*. PhD thesis, School of Earth Sciences, Faculty of Science, University of Melbourne.
- Torok, S.J. and Nicholls, N. 1996b. A historical annual temperature dataset for Australia. *Australian Meteorological Magazine*, **45**: 251-260.
- Torok, S.J., Morris, C.J.G., Skinner, C. and Plummer, N. 2001. Urban heat island features of southeast Australian towns. *Australian Meteorological Magazine*, **50**: 1-14.
- Tothill, J.C. and Gillies, C. (1992). The pasture lands of northern Australia: Their condition, productivity and sustainability. Tropical Grasslands Society of Australia Occasional Publication No. 5.
- Trewin, B.C. (2001). *Extreme Temperature Events in Australia*. PhD thesis, School of Earth Sciences, Faculty of Science, University of Melbourne.
- Wackter, D. J., and Bayly, P.V. (1987). "The Effectiveness of Connecticut's SIP on Reducing Ozone Levels from 1976 through 1987". *Air Pollution Control Association Specialty Conference on "The Scientific and Technical Issues Facing Post-1987 Ozone Control Strategies,"* Hartford, Connecticut (November 1987).
- Walker, B. H. and Weston, E.J. (1990). Pasture development in Queensland- a success story. *Tropical Grasslands*, **24**, 4, 257-268.
- WBM Oceanics Australia, (1998). Overview of the Burnett Catchment Flora and Fauna, Department of Natural Resources.
- Whetton, P. (2001). Methods used to prepare the ranges of projected future change in Australian region temperature and precipitation. CSIRO Report, 7May 2001. 4pp.

- White, N., Sutherst, R. W., Hall, N. and Whish-Wilson, P. (2004): The vulnerability of the Australian beef industry to impacts of the cattle tick (*Boophilus microplus*) under climate change. *Climatic Change* (in press).
- White, B.J. (1972). Supply projections for the Australian beef industry. *Review of Marketing and Agricultural Economics* **40**, 1-12.
- Yee Yet, J.S., Silburn, D.M., McKeon, G.M. (1999). Cover-runoff equations which improve the simulation of runoff in pasture growth models. In: D. Elridge and D Freudenberger (eds) *People and Rangelands: Building the Future. Proceedings VIth International Rangelands Congress*, July 1999, Townsville, Australia. p. 849-50.

Appendix A

Climatic variables available from STARDEX for trend analysis

1. Mean Tmax
2. Mean Tmin
3. Mean Tmean
4. Mean diurnal temperature range
5. 10th percentile diurnal temperature range
6. 90th percentile diurnal temperature range
7. Tmax 10th percentile
8. Tmax 90th percentile
9. Tmin 10th percentile
10. Tmin 90th percentile
11. Number of frost days $T_{min} < 0^{\circ}\text{C}$
12. Number of days without defrost (ice days) $T_{max} < 0^{\circ}\text{C}$
13. Growing degree-days > threshold
14. Intra-annual extreme temperature range
15. Growing Season Length
16. Heat Wave Duration
17. Percentile Heat Wave Duration
18. Cold Wave Duration
19. Percentile Cold Wave Duration
20. Frost Season Length (0°C)
21. Percentage days $T_{max} < 10\text{th percentile}$
22. Percentage days $T_{max} > 90\text{th percentile}$
23. Percentage days $T_{min} < 10\text{th percentile}$
24. Percentage days $T_{min} > 90\text{th percentile}$
25. Mean climatological precipitation (mm/day)
26. 20th percentile of rainday amounts (mm/day)
27. 40th percentile of rainday amounts (mm/day)
28. 50th percentile of rainday amounts (mm/day)
29. 60th percentile of rainday amounts (mm/day)
30. 80th percentile of rainday amounts (mm/day)
31. 90th percentile of rainday amounts (mm/day)
32. 95th percentile of rainday amounts (mm/day)
33. Fraction of total precipitation above annual 20th percentile
34. Fraction of total precipitation above annual 40th percentile

35. Fraction of total precipitation above annual 50th percentile
36. Fraction of total precipitation above annual 60th percentile
37. Fraction of total precipitation above annual 80th percentile
38. Fraction of total precipitation above annual 90th percentile
39. Fraction of total precipitation above annual 95th percentile
40. Number of days precipitation $\geq 10\text{mm}$
41. Maximum number consecutive dry days
42. Maximum number consecutive wet days
43. Mean wet-day persistence
44. Mean dry-day persistence
45. Correlation for spell lengths
46. Mean wet spell lengths (days)
47. Median wet spell lengths (days)
48. Standard deviation wet spell lengths (days)
49. Mean dry spell lengths (days)
50. Median dry spell lengths (days)
51. Standard deviation dry spell lengths (days)
52. Greatest 3-day total rainfall
53. Greatest 5-day total rainfall
54. Greatest 10-day total rainfall
55. Simple Daily Intensity (rain per rainday)
56. Percentage of total rainfall from events $>$ long-term 90th percentile
57. Number of events $>$ long-term 90th percentile